Recherche de nouvelles sources de résistance à la verticilliose chez Medicago sp

Amir Hossein Fartash

THÈSE

En vue de l'obtention du

DOCTORAT DE L'UNIVERSITÉ DE TOULOUSE

Délivré par :

Institut National Polytechnique de Toulouse (Toulouse INP)

Discipline ou spécialité :

Ecologie Fonctionnelle

Présentée et soutenue par :

M. AMIR HOSSEIN FARTASH

le lundi 24 octobre 2022

Titre :

Search for new sources of resistance to Verticillium wilt in Medicago

---

Ecole doctorale :

Sciences de l'Univers de l'Environnement et de l'Espace (SDU2E)

Unité de recherche :

Laboratoire Ecologie Fonctionnelle et Environnement (LEFE)

Directeur(s) de Thèse :

MME MARTINA RICKAUER

M. ASA EBRAHIMI

Rapporteurs :

M. DIEGO RUBIALES, CSIC BARCELONE

MME JULIA BUITINK, INRA ANGERS

Membre(s) du jury :

M. NACEUR DJEBALI, CENTRE DE BIOTECHNOLOGIE DE BORJ CEDRIA, Président

M. ASA EBRAHIMI, ISLAMIC AZAD UNIVERSITY TEHERAN, Membre

M. LAURENT GENTZBITTEL, ACADEMIE DES SCIENCES DE RUSSIE MOSCOU, Membre

MME CECILE BEN, TOULOUSE INP, Membre

MME MARTINA RICKAUER, TOULOUSE INP, Membre

“Everything will be okay in the end.

If it is not okay, it's not the end"

John Lennon

Acknowledgement

It is not without emotion that I would like to thank all the people who have supported me from near or far and to the extent of their ability in this project.

I would like to warmly thank my thesis supervisors, Martina Rickauer and Asa Ebrahimi, who were able to pass on their passion for microbiology and plant genetics to me right from my studies at ENSAT and Iran Azad university. It would not be an exaggeration to say that they were, are, and will be more than official supervisors to me. Their support and encouragement were the main factor that gave me the courage to complete this project, and I will never forget their role for my present work and future career.

Also, I thank Laurent Gentzbittel and Cécile Ben for their contribution to this project and in particular for their help in learning and improving new skills such as statistics, data science, R program and Linux commands.

In addition, I would like to thank Julia Buitink, Diego Rubiales, and Naceur Djebali who accepted to evaluate this work; undoubtedly, their valuable and precise comments on my manuscript enriched the current manuscript.

Thanks to Nathalie Séjalon-Delmas, Pierre Maury, Mokhtar Benkada, Seddik Bendahmane, Yassine Mabrouk, and Jean Kallerhoff for the discussions and pieces of advice provided, particularly during the four thesis committees.

Thank you to Afsaneh Mohammad Pourfard, head of Iranian NanoBioTechnologist company (INBTCo.), Tehran, Iran, for providing me with a scholarship and also to the French embassy in Tehran which partially granting me through PHC Gundishapur N° 38423VK for supporting field trips to Iran.

Thanks to Mojtaba Ghalandar for providing us with the *Verticillium alfalfae* sample (MG-2) and helping us during the field sampling in Arak. Also many thanks to our friends who helped us a lot during our field sampling in Iran such as Aliakbar Heidari (Esfahan), Setare kochaki (Tehran), Kazem Sabagh(University of Yazd), and Reza Darvishzadeh (University of Urmia).

I would like to thank the GENOTOUL-bioinfo (calculation cluster) and GENOTOUL - GeT (Génome & Transcriptome) platforms and more particularly Sandra Fourré for her help in performing the qRT-PCR.

I would like to thank Mélanie Mazurier since the current study, was more and less the extension of her project and I used some of her results for the comparison of our two projects. She helped me a lot during the past years in different ways such as commenting on my results, providing some R codes, etc …

I would like to thank Melanie Pestre, Enzo Carrières, and Mathieu Volpilière, BTS student trainees in our laboratory for their technical assistance throughout this thesis.

Special thanks to Annick Corrège, Franck Gilbert, and Dirk S. Schmeller, Geneviève Soucail, and Adrien Bru for their support in administrative tasks and their logistical support.

I would like to thank Zahra Pakbaz, Yanis Amokrane, Insaf Djouider, Manel Chaouachi, Loubna El Madouri, Henar Margenat, Nikola Zsolnay for our scientific and cultural exchanges; their Inspirational and motivational words such as "Don't worry, it will work, it has to; there is no other option, ..." have contributed to the continuation of my work when nothing worked.

Also, I want to acknowledge the contribution of Maoulida Toueni and Abed Sbeiti whose results were important stepstones for my thesis.

I would like to thank Williams Exbrayat, OMP Open Archive Manager, who provided me with articles to which I had no access for literature review.

Also, I would like to thank Colette, Flor, Geneviève, and Christiane; the nice and kind people who I lived with and who became like my family; they were with me in all of the good and hard moments and special thanks to Emma and Marc Afshar who helped me in different ways - I never ever can pay back their kindness. .

Finally, hoping I have not forgotten anyone, I would like to thank my family (My Mother, Father, and kindest Brother) alongside Hassan Shafinouri, Mahboubeh Mohhamad Pour, Farzaneh Behzadi, and Raya Waxler who have always been by my side, even when my passion for research made me run away from them and from my country.

Résumé

L'objectif de cette étude est d'explorer le contrôle génétique de la résistance *de M. truncatula* envers *V. alfalfae* dans un contexte de réchauffement climatique et de menace d'arrivée de nouveaux pathogènes par le commerce mondial.

Pour obtenir une nouvelle souche de *Verticillium alfalfae*, des plants de luzerne présentant des symptômes de verticilliose ont été collectés lors de plusieurs sorties sur le terrain en Iran. Suite à l'isolement de champignon à partir des plantes échantillonnées, dix isolats de *V. alfalfae* ont été identifiés par PCR avec des amorces spécifiques à l'espèce. Sept isolats ainsi que l'isolat français V31-2 ont été étudiés pour les paramètres de croissance végétative à 20 °C, 25 °C et 28 °C. La température optimale pour la croissance radiale et la sporulation était de 25 °C suivie de 20 °C. L'analyse statistique révèle l'existence de deux groupes distincts ; l'un contenant tous les échantillons iraniens et l'autre groupe contenant l'isolat français.

L'isolat iranien de *V. alfalfae* AF-1 a été sélectionné pour une étude de génétique d'association (GWAS) avec 242 accessions de *M. truncatula* de la collection HapMap afin d'identifier les loci ou les gènes impliqués dans le contrôle génétique de la résistance. Les plantes ont été inoculées aux racines avec des spores d'AF1 et les symptômes ont été notés sur une échelle de 0 à 4 pendant 4 semaines dans une chambre de culture à 25 °C (une température plus élevée par rapport aux études précédentes à 20 °C). Le score maximal des symptômes (MSS, symptôme à la fin de l'expérience) et l'aire sous la courbe de progression de la maladie (AUDPC) ont été calculés

Les expériences de phénotypage ont été réalisées dans une conception en blocs augmentés (3 répétitions indépendantes composées chacune de quatre blocs indépendants) en incluant chaque fois 4 lignées (F83005.5, DZA315.14, DZA45.5 et A17) comme contrôle pour corriger les données contre les effets de bloc si nécessaire. Cinq modèles statistiques GWAS ont été testés impliquant deux modèles linéaires généraux (GLM) et trois modèles linéaires mixtes (MLM). L'analyse par Q-Q plot a montré que le MLM Q-Model est le modèle le mieux ajusté pour les deux traits (AUDPC et MSS). En utilisant le modèle le mieux ajusté, 30 *locus* associés à la

résistance à l'AF1 ont été détectés par un polymorphisme de nucléotide unique (SNP) significatif pour les deux traits. Ces *loci* étaient tous différents de ceux identifiés précédemment avec un isolat français à 20 °C. Les régions de 10 kb entourant chaque SNP ont été explorées et les gènes situés dans cette zone ont été considérés comme des gènes candidats. Parmi 122 gènes candidats putatifs, sept gènes ont été sélectionnés pour des études d'expression.

Pour évaluer expression, 12 accessions parmi les plus sensibles et les plus résistantes ont été inoculées aux racines. Les racines et les parties aériennes ont été récoltées 0,4,24 et 96 heures après l'inoculation, et les échantillons ont été regroupés en un groupe sensible et un groupe résistant pour masquer les différences individuelles entre les accessions. L'expression génique a été analysée par qRT-PCR et l'analyse des données a été effectuée par le calcul de $\Delta\Delta$CT et le facteur d'induction dans les plantes inoculées par rapport aux plantes non-inoculées. Les valeurs CT ont été normalisées par rapport à la moyenne harmonique de deux gènes de référence codant pour l'actine et l'histone H3L.

Les résultats de la qRT-PCR ont montré que tous ces gènes candidats étaient exprimés dans les racines et que leur expression était augmentée après inoculation dans les plantes résistantes et sensibles.

En conclusion, les résultats indiquent qu'un simple changement de température combiné à une nouvelle souche pathogène modifie entièrement l'architecture du contrôle génétique de la résistance au pathogène. Cela devrait être un sérieux avertissement aux sélectionneurs, aux décideurs politiques et aux institutions qui contrôlent l'échange de matériel végétal.

Mots clés : Stress biotique / Changement climatique / Expression génique / Étude d'association à l'échelle du génome / Légumineuses / Medicago sativa / Résistance quantitative aux maladies / Maladies des racines / Flétrissement vasculaire.

Abstract

The objective of this study is to explore the genetic control of resistance in *M. truncatula* toward *V. alfalfae* in a context of global warming and the threat of arrival of new pathogens by global trade.

To obtain a new strain of *Verticillium alfalfae*, alfalfa plants with symptoms of Verticillium wilt were collected during several field trips in Iran. Following fungal isolation from the sampled plants, ten *V. alfalfae* isolates were identified by PCR with species-specific primers., Seven isolates along with the French isolate V31-2 were studied for vegetative growth parameters at 20 °C, 25 °C and 28 °C. Optimum temperature for radial growth and sporulation was 25 °C followed by 20 °C. Statistical analysis reveals the existence of two distinct groups; one containing all Iranian samples and the other group containing the French isolate.

The Iranian *V. alfalfae* isolate AF-1 was selected for a Genome wide association study (GWAS) with 242 *M. truncatula* accessions from the HapMap collection to identify loci or genes involved in the genetic control of resistance. Plants were root-inoculated with spores of AF1 and symptoms were scored on a scale from 0 to 4 during 4 weeks in a growth chamber at 25 °C (a higher temperature compared to previous studies at 20 °C). Maximum symptom score (MSS, symptom at the end of the experiment) and Area under disease progress curve (AUDPC) were computed.

The phenotyping experiments were performed in an augmented block design (3 independent repeats each of which consisted of four independent blocks) while 4 lines (F83005.5, DZA315.14, DZA45.5, and A17) were used as check lines to correct the data against block effects if necessary.

Five GWAS statistical models were tested involving two General Linear models (GLM) and three Mixed Linear Models (MLM). Analysis by Q-Q plot showed that the MLM Q-Model is the best-fitted model for both traits (AUDPC and MSS). Using the best-fitted model, 30 loci associated to resistance towards AF1 were detected through significant Single Nucleotide Polymorphism (SNP) for the two traits. These loci were all different from those identified previously with a French isolate at 20 °C. The regions of 10 kb surrounding each SNP were explored and genes located in this area were considered

as candidate genes. Among 122 putative candidate genes, seven genes were selected for expression studies.

To evaluate their expression, 12 of the most susceptible and the most resistant accessions were root-inoculated. Roots and aerial parts were harvested 0, 4, 24 and 96 hours after inoculation, and the samples were pooled in a susceptible and a resistant group to mask the individual differences among accessions. Gene expression was analyzed by qRT-PCR and data analysis was performed through calculation of $\Delta\Delta$CT and fold change of expression in inoculated plants versus mock-inoculated plants. CT values were normalized against the harmonic mean of two reference genes encoding Actin and Histone H3L.

The qRT-PCR results showed that all selected candidate genes were expressed in roots and that their expression was increased after inoculation in both resistant and susceptible plants. The induction was consistently higher and more durable in resistant plants compared to susceptible ones, confirming the involvement of the identified loci in resistance.

In conclusion, the results indicate that a simple shift in temperature combined with a new pathogen strain entirely changes the architecture of genetic control of resistance to the pathogen. This should be a serious warning to breeders, and policy makers and institutions that control the exchange of plant material.

Key words: Biotic stress / Climate change / Gene expression / Genome-wide association study / Legumes / Medicago sativa / Quantitative disease resistance / Root diseases / Vascular wilt.

Abbreviations

AIL: Advanced Intercross Line

AM: Association mapping

ANOVA: Analysis of Variance

AUDPC: Area Under Disease Progress Curve

BBSRC: Biotechnology and Biological Sciences Research Council

BLUE: Best Linear Unbiased Estimator

cDNA: complementary DNA

cAMP: cyclic AMP

cM: Centi-Morgan

CNV's: Copy Number Variants

CTAB: Cetyltrimethylammonium Bromide

DNA: Deoxyribonucleic Acid

dpi: Days-Post Inoculation

EM: Expectation Maximization

ETI: Effector-Triggered Immunity

ETS: Effector-Triggered Susceptibility

FDR: False Discovery Rate

FISH: Fluorescence in Situ Hybridization

GBS: Genotyping-By-Sequencing

GLM: General Linear Model

GWAS: Genome-Wide Association study

HR: Hypersensitive Response

INDELs: insertions/ deletions

ITS: Internal Transcribed Spacer

K matrix: Kinship Matrix

LD: Linkage Disequilibrium

LD: Linkage disequilibrium

LG: Linkage Groups

LS: Lineage-Specific

Lsmeans: Least-Squares Means

MAF: Minimum Allele Frequency

MAGIC: Multiparent Advanced Generation Intercross

MAMPs: Microbe-Associated Molecular Patterns

MAPKs: Mitogen-Activated Protein Kinase

MLM: Mixed Linear Model

MLPA: Multilocus Phylogenetic Analysis

MSS: Maximum Symptom Score

NAM: Nested Association Mapping population

NGS: Next Generation Sequencing

NLP: Necrosis and Ethylene-Inducing-Like Protein

NSF: National Science Foundation

P3D: Population Parameter Previously Determined

PAMPs: Pathogen-Associated Molecular Patterns

PCR: Polymerase Chain Reaction

PDA: Potato Dextrose Agar

PDB: Potato Dextrose Broth

PRRs: Pattern Recognition Receptors

PTI: PAMP-Triggered Immunity

Q Matrix : Population Matrix

Q-Q Plot : Quantile-Quantile plots

qRT-PCR: Quantitative real-time PCR

QTL : Quantitative Trait Loci

RELM: Restricted Maximum Likelihood

RILs: Recombinant Inbred Lines

ROS: Reactive Oxygen Species

RPM: Round Per Minute

SA: Salicylic Acid

SAR: Systemic Acquired Resistance

SGE: SA glucose ester

SNP: Single Nucleotide Polymorphism

SNPs: Single Nucleotide Polymorphisms

SSRs: Single Sequence Repeats

TE8: Tris-EDTA (pH 8.0)

WA: Water Agar

WGAS: Whole Genome Association Study

List of Figures

List of tables

List of Supplementary Figures

List of Supplementary Tables

Table of Contents

I - Introduction

I.1. Plant - Pathogen interactions

Plants are continuously confronted with microorganisms in their environment. Only small parts of them are pathogenic and will colonize the plant and cause disease symptoms (Agrios 2005). Among pathogenic microorganisms, fungi form the most important group.

Obligate and nonobligate pathogenic fungi vary in the ways they attack and colonize their host and obtain their nutrients (Agrios 2005). Both first need to penetrate through the plant cell wall by forming specific structures called appressoria and/or by secreting enzymes to degrade the cell wall components.

Obligate pathogens (also called biotrophs) need living cells to acquire their nutrients, so they will not damage the plant cell membrane and enter the cytoplasm, but instead they form specific feeding structures called haustoria in close contact with the host cell membrane (Mukhtar et al. 2016). Most of them are highly specific with regard to the plant host probably as a result of co-evolution and requirement of specific nutrients that are produced or are accessible to the pathogen only in its host (Westwood et al. 2010).

Nonobligate pathogens do not need to keep their host alive. Some of them (called hemibiotrophs) start as biotrophs during early stages of colonization but kill the host cells at later stages when the infectious propagules are formed. Others (necrotrophs) kill the host cells early during infection with toxins, and feed on the content of dead cells. In contrast to obligate pathogens, non-obligate have a wide host range, probably due to the fact that for their invasion they rely on non-specific enzymes or toxins which alter substances or processes commonly found in all plants (Ainsworth and Sussman 2013).

1.1. Development of Disease

The disease development relies on three factors: a pathogen, a susceptible host plant and favourable environmental conditions.

Each of these factors can represent a wide range of variability and changes in each factor can manipulate the extent of disease intensity within the individual plant and in plant populations.

The interaction of the three factors has often been visualized as a triangle, which commonly is known as the “disease triangle” (Figure 1)(Agrios 2005). Each side of the triangle presents one factor.

However, recently “Time” has been integrated as a fourth important factor (fourth dimension) in this model and evolved it to a “disease pyramid” (Figure 1) (Francl 2001). Generally, for infection and disease development, a period of time is required since hosts come in contact with pathogens in a favorable environment (Ainsworth and Sussman 2013). Even in situations when favorable environmental conditions continue for an extended period of time, disease would not occur immediately (Allen 2012).

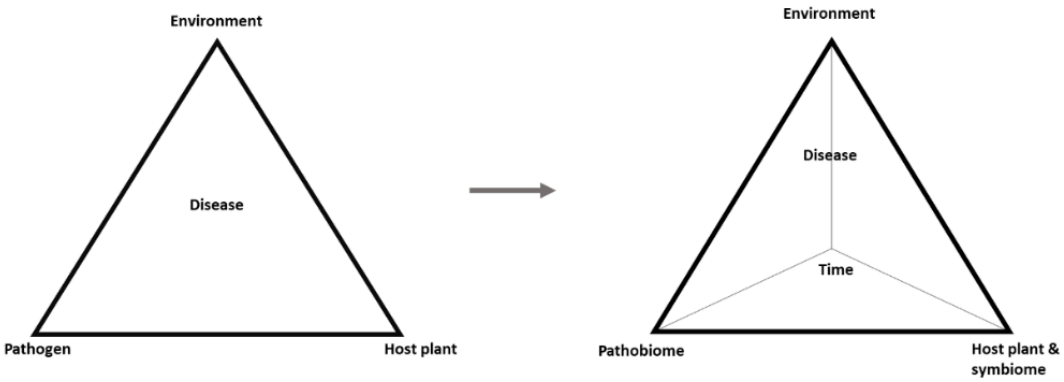

Figure 1: The disease triangle and the disease pyramid.

Source: Manna and Seo,2021.

The advent of new technologies such as next-generation sequencing has offered cost-effective and convenient ways to explore the extraordinarily diversified microorganisms' world, notably the microbiome in various environments. With increased knowledge of the distribution and effect of endophytes it is now accepted that the microbiome of host plants plays a critical role in host immunity and shapes the disease outcome (Teixeira et al. 2019; Tiwari et al. 2022). Hence, a different model of the disease pyramid proposes to integrate the host microbiome as the fourth dimension that manipulates the disease outcome (Figure 2) (Bernardo-Cravo et al. 2020).

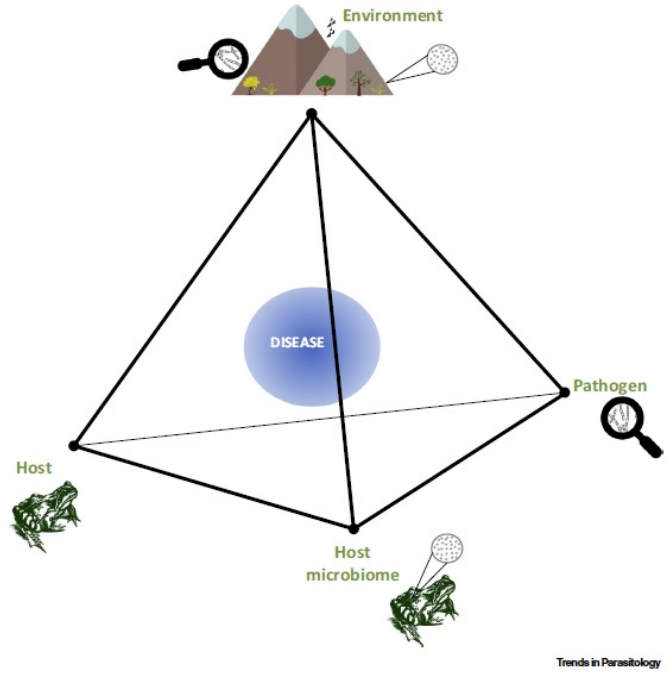

Figure 2: The disease pyramid: A quadruple-approach between host, pathogen, environment and host microbiome that determines the outcome of a disease.

Source : Bernardo-Cravo *et al*. ,2020.

1.2. Disease Cycle

In each kind of disease, there are interconnected successive stages that lead to the development of the disease and the pathogen, which is known as the “disease cycle” (Figure 3)(De Wolf and Isard 2007; Agrios 2005). Although in some cases the disease cycle is similar to the pathogen life cycle, it generally points out the advent, development and longevity of the disease caused by the pathogen rather than of the pathogen itself.

The distinct events in a disease cycle are (Agrios 2005)

1. Inoculation
2. Pre-Penetration
3. Penetration
4. Infection
5. Invasion
6. Colonization
7. Dissemination of the pathogen

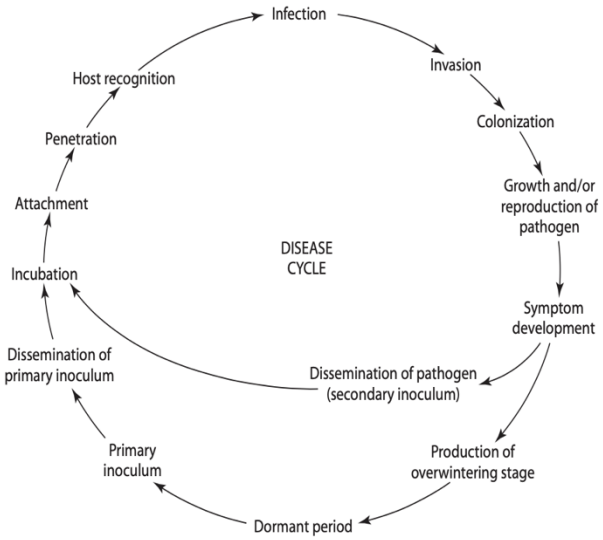

Figure 3:Disease cycle.

Source : Agrios, 2005

The following will try to explain all of these levels focusing on Fungi domain

1.2.1. Inoculation

Inoculation is the initial meeting of a pathogen with a plant's organ where contamination is feasible. The pathogen that comes into contact with the host plant is called inoculum (Schumann and D'Arcy 2010). The inoculum can be any section of the pathogen that is able to start infection. For example, in fungi, it could be a part of mycelium, sclerotia or spore. The inoculum can be a single individual (e.g., only one spore) or of million hundreds of individual spores. Generally, one unit of inoculum of a pathogen is called "propagule" (Guest 2017; Agrios 2005).
An inoculum that endures dormant in the winter/ summer and causes the primary infection in the spring/autumn is called "primary inoculum"; the infection which it is causes is called "primary infection". An inoculum that is produced from primary infections is called a "secondary inoculum" and will cause "secondary infection". There is a positive correlation between the severity of disease and the abundance of inoculum (Schumann and D'Arcy 2010; Agrios 2005).

1.2.2. Pre-Penetration

The step of pre-penetration can be further divided into three parts such as:

- Recognition of host and pathogen
- Attachment to the host-surface
- Spore germination and formation of appressoria

1.2.2.1. Recognition of host and pathogen

When a pathogen is in direct contact with the host both may perceive the presence of the other by signals such as topography of the surface, plant compounds or pathogen-

derived elicitor molecules. This mutual recognition will lead to a response in the pathogen to favour penetration, and in the plant to defend itself against the pathogen (Figure 4).

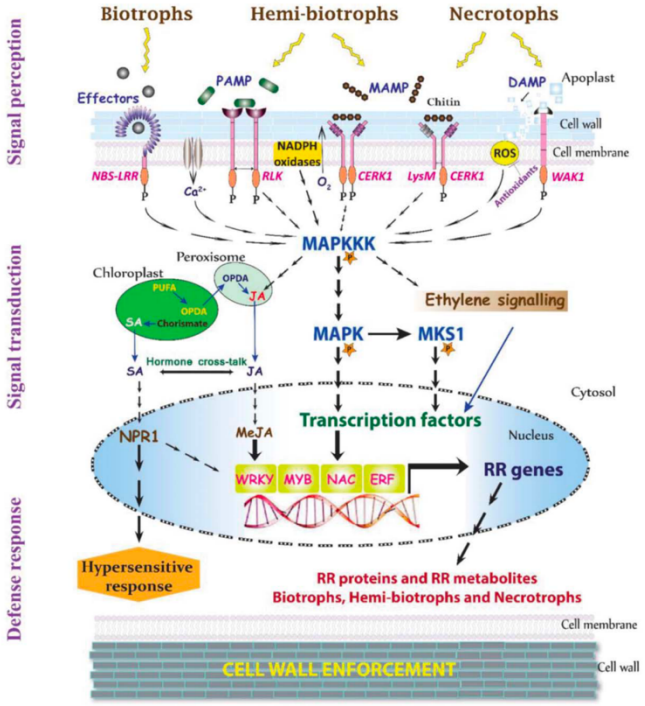

Figure 4: The early events in host-pathogen interaction.

Generally, all pathogens produce elicitors (PAMP/MAMP), except for specialized pathogens which also produce effectors. Plants detect effectors /elicitors and active their immune response, through triggering a hierarchy of R genes (elicitor recognition receptor, effector recognition receptor, transcription factor (TF), mitogen-activated protein kinase (MAPK), phytohormone), ultimately to produce resistance-related proteins (RRPs) and metabolites (RRMs), that directly suppress the pathogen advancement. The elicitors are recognized by host membrane-localized elicitor recognition receptor, while the effectors are recognized by effector recognition receptor (PRR produced by R genes). Simultaneously, a number of secondary messengers such as calcium ions, reactive oxygen species (ROS), and plant hormone-mediated defense pathways (Ethylene, JA, and SA) are activated following stress, which trigger downstream genes resulting in hypersensitive response or reduced susceptibility. Finally, the signal perceived by receptor kinases are transmitted through cytosolic protein kinases to activate an array of plant transcription factors (ERF, MYB, NAC, and WRKY), which regulate several R genes to produce RRPs and RRMs. These RMs or their conjugate products that are deposited to enforce the secondary cell wall, thus containing the pathogen to initial infection area.

Source : Kushalappa et al., 2016.

For example, fatty acids which are present in the plant cuticle can trigger the production of enzymes such as cutinase in the pathogen, and initiate the formation of appressoria (Figure 5-Figure 6). Pectin which is present in the middle lamella of the host cells triggers the production of pectinases which will facilitate the colonization of

the intercellular space.(Delaunois et al. 2014). Specific phenolic compounds such as strigol or isoflavones released from the plant (Le Roy et al. 2016; Mishra, Upadhyay, and Shukla 2017) will induce expression of various avirulence (or virulence) genes in the pathogen such as Avr9 in the tomato pathogen *Cladosporium fulvum* (Blatt et al. 1999) or vacuolar protein sorting-associated protein 9 (VPS9) and RGD-binding gene in the barley pathogen *Puccinia graminis* (Nirmala et al. 2011) which finally leads to infection.

In parallel, a host plant may also recognize the presence of the pathogen by molecules on the surface or secreted by the pathogen, such as Pathogen-associated molecular patterns or Microbe-associated molecular patterns (PAMPs, MAMPs) which are non-specific. In addition to such non-specific molecules, others are encoded directly or indirectly by avirulence genes and will be recognized only by plants that carry the corresponding resistance gene. This will lead to the triggering of Defense reactions (Figure 4).

1.2.2.2. Attachment to the host-surface

Before starting the penetration process and the colonization of plant tissues, pathogens have to be in direct contact with the outermost surface of the targeted organ of the plant. Attachment starts via adherence of spore to sticky materials that differ naturally in architecture and in environmental factors in which they demand it to become adhesive.

The propagules of fungi and oomycetes have a mucilaginous surface which contains a mixture of insoluble polysaccharides, glycoproteins, and fibrillar components (Nicholson and Epstein 1991; Guest 2017). This mixture becomes adhesive under conditions of high moisture (e.g., dew, high relative humidity of air, rain), and propagules will be able to stick to the host plant surface which is often very hydrophobic. Some will secrete a mucilage at the tip of the spore in order to attach to the plant surface (Rumbolz et al. 2000; Nicholson et al. 1988).

1.2.2.3. Spore germination and formation of appressoria

Spores are equipped with a prevention mechanism that inhibits germination before they detect stimulation signals or when they are surrounded by too many spores(Chitarra et al. 2004; Ugalde and Rodriguez-Urra 2016). When the spore detects such stimulation signals, it gets activated (breaks dormancy) and will synthesize the cell membrane and cell wall to form the germ tube (Sephton-Clark and Voelz 2018; Agrios 2005) which will later differentiate the appressorium (Figure 6). The germ tube perceives some physical and chemical signals from host surface such as plant hydrophobicity, surface topography or molecules (e.g., cutin) which will trigger the differentiation of appressoria. In the absence of such signals, the development of a germ tube would be stopped when spore accumulated supplies run out.

Signaling pathways associated with these early infection steps often involve mitogen-activated protein kinase (MAPKs) and their upstream regulatory kinases, and cyclic AMP (Jiang et al., 2018a, b; N. Lee et al., 2003).

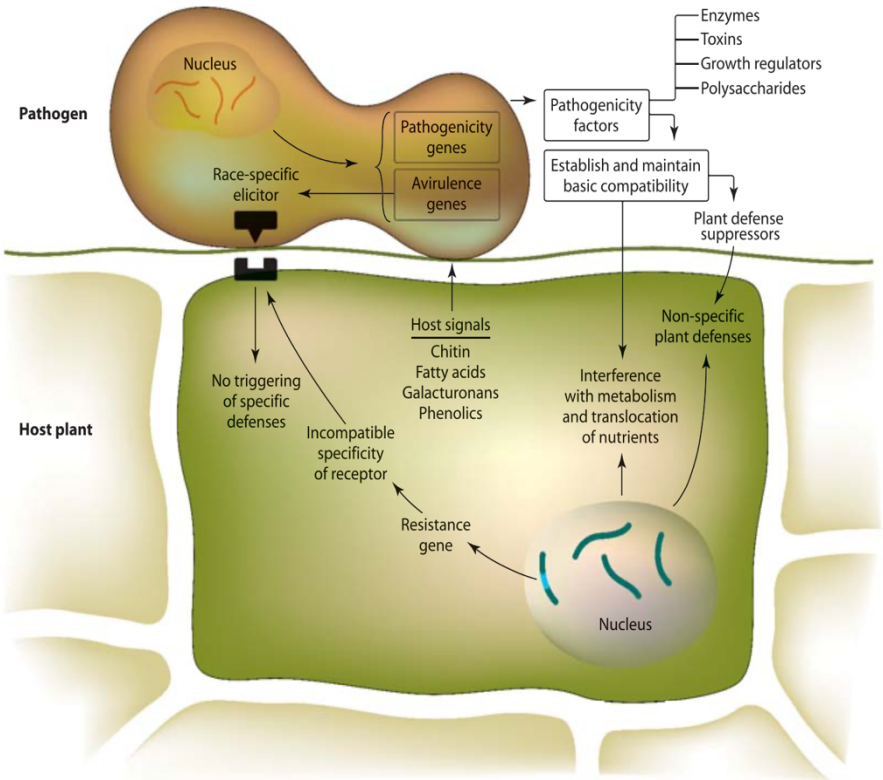

Figure 5: Signal exchange and responses between plant and pathogen at early steps of infection.

Source: Agrios, 2005.

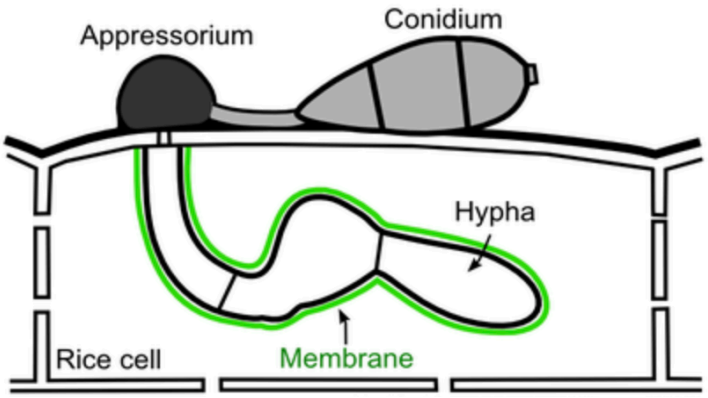

Figure 6: Appressorial nucleus and formation of the penetration peg.

Schematic diagram illustrating the question of how an appressorium forms and enters the filamentous invasive hyphae into host plant.

Source : Valent and Khang, 2010.

1.2.3. Penetration

Fungal penetration into the host cells or tissues takes place through one of the following strategies (Figure 7)

1. Direct penetration
2. Penetration through natural opening of host plants
3. Penetration through wounds

1.2.3.1. Direct Penetration

For fungi, direct penetration into the host plant is possible mostly through the function of appressoria.

After differentiation of a germ tube into an appressorium (Figure 6), it attaches tightly to the host surface and secretes enzymes that break down the cuticle layer. In addition, the appressorium will form a thick cell wall that is often melanized and will build up

high turgor pressure through accumulation of glycerol. De Jong et al. (1997) reported the increase of turgor pressure inside the appressorium which leads penetration hyphae to introduce into the underlying epidermal cells through the plant cuticle. While the initial transfer of lipid and glycogen reserves to the evolving appressorium is regulated by the MAPK1, glycerol biosynthesis is regulated by the cAMP-PKA signaling pathway (Rajput et al. 2019; F. Liu et al. 2017). In addition to applying mechanical forces the appressorium secretes cell-wall loosening enzymes to facilitate the growth of the penetration peg into the cell (Schumann and D'Arcy 2010; Agrios 2005).

Production of the penetration peg needs the localization of actin to the hyphal tip and accelerated biosynthesis of the cell wall while the hypha grows into the cuticle and epidermal cell wall layers. It is reported that the MAP kinase pathway is responsible for the regulation of the production of penetration hyphae (Y. Li et al. 2016) (Figure 7).

1.2.3.2. Penetration through natural opening pores of host plants

Stomata and hydathodes are natural openings for pathogen entry into the host plants. Stomata are open during the day and during the night. Typically, fungal spores germinate on the host plant surface and then the germ tube can enter and grow through the stoma. The hypha develops in sub stomata pit and by the means of haustoria directly occupies the cells of the host plant (Figure 7)(Guest 2017).

Hydathodes are pores at the edge of leaves which are linked to veins and their main function is to discharge water by guttation drops. Some bacteria and a few fungi introduce to host plant through these type of pores (Figure 7).

Lenticel is a permeable tissue with large intercellular pits that can be found on the periderm of secondary thickened organs, stems, tubers and fruits. Lenticels act as pores and provide a pathway for direct gas exchange between the internal tissues and the environment (Priestley 1922). They also allow the penetration of some bacteria and a few fungi (Figure 7); however pathogen penetration through lenticels seems to be less efficient than penetration through wounds (Agrios 2005).

1.2.3.3. Penetration through wounds

Most of the pathogens such as fungi can enter the host plant through wounds which are caused by various factors such as hail damage, wind breakage, insects, animals feeding or human practices (transplanting, pruning, ...) (Figure 7) (Schumann and D'Arcy 2010; Agrios 2005). Pathogens depending on wounds for entering often develop mainly on the wounded tissue before they move toward intact and healthy tissue.

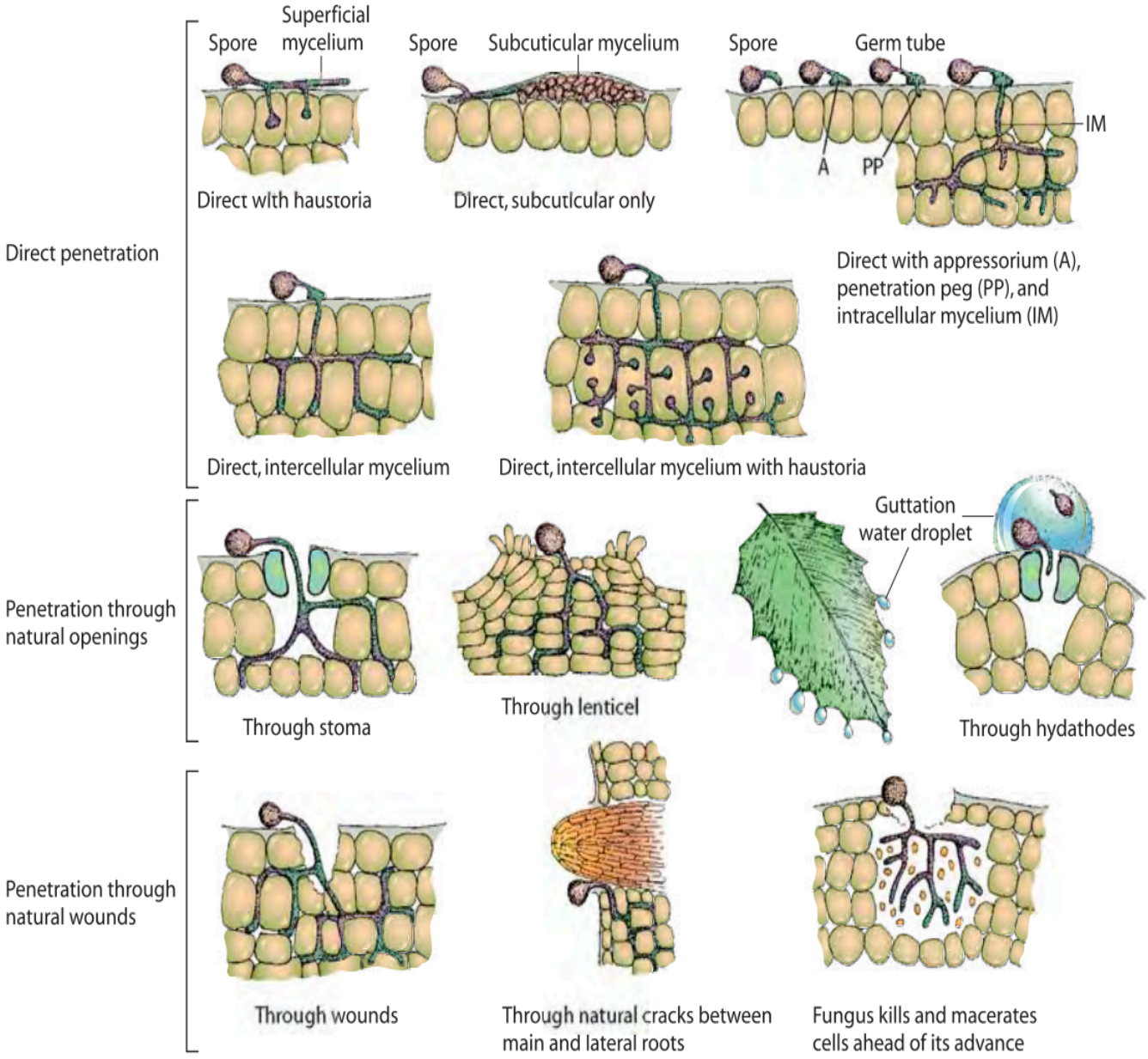

Figure 7: Different approaches and tactics of fungal for invasion and penetration to the host cells.

Source : Agrios, 2005.

1.2.4. Infection

Infection is defined as the phase where the pathogen initiates colonizing the susceptible tissues or cells of the host plant and obtaining its essential nutrients from

the host plant. (Dufresne and Osbourn 2001; Matta and Kerling 1964). Infection and colonization are two simultaneous events of disease development.

The appearance of symptoms is the result of a prosperous infection in the host plant; however, not all of the symptoms appear at the time of infection. The time between inoculation and the emergence of symptoms is called incubation time and varies greatly (from a few days to a few weeks), since it depends on numerous factors and conditions such as the pathogenicity of the pathogen, genetics of host plants, maturity of the plant, environmental factors.

Whereas the pathogen secretes biologically active molecules such as enzymes, hormone and toxins which affect host cell structure and metabolism, the host plant responds with numerous defense mechanisms which end up in different degrees of protection against the pathogen (Fradin and Thomma 2006; Casadevall and Pirofski 1999).

As mentioned earlier, for a successful infection to occur, some conditions must be met that are symbolized by the disease triangle. For example, environmental conditions such as moisture and temperature must be proper for pathogen development or the pathogen must be in a pathogenic phase that can infect the host plant (Agrios 2005; De Wolf and Isard 2007).

1.2.5. Invasion

Pathogens invade host plants in several ways (Figure 7). For example, some fungi invade the xylem vessels of plants as in the case of vascular wilt diseases; they will be confined to these vessels in the roots and stem and only in the final stages colonize other tissues (Bishop and Cooper 1983). Others for example produce mycelium which develops solely within the cuticle and the epidermis cells such as in the case of apple scab (Bowen et al. 2011) , Powdery Mildews (Yarwood 1957).

1.2.6. Colonization

Commonly; colonization means the growth and reproduction of pathogen on or in the infected host's cells and tissues transmission of pathogens among the host plant.
Generally, fungi attack and occupy the tissue of the host plant through growing either on the host surface or into host plant tissues and cells. The fungal infection starts by the colonization of a single cell and then after starts to grow and branch out all over the infected tissue; this cycle will repeat more or less till the fungal scatter all over the host plant; usually, the colonization has different patterns, for example in the fungi which produce vascular wilt disease, when they colonize one vessel for colonizing the adjacent vessel they produce spores and then the spores are transmitted to the next vessel by the means of sap stream, and again in the new vessel cell they germinate and produce mycelium and this cycle will be repeated for colonization of the next vessel cell (Fradin and Thomma 2006).
At the end of the colonization process, the pathogen will reproduce, either sexually or asexually, and the released propagules will start a new infection cycle.

1.2.7. Dissemination of the pathogen

Fungi are which can move short distances on their own and thus can migrate from one host to another one very close to it (Schumann and D'Arcy 2010; Aylor 1986). Their hyphae not only can grow between tissues in contact but also sometimes through the soil toward nearby roots. Both of these means of dissemination, however, are quite limited.
Fungal spores on the other hand can be disseminated over longer distances. They are ejected effectively from the sporocarp or sporophore by a sprinkling or puffing action that results in the successive or simultaneous discharge of spores up to few centimeters above the sporophore (Dietzel et al. 2019; Agrios 2005; Rieux et al. 2014). Spores can then be carried by air, water, insects or other animals, far away from the infected host plant.

Almost all dissemination of pathogens responsible for plant disease outbreaks, and even for disease incidence of less economic importance, is carried out by this way (Dietzel et al. 2019; Rieux et al. 2014).

1.3. Plant resistance and defense reactions

Before or during entering the host, plant pathogens can be perceived by elicitor molecules also called PAMPs (Pathogen-Associated Molecular patterns) or PMAMPs (Microbe-Associated Molecular Patterns). Some elicitors may be constituents of the pathogen cell surface like chitin, chitosan, ß-glucan from which fragments are released by the actions of host enzymes such as chitinase and ß-glucanase, respectively (Sánchez-Vallet, Mesters, and Thomma 2015; Pusztahelyi 2018).

After the introduction of the pathogen into the host plant pathogens may synthesize and release compounds called effectors which aim to weaken the host but will trigger a hypersensitivity response when the host carries a resistance gene which product recognizes the effector (Bu et al. 2014; Mur et al. 2008).

In general, once elicitors and effectors are recognized by the plant, they will induce the transcription of host plant genes that are responsible for different types of the Defense response and thus the pathogen becomes less destructive (T. Nürnberger 1999; Thorsten Nürnberger and Brunner 2002).

Three outcomes are possible:

Host plant compounds early suppress the growth of the pathogen which results in no disease (Nishad et al. 2020)

Host plant detects the pathogen by its elicitors and initiates Defense reaction cascades which results in limitation of pathogen growth and less severe diseases (Q. M. Gao et al. 2015; O'Brien et al. 2012)

Host plant Defense reaction are bypassed or suppressed by pathogen effectors which results in serious disease (Naveed et al. 2020; Thaler, Humphrey, and Whiteman 2012)

It should also be noted that due to genetic changes, pathogens can gain the ability to attack the hosts that previously were immune to the pathogen or vice versa (Jones and Dangl 2006). Despite all of these, each plant species is only susceptible to only comparatively small groups of plant pathogens (Cheng et al. 2013).

1.3.1. The plant immune system

Plants constantly have to cope with attacks from all kinds of pathogens and pests. In this confrontation after infection, they can employ two layers of immunity. The first layer includes the perception of pathogen structures known as Pathogen-associated molecular patterns (PAMPs); since all Microbes are not pathogenic to plants, the term Microbe-associated molecular patterns (MAMPs) is also used (Boller and Felix 2009; Bigeard, Colcombet, and Hirt 2015; de Wit 2007). The MAMP/PAMP perception takes place at plasma membrane level through ubiquitous and conserved receptors which are known as pattern recognition receptors (PRRs)(Sánchez-Vallet, Mesters, and Thomma 2015).

When these receptors detect MAMP/PAMPM in the plasma membrane, they bind and start an active defense response that is known as PAMP-triggered immunity (PTI) that lead to overcome the pathogen (Bigeard, Colcombet, and Hirt 2015; Jones and Dangl 2006).

However, during this constant survival warfare between plants and pathogens, the pathogen in order to overcome plant immunity, evolved new strategies such as secreting some proteins into the cytoplasm which are known as an effector protein, that finally lead to suppress the PTI. This situation is known as effector-triggered susceptibility (ETS) (Naveed et al. 2020).

In response to pathogen effectors, the plants also evolved, and developed receptors that particularly recognize the pathogens' effectors. This is the second layer of immunity which is known as the effector-triggered immunity (ETI) (Jones and Dangl 2006).

ETI is often leads to a hypersensitive response (HR) and subsequently is followed by systemic acquired resistance (SAR) (P. P. Liu et al. 2010).

The nonstop co-evaluation between plant-pathogen stimulates the formation of new effectors on side of the pathogen to suppress the ETI (Boller and Felix 2009). On the other hand, the plant also developed new resistance (R genes) proteins to detect effectors to re-solidate/reestablish the ETI (Boller and Felix 2009).

Together, these four successive stages: detection of MAMPs/PAMPs through PRRs, suppression of PTI though pathogens effectors, recognition of pathogens effectors

through PTI and finally mutual evolution of plants' R genes and pathogens' effectors is known as zigzag model that proposed by Jones and Dangl (2006) (Figure 8).

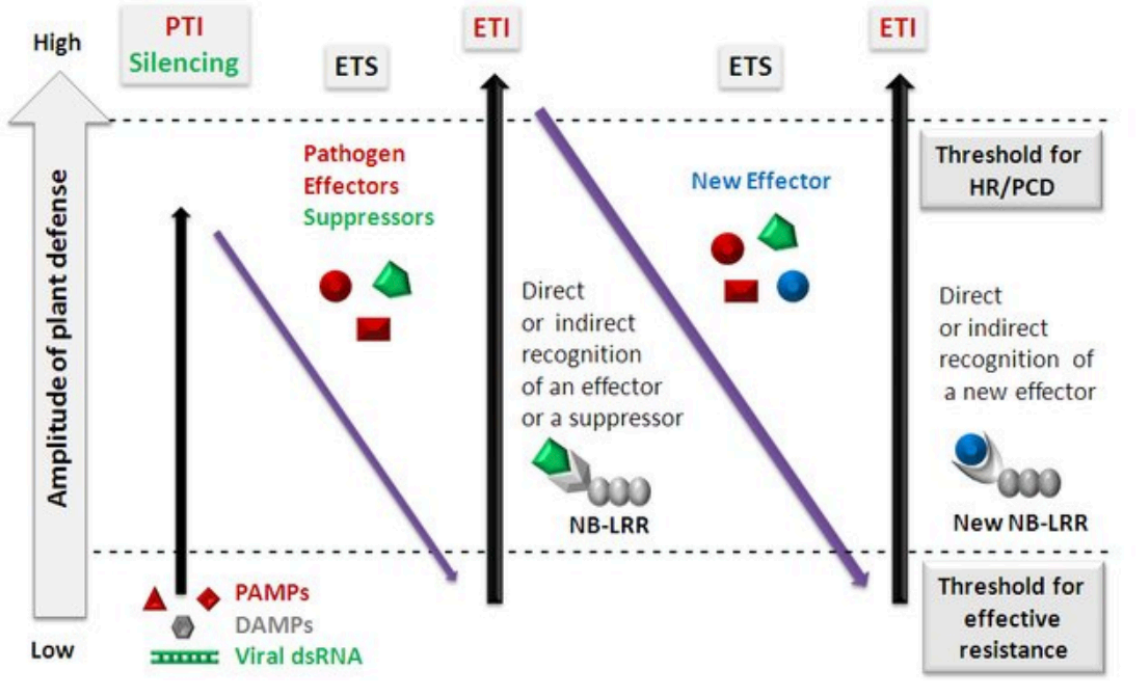

Figure 8: Zig-zag model for evolution of innate immunity.

PAMPs, pathogenesis-associated molecular patterns; PTI, PAMP-triggered immunity; ETS, effector-triggered susceptibility; ETI, effector-triggered immunity; Avr, avirulences; R, resistance proteins; HR, hypersensitive response, NB-LRR: Nucleotide-binding leucine reach repeats.

Source : Zvereva and Pooggin, 2012.

1.3.2. Signal transduction in plant immunity

Upon recognition of MAMPs/PAMPs or effectors, sets of signal transduction cascades pathways in plant cells have been proposed to mediate defense responses.

1.3.2.1. Ion fluxes

Accelerated changes in ion fluxes are reported as an early response of plants' cells. These changes in ion flux include boosted influx of Ca^{2+}, H^{+} (Zimmermann *et al.*, 1999; Lecourieux *et al.*, 2006) and efflux of Na^{+}, K^{+} (Amano et al. 1997). Various

reports suggest that the calcium ion covers two main functions in plant resistance response, including activating other signaling components such as calcium-dependent protein kinases (CDPKs), as well as acting as a second messenger to promote the opening of other membrane channels (Bredow and Monaghan 2019; X. Gao, Cox Jr., and He 2014). Also, extracellular alkalinization as a result of H^+ influx is reported which is detected through several signaling or regulatory pathways (Zimmermann et al. 1999; Mur et al. 2008) *i.e.* induced transcription level of several defense-related genes and production of ROS in potato cells in response to *Phytophthora infestans* (Moroz et al. 2017).

Some studies reported that ion fluxes are particularly involved in synthesis of salicylic acid, reactive oxygen species (ROS) production and phytoalexin production (Mur et al. 2008; Ahuja, Kissen, and Bones 2012; Thorsten Nürnberger and Scheel 2001)

1.3.2.2. Oxidative burst

Expeditious and transient production of ROS such as HO·, H_2O_2, and O_2^- which is known as oxidative burst, also is an early response of plants' cells upon the recognition of MAMPs/PAMPs or effectors (Wojtaszek 1997).

Cell wall peroxidases and plasma membrane NADPH oxidase were reported to be responsible for production of H_2O_2 and O_2^-, respectively (Liszkay, Kenk, and Schopfer 2003; Chisholm et al. 2006; Kámán-Tóth et al. 2019).

It can be said that the ROS are very important molecules in the plant resistance with multifaceted effects. Different roles have been suggested for ROS such as synthesis of salicylic acid (Wrzaczek, Brosché, and Kangasjärvi 2013), expression and regulation of defense-related genes (Herrera-Vásquez, Salinas, and Holuigue 2015; H. Huang et al. 2019) , stimulation and activation of mitogen-activated protein kinase (MAPK) cascades (Son et al. 2011; Jalmi and Sinha 2015),production of phytoalexin (J. Zhao, Fujita, and Sakai 2007), induction of HR, SAR and also contributing to EIT (Jwa and Hwang 2017; Zurbriggen, Carrillo, and Hajirezaei 2010).

1.3.2.3. Activation of MAPK cascades

Mitogen-activated protein kinases (MAPKs) are a class of highly conserved proteins kinase in eukaryotic cells which play a vital role in signal transduction pathways and modulate physiological cell responses toward changes in the environment (Hamel et al. 2012). Activation of mitogen-activated protein kinases (MAPKs) cascades is actually the primary response to PAMPs. The MAPKs cascade involve three-component signal MAPK kinase kinases (MAPKKKs or MAP3Ks), MAPK kinases (MAPKKs), and MAPKs in which an activated MAPKKK activates a MAPKK through phosphorylation and subsequently phosphorylates and activates a MAPK (R. E. Chen and Thorner 2007; Nurnberger et al. 2004). In eukaryotic cells MAPKs cascades contribute in different cell process such as signal transduction and plant/ animal immunity and defense (Thorsten Nürnberger and Brunner 2002). The activation of MAOK cascade during PTI signaling activates WRKY transcription factors, a large family of transcription factors with a WRKY DNA-binding domain. In plants WRKY transcription factors play a vital role in various aspects such as regulation of plant abiotic and biotic stresses tolerance (Ding et al. 2013; Nurnberger et al. 2004), hormone signaling (Dong, Chen, and Chen 2003; Schluttenhofer et al. 2014), primary or secondary metabolism (Devaiah, Karthikeyan, and Raghothama 2007; H. Wang et al. 2007).

Also, MAPKs play an effective role in regulating microtubule dynamics and organization which finally leads to the cytoskeletal reorganization(Samaj 2003).

MICROTUBULE ASSOCIATED PROTEIN 65-1 (MAP 65-1) was the first MAPK-related substrate, its contribution to the regulation of the dynamic of microtubule was reported by the Sasabe and Machida (2006).

1.3.2.4. Plant hormonal signaling

Plants hormones are responsible for nearly all features of plant development and response to the environment.

Extensive studies and analyses have focused on the functions of auxin (IAA), ethylene (ET), jasmonates (JA), and salicylic acid (SA) in the regulation of plant defense

responses toward abiotic and biotic stresses (Alonso and Stepanova 2004; Y. Xu et al. 1994; W. Liu et al. 2003; Chini et al. 2018; Yang et al. 2019).

it is accepted that ET and JA are involved in resistance against necrotrophic pathogens, physical wounding, some phloem feeding insects and herbivores insects, while SA activates resistance towards biotrophic pathogens, hemibiotrophic pathogen and some phloem feeding insects(Okada, Abe, and Arimura 2015; Thaler, Humphrey, and Whiteman 2012). Also, SA contributes to SAR and accumulation of PR proteins (Durrant and Dong 2004).

The mutual interaction and cross talk between phytohormones signaling pathways especially ET/JA and SA allows a very vital and precise regulatory mechanism for plant immunity system (Yang et al. 2019; van Wees et al. 2000; Kunkel and Brooks 2002).

There are several reports on mutual phytohormones' antagonistic effects that contribute to plant defense responses such as antagonistic interaction between the SA and JA signaling pathways (Takahashi et al. 2004; Phuong et al. 2020; Kunkel and Brooks 2002), between the SA and auxin (Kong et al. 2020; D. Wang et al. 2007) and also between SA and JA (Niki et al. 1998).

Considering auxin and plant defense, although there are less studies in comparison to ET, JA and SA, Kazan and Manners (2009) reported that auxin plays a pivotal role in the both plant development and defense, in fact linking development to defense. There are studies that reparteed the role of auxin signaling, synthesis and also transport in plant defense against abiotic and biotic stress (Čarná et al. 2014; Djami-Tchatchou et al. 2020; Grunewald et al. 2009).

1.3.2.5. Expression of Defense Genes

The most important key point for an effective defense against pathogens is the rapid induction and regulation of spatial and temporal expression patterns of specific defense genes. In a transcriptome study of *Arabidopsis* treated with the bacterial PAMP flg22, about 2460 genes were upregulated or downregulated after only 30 minutes; some of these genes contributed to the induction of different protective enzymes, signal transduction and perception, biosynthesis of phytoalexin, hormone signaling (Navarro et al. 2004).

In this transcriptome study a considerable overlap between the tobacco Avr9 race-specific defense response and the Arabidopsis flg22 response was observed, leading to the hypothesis ETI applies the immune system mechanism from preexisting PTI mechanism (Navarro et al. 2004).

Also, Pathogenesis-related proteins (PR) like Thaumatin-like protein, ß-1-3 glucanase, chitinase play a prominent role in defense mechanisms by attacking the pathogen's cell wall (VAN LOON and VAN STRIEN 1999; Viswanathan et al. 2005). These PR are regulated through crosstalk of immune signaling pathways (De Vleesschauwer, Xu, and Höfte 2014; Closkey and Fieldwick 2004; Klessig, Choi, and Dempsey 2018).

I.2. Verticillium Wilt

2.1. Disease and Host range

Verticillium wilt is a vascular disease caused by several species of the fungal genus *Verticillium*. It is categorized as one of the most destructive fungal diseases all over the world (Inderbitzin et al. 2011). Generally, Verticillium wilts are diseases of dicotyledonous plants in temperate, tropic and subtropical regions (Inderbitzin and Subbarao 2014; Pegg and Brady 2002). Although monocotyledons are generally resistant to this pathogen, some species can be hosts for survival structures in superficial root tissue as reported for *V. dahlia* in tulip, onion and others (Fradin and Thomma, 2006; Malik and Milton 1980).

V. dahliae can affect more than 200 host plants from more than fourteen different plant families (Pegg and Brady 2002; Inderbitzin and Subbarao 2014); tomato, eggplant, pepper, potato, peppermint, chrysanthemum, cotton, asters, fruit trees, strawberries, raspberries, roses are some of the economically important crops which are hosts to *V. dahliae*. Other species have a much more restricted host range. *V. alfalfae* has been isolated only from alfalfa (*Medicago sativa*), *V. isaacii* and *V. klebahnii* from artichoke and lettuce respectively (Inderbitzin et al. 2011), *V. longisporum* infects only plants of the *Brassicaceae* family (Fahleson et al. 2003), *V. nubilum* attacks tomato and potato (Ivor Isaac 1953).

In terms of geographical distribution, *Verticillium* is mostly found in temperate regions and then in subtropical regions (Inderbitzin et al. 2011; Hawksworth and Talboys 1970; Pegg and Brady 2002), with some reports of, the presence of Verticillium in tropical regions (Inderbitzin & Subbarao, 2014; Tai et al., 2018).

Economic losses in excess of 50 % have been reported for many high value crops such as alfalfa (H. C. Huang 2003; Pegg and Brady 2002), cotton (Land et al. 2017), Lettuce (Atallah, Hayes, and Subbarao 2011), potato (Atallah et al. 2007), strawberry and tomato (Wilhelm and Paulus 1980).

Verticillium species are soil-borne pathogens that can survive in the soil even in the absence of a host for at least 14 years through resting structures (Wilhelm; S. 1955;

Inderbitzin and Subbarao 2014). Infection of the host is launched through penetration of roots and gradual colonization of the vasculature up into the shoots (Fradin and Thomma 2006). Field symptoms normally consist of tissue necrosis and wilting, usually near the end of the disease cycle that is overlapping with host maturity (BLACKHURST 1963). Up to now, the best approach to control *Verticillium* is soil fumigation but because of environmental concern, this approach has been phased out since 1st January 2005 under the Protocol of Montreal and the Clean Air Act (Enebak 2012).

2.2. Taxonomy

Verticillium is a small genus in the family *Plectosphaerellaceae*, subclass *Hypocreomycetidae*, class *Sordariomycetes* in the phylum *Ascomycota* (Zare 2007; N. Zhang et al. 2006).

The family *Glomerellaceae* (N. Zhang et al. 2006) that harbors *Colletotrichum*, the pathogen which causes anthracnose diseases (Latunde-Dada 2001) is closely related to *Verticillium* (Figure 9).

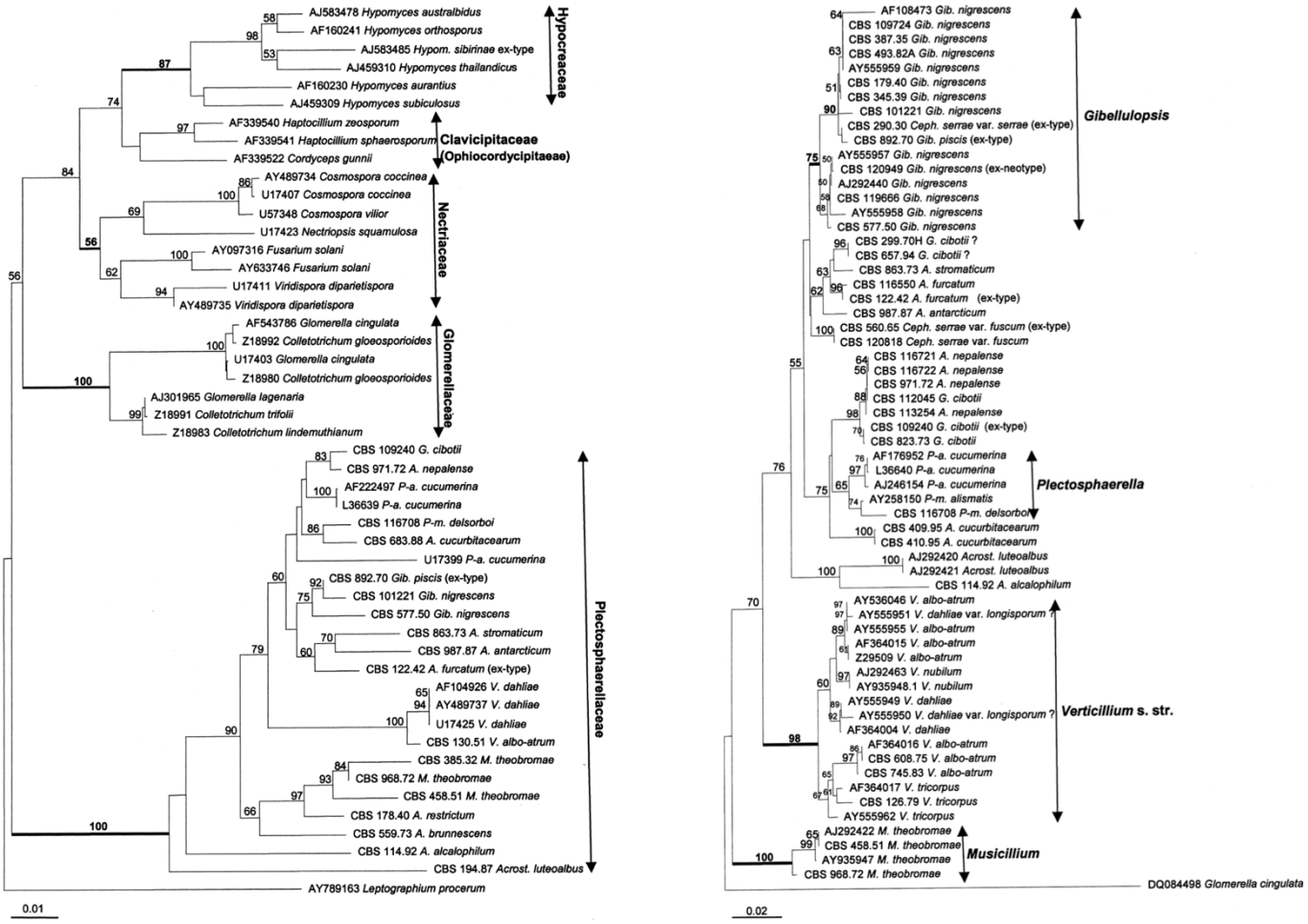

Figure 9: The estimated phylogenetic tree of pathogenic fungi.

sequences used for alignment were Left: nuclear large subunit ribosomal DNA (LSU), Right: ITS operon (ITS1 and ITS2, including the 5.8S gene).

Numbers above branches indicate bootstrap support values. A. = *Acremonium*, Acrost. = *Acrostalagmus*, G. = *Gliocladium*, Gib. = *Gibellulopsis*, P-a. = *Plectosphaerella*, P-m. = *Plectosporium*, M. = *Musicillium*, V. = *Verticillium*.

Source: Zare *et. el.*, 2007

Several agents of vascular wilt diseases can be found among the more distant relatives such as *Ceratocystis fagacearum* (Juzwik et al. 2011) and *Fusarium oxysporum* (Michielse and Rep 2009) belonging to the *Hypocreomycetidae* subclass and *Ophiostoma novo-ulmi* (Brasier 1991) which is placed in the *Sordariomycetidae* subclass. It is supposed that the ability to colonize the xylem and trigger symptoms of vascular wilt has evolved several times in the *Sordariomycetes* class since *Ceratocystis*, *Fusarium* and *Ophiostoma* are not closely related to each other or to *Verticillium*.

Generally, *Verticillium* species are morphologically described by the presence of resting structures and by elongate conidiogenous cells that are organized in whorls (Verticillo) along a vertical axis (Figure 10). However, the use of these features for classification has led to misclassifications, so that some pathogens were included in this group that were completely unrelated as for instance *Musicillium theobromae* a nonvascular wilt pathogen of banana which formerly was known as *Verticillium theobroma*e (Zare 2007; Pegg and Brady 2002).

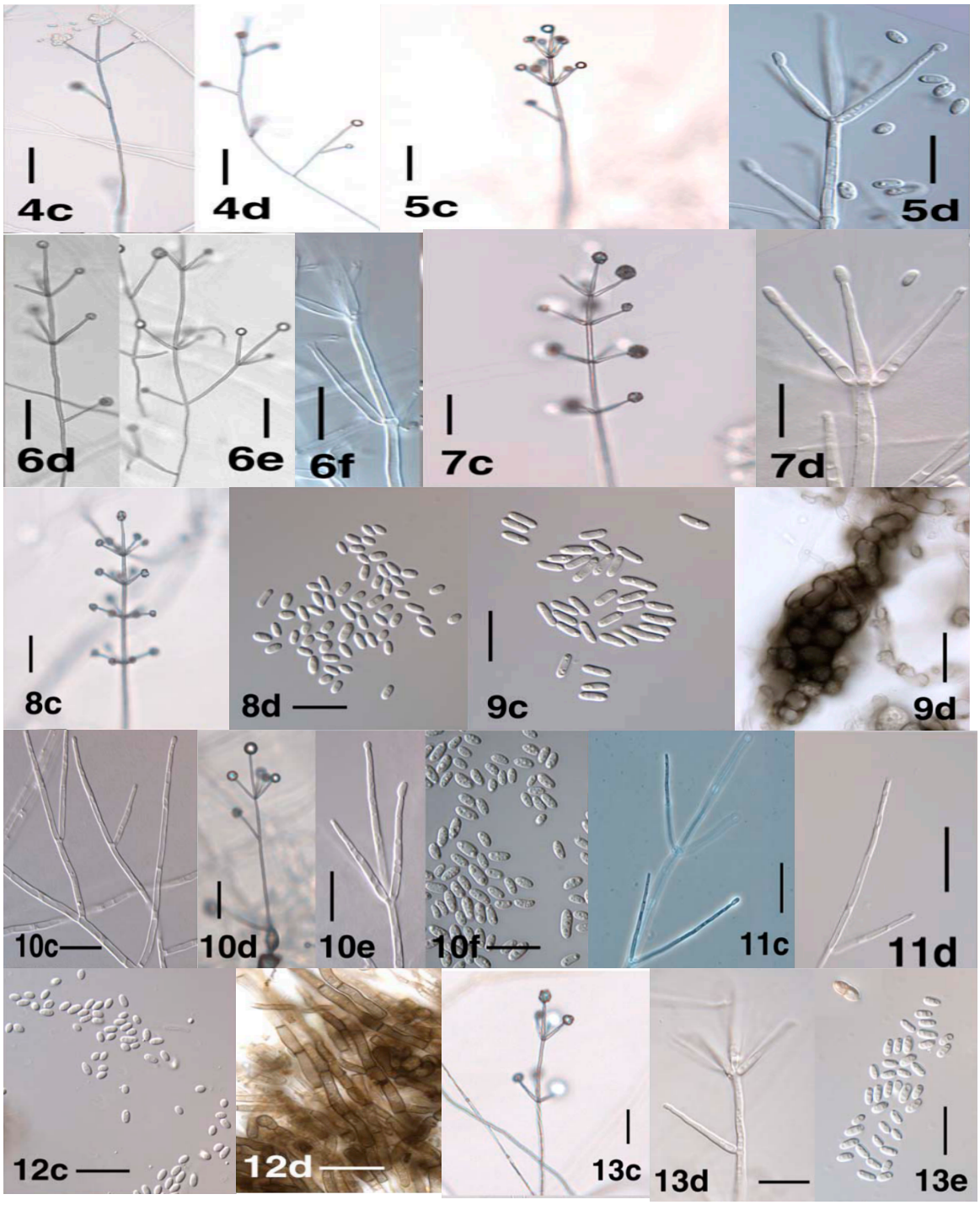

Figure 10- Conidiophores and Phialide of *Verticillium* Species.

4c. Conidiophore of *Verticillium albo-atrum* strain PD748. 4d. Branched conidiophore of *Verticillium albo-atrum* strain PD670. 5c. Conidiophore of *Verticillium alfalfae* strain PD682. 5d. Phialide of *Verticillium alfalfae* strain PD489. Conidiophore of *Verticillium dahliae* strain PD322p. 6e. Branched conidiophore of *Verticillium dahliae* strain PD322. 6f. Whorl phialide of *Verticillium dahliae* strain PD322. 7c. Conidiophore of *Verticillium isaacii* strain PD618. 7d. Phialides of *Verticillium isaacii* strain PD660 as part of an apical whorl. 8c. Conidiophore of *Verticillium klebahnii* strain PD659. 8d. Conidia of *Verticillium klebahnii* strain PD401. 9c. Conidia of *Verticillium longisporum* strain PD348 after 35 days on PDA. 9d. Elongate microsclerotium of *Verticillium longisporum* strain PD356 after 35 days on PDA. 10c. Branched conidiophore of *Verticillium nonalfalfae* strain PD616. 10d. Conidiophore of *Verticillium nonalfalfae* strain PD616. 10e. Phialide of apical whorl of Verticillium nonalfalfae strain PD616. 11c. Conidiophore of *Verticillium nubilum* strain PD621. 11d. Apical phialide of *Verticillium nubilum* strain PD621. 12c. Conidia of *Verticillium tricorpus* strain PD685 after 38 days on PDA. 12d. Resting mycelium of *Verticillium tricorpus* strain PD685 after 38 days on PDA. 13c. Conidiophore of *Verticillium zaregamsianum* strain PD736. 13d. Solitary phialide of *Verticillium zaregamsianum* strain PD733. 13e. Conidia of *Verticillium zaregamsianum* strain PD736.

Adapted from Inderbitzin, P., Bostock, R. M., Davis, R. M., Usami, T., Platt, H. W., & Subbarao, K. V., 2011.

The classification and taxonomy of *Verticillium* have been challenging and full of disagreements (Hawksworth and Talboys 1970). The phylogenetic relationships between *Verticillium* species have been established by the extensive work of Inderbitzin *et al.* (2011) through a multilocus phylogenetic analysis (MLPA). It is now widely accepted that the genus *Verticillium* comprises ten different species. The best known *Verticillium* species, which is the most economically important and widely distributed, is *Verticillium dahliae* (Klosterman et al. 2011; Pegg and Brady 2002). The other species are *V. albo-atrum*, *V. alfalfae*, *V. isaacii*, *V. klebahnii*, *V. longisporum*, *V. nubilum*, *V. nonalfalfae*, *V. tricorpus* and *V. zaregamsianum*. Although they have a less wide distribution and a limited host range, they cause significant annual damage and losses on a global scale (Inderbitzin et al. 2011).
Morphological identification of *Verticillium* species is thus not reliable and the result should be confirmed by DNA sequencing and/or analyses through species-specific PCR assays (Inderbitzin et al. 2013).

2.3. Life Cycle and disease

Verticillium species is a soil-borne pathogen whose life cycle can be divided into three different stages: dormant, parasitic, and saprotrophic (Figure 11). In the dormant stage, the fungus survives in specific structures known as resting structures. Different types of resting structures such as dark resting Mycelium, microsclerotia and chlamydospores can be observed, and each *Verticillium* species harbors one or more than one type of these resting structures (Barbara and Clewes 2003). Protecting the fungus against harsh conditions and keeping it viable is their most important task. For instance it is reported that some chlamydospores and conidia can be viable more than 22 years (Devine and Dikeman 2014). More specifically *V. dahliae* microsclerotia can retain viability up to 14 years (Schnathorst 1981; Short et al. 2015).
The resting structures germinate under the influence of root exudates in the rhizosphere of host plants (MOL, SCHOLTE, and VOS 1995), and emerging hyphae can cross a short distance to get in contact with their potential hosts. They penetrate the plant through the root tip, root elongation area or the regions where lateral roots emerge and grow straight towards the stele. This is the beginning of the parasitic stage

(Bishop and Cooper 1983). Vascular infections are successful only when the endodermis has not been developed well or where the endodermis has been damaged (Pegg and Brady 2002). After penetration into the central cylinder, the fungus enters the vascular system where it forms conidia. The conidia are transported through the sap stream and stopped at vessel end walls or in pit cavities which are known as trapping sites. To overcome trapping sites, they have to germinate, and the hyphae will penetrate into the next adjacent vessel and sporulate to continue the colonization process (Bishop and Cooper 1983). Masses of fungal hyphae and conidia in the colonized xylem vessels, along with the secretion of material produced by the plant with the aim of suppressing *Verticillium* growth result in clogging of the xylem and affect water transport. Finally, this causes a decrease in respiration and photosynthesis (Hampton, Wullschleger, and Oosterhuis 1990), and lastly wilting. In addition, the *Verticillium* species secrete several toxic compounds such as LysM or necrosis and ethylene-inducing-like protein (NLP) (Klosterman et al. 2011). NLP is responsible for rapid tissue necrosis induction and, as LysM, leads to reduction or inactivation of plant host immunity (Oome et al. 2014; Kombrink and Thomma 2013). The time required for symptoms to appear varies depending on the *Verticillium* species and the host plant and on environmental conditions.

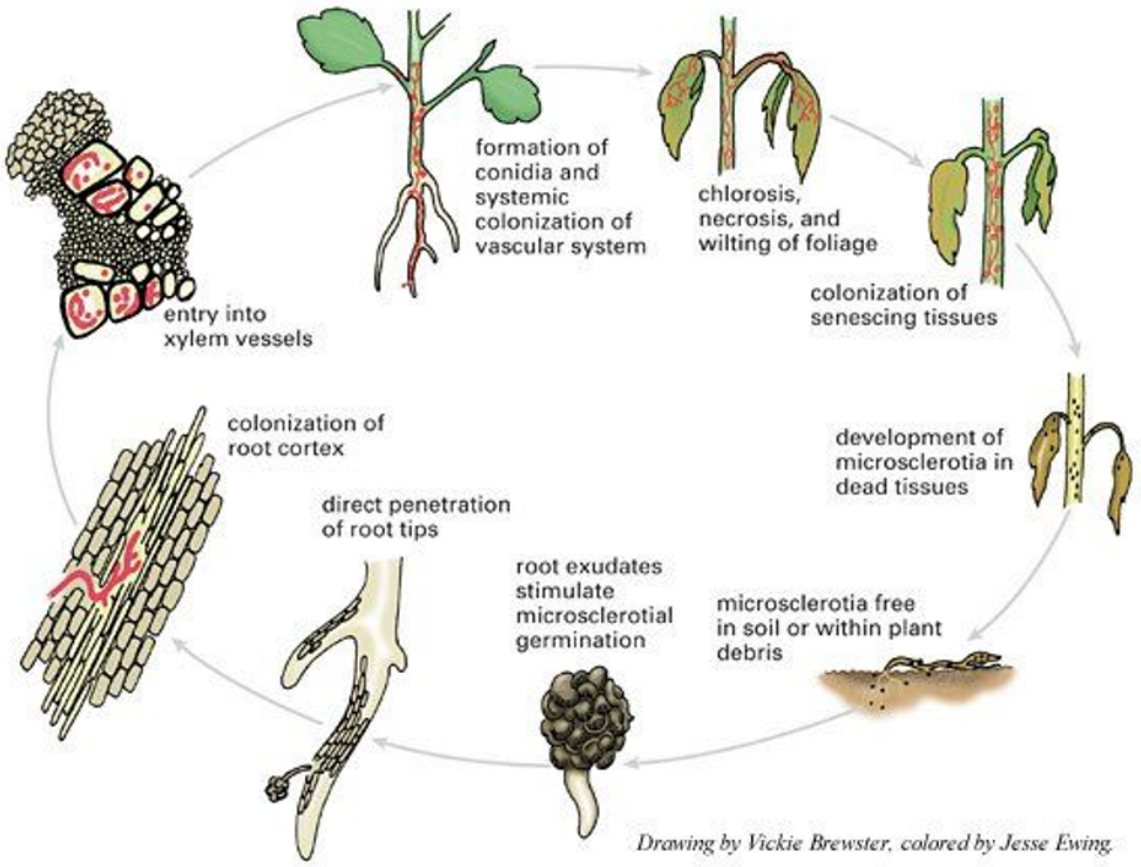

Figure 11: ***Verticillium*** **Spp. disease cycle.**

Source: Berlanger and Powelson, 2000.

The saprophytic stage begins during and after plant senescence. At this stage, all parts of the host plant are heavily colonized. Resting structures are formed within the infected plant and can be dispersed through the plant decomposition into the soil and start a new cycle of disease (Fradin and Thomma 2006).

2.4. *Verticillium* Genomics

The *Verticillium* sequencing project is part of the Fungal Genome Initiative at the Broad Institute of Harvard and MIT. The aim was to release 7X genome sequence coverage for V. dahliae (strain VdLs.17) and 4X coverage for V. alfalfae formerly V. albo-atrum (strain VaMs.102) (Klosterman et al. 2011). The *Verticillium* comparative genomics database can be accessed and is available for download (https://www.broadinstitute.org/scientific-community/science/projects/fungal-genome-initiative/*verticillium*-comparative-genomics-pro). All genomes were produced through a shotgun approach and Sanger sequencing (Klosterman et al. 2011).

The Comparative genome statistics of *V. alfalfae* and *V. dahliae* are shown in (Table 1).

The read data of *V. dahliae* (Ls.17) DNA sequence was assembled into scaffolds, which were positioned onto chromosomes by comparing them to an optical map (Schwartz et al. 1993) prepared at ~300X physical coverage with restriction enzyme AflII. The map revealed that, similar to *V. alfalfae*, *V. dahliae* (Ls.17) harbored eight chromosomes (Table 1)(Klosterman et al. 2011).

Table 1: Comparative genome statistics of *V. alfalfae* and *V. dahliae*.

Assembly statistics	***V. dahliae* – VdLs.17**	***V. albo-atrum* – VaMs.102**
Total contig length (Mb)	32.9	30.3
Total scaffold length (Mb)	33.8	32.8
Average base coverage (Fold)	7.5	4
Quality score (% Q40)	95.21	84.58
N_{50} contig (kb)	43.31	14.31
N_{50} scaffold (Mb)	1.27	2.31
Linkage groups	8	Nd*
GC-content (%)	55.85	56.06
Protein-coding genes #	10,535	10,221
tRNA genes	230	223

*Nd – No data # Protein-encoding genes were annotated using a combination of manually curated genes, in addition to EST BLAST alignments, and *ab initio* gene predictions made by FGENESH, FGENESH+ (http://linux1.softberry.com), and GENEID (http://genome.crg.es/software/geneid). Additionally, protein-encoding genes were predicted based on BLASTs of known genes available in public databases. BLAST matches with E values<1e-10 were considered to be usable BLAST evidence. HMMER [90] searches were also performed using the Pfam library to find Pfam domains on six-frame translations of the genomic sequences.
doi:10.1371/journal.ppat.1002137.t001

Source: Klosterman et al.,2011.

Out of 52 scaffolds of *V. dahliae* (Ls.17) 30 were successfully positioned on the chromosomes (Figure 12). No optical map is available for *V. alfalfae*, Because of the high sequence identity between *V. alfalfae* VaMs.102 and *V. dahliae* Ls.17 (92% identity), the genome of *V. alfalfae* VaMs.102 was assembled into 26 scaffolds using *V. dahliae* Ls.17 as a reference (Klosterman et al. 2011).

Although the genome assemblies of *V. alfalfae* VaMs.102 and *V. dahliae* Ls.17 were highly similar in length, the alignment between these two species disclosed the presence of four regions in *V. dahliae* Ls.17 of 300–350 kb each that were absent in *V. alfalfae* VaMs.102 (Klosterman et al. 2011) (Figure 12). These four regions were named lineage-specific (LS) regions LS1 to LS4 and their size is highly variable among different *V. dahliae* strains (Klosterman et al. 2011). The LS regions harbor genes with putative or known functions in pathogenicity and virulence. The best known is *Ave1* encoding the effector and race determinant of *V. dahliae* which is localized in the LS3 region (de Jonge et al. 2013).

The number of predicted protein-encoding genes were estimated 10,221 and 10,525 for *V. alfalfae* VaMs.102 and *V. dahliae* Ls.17, respectively (Table 1) (Klosterman et al. 2011). These estimations are in perfect match with other plant pathogens in the *Sordariomycetes* class such as *Neurospora crassa* with 10,082 genes (Galagan et al. 2003) or *O. ulmi* with 8,639 genes (Khoshraftar et al. 2013).

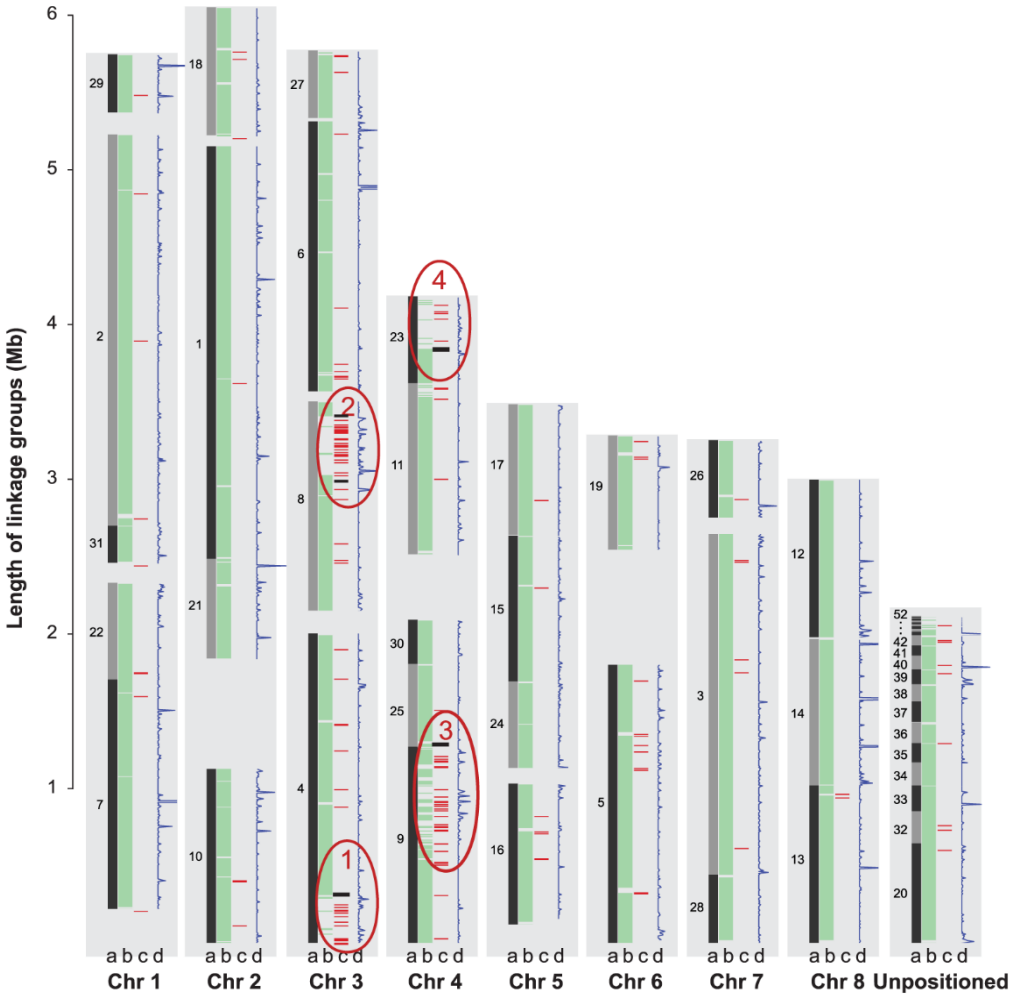

Figure **12**: **Global view of syntenic alignments between *V. dahliae* (Ls.17) and for *V. alfalfa* (Ms.102).**
Vd linkage groups (black bars) are shown as the reference, and the length of the light grey background to the left of each linkage group (in the scale of Mb) is defined by the *Vd* optical map. For each chromosome, column **a** represents the *Vd* genomic scaffolds positioned on the optical linkage groups separated by scaffold breaks. Scaffold numbers are adjacent to the blocks; column **b** displays the syntenic mapping of *Vaa* scaffolds; column **c**, color red shows the density of transposable elements calculated with a 10 kb window; and color black represents the AT-rich regions; column **d** represents the density of ESTs calculated with a 10 kb window. Four LS regions that lack similarity to the genome of *Vaa* but are enriched for TEs are highlighted in red ovals and numbered as LS1, 2, 3, and 4. https://doi.org/10.1371/journal.ppat.1002137.g004

Source : Klosterman et al., 2011.

I.3. Legume plants

3.1. Legumes and their role in agronomy

Legumes are a highly popular crop for farmers and consumers; they are regarded as the second most important family of crop species after grasses (C. A. Watson et al. 2017).

Legumes is the generic name for members of the Fabaceae family (Leguminosae). This family comprises 800 genera and 20,000 species (Lewis et al. 2005; Stagnari et al. 2017) and corresponds to the third largest family of flowering plants. Table 2 represents the taxonomy of legume plants.

Table 2: The Taxonomy of the Legume plants.

Kingdom	Plantae – plantes, Planta, Vegetal, plants
Subkingdom	Viridiplantae – green plants
Infrakingdom	Streptophyta – land plants
Superdivision	Embryophyta
Division	Tracheophyta – vascular plants, tracheophytes
Subdivision	Spermatophytina – spermatophytes, seed plants,phanérogames
Class	Magnoliopsida
Order	Fabales
Family	Fabaceae – peas, legumes

(https://www.itis.gov/servlet/SingleRpt/SingleRpt?search_topic=TSN&search_value=183623#null)

Legumes are widespread across the world, cultivates species occupy 12–15% of available arable land (Ferguson et al. 2010) but mainly they are found in mild to cold regions (L. Watson and Dallwitz 1996). According to the FAO annual Reports, legume production (pulses) was estimated more than 89 million tons (https://www.fao.org/faostat/en/#compare) in 2020 around the world (Figure 13).

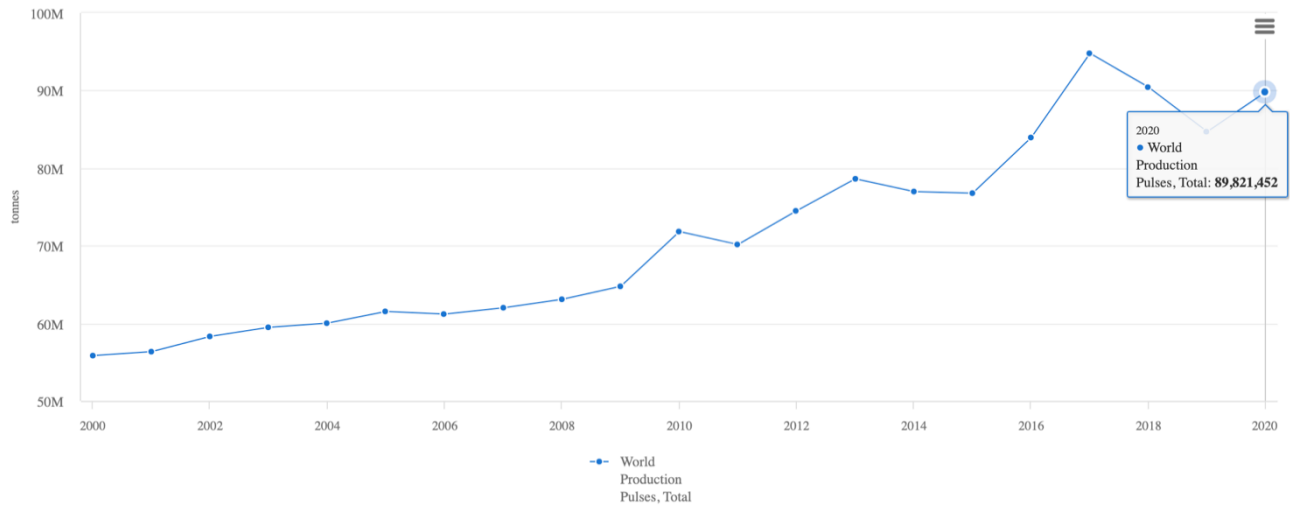

Figure 13: Annual statistics of leguminous production in the last decade.

Source : https://www.fao.org/faostat/en/#compare

Legumes offer several central performances like

1. at food-system levels: Legumes are considered as a valuable and low priced source of high-quality protein (Graham and Vance 2003; Tharanathan and Mahadevamma 2003; Stagnari et al. 2017). Pulses (grain legumes) such as bean, pea, chickpea, soybean are widely used as food for humans, and forage plants such as alfalfa, vetch or trefoil, as well as byproducts of pulses (e.g. soybean meal) are essential components of animal feed (Siddique et al. 2012). Combinations of legumes and monocots have been found suitable for pastures due to their superior yield and quality (Gultekin et al. 2021; Catalano et al. 2015).
2. At cropping-system levels: Generally, grain legumes are not susceptible to the same pests and diseases as the main cereal crops (Zander et al. 2016) and also they assist in weed controlling (Seymour et al. 2012). These features lead them to be suitable as break crops in wheat-based rotations, to break the cycles of pests and diseases. (Jensen, Peoples, and Hauggaard-Nielsen 2010; Köpke and Nemecek 2010; Stagnari et al. 2017).

3. At the production-system level: Due to their symbiosis with nitrogen-fixing rhizobia, legumes do not need nitrogen fertilizers. This makes them extremely suitable for incorporation in low input cropping systems like organic farming, moreover they have a firm role in mitigating greenhouse gases emissions due to the reduced application of animals' manure and subsequently, nitrogen runoff (Lemke et al. 2007; Lötjönen and Ollikainen 2017). In addition, a part of the fixed nitrogen is secreted into the rhizosphere improving soil fertility. Some of the associated rhizobia also improve P accessibility. Latati *et. al*. (2016) reported an increase in the availability of P at rhizosphere level in intercropping cowpea–maize in comparison to sole maize cropping. Due to their high seed oil content legumes such as soybean and *Pongamia pinnata* (*Millettia pinnata*) have gained considerable attraction as future biofuel sources (Ferguson et al. 2010; P. T. Scott et al. 2008). These cases illustrate the importance of legumes in agronomy and sustainable agriculture, and in order to achieve the ultimate goals of sustainable agriculture (protection of the environment, expansion of the natural resource base of earth, and preserve/improve soil fertility), more attention to this plant family in agricultural research seems vital.

3.2. The genus *Medicago*

Medicago is a genus of annual flowering plants with the presence of trifoliate leaves as one of the main features. Medicago covers at least 87 species, some of them autogamous and some out-crossing. In a study applying Fluorescence In Situ Hybridization (FISH) Rosato *et al.* (2012) reported that the number of chromosomes in *Medicago* varies from 2n = 14 to 48. Alfalfa (*Medicago sativa*) is the most famous species of this genus (Gholami et al. 2014) due to its agricultural value.

Medicago originates from the eastern Mediterranean region (from northwestern Iran to Azerbaijan) (Westgate 1908) and was introduced to Europe by Darius the Great (550 – 486 BC), where it began to spread during the time of the Roman Empire (Mikaili and Shayegh 2011). The most favorable condition for Medicago species growth are cool temperature (between 11.7 and 21.1 °C) and short photoperiod (Quiros and Bauchan 2015; Ahmed, Durand, and Escobar-Gutiérrez 2019).

3.2.1. Alfalfa (*Medicago sativa*)

Alfalfa (*Medicago sativa* L.) is the most productive and widely grown forage legume. It is a high-quality, long-lasting and productive legume adapted to both hay and grazing (Casler and Undersander 2018).

Alfalfa is a perennial, outcrossing, autotetraploid species (2n = 32) with a large genome. Morphologically it is an erect plant with main stems arising from a large crown. Branches also occur from axillary buds on the stems (Figure 14). *Alfalfa* has a strong, deep taproot that makes it well adapted to any soil condition. It has a good tolerance to cold and freezing, although, may get damaged in cold, open winters (Casler and Undersander 2018; Pennycooke, Cheng, and Stockinger 2008; Adhikari et al. 2021). Among all forage crops, alfalfa has the highest nutritive value (Gashaw 2016). In addition combining alfalfa with other forage crops increases the yield ratio as well as the crude protein content of the produced crops (Popp et al. 2000; Capstaff and Miller 2018).

Figure 14: The close up a *Medicago sativa* in the field and its morphology.

Source : https://www.tropicalforages.info/text/entities/medicago_sativa.htm

Alfalfa is usually planted in the fall or spring season on well-drained soil with a neutral pH (6.8 – 7.5) and a constant amount of Phosphorus and potassium (Undersander, D., Cosgrove, D., Cullen, Ei., Grau and Rice, M. E., Renz, M., Sheaffer, C., Shewmaker, G., Sulc 2011). It is harvested three to four times a year (Undersander, D., Cosgrove, D., Cullen, Ei., Grau and Rice, M. E., Renz, M., Sheaffer, C., Shewmaker, G., Sulc 2011) but in some regions harvests are possible up to 7 times per a year (Ferreira et al. 2015)

The annual average yields are commonly around 20-35 tons per hectare ("National Alfalfa & Forage Alliance" 2019).

Alfalfa was called Medic in Latin, a name that invoked the Medes (ancient Iranian citizens) (Bilello 2016), and evolved later to Medicago. Within the sixteenth century, it was introduced into the American continent (Westgate 1908).

3.2.2. Barrel medic (*Medicago truncatula*)

Medicago truncatula (Barrel clover, barrel medic, barrel medick, strong-spined medic, Caltrop medic, Cylindrical bur medic or truncated alfalfa) (Affouard et al. 2020) is a small annual legume originating from the Mediterranean regions (Garmier et al. 2017). It is a wild plant but also a forage crop for pastures in Australia (Rose 2008; Garmier et al. 2017). *M. truncatula* presents a high level of synteny with other important legumes such as alfalfa, pea, soybean, and *Lotus japonicus* (Figure 15) (Nevin Dale Young, Mudge, and Ellis 2003; Frugoli and Harris 2001; Choi et al. 2004).

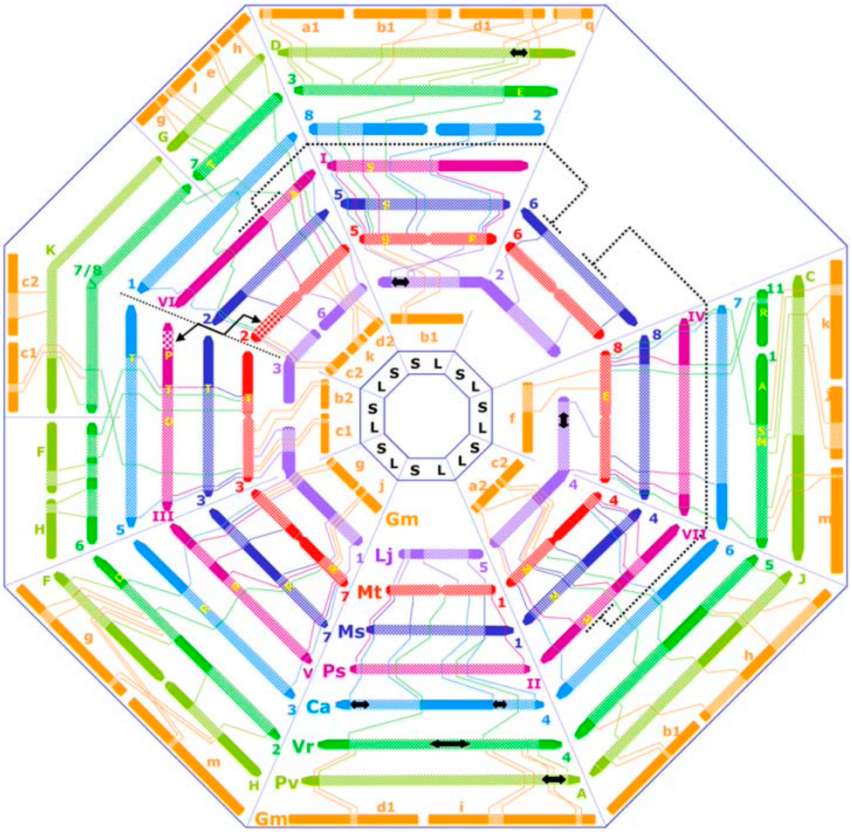

Figure 15: Synteny between *M. truncatula* and seven other important legume species.

Mt, *M. truncatula*; Ms, *M. sativa*; Lj, *L. japonicus*; Ps, pea; Ca, chickpea; Vr, mung bean; Pv, common bean; Gm, soybean. Syntenic blocks are illustrated to scale based on genetic distance.

Source: Zhu *et. al.*,2005.

Due to its small genome size (~ 450 Mbp), diploid genome (2n = 16), high self-fertility, high level of natural diversity, short generation time and high transformation efficiency it has been established as model species for legume plants (Frugoli and Harris 2001; N. D. Young et al. 2011; Kang et al. 2016).

M. truncatula is a semi prostrate plant with ascending low growing stems to 10- 60 cm high with trifoliate leaves while each leaflet is rounded, 1-2 cm long, sometimes with a dark spot in the center. The flowers are yellow and produced individually or in small inflorescences of two to four flowers. The fruits are small pods in barrel-shaped format and mature pods are light yellow to dark in color (Figure 16) (Moreau 2006; Barker et al. 1990; Kamaté et al. 2000)

Figure 16: Morphological characteristics of leaves, flowers, pods and seeds of *Medicago truncatula*.

Source: https://legumeinfo.org/organism/Medicago/truncatula

M. truncatula includes many different accessions adapted to the diverse environmental conditions of their growing sites. Pure lines were obtained after selfing under controlled conditions. Within the collection of several hundred lines, Jemalong A17, derived from the Australian cultivar Jemalong is the reference line (Barker et al. 1990; Garmier et al. 2017) and had been used as the fixed parental line in most crosses to obtain RILs populations (Figure 17). Its complete genome sequence was obtained by an international consortium with funding from the US National Science Foundation (NSF) and the European Sixth Framework Program (FP6) starting in 2003. Chromosomes 1, 2, 4, 6, 7 and 8 were sequenced by the United States, chromosome 3 by the United Kingdom (European and Biotechnology and Biological Sciences Research Council - BBSRC- funds) and chromosome 5 was done by France (European funds and INRA), through the Sanger method (N. D. Young et al. 2011).

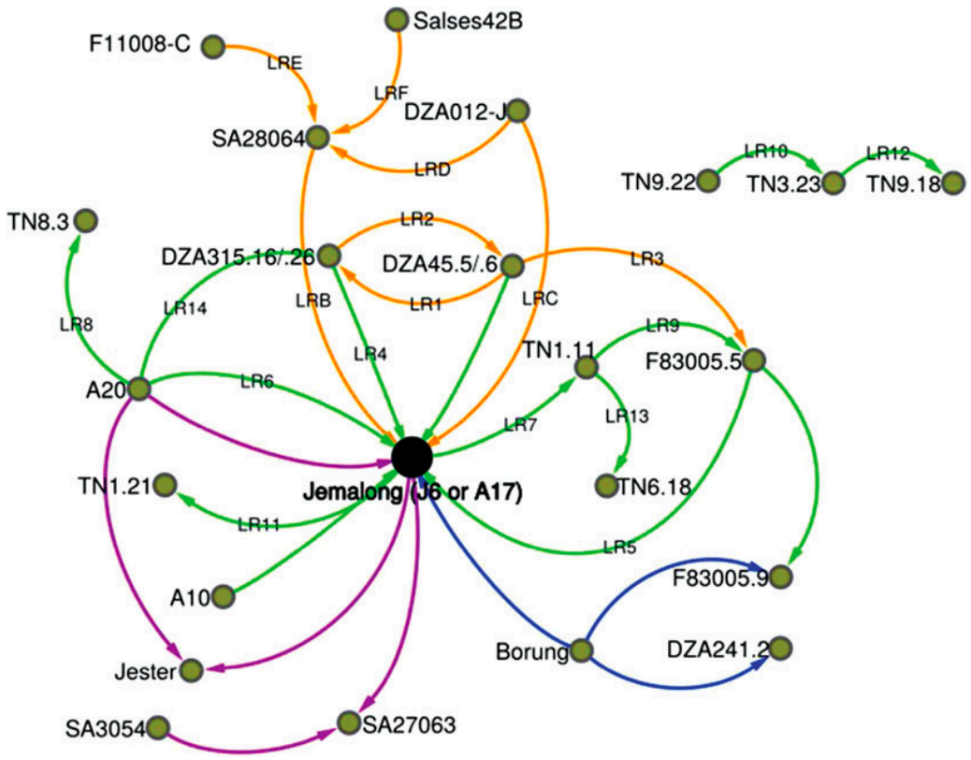

Figure 17: Schematic representation of crosses to obtain the different RIL populations (LR) of Medicago truncatula.

Purple lines: crosses done by Australian groups; Orange lines: crosses done by INRAe Montpellier; Blue lines: crosses done by INRAe Rennes; Green lines: crosses done by University of Toulouse/CNRS/INRAe.

Source : Garmier *et. al*, 2017.

Since preliminary studies on the genome of *Medicago truncatula* showed that most of its genes were located within the euchromatic regions of the arms of the chromosomes and that they were rather absent from the heterochromatin (Kulikova et al. 2001); the sequencing project targeted the euchromatin portion of the *Medicago truncatula* genome (i.e. between 280 and 300 Mb).

The Mt3.5 version of the *Medicago truncatula* genome released in 2011 was obtained and assembled using the six A17 BAC and one fosmid libraries (N. D. Young et al. 2011). By sequencing mainly through the Sanger paired-end sequencing method 2,536 BACs (Bacterial Artificial Chromosomes), 246 Mb were assembled by overlapping of the BACs while 104.2 Mb were not anchored in the pseudomolecule and were sequenced by Illumina sequencing technology at a depth of 40X. Nearly 94% of the genes expressed were sequenced, *i.e*. 62,388

genes predicted by the IMGAG consortium using the EuGene pipeline including 14,322 annotated genes (Foissac et al. 2008; Tang et al. 2014; N. D. Young et al. 2011).

In 2014, the new genome assembly of *Medicago truncatula* (Mt4.0) incorporates sequences obtained by the Illumina (>50X), Sanger and Roche 454 sequencing methods and was made from the genetic map of the RILs population LR4 (A17xDZA315 .16), developed within our laboratory. This new assembly made it possible to anchor 75.8 Mb of the 104.2 Mb not anchored in the Mt3.5 version: the total length of the genome obtained is 384.5 Mb (i.e. an anchoring of 93% of the sequences against 71% for the Mt3.5 version). The annotation of this genome was carried out using the EVM and MAKER pipelines, and made it possible to highlight the presence of 50,894 genes, i.e. 82% of the annotated genes on the MT3.5 version of the genome (31,661 genes at high confidence and 19,233 low confidence) (Figure 18) (Tang et al. 2014).

In 2018, to further improve the genome assembly Mt4.0, high-depth (> 100X) long-read (PacBio) sequencing, as well as previous and new technologies such as BioNano technology optical maps were used. By his way, a highly contiguous reference genome of 430 Mb was generated in only 64 sequence contigs (including 3.59 Mb in 32 unanchored contigs) that was termed Mt5.0.

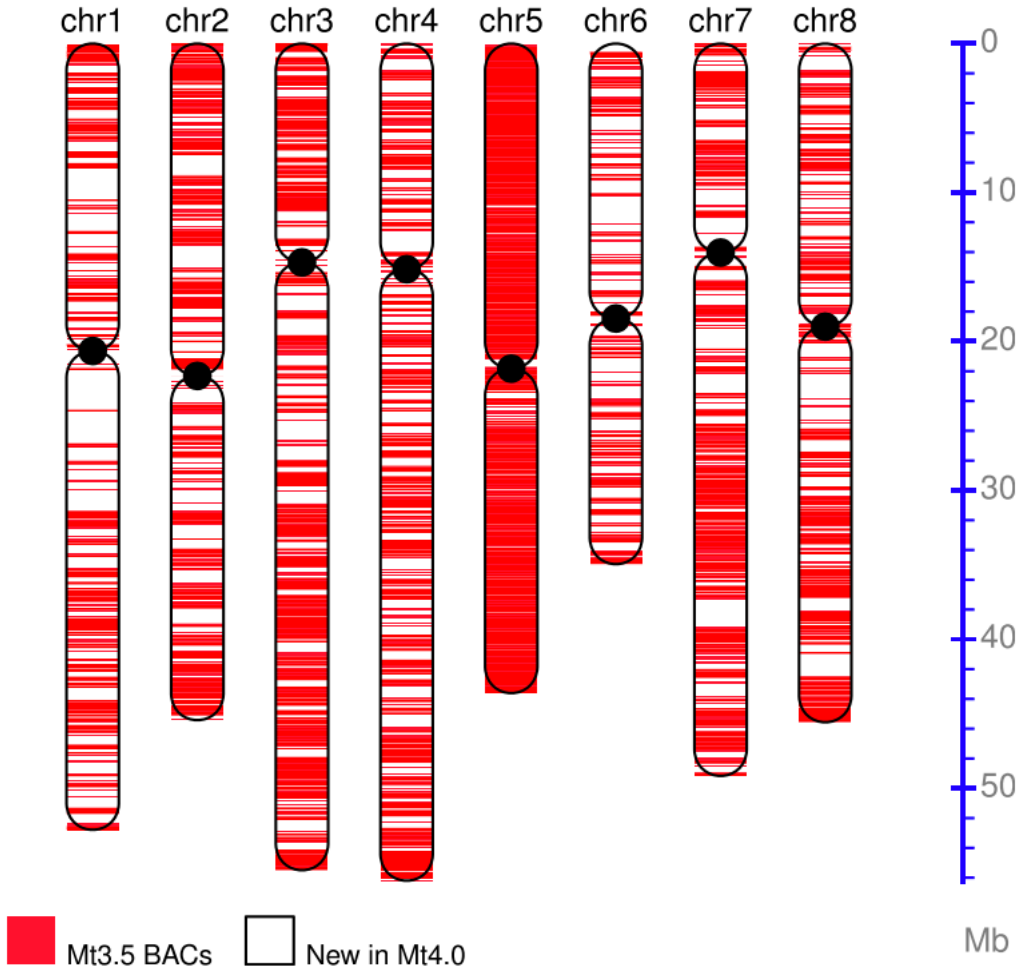

Figure 18: *Medicago truncatula* genomic sequence Mt4.0 compared to Mt3.5 in term of increased amount of chromosome-anchored sequences.

Red-colored segments of the chromosomes represent BAC sequences used in Mt3.5 and the white areas on the chromosomes represent newly anchored sequences in Mt4.0.

Source : Tang *et. al.*, 2014.

I.4. Genetic and Genomics approaches to study Plants' resistance

4.1. Gene mapping: QTL detection and GWAS

Generally, the approaches for mapping genes on chromosomes are based on two types of methods, family mapping and population mapping (Stram 2014).In family mapping, populations are obtained by crossing two homozygous lines which are used for Quantitative trait loci (QTL) mapping studies (Slate 2005). So, these populations are closely related families which arise from common parents using particular mating patterns (Myles et al. 2009).

In the population mapping approach, broadly known as association mapping (AM) diverse sets of individuals from different natural populations are chosen as the mapping population. These populations may also be considered as groups of several small families for example even as small as one individual per family. Since association mapping uses Linkage disequilibrium (LD) between molecular markers and the quantitative trait loci (QTL)/ genes for detecting marker-trait associations, it is also known as LD mapping. Genome-Wide Association study (GWAS) or Whole Genome Association Study (WGAS) relies on sequence information provided by genomics (Ogura and Busch 2015).

The association mapping approach was developed by human geneticists to find genetic risk factors for human disease. These genetic factors then can be used to predict who is at risk for a certain disease, to understand the biological aspects of diseases in order to develop treatments and also to introduce new prevention strategies (Bush and Moore 2012). The first reported GWAS dated back to 2002 in which human geneticists found two significant SNPs associated with susceptibility to myocardial infarction (Ozaki et al. 2002).

Subsequently, association mapping was introduced to plant genetics and the first report related to plant GWAS was published in 2005, about the resistance of *Arabidopsis thaliana* towards the bacterial pathogen *Pseudomonas syringae* (Aranzana et al. 2005).

Since LD analysis exploits all the possible recombination events that have happened between the different genes and the molecular marker loci within the population, the association mapping approach is able to detect markers much closer to the genes of interest in comparison to conventional linkage mapping that uses only the recombination events occurring after the mating of two selected parents (Ruggieri et al. 2014).

Although by comparing Association mapping and conventional linkage mapping, we find more advantages on the association mapping side this is not always the case and there are still some advantages with linkage mapping (Table 3).

Table 3: A comparison between linkage and association mapping approaches.

Feature	Linkage mapping	Association mapping
QTL effect size	Effective for moderate to large effect QTLs; ineffective for QTLs with small effect size	Effective for QTLs with much smaller effect size than in linkage mapping
Effectiveness with low allele frequencies	Effective [a]	Ineffective
Number of alleles detected per locus	Only two alleles can be detected	All the alleles present in the sample are detected
Type of information on marker alleles used for mapping	Information on identity by descent	Current approaches use information on identity by state
Need for QTL result confirmation/validation	Confirmation as well as validation required	Often confirmation is done by replication studies
Populations used for mapping	Produced by crossing selected parents	Natural populations, breeding materials, germplasm lines, lines produced from multiple crosses
Recombination events exploited	Those occurring after the crosses are made	All the recombination events that occurred since the LD was created
Identified markers linked to QTL/gene	Few to several centimorgans (cM) away from gene/QTL	Much closer than those by linkage mapping
Mapping based on	Recombination frequency between the loci	Linkage disequilibrium (LD) between the loci
Familial relatedness	Minimized by controlled crossing	Minimized by kinship coefficient estimation and its use in association mapping
Population structure	Minimized by controlled crossing	Minimized by estimation of *Q* or *P* and its use in AM
Feasibility in different species	Feasible in annual and biennial species, not feasible in perennial species	Feasible in annual, biennial, and perennial species
Integration of QTL discovery with breeding	Novel breeding schemes proposed for the purpose	Integration feasible when breeding materials are used for AM
Number of markers needed to cover the whole genome	Low (10^2) to moderate (10^3)	High (10^5 for small genomes) to very high (10^9 for large genomes)
Conclusions applicable to	The concerned populations unless validated in other materials	The concerned species or subspecies

[a] Allele frequencies increase as a result of biparental crosses

Source : Singh BD and Singh AK.2015.

4.2. The Steps of the Association mapping Procedure

Generally, the association mapping approach involves different steps

1. Collecting association mapping population
2. Genotyping population
3. Phenotyping
4. Association mapping analysis

4.2.1. Collecting association mapping populations

A successful association mapping needs a large random sample from a natural population, a core collection that could involve double haploids, backcrosses, recombinant inbred lines, and near isogenic lines of the concerned species (Al-Maskri, Sajjad, and Khan 2012).

The existence of the greatest possible genetic diversity in the association mapping population is the most important feature of this collection (the more variety, the more success in association mapping) (Basak, Uzun, and Yol 2019). Association panel, association mapping panel are the other synonyms which are used for association mapping populations in the literature.

4.2.2. Genotyping

Having a good, precise, and comprehensive collection of genotyping datasets from the association panel is critical for association mapping. Currently, the development of High-throughput genotyping approaches, such as Next Generation Sequencing (NGS), Genotyping-By-Sequencing (GBS), and other approaches, have boosted the ability to collect huge genotyping datasets just in a short period which enables scientists to focus on further studies of important economic plant traits (Pavan et al. 2020). Single Nucleotide Polymorphisms (SNPs) introduced through point mutations (Z. J. Liu and Cordes 2004) are among the markers predominantly used in genotyping

approaches because of benefits such as their high abundance in the genome and their occurrence throughout the entire genome (noncoding regions and coding regions of the genome) (Wenne 2018; Z. J. Liu and Cordes 2004). After preprocessing of genotyping data such as filtering based on quality control, concatenating the reads to create a map (for each individual accession in the association panel) and finally aligning with the reference genome, the map is ready to use for calculating and highlighting genomic derived features such as allele frequency, SNPs and tag-SNPs in the population, haplotype blocks, Linkage disequilibrium (LD), population structure (Matrix Q) and Kinship (Matrix K). A collection of different associated SNPs that always occurs together along the same chromosome is called a haplotype (Manfred Schwab 2011; Morton 2005) which are very helpful and a key concept in genomic research.
There are various software that aim to calculate genomic derived features in the population such as STRUCTURE (Porras-Hurtado et al. 2013), TASSEL (Bradbury et al. 2007), different R packages(R Core Team 2020) and so on.

4.2.3. Phenotyping

Precise phenotyping of the association panel is an absolute requirement to achieve effective conclusions. There are several reports suggesting that an increase in the number of association panel units used for phenotyping increases the power of association mapping much more than a rise in the number of markers applied for genotyping (Manchia et al. 2013; Ingvarsson and Street 2011). The human-related phenotyping error is usually regarded as the main reason for irreproducible results in association mapping (Barendse 2011). Replicated phenotypic evaluations over locations and years not only improve the association mapping result by taking into account the environment-genotype interaction effects that are highly influential for quantitative traits but also enrich the statistical power of QTL detection (Z. Zhang et al. 2010; Stich et al. 2008; C. Zhu et al. 2008).
To achieve high statistical power in association mapping, regular repeated phenotypic evaluation should be planned based on an efficient and suitable experimental design and phenotypic results analyzed through fitting statistical approaches. Among the

different experimental designs augmented design, nested design and randomized block design (Kumar et al. 2017; Prioritization 2020; Yu and Buckler 2006; Sukumaran et al. 2012) are very common in association mapping.

It should also be mentioned that association mapping can be divided into two approaches based on how to treat phenotypic data. The phenotypic data from different replicates can be averaged and the adjusted entry mean values are then used for association analysis; this is referred to as two-stage association mapping. In contrast to this approach, there is the one-stage association mapping in which phenotypic data (from all the replicates) are directly used for association analysis (Stich et al. 2008). A study comparing these two approaches disclosed differences between them although the differences were rather small. The report suggests that applying the two-stage approach will not increase the empirical type I error rate too much in comparison to the one-step approach (Stich et al. 2008) and seems more precise and convincing.

4.2.4. Association mapping analyses

A regression analysis of relatedness between the phenotypic values and the genotype data is applied (M. Wang et al. 2012) based on different models to detect the QTLs governing the traits of interest. It should be noticed that the best-fitted model will be selected based on a comparison of the different models' outcomes. Based on the applied model the kinship (K matrix) and population structure (Q matrix) may be used as covariates (Hoffman 2013) to minimize false (Spurious) associations between the markers and the detected QTLs. As these analyses are computationally intensive, special and suitable facilities are needed in terms of both hardware (Cluster network) and software (Linux platform).

4.3. Association Mapping approches

Association mapping can be grouped into two typical approaches such as Genome-Wide Association Studies (GWAS) and the candidate gene approach. In the GWAS approach, high-density markers scattered all over the genome are applied for genotyping (Pavan et al. 2020). For the genotyping process, this should take into account that in allogamous species more dense markers are needed than for autogamous species as the LD blocks are more stable (Myles et al. 2009; Pavan et al. 2020). For example Garris et al. (2005) reported that the LD in rice (Oryza sativa) can extend to 100 kb or more; so as the LD increases, fewer markers are needed (Sorkheh et al. 2008) (Table 3). Generally, in the GWAS approach, all the loci engaged in the variation for the trait of interest can be detected.

The other approach is known as candidate genes approach. It is based on available data of gene variance that are presumed to contribute to governing a trait. of interest. These genes are studied in order to test their contribution to the trait (M. Zhu and Zhao 2007). The candidate gene study only explores limited regions of the genome where selected candidate genes are located (Patnala, Clements, and Batra 2013). Usually, candidate genes are selected through the meta-analysis of data driven from QTL analysis, comparative genomics, transcriptome data, and gene functional annotation (Kankanala, Nandety, and Mysore 2019; Patnala, Clements, and Batra 2013) along with a detailed literature review. In this approach, since it focuses only on specific genomic regions, the number of applied markers will decrease. Through this approach, it is possible to detect significant QTLs which genome wide association study fails to detect (Amos, Driscoll, and Hoffman 2011). The use of this approach in conjunction with GWAS ends up to improving the accuracy of QTL detection and statistical power (Gupta, Kulwal, and Jaiswal 2014).

4.4. Plant Populations Used for Association Mapping

One of the most important issues affecting the success or failure of association mapping is the population that is analyzed in the study. Association mapping can apply to natural populations, family-based populations, biparental and multiparent populations (Bartoli and Roux 2017; Zhou and Huang 2019). Among multiparent populations, multiparent advanced generation intercrosses (MAGIC) and nested association mapping (NAM) populations are very popular and useful not only for association mapping but also for linkage mapping (Cavanagh et al. 2013; Zhou and Huang 2019).

4.4.1. Population-Based Association Panels

Association mapping is applicable in all random mating populations with substantial LD in genomic regions engaged in the control of the trait of interest. Generally, the association panel samples are selected from a natural population, breeding population (Xiao et al. 2017) and synthetic populations (Mazaheri et al. 2019; Luo et al. 2020). The association panel whose samples are selected from a germplasm collection can be one of two random samples or a "core collection" of germplasm accessions (Singh and Singh 2015).

The diverse types of populations are discriminated based on various features such as the mapping resolution, the LD level, and the power of QTL detection Table 3 (Table 3). Generally, based on the different literature reviews, the different populations which can be used in association mapping studies can be graded as follows based on their population structure and familial relatedness (Kinship) (C. Zhu et al. 2008; Yu et al. 2006)(Table 3)

i. Ideal population with little familial relatedness and population structure
ii. Population with mild familial relatedness and population structure

iii. Population with mild familial relatedness but slight population structure
iv. Population with slight familial relatedness but mild population structure
v. Population with floating familial relatedness and strong population structure

4.4.2. MAGIC Populations

MAGIC is the short form of the “Multiparent Advanced Generation Intercross” populations and include a set of Recombinant Inbred Lines (RILs) which are assembled from a complex intercross or a set of crosses holding multiple parents. The parental lines depend on the aim of the research or their origin can be selected among clones, inbred lines, or individuals selected. The MAGIC can be regarded as an extension of an Advanced Intercross Line (AIL), intercrossing of individuals of F2 and later generations which for the first time had been proposed and applied in animal science (mice) (Mott et al. 2000) while termed as “heterogenous stock”; later Mackay and Powell coined “MAGIC” term (Mackay and Powell 2007), instead of heterogenous stock and introduced this concept to plant science.

The main difference between MAGIC and AIL is the collaboration of numerous parents in the construction of MAGIC.

To produce a MAGIC population, the first step is to construct complex cross parental lines and then develop RILs from these complex cross parental lines. To establish the complex cross parental lines, after selecting parental lines, usually eight different lines, the parental lines are crossed in pairs to develop different single crosses, then after the newly derived single crosses again cross in pair to construct two double crosses. Subsequently, the two produced double crosses, crosses together to construct multiple parental lines. Then the single seed descent approach is applied to develop the RILs MAGIC population (Figure 19).

These populations can be applied in association mapping and linkage mapping and due to the several recombination events occurring during the construction of the MAGIC population, the resolution of QTL increases dramatically. The MAGIC

population have been developed in maize, wheat and rice and employed for QTL mapping (Arrones et al. 2020; Jiménez-Galindo et al. 2019; Dell'Acqua et al. 2015; Bandillo et al. 2013; Novakazi et al. 2020; M. F. Scott et al. 2020; Mackay and Powell 2007).

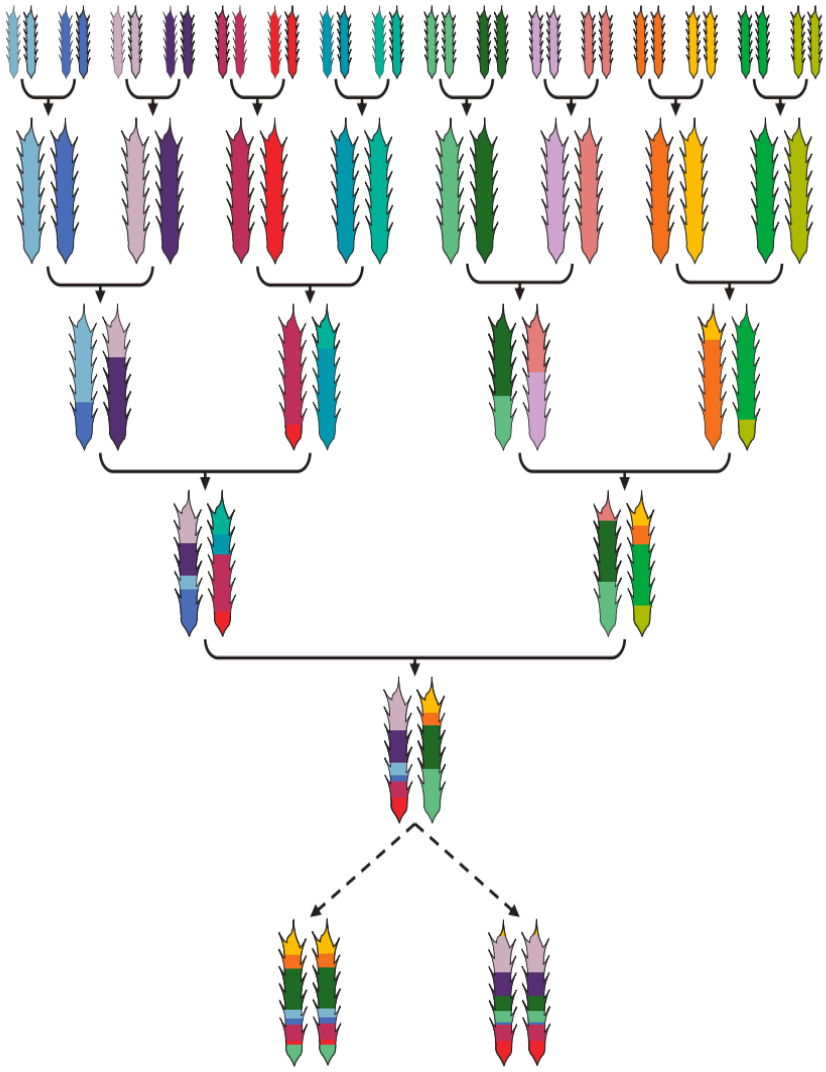

Figure 19: The multi-parent advanced generation inter-cross (MAGIC) design.

Source : M. F. Scott *et. al*.,2020.

4.4.3. NAM Populations

Nam stands for Nested Association Mapping population and was developed for identifying the genetic architecture of complex traits in maize by Yu et al. (2008). NAM populations exploit the positive features of the association mapping approach (historic recombination events, higher resolution) and QTL mapping approach (recent recombination events, a smaller number of markers) to have high allele richness, high statistical power and high mapping resolution.

To construct a maize NAM population 25 diverse maize were chosen as the parental lines (founders) and each of them was crossed to the maize reference line (maize inbred line B73) to produce F1 populations. The F1 plants derived from every 25 crosses were selfed independently for 6 successive generations and the single seed descent approach was applied to create a total of 200 RILs per family. Finally, a total of 5000 RILS were constructed within the NAM population (Figure 20) (Yu et al. 2008). Similar NAM populations have been developed for other plant species such as barley, wheat, rice, oilseed rape (Hu et al. 2018; Ren et al. 2018; Schnaithmann, Kopahnke, and Pillen 2014; Fragoso et al. 2017).

In contrast to the positive aspects of the NAM population, there is a statistical challenge which corresponds to the estimation of the probability that alleles of various loci that are not only identical by descent but also are identical by state. Although this concern potentially can be ignored because of existence of the powerful statistical models and the advent of new sequencing technologies. However, there are still some ambiguous points that should be answered such as the criteria for selection of parental lines and their optimum numbers to construct a NAM population, the number of reference line that can be used to construct the NAM and the essential modification of experimental design based on the population structure of plant species under study (Myles et al. 2009).

.

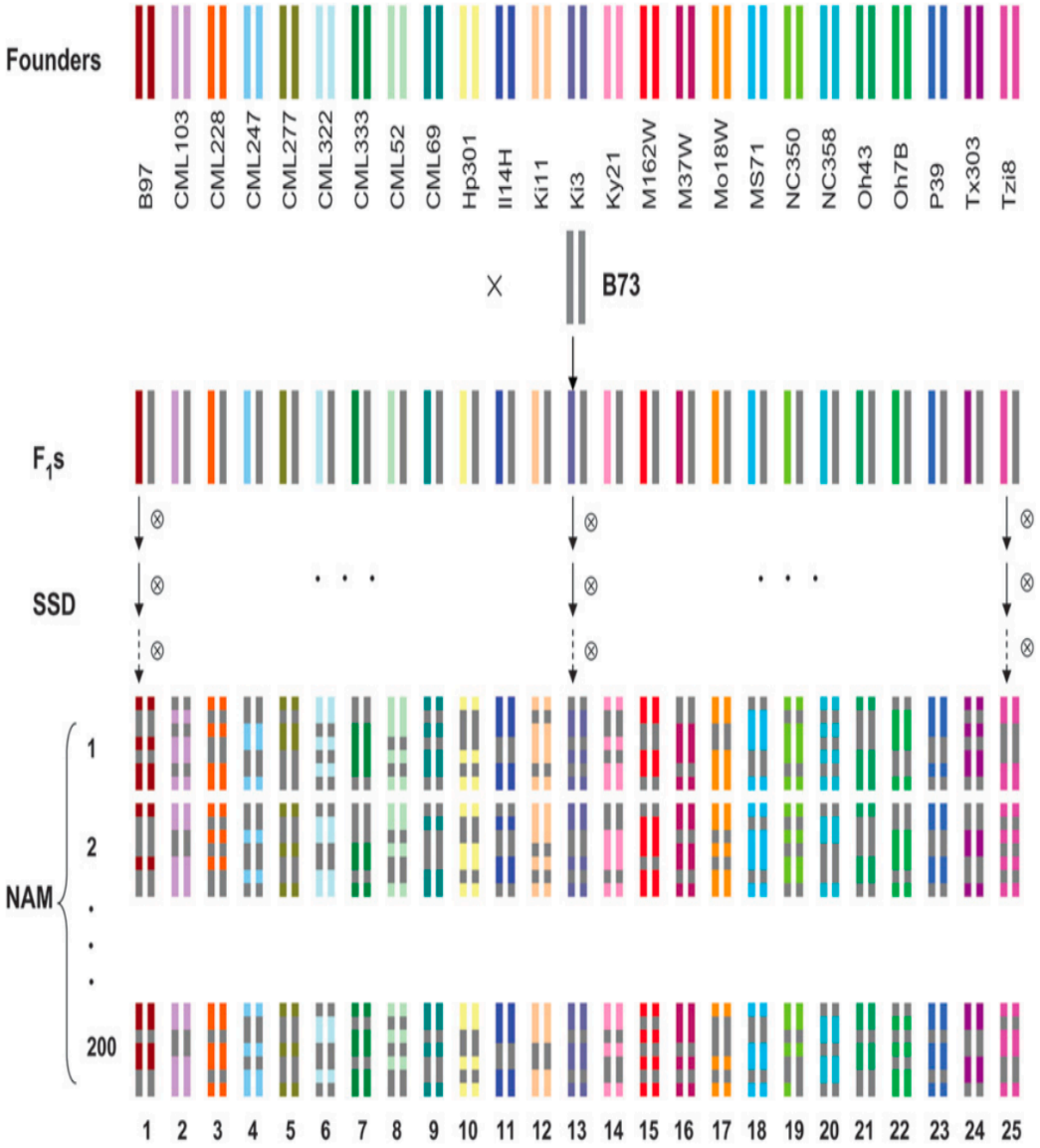

Figure 20: The nested association mapping (NAM) design.

Source: Yu *et. al.*, 2008.

4.5. Linkage Disequilibrium

Linkage disequilibrium (LD) was introduced by Jennings (1917) and Lewontin developed its estimation later (R. C. Lewontin 1964). In different Literatures LD have been addressed as an allelic association, gametic phase disequilibrium, or gametic disequilibrium (Flint-Garcia, Thornsberry, and Buckler 2003). LD is very crucial in association studies. For instance, the amount of LD in a population can impact several factors in a study, such as the marker number, marker density and the sample size (Flint-Garcia, Thornsberry, and Buckler 2003). It is very important to master the LD concept and to specify LD extent in the species under study.

LD refers to the non-random association of alleles at different loci in a population (Flint-Garcia, Thornsberry, and Buckler 2003; Morton 2005). In a random mating population, the genes and subsequently the genotype frequencies remain unchangeable during successive generations. Some factors result in a shift in genes and genotypes frequencies. These factors are known as “evolutionary factors” and include mutation, selection, migration and random drifts (Flint-Garcia, Thornsberry, and Buckler 2003; Balding 2006).

Consider one locus on a chromosome that consists of two alleles “A_1” and “A_2”, with a frequency of “p” and “q” respectively. The expected genotype frequencies at this specific locus are p^2 (A_1 A_1), 2pq (A1 A2) and q^2 (A_2 A_2), following the binomial square of equation $(a + b)^2$ which in population genetics is known as Hardy-Weinberg equilibrium. When the population is in Hardy-Weinberg equilibrium, there is no statistically significant variation between expected genotype frequencies and observed genotype frequencies. Once this equilibrium is violated by one or some of the evolutionary factors there would be a statistically significant difference between expected genotype frequencies and observed genotype frequencies.

Now consider two independent loci (A, B) on a same chromosome carrying four different alleles (A_1, A_2 and B_1, B_2) in a population. As a general rule, the expected frequency of allelic combination for A_1 B_1 would be p (A_1) Multiple by p (B_1) and so on. Therefore, the expected genotypic frequencies for all possible gametic combinations “A_1 B_1”, “A_1 B_2”, “A_2 B_1” and “A_2 B_2” would be p A_1 B_1, p A_1 B_2, p A_2 B_1, and p A_2 B_2, respectively (Figure 21).

Allele	A_1 (0.6)	A_2 (0.4)	Total = 1
B_1 (0.8)	A_1 B_1 (0.6) * (0.8) =0.48	A_2 B_1 (0.4) * (0.8) = 0.32	
B_2 (0.2)	A_1 B_1 (0.6) * (0.2) = 0.12	A_2 B_2 (0.4) * (0.2) = 0.08	
Total = 1	Total = 1		

Figure 21: The frequencies of different allelic combinations.

The frequencies are produced by independent segregation of alleles of two genes (A_1/A_2 and B_1/B_2). This results an estimation of "zero" for D (a measure of LD).

Again, if the equilibrium is violated by evolutionary factors there would be a statistically significant difference between p A_1 B_1.p A_2 B_2 and p A_1 B_2.p A_2 B_1 that is known as disequilibrium. As soon as the causal factor(s) stopped, after each generation of random mating this difference reduces to half of its amount in the previous generation, so it is expected that after several generations the loci in the population will proceed toward equilibrium (Singh and Singh 2015).

In order to estimate LD several approaches have been introduced. Generally, to estimate between two loci which involved two alleles, these approaches were modified to generalized their application in other situations. To validate the statistical significance of LD estimation when the two loci have two alleles Fisher's exact test is applied (Mackay and Powell 2007; Fisher 1935; Flint-Garcia, Thornsberry, and Buckler 2003); once there are more than two alleles at loci multifactorial permutation analysis are applied (Bruce S. Weir 1996; Flint-Garcia, Thornsberry, and Buckler 2003).

4.5.1. Calculating LD

4.5.1.1. Two biallelic Loci

To calculate the extent of LD between two loci having two different alleles there are different statistics such as D, D', r2, d, Q, δ, δ* and λ (Table 4) and they take account to the different features of nonrandom association (Slatkin 2008).

D which was introduced in 1918, is the primitive approximation of LD, and although it is not common anymore, the other statistics are derived from it. D is calculated as the difference between the expected allelic combination (haplotype) frequency and the observed one in a population (Guo 1997; Calabrese 2019) (Table 4). It should be considered that two alleles are in positive LD when their combinations are observed more frequently than expected and in contrast, they are in negative LD when they are observed together less frequently than expected (Manfred Schwab 2011) (Table 5).

D would be highest when allele frequencies both are 0.5 but its weakness is that it is very sensitive when the extreme values of allele frequencies exist (0 or 1). D cannot be calculated in such a situation (Gaut and Long 2003; Manfred Schwab 2011).

Table 4: Different equations used for calculation of the diverse estimates of LD.

LD estimate	Formula	Remarks
D	$(pA.\ pab) - (pA.\ paB)$ or $pAB - (pA\ .\ pB)$	Depends on allele frequency; not in common use
D'^{a}	D/min $(pA.pb, pa.pB)$ when $D>0$	Most often used in plants
	D/min $(pA.pB, pa.pb)$ when $D<0$	
r^2 or Δ^2	$D^2/(pA{\cdot}pa{\cdot}pB{\cdot}pb)$	Most often used in plants
δ^{a}	$D/pB.pbb$	Approximation of δ*; also known as λ and P_{excess}
δ^{*a}	$\frac{pA[\{(pAB/pA)/(paB/pa)\}-1]}{1+pA[\{(pAB/pA)/(paB/pa)\}-1]}$	Frequently used in epidemiology
D	$D/(pB.pb)$	Specifically recommended for case-control studies
Q	$D/(pAB.pab + pAb.paB)$	Used in case-control studies; range −1 to +1
λ	$(pAB.pab)/(pAb.aB)$	Used in population genetics

Based on Devlin and Risch (1995)

[a]When disease causing allele is rare and the sampling of haplotypes is random, $\delta = \delta^* = D' = [D/(pa.pB)]$, where B is the allele producing disease and A and a are the marker alleles

Source: Singh BD and Singh AK.2015.

Table 5: Frequencies of Haplotype under linkage disequilibrium.

HAPLOTYPE	OBSERVED FREQUENCY	A_2 AND B_2 IN NEGATIVE LD	A_2 AND B_2 IN POSITIVE LD
A_1B_1	X_{11}	$X_{11} < p_1 \times q_1$	$X_{11} > p_1 \times q_1$
A_1B_2	X_{12}	$X_{12} > p_1 \times q_2$	$X_{12} < p_1 \times q_2$
A_2B_1	X_{21}	$X_{21} > p_2 \times q_1$	$X_{21} < p_2 \times q_1$
A_2B_2	X_{22}	$X_{22} < p_2 \times q_2$	$X_{22} > p_2 \times q_2$

Source: Manfred Schwab, 2011.

Lewontin (1964) suggested that this problem can be fixed by estimating a standardized form of D known as D', through dividing calculated D by its theoretical maximum frequency of observed allele

$$|D'| = DA_2B_2 / \min (pA_1.pB_2, pA_2.pB_1) \text{ when } DA_2B_2 > 0$$

$$|D'| = DA_2B_2 / \min (pA_1.pB_1, pA_2.pB_2) \text{ when } DA_2B_2 < 0$$

In fact, D' reduces the trace of low allele frequency in the population in LD estimates. D' is in the range of 0 and 1 (Flint-Garcia, Thornsberry, and Buckler 2003; Singh and Singh 2015). When it is 1 it can be interpreted that no (historical) recombination events have occurred between two loci and there is complete LD, while the moderate value

of D' is not very useful for interpretation (Singh and Singh 2015). D' manifests both negative and positive linkage disequilibrium (Table 4).

The weakness of D' is that a small size of population extremely affects it, especially for loci with rare alleles. Ardlie *et al.* (2002) reported that in this situation D' can present high values while the loci are in equilibrium, so this cannot be used for comparison of different studies.

To overcome the limitation of D', r^2 or Δ^2 has been proposed as the linkage disequilibrium index which technically is the Pearson correlation coefficient among the alleles of two given loci (Singh and Singh 2015; VanLiere and Rosenberg 2008). r^2 computes

$$r^2 = D^2 / (pA_1.pB_1, pA_2.pB_2)$$

ranges from 0-1; 0 presents a situation where the alleles of two genes segregate independently while 1 corresponds to the situation where two loci are in complete LD. In association studies, r^2 is more practical since it is less affected by extreme allele frequencies (rare or abundant).

4.5.1.2. Two loci with Several Alleles

Generally, most of the (important) traits in a population are controlled by genes/QTLs that have more than two alleles. In this situation Hedrick (1987) propose to compute D' for each allele pair of two loci and subsequently weighed average of D' computes through following formula to achieve a general estimation of LD among all the alleles at two loci

$$D' = \sum_{i=1}^{k} \sum_{j=1}^{l} p_i q'_j \left| D'_{ij} \right|$$

In this formula, p_i and q_j are the frequencies of i^{th} and j^{th} alleles at the two loci that have k and l alleles, respectively.

One of the positive advantages of D' is that it is much less affected by allelic frequencies however difficulties in deducing the haplotype block when there are more than one heterozygous locus and multiple loci; is the disadvantage of this method (Slatkin 2008). To overcome this limitation expectation maximization (EM) algorithm is proposed to capture the maximum likelihood estimation of gene frequencies for LD calculation (Gupta, Rustgi, and Kulwal 2005).

4.5.1.3. Multiple *loci*

To capture multilocus LD estimation there are two approaches

1. Top-down decomposition approach
2. Bottom-up decomposition approach

Generally, multi locus LD is estimated through the bottom-up decomposition approach: in the first phase the LD is captured for the individual loci and then the multilocus LD will be captured (R. Lewontin 1974). To treat multilocus data there are different methods such as the estimate λ, least-square methods, composite likelihood methods, entropy-based method and haplotype segment sharing methods. In the λ method, the λ is calculated for each marker/gene subsequently the λ is used to calculate the log-likelihood for LD.

In the other decomposition approach (Top-down), the coefficients of higher-order LD are captured then decomposed into the lower-order LD (Gupta, Rustgi, and Kulwal 2005).

Today most of the algorithms used to capture the higher-order LD were suggested by Geiringer (1944). However, Gorelick and Laubichler (2004) presented an algorithm for the top-down decomposition approach to calculate the higher-order LD but it was also a developed model based on the Geiringer 's algorithms.

Overall, even nowadays calculating LD for multiple locus are vital for fine QTL mapping and the applied methods and algorithms are still in the developing and refining process (Singh and Singh 2015).

4.5.2. Graphic Representation of LD

In general, LD estimates are captured for pairs of loci. Pairwise LD estimates for numerous markers can be illustrated graphically to get a concept of the pattern of LD blocks; in another word the genomic segments exhibiting persistence of LD (LD decay), in the species. The LD decay plot and color-code triangle LD plot (LD heatmap, linkage disequilibrium matrix plot) are the two graphical display methods to display LD values.

LD decay is a concept that addresses the decline in the LD amount between two loci because of recombination events between them. As a general pre-assumption when a new mutation occurs, it will create a complete LD with the neighboring alleles (Flint-Garcia, Thornsberry, and Buckler 2003; Singh and Singh 2015); as a result, this new mutant allele will attach to the neighboring alleles and ignore the recombination events. In the meiotic cell division (prophase I), the recombination events contribute to shuffling genetic materials between chromosomes that lead to a decline in the magnitude of the LD which is known as LD decay.

The time of mutation is a factor that affects LD decay, for example. the amount of LD will be higher in the new mutations than LD amount in the older mutations since more recombination events are expected to happen in the older mutations than the new ones. So, the analysis of LD can also be applied to determine the historical background of genetic variation in terms of the contribution of recombination and mutation regarded to the magnitude of LD in a population(Flint-Garcia, Thornsberry, and Buckler 2003).

In LD decay plot graphical method, LD pairwise estimated values (r^2 or D') are plotted against physical distance (in bp or kb) or genetic distance (in cM) among pairs of the markers. In this graphical method the x-axis is designated to the estimated values of LD pairwise while the Y-axis represents the genetic or phisical distance (Figure 22). In this method to represent the generalized relationship between estimated values of r^2 and the genetic/physical distance the nonlinear logarithmic regression curve of r2 values at the genetic/physical distance is calculated and plotted (Abdurakhmonov and Abdukarimov 2008).

The LD decay plot may illustrate either the pairwise estimated value of LD in the particular section of the genome or summarize the LD values among pairs of markers distributed throughout the whole-genome.

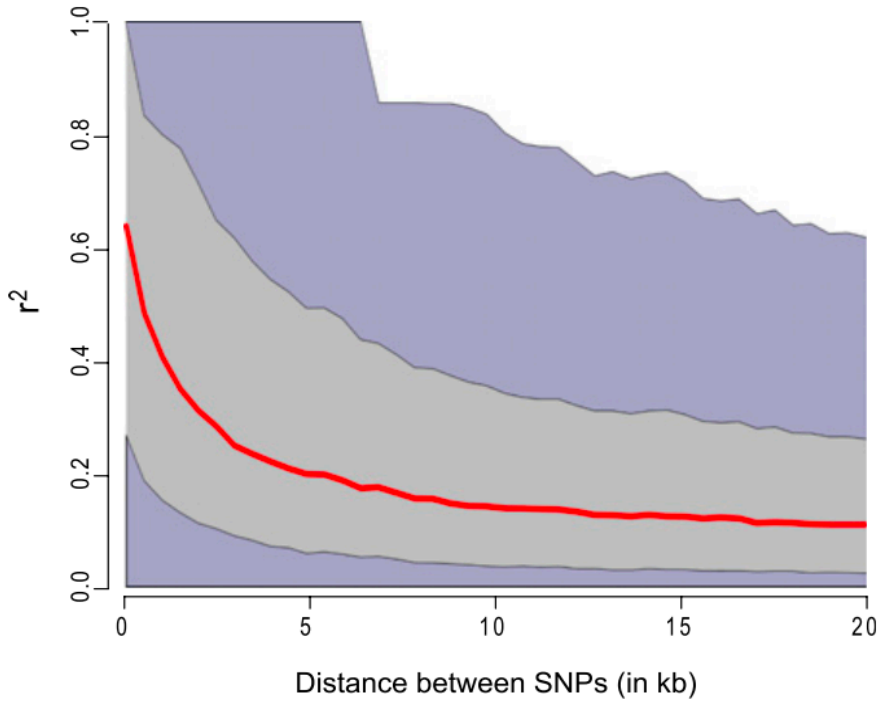

Figure 22:*M. truncatula* LD decay plot.

Source : Branca *et. al.*, 2011

The color-code triangle LD plot (LD heatmap, linkage disequilibrium matrix plot) is another graphical display method to display LD values. The triangle plot illustrates significant values of LD within several pairs of markers and their p-values either in a single gene or specific region of the genome. In this method the values of pairwise LD; depicts on both X– and Y-axis where r^2 values and p-values that derived from the 1000 permutation test, are depicted above and under the diagonal, respectively. The color of the cell depends on the p-value and normally is shown in the color-code bar alongside the triangle LD plot. The large red blocks throughout the diagonal indicate the high level of the LD within loci that are situated in the blocks and convey this message that since the formation of the LD blocks there has been no recombination (or very limited) among these loci (Figure 23). This type of graph is generated by some programs such as TASSEL (Trait Analysis by Association, Evolution and Linkage), GOLD (Graphical Overview of Linkage Disequilibrium), and some R-program packages such as LDheatmap, PowerMarker.

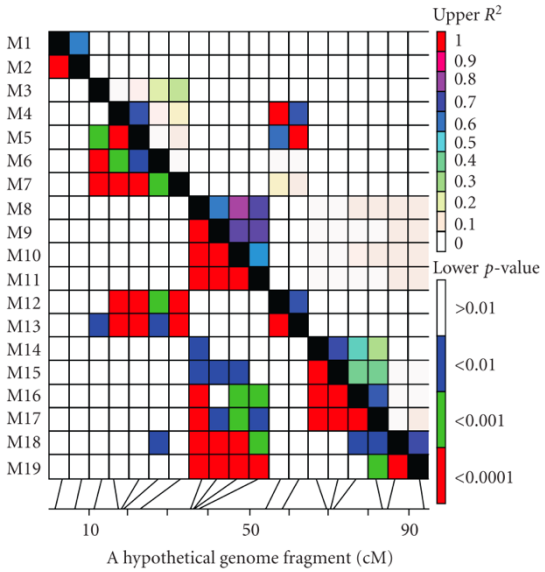

Figure 23: The triangle LD plot.

Source: Abdurakhmonov and Abdukarimov, 2008.

II - Objectives of the study

The interaction between *Medicago truncatula* and *V. alfalfae* and objectives of the Thesis

Earlier investigations in our group with a French isolate (V31-2) have demonstrated that *V. alfalfae* is a true pathogen of *M. truncatula* and that the colonization pattern in this model plant follows the same typical pattern as for other vascular wilt pathogens (Ben et al. 2013). Resistant and susceptible lines were identified and some major and minor QTLs for resistance against V31-2 were detected in different RILs populations. Notably, a major QTL *MtVa1* was identified in two RILs populations (LR4 and LR5) where resistance was introduced by the A17 parent. Another major QTL *MtVa2 and* a minor QTL *MtVa3* were detected in the LR3 population where resistance was introduced by the DZA45.5 parent. Resistance to a *V. non-alfalfae* strain (former *V. albo-atrum*) LPP0323 was controlled by another 4 QTLs (Negahi et al. 2014).

By using a transgenic V31-2 strain expressing the GFP reporter gene it was shown that the resistant line A17 after initial fungal penetration and colonization of xylem vessels eliminated the fungus from its roots (Toueni et al. 2016).

A transcriptional study in a resistant (A17) and a susceptible (F83005.5) (Toueni et al. 2016) showed that in response to *V. alfalfae* V31-2 inoculation genes related to secondary metabolism and oxidative stress were induced in both the resistant and susceptible line. The specific gene expression response of the susceptible line indicated upregulation of the signaling pathways involving the hormones ethylene, jasmonic acid and auxin, whereas pathways involving salicylic acid and abscisic acid were downregulated. The resistant line exhibited upregulation of genes related to defense mechanisms.

All previous genetic studies showed that resistance to *Verticillium alfalfae* in *M. truncatula* is a quantitative disease resistance or “QDR” involving major and minor QTLs.

The available genomic data derived from the international Medicago HapMap project enabled to perform a whole-genome approach to further investigate the genetic control of resistance to *V. alfalfae*. So in the first GWAS the response of 261 accessions

towards V31-2 were evaluated (Mazurier 2018). It revealed several new QTLs for partial resistance to *V. alfalfae* V31-2 and confirmed the previously identified major QTL *MtVa1* on linkage group 7. Subsequently, the functional validation of candidate genes was initiated, with a focus on the genes located on linkage group 7. Through an in vitro transgenic root inoculation system, the contribution of the gene *Medtr7g070480* encoding a SEC14 protein was confirmed. The expression of this gene was suppressed through an artificial microRNA (amiR) in the A17 (resistant) and F83005.5 (susceptible) accessions and resulted in diminution of the colonization of the roots by V31-2.

In a second GWAS performed on 90 Tunisian accessions (Soliman population) different candidate genes were identified compared to those identified from the Medicago HapMap collection, implying a possible local adaptation towards V31-2 (Mazurier 2018).

The phenotyping data derived from the first GWAS were applied in the prediction pipeline known as WhoGEM, developed in 2019. WhoGEM is based on admixture proportions and quantitative phenotypic variables using geographical coordinates as covariates for admixture analysis. This developed algorithm suggested that resistance against *V. alfalfae* V31-2 is structured by the geographical origin of the plants, accessions are rather susceptible in the eastern Mediterranean regions and resistant in the western regions (Gentzbittel et al. 2019).

This suggests a possible co-evolution between *M. truncatula* and *V. alfalfae* and led to the idea to analyze how these accessions would respond to a *V. alfalfae* strain that is isolated from the eastern part of the Mediterranean basin. Such a study would also be of interest for a more practical issue, i.e., the introduction of new pathogens by global trade for which native plants may not have the appropriate ability of perception and/or defense. In order to take into account additional effects of global warming, the new isolate should be from a region with higher temperatures than the origin of strain V31.2.

Hence, the present project concerns a GWAS analysis of the response of *M. truncatula* towards a strain from Iran, at higher temperature compared to previous studies.

Therefore, this study was proceeding by the following steps

- Obtain *Verticillium alfalfa* isolates from Iran
- Characterize these isolates by growth and sporulation properties
- Perform GWAS with one of these isolates and the *M. truncatula* HapMap population in order to identify loci involved in resistance
- Identify genes underlying these loci and study their expression in response to *V. Alfalfa*

As a side project, study of Iranian *M. truncatula* accessions for resistance and susceptibility to *V. alfalfae was initiated.*

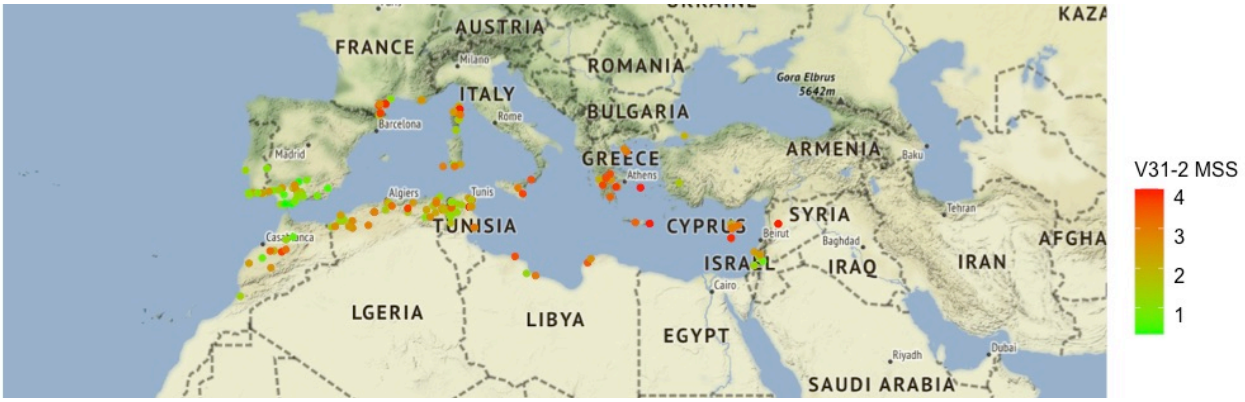

Figure 24: Geographical distribution of the 211 *Medicago truncatula* accessions and their response to the French *V. alfalfae* (V31-2) isolate.

Each accession is represented by a point whose color varies consistent with the MSS corrected value.

III - Material and Methods

III.1. Material

1.1. Plants

1.1.1. *Medicago truncatula* accessions from HapMap project

A set of 242 *Medicago truncatula* accessions was selected from the HapMap collection and was multiplied in our greenhouse (Table S. 1). The plants were grown in soil/sand mixture in the greenhouse for seed production, for inoculation experiments they were grown in jiffy substrate (Jiffy-7®, reference 31130105- 33mm) (Figure 25) or sand /perlite mixture (2/3 sand + 1/3 perlite) in plug trays (alvéoles) (27 ml) in a growth chamber with 25 °C day/23 °C night temperature and a photoperiod of 16h.

Figure 25- Jiffy Substrate.

1.1.2. Iranian *Medicago* species

A set of 4 *M. truncatula* accessions and one *M. scutellata* were obtained from the Research institute of forests and rangelands (Table S. 2). As Iranian accessions were wild-type, they cannot be used directly for in depth studies but have to be fixed genetically by selfing. In order to fix them, they were planted in the greenhouse for two successive generations by means of single-seed descendants (SSD) method.

1.2. Fungal isolates

Verticillium alfalfae isolates were obtained from diseased alfalfa (*Medicago sativa*) plants during two field trips in Iran in 2017 and 2018 (Table 6). They were cultured as monospore isolates on Potato Dextrose Agar (PDA) medium and spores were stored as glycerol stocks at -80 °C. The Iranian *Verticillium alfalfae* MG2 (formerly *V. albo-atrum*) was provided by M. Ghalandar (Arak, Iran); (Ghalandar et al. 2004). The French *V. alfalfae* strain V31.2 (Ben et al. 2013) and *V. non-alfalfae* LP0323 and *V. dahliae* strain JR2 (Negahi et al. 2013) were used for comparisons.

Table 6: Location, numbers of farms sampled in different parts of Iran.

Sampling site (Province)	Number of sampled fields
Arak	8
Hamedan	1
Isfahan	9
Karaj	2
Tehran	9
Urmia	5
Yazd	6

1.3. Bioinformatics data

SNP data were obtained from the *Medicago truncatula* HapMap project (Stanton-Geddes et al., 2013, http://www.medicagohapmap.org/). On the *Medicago truncatula* genome, there are over 37 million SNPs, or on average one SNP per every 450bp. The Kinship matrix and Population structure were computed based on the 840 K SNP dataset which has been described earlier (Gentzbittel et al. 2019).

The GENOTOUL bioinformatics platform Toulouse Occitanie (BIOINFO GENOTOUL, https://doi.org/10.15454/1.5572369328961167E12) has provided computing and storage resources.

III.2. Methods

2.1. Characterization of Iranian *Verticillium alfalfae*

2.1.1. Isolation of fungal strains and primary selection of *Verticillium alfalfae*

Collected samples were dried between paper for conservation. Their stems were cut into two cm long fragments above the first node and surface sterilized in 70% ethanol for 15 seconds followed by 6 minutes in 0.96% commercial bleach then rinsed three times in sterile water. The sterilized stems were incubated on Potato dextrose agar (PDA) medium containing 50 µg/ml streptomycin at 25 °C. After three days, outgrowing mycelium was subcultured onto fresh PDA, and purified by further subculturing. Monospore cultures were prepared when isolates were pure by visual assessment. A spore suspension was prepared from 2-week-old cultures by adding 20 ml of sterile distilled water to the culture and gently rubbing the surface with a bent Pasteur pipette to release conidia. The concentration of spore suspensions was determined under a microscope with a Malassez counting chamber and was adjusted diluted to a final concentration of 100 spores per milliliter. Drops of 5 µL were put on PDA and growing mycelium was subcultured on PDA immediately. For conservation, glycerol stocks were prepared from spore suspensions of each monospore isolate by mixing 500 µL of sterile glycerol 50% with 500 µL of spore suspension (concentration > 10^6 spores/ml) in a sterile microtube and freezing the tube in liquid nitrogen. The tubes were stored at -80 °C.

After purification, the isolates were cultured on water agar (WA) media and incubated at 25 °C for two weeks. Then a part of the medium was cut and taken out at the periphery the grown mycelium and the cultures were further incubated. Within three to five days, the edges of evacuated parts were observed under the microscope (Figure 26) and the samples which had developed the characteristic form of *Verticillium* sp. conidiophores, were retained for further steps.

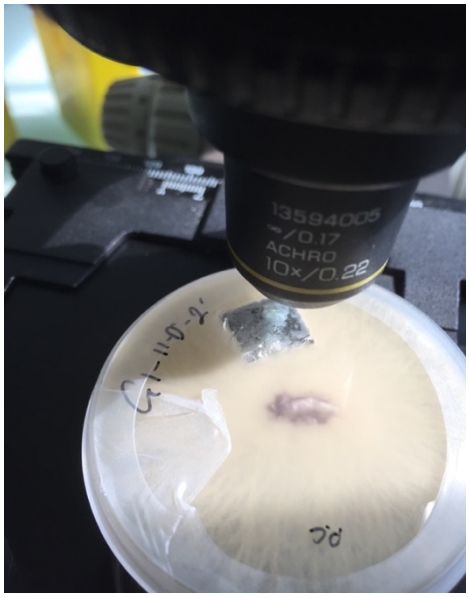

Figure 26: Observation of isolates under the microscope.

A square part of the water agar medium was removed to observe hypha growing in the empty space.

2.1.2. Extraction of Fungal DNA

Selected isolates based on visual identification were grown on Potato Dextrose Broth (PDB) medium at 25 °C in the dark on a shaker (90 RPM) for two weeks and the mycelia were harvested by filtration (Whatman® Grade 1 filter paper) and stored at -20 °C.

For DNA extraction, frozen mycelia were ground to a fine powder with a mortar and pestle under liquid nitrogen. About 100 mg powder was transferred to a 2-mL Eppendorf tube and 650 µL of CTAB extraction buffer (2% CTAB) (Table S. 3) preheated to 60 °C were added to every sample. After mixing, 10 µL proteinase K (20 mg/ml) was added and the samples incubated at 65 °C for 30 minutes with gentle shaking. The incubation was followed by nine minutes centrifugation at 10000g at room temperature; subsequently, 600 µL of supernatant was transferred to a fresh microtube, and a 600µL of phenol/chloroform/isoamyl alcohol (25:24:1) were added. Thereafter the samples were again centrifuged for nine minutes at 10000g. The aqueous phase was transferred to a fresh microtube and 500 µL of chloroform/ isoamyl alcohol (24:1) were added and tubes were mixed gently followed by centrifugation for nine minutes at 10000g. Thereafter, the aqueous phase was transferred to a fresh microtube and DNA was precipitated by the addition of 300 µL isopropanol, incubation

at -20 °C for 20 minutes, subsequent centrifugation for 15 minutes at 13000g at 5 °C. The pellets were washed with cold 70% ethanol, dried and dissolved in 50 µL TE8. The quality of extracted DNA was assessed with a nanodrop (NanoDrop nd-1000 Spectrophotometer).

The concentration of all extracted fungal DNA samples was adjusted to 5ng/µL for PCR.

2.1.3. Polymerase chain reaction

PCR was performed with 10µL fungal DNA (5ng/µL) in a reaction volume of 25 µL. The reaction mixture for one reaction is shown in Table 7.

Table 7: PCR mix used for ITS1 – ITS4, species-specific primers and SSR amplification.

Reagent	Concentration of stock solution	Volume (µL)
Water	-	U.T.* 25 µL
PCR buffer	10x	2.5
MgCl2	50 mM	1.25
dNTP	10 mM	0.5
Forward primer	10µM	2.5
Reverse primer	10 µM	2.5
Taq polymerase	35 U/µL	1
Fungal DNA	5 n*g*/µL	10

*: Up to

Two species-specific primers were used for the final identification of isolates; *V. alfalfae* specific primer (AlfF - AlfD1r) (Inderbitzin et al. 2013) and *V. non-alfalfae* specific primer (NOF/NonUR) (Inderbitzin et al. 2013). To assess the quality of all extracted samples, a PCR amplification with the fungal universal primers (ITS1 – ITS4) was performed.

Amplification was performed in a programmable heating block (Geneamp PCR system 9700). Table 8 represents the amplification program.

The annealing temperature was set to 62 °C for *V. alfalfae* specific, 65 °C for *V. non-alfalfae* specific primers and 50 °C for ITS.

Amplicons were electrophoresed on a 1.5% agarose gel containing Ethidium bromide and were visualized as described above.

Two negative controls were included in all of the PCR amplification: sterile MilliQ water instead of DNA and DNA from JR2 (*V. dahliae*); isolates MG2 and V31.2 were considered as positive controls.

The PCR products were visualized on the 1% agarose gel supplemented with Ethidium bromide. DNA bands visualized through the Quantum st5 gel documentation system.

Table 8: PCR program used for the amplification of fungal universal primer, species-specific primers and SSR primers.

Step	Number of Cycles	Temperature	Time
Preliminary denaturation	1	94 °C	5 Min
Denaturation	30	94 °C	1 Min
Annealing		Depending on primer	1 Min
Elongation		72 °C	2 Min
Final elongation	10	72 °C	10 Min

2.1.4. Genotyping of *V. alfalfae* isolates

To detect genetic differences among all selected strains, the genotyping approach through SSR markers was recruited.

In addition to designed SSRs markers, some other primers such as mating types (Inderbitzin et al. 2011), a primer corresponding to histone 4 (Glass and Donaldson 1995) and also some SSR markers from a previous study (Mahiout 2017) were used to explore the divergence of different confirmed *V. alfalfae* isolates (Table 9).

PCR conditions and amplification for genotyping were carried out in a programmable heating block (Geneamp PCR system 9700) according to Table 7-Table 8.

Table 9: Properties of designed SSR primer for genotyping *V. alfalfae*.

Name	Primer Direction	sequences (5 '-> 3')	Predicted Annealing Temperature (°C)	Optimized Annealing Temperature (°C)	Product size(bp)	Source of Primer
Va1.23	Va1.23F	GGGGCTCCTCTTCTTAGCTT	62	55	192	designed
	Va1.23R	TACTCGGGGGAACTATCCGT	62			
Va1.24F	Va1.24F	TGACCCACTTGCACCTATGA	60	55	192	designed
	VA1.24R	GGGTAGGATGGTACGGATGA	62			
VA1.25	VA1.25F	GCACTCAACTGCGAAAAACA	58	57	193	designed
	VA1.25R	GAGAGAGAAAGCGAGCGAGA	62			
Va1.2	Va1.2F	CGCTAGTCTTGGACGGAGAG	64	58	203	designed
	Va1.2R	CACTGAAGGCTCTGACGTTG	62			
Va1.2(4)	Va1.2F(4)	CCACTCCGTACAAGGTGACA	62	55	169	designed
	Va1.2R(4)	CACAAGGTGCTTCCATGTTG	60			
Va1.2'.3	Va1.2'F3	GGGCAAGGCAGTAGTAGCAT	62	57	165	designed
	Va1.2'R3	CCCACCGAGACTGTTATCGT	62			
Va1.2'.5	Va1.2'F5	CGAGGGTCGTCTCTTTGCT	60	57	195	designed
	Va1.2'R5	GCATCTACCAGCGCCTCTAC	62			
Mat1	ALF3	AGCGAGGTAGGCCAGCAGGT	57	50	1116	(Inderbitzin et al. 2011)
	Mat1-1r	CAGTCAGATCCAACCTGCTGGCC	55.5			
Vd M	Vd M2F	GCTATCCGCCGTCTCGCT	60	57	247	(Papaioannou et al. 2013; Glass and Donaldson 1995)
	Vd M1R	GGTACGGCCCTGGCGCTT	62			
M13	M13	GAGGGTGGCGGTTCT	52	50	650 -1800	(Mahiout 2017)
(ATC)5	(ATC)5	ATCATCATCATCATC	37	37	900 – 2000	
(GAA)5	(GAA)5	GAAGAAGAAGAAGAA	37	37	550 – 2200	
(TGTC)4	(TGTC)4	TGTCTGTCTGTCTGTCTGTC	45	45	Diverse band size	

2.1.4.1. Designing of new SSR markers

Verticillium alfalfae genomic sequences were obtained through the Nucleotide database of NCBI. These data are accessible at (https://www.ncbi.nlm.nih.gov/nuccore/?term=verticillium+alfalfae+genomic+sequence). All records were explored one by one; the whole nucleotide sequence of each record was called in FASTA format and divided into several fragments of around 800 - 1000 bp. Each chunk was copied in FASTA format and subsequently pasted into the Simple Sequence Repeat Identification Tool (SSRIT) portal (https://archive.gramene.org/db/markers/ssrtool). In this portal, the maximum number of the motif-length group was set to trimer and the minimum number of repeats was set to 5. After selecting these criteria, the FIND SSRs option was selected and the portal based on the input FASTA sequences data and the regulated options would either suggest some SSRs or would not be able to find any (Figure 27).

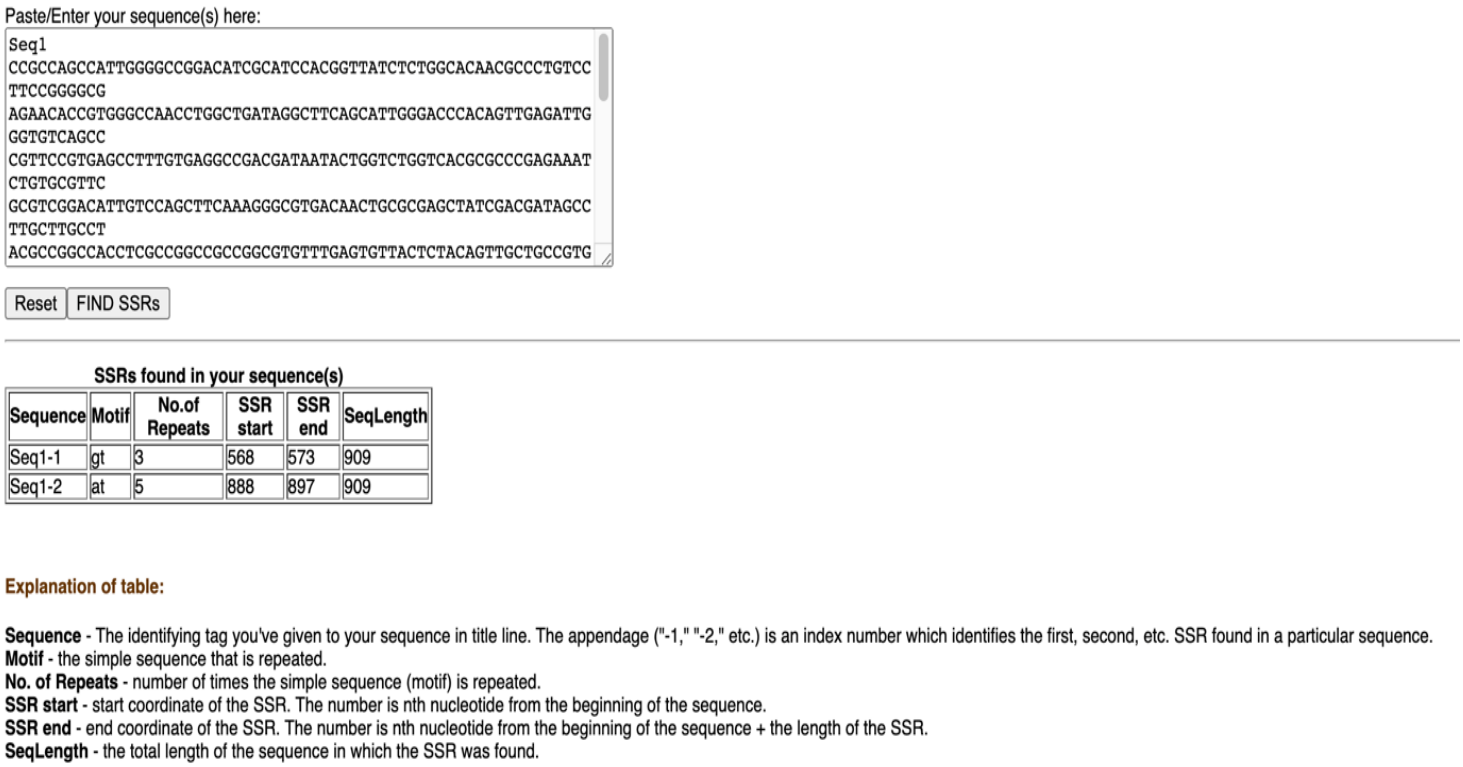

Paste/Enter your sequence(s) here:

```
Seq1
CCGCCAGCCATTGGGGCCGGACATCGCATCCACGGTTATCTCTGGCACAACGCCCTGTCC
TTCCGGGGCG
AGAACACCGTGGGCCAACCTGGCTGATAGGCTTCAGCATTGGGACCCACAGTTGAGATTG
GGTGTCAGCC
CGTTCCGTGAGCCTTTGTGAGGCCGACGATAATACTGGTCTGGTCACGCGCCCGAGAAAT
CTGTGCGTTC
GCGTCGGACATTGTCCAGCTTCAAAGGGCGTGACAACTGCGCGAGCTATCGACGATAGCC
TTGCTTGCCT
ACGCCGGCCACCTCGCCGGCCGCCGGCGTGTTTGAGTGTTACTCTACAGTTGCTGCCGTG
```

Reset | FIND SSRs

SSRs found in your sequence(s)

Sequence	Motif	No.of Repeats	SSR start	SSR end	SeqLength
Seq1-1	gt	3	568	573	909
Seq1-2	at	5	888	897	909

Explanation of table:

Sequence - The identifying tag you've given to your sequence in title line. The appendage ("-1," "-2," etc.) is an index number which identifies the first, second, etc. SSR found in a particular sequence.
Motif - the simple sequence that is repeated.
No. of Repeats - number of times the simple sequence (motif) is repeated.
SSR start - start coordinate of the SSR. The number is nth nucleotide from the beginning of the sequence.
SSR end - end coordinate of the SSR. The number is nth nucleotide from the beginning of the sequence + the length of the SSR.
SeqLength - the total length of the sequence in which the SSR was found.

Figure 27: A scheme of the Simple Sequence Repeat Identification Tool portal and report corresponding to Simple Sequence Repeat Identified throughout the inputted sequences.

If the portal reported any SSR then the sequences flanking the SSR would be copied and past into primer 3 portal (https://www.bioinformatics.nl/cgi-bin/primer3plus/primer3plus.cgi) to design different sets of primer. To have a successful primer design for SSR regions, primer GC content was set to the range of 30%-50%, the maximum difference for T_m between each primer strand was set to the 5 °C and the product size ranges was set to 300 bp maximum.

The designed primers then were blasted by the basic local alignment tool of the NCBI database to check for specific binding with *V. alfalfae* genome and then based on the obtained result the best primer pairs were selected.

If the recommended annealing temperature (by the primer 3 portal) for PCR did not result in a clear band pattern on agarose gel the best annealing temperature for the primer pair was achieved by trial and error.

2.1.5. Analysis of *V. alfalfae* growth

To investigate the effect of temperature on vegetative and reproductive features of strains two parameters were examined: hyphal growth and the amount of produced spores after two weeks.

Small disks (0.8 cm) of mycelium were punched from the border of 2-week-old cultures and inoculated in the center of Petri dishes containing 15 ml PDA. The diameter of the colony was measured at regular intervals for 2 weeks at 20 °C, 25 °C, and 28 °C in the dark.

To evaluate growth of the fungal cultures the radius was measured in two perpendicular directions (Figure 28). Finally, the mean value of two measured radii was calculated for each time point per each Petri dish and used for further analysis.

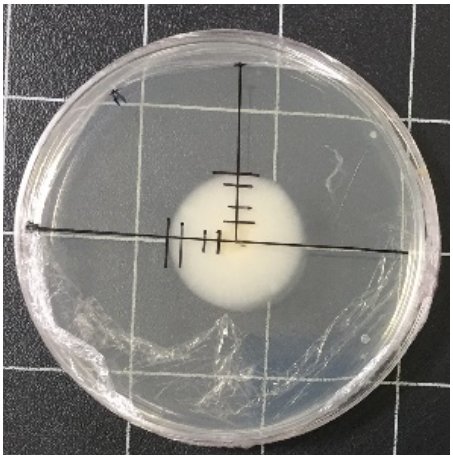

Figure 28: Measurement of radial growth.

After 14 days, 20 mL of sterile water was added to every Petri dish and the surface of the mycelium was rubbed gently with a bent glass Pasteur pipette to release the conidia and their concentration was determined with a Malassez counting chamber.

The study was performed in 3 independent experiments and included 2 independent blocks through split-plot design arranged in RCBD experiments where the whole-plot factor was assigned to temperature (3 separate incubators used for 20 °C, 25 °C, and

28 °C) and split-plot factor was assigned to the fungal strains. In each experiment 3 Petri dishes were used per strain per temperature.

The linear mixed model was used to analyze the effect of temperature and strains on hyphal growth and sporulation as follows (Equation 1):

Equation 1: Mixed linear model used to model the effect of temperature and strains on hyphal growth and sporulation

$$Y_{ijkl} = \mu + \text{Design matrix} + \text{Strains}_i + \text{Temperature}_j + \text{Block}_k + \text{Repeat}_l + \epsilon_{ijkl}$$

where μ is the grand mean of the trait (hyphal growth or spore production), temperatures and different strains were regarded as fixed effects while blocks and repeats were regarded as random effects; then the best linear unbiased estimates (BLUEs) were extracted for all strains using restricted maximum likelihood (RELM).

An analysis of variance (ANOVA) was implemented using the lmer function through the lmerTest package (Kuznetsova, Brockhoff, and Christensen 2017).

The least square means (LSmeans) (Lenth 2016) for each strain was computed based on a function of strain and temperature and the grouping was performed by the Tukey method.

2.1.6. Plant inoculation

M. truncatula seeds were manually scarified with sandpaper (P180) and incubated at 5 °C in Petri dishes between 2 layers of humid filter paper for 2-3 days, then were transferred to room temperature. The germinated seeds were transplanted in Jiffy substrate (jiffy®-7 -31130105-33cm) and then kept in a growth chamber at the conditions described previously. The jiffies were covered with a mini greenhouse for the adaptation process during 3 days after transmission of the jiffies to the growth chamber the mini greenhouse was removed completely however in the two first days the door of the mini greenhouse was opened graduality.

Ten-day-old seedlings were subjected to root inoculation by cutting 1 cm of the bottom of the Jiffy pots containing root tips. They were dipped in conidial suspension (10^6

spores ml^{-1}) prepared from 2-week-old cultures on PDA for 30 minutes, and then transferred to trays covered with moist soil and incubated in the growth chamber. Symptom development was scored regularly on a scale from 0 to 4 as described by Ben *et al*. (Ben et al. 2013) during 4 weeks (Figure 29).

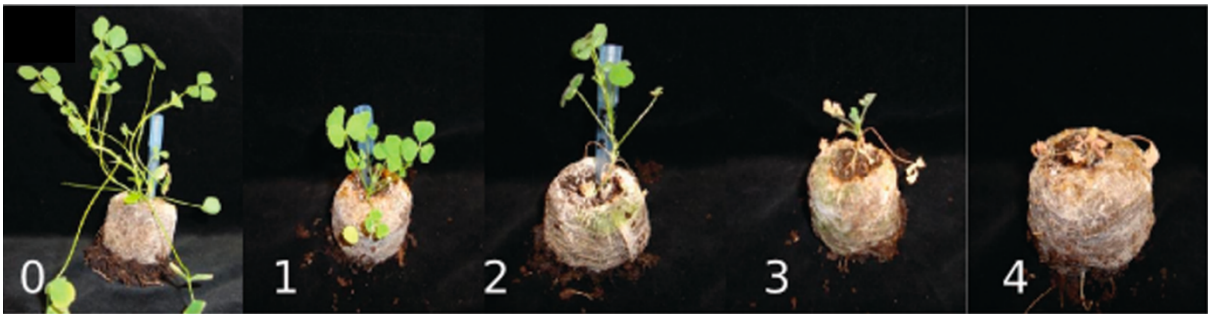

Figure 29: Scale of verticillium wilt symptoms in *Medicago truncatula*.

0 represents when there is no symptom, 1 represents when one young leaf is chlorotic or necrotic, 2 represents when half of the leaves are chlorotic or necrotic, 3 represents when the most leaves are chlorotic or necrotic except the apex leaves and 4 represents the dead plant.

Source: Ben et. al. 2013.

2.1.7. Parameters used to estimate the disease intensity

2.1.7.1. Area Under the Disease Progress Curves

The first parameter used to estimate the disease intensity was Area Under the Disease Progress Curves (AUDPC) which is a measure of quantitative disease resistance that involves sequential disease assessments through a trapezoidal method and linear regression function (Jeger and Viljanen-Rollinson 2001; Hernandez, Crossa, and Castillo 1993). The AUDPC is a handy quantitative review of disease intensity that integrates the time of start and evolution of symptoms (Shaner 1977; Haynes and Weingartner 2004).

In this study the AUDPC was calculated for all of the inoculated plants individually (Figure 30) through the agricolae package (Mendiburu and Yaseen 2017) of the R software (R Core Team 2020). The graphs were drawn using the ggplot2 (Wickham 2016) and lattice (Sarkar 2008) packages.

2.1.7.2. The Maximum Symptom Score

The Maximum Symptom Score (MSS) is the disease score at the last day of symptom scoring (Figure 30). Since there were not many changes in the development of symptoms after 28 days post inoculation, the 28th day was fixed as the last day of symptom scoring.

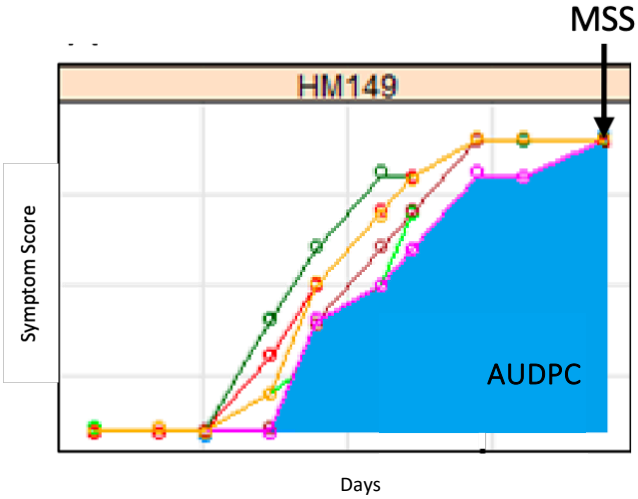

Figure 30: Parameters used to estimate the disease intensity.

The curves represent the progression of the disease symptoms for individual plants of accession Hm149. The blue area represents the Area Under the Disease Progress Curve (AUDPC) of one inoculated individual and the MSS is the score of disease intensity at the last day of symptom scoring (Black arrow). Source: Mazurier,2018.

2.1.8. Pathogenicity test

To determine the pathogenicity of Iranian isolates, a pathogenicity test was applied with these isolates and some other *V. alfalfae* confirmed isolates that were available in the lab (Table 10).

Root inoculation and symptom scoring was performed as described above. The study was carried out in 3 independent experiments each consisting of 2 blocks in augmented block design. The inoculated accessions were selected based on the *M. truncatula* population structure study (Gentzbittel et al. 2019). Two representatives

from each of the 8 population subgroups were chosen (Table 11). The two accessions F83005.5 and A17 were included systematically in all repeats as “check lines” to determine the effects of blocks. Data transformation was applied where the data did not follow the normal distribution.

Table 10: *Verticillium alfalfae* strains used for pathogenicity test.

Strain Name	Origin
2.1.B	Iran (Arak province)
4.3.A	Iran (Hamedan province)
AF1	Iran (Arak province)
Mg2	Iran (Arak province)
V31.2	France (Occitania)
VA107	USA (Radišek, Jakše, and Javornik 2006)
LUC	Great Britain (Radišek, Jakše, and Javornik 2006)

Table 11: *M. truncatula* accessions used for pathogenicity test.

Accession	HapMap ID	Population	Origin
L000049	HM016	SA09707	Tunis
L000154	HM010	SA24714	Italy
L000163	HM001	SA22322	Syria
L000174	HM002	SA28064	Cyprus
L000239	HM012	SA26063	Morocco
L000368	HM008	DZA012.J	Algeria
L000530	HM006	F83005.5	France
L000542	HM014	DZA233.4	Algeria
L000543	HM011	DZA327.7	Algeria
L000544	HM003	ESP105.L	Spain
L000555	HM009	GRC020.B	Greece
L000648	HM013	Salses42B	France
L000651	HM007	Salses71B	France
L000734	HM005	DZA315.16	Algeria
L000736	HM004	DZA045.6	Algeria
L000738	HM101	A17_Varma	Unknown

2.2. Phenotyping

2.2.1. Evaluation of the response of the *M. truncatula* HapMap collection to *Verticillium alfalfae*

The study of response of 242 *M. truncatula* accessions from HapMap collection (Table S. 1) to *V. alfalfae* (phenotyping) was implemented in three independent experiments each consisting of 4 different independent blocks through Augmented block design (Figure 31). The four accessions F83005.5, DZA315.14, DZA45.5, and A17 (for which their response to *V. alfalfae* V31-2 has been already studied in our group, (Ben et al. 2013)) were included systematically in all blocks as “check lines” to estimate the block effects of each repeat and then if necessary, data were corrected either through Least square means (Lsmeans or marginal means) or through Type I sum of squares.
In total, 8442 plants were inoculated and symptom development assessed during the phenotyping process.

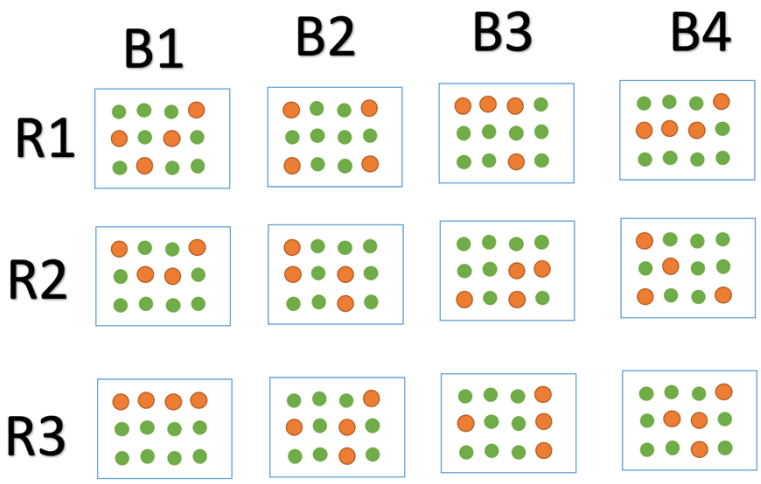

Figure 31: Plan of the augmented block design.

Each dot represents an accession. The orange dots represent the four "Check lines" included systematically in each block. The green accessions are all different from each other.

For data analysis, two approaches were applied in parallel, where all *M. truncatula* accessions were regarded as fixed effects while the blocks and the repeats were

regarded as random effects. Each repeat contained 6 –12 plants per accession while the check varieties were consistently 6 plants per block.

In the first approach, the block effects were estimated at the end of each repeat and the breeding values were adjusted based on block effects. The linear mixed model used in this approach was determined as is shown in Equation 2.

Equation 2: Mixed linear model used to model the corrected values of AUDPC and MSS from Augmented block design and calculate breeding values.

$$Y_{ijk} = \mu + \text{accessions}_i + \text{Block}_j + \text{Repeat}_k + \epsilon_{ijk}$$

While Y_{ijk} is the numerical value of the phenotypic parameter for the i^{th} accession in the j^{th} block of the k^{th} Repeat; μ is the grand mean of the trait (AUDPC or MSS) and ϵ_{ijk} is the residual of the model.

In the second approach, all raw phenotypic data (all blocks within all repeats) were put together and the breeding values were calculated through the following mixed linear model Equation 3.

Equation 3 Mixed linear model used to model the raw values of AUDPC and MSS from Augmented block design and calculate breeding values.

$$Y_{ijk} = \mu + \text{Design matrix} + \text{accessions}_i + \text{Block}_j + \text{Repeat}_k + \epsilon_{ijk}$$

Estimated breeding values related to the traits (AUDPC and MSS) were calculated as BLUEs (Best Linear Unbiased Estimation) using restricted maximum likelihood (RELM); data transformation was deployed whenever it was needed (based on the Shapiro-Wilk test result) and was used in Genome-wide association mapping.

An ANOVA was performed using the lmer function of the lmerTest package (Kuznetsova, Brockhoff, and Christensen 2017).

Grouping of all accessions according to the desired trait was performed by the Tukey method based on the calculated least-square means (LSmeans)(Lenth et al. 2021) of the models as a function of accessions.

To calculate broad sense heritability (H^2) the variance components method was used on raw phenotypic data while the blocks and repeats were regarded as fixed effects and the accessions were regarded as a random effect.

2.2.2. Evaluation of the response of Iranian *Medicago* species to *V. alfalfae* isolates

Iranian *M. truncatula and M. scutellata* (Table S. 2) were root inoculated by Iranian *V. alfalfae* (AF1) and French *V. alfalfae* (V31-2) at 25 °C.
Since the genetic fixation process is a time-consuming procedure, a preliminary study was performed with only one repeat (due to the lack of a sufficient number of seeds). An analysis of variance (ANOVA) was performed using the lm function of the stats package (R Core Team 2020). The least square means (Lsmeans) (Lenth 2013) for AUDPC and MSS were computed and the mean comparison grouping was performed by the Tukey method.

2.3. Genome-wide association study

2.3.1. Genome-wide Association mapping

To fine map the genomic regions of *M. truncatula* with additive effects associated with AUDPC and MSS, TASSEL 5.2.50 was used (Bradbury et al. 2007).
In order to increase the probability of detecting causal SNP-phenotype association, increase the statistical power and to limit the number of false positives, SNPs were filtered with a minimum allele frequency (MAF) of 5% (Marees et al. 2018) and a minimum count to 200 bp which resulted in 5,671,743. Population structure (Q matrix) and the kinship matrix (K matrix) used in this study had been earlier reported by Gentzbittel *et al.* (Gentzbittel et al. 2019).
A total of five GWAS statistical models were tested including General Linear models (GLM) without any correction for population structure (naive model), GLM Q-Model with Q-matrix that considers the correction for population structure (GLM fixed effects

model) and three mixed linear models (K model, Q model and K + Q model). To reduce computing time P3D algorithm (Z. Zhang et al. 2010) was used for mixed models.
In the naive model (the simplest GLM model), only the SNP matrix was used and no correction for population structure was considered as is shown in Equation 4.

Equation 4: The simplest GLM model (naive model) used for association study

$$Y = X\beta + \epsilon$$

where Y represents the observation vectors or breeding values corresponding to the AUDPC or MSS, X is contained SNPs marker matrix, β refers to the unknown vector of allelic effects to be estimated and ϵ is the residuals.
In the GLM Q-Model (GLM fixed effects model) which is the generalized model of the naive model, population structure is incorporated as a fixed cofactor. This model can be conceptually represented as Equation 5.

Equation 5: The GLM fixed-effects model used for association study.

$$Y = X\beta + \epsilon$$

where Y represents the observation vectors or breeding values corresponding to AUDPC or MSS, X is contained SNPs marker matrix and population structure, β refers to the unknown vector of allelic effects to be estimated and ϵ is the model's residuals.
The Mixed Linear Model (MLM) taking into account the ancestry and cryptic relatedness among individuals and also the population structure; the MLM model used in this study can be addressed as Equation 6.

Equation 6: The Mixed Linear Model (MLM) used for association study

$$Y = X\beta + \mathrm{ZU} + \epsilon$$

In this equation, Y represents the observation vectors or breeding values corresponding to AUDPC or MSS, X contains SNPs marker matrix and also population structure (Q matrix) which are fitted as a fixed effect, β is an unknown vector including the effect of alleles at the SNP that has to be estimated, Z represents the known matrices of genetic effects that are fitted as a random effect, and finally ϵ is the model's residuals.

U and ϵ are random effects that should be estimated. U follows standard normal distribution with a mean of zero and variance σ²a (additive genetic variance). On other hand ϵ also follows standard normal distribution with homogeneous variance σ²e (residual variance); so

$$Var\begin{pmatrix} U \\ \epsilon \end{pmatrix} = \begin{pmatrix} G & 0 \\ 0 & R \end{pmatrix}$$

Where G = σ²a.K and R = I.σ²e with K, kinship matrix between individuals. G and R in this formula represent the covariance matrix for the random effect and the residuals in the mixed model, respectively.

For the K model the K matrix (Kinship matrix) was used as a random effect (Equation 6), whereas for the Q-Model, the Kinship identity matrix was used as a K matrix regarded as a random effect (Equation 6). Finally, for the K + Q model, both the K matrix (as random effects) and the Q matrix (as fixed effects) were used (Equation 6). All types of modeling and calculations were performed on the calculation cluster of the GENOTOUL-Bioinfo platform (http://bioinfo.genotoul.fr/).

To evaluate and select the best fitted model in this study among all of the models, the Q-Q plot (D. Turner 2018) was computed for each model separately and the best fitted model for each trait was selected based on the Q-Q plot result.

To illustrate the association of significant SNPs with AUDPC and MSS the Manhattan plot was outlined for each trait separately. For plotting the Manhattan graph the association score of SNPs were calculated through p-values of all SPNs as is shown in Equation 7

Equation 7: Calculation of SNPs association score.

$$\text{SNPs association score} = -\log_{10}(\text{p values})$$

To correct for multiple testing problem, Bonferroni and False Discovery Rate (FDR) corrections were used. Multiple testing adjustment was conducted at α = 0.05 to reduce type II error and also to correct for the effective turn of independent tests.

2.3.2. Selection of candidate genes and primer design

The suggestive line which was proposed by the qqman R package (D. Turner 2018) was very close to the FDR, thus it was selected as the main threshold for selecting the significant candidate SNPs. So, SNPs with association score values equal or greater than 5 were selected and the regions 10 kb upstream and downstream of these SNPs were explored through the jbrowser site (Buels et al. 2016). Genes with functional annotation associated to defense pathways which were located within these areas were considered as possible candidate genes. In addition; two genes that encode hypothetical proteins were included for further steps because of their high association score.

The full sequence of selected candidate genes was obtained through *(*http://www.medicagohapmap.org/fgb2/gbrowse/mt40/*)*. Primers for qRT-PCR were designed using the primer3plus web interface (Untergasser et al. 2012). in order to increase the specificity of the amplification and to avoid any DNA amplification in qRT-PCR, the primers were designed based on exon-exon junction. Primer GC content was set to 50%, the minimum, optimum and maximum temperature for primer T_m was set to 56 °C, 58 °C and 60 °C, respectively; the maximum difference for T_m between sense and antisense primer strand was set to 1 °C and the product size range was set to 150 - 200 bp. In a first step 10 different pairs of primers were designed for each gene.

The designed primers were checked for stability (forming of secondary structures) through the NCBI database and Primer3 web interface also in terms of specific amplification through blast against the A17 genome (http://www.medicagohapmap.org/tools/blastform).

Among all designed primer pairs, for each gene, one primer pair which represented the highest stability was selected and ordered from Thermo Fisher Scientific France for synthesis.

2.4. Gene expression study

2.4.1. Sample preparation

Gene expression in *M. truncatula* roots was studied with material from three independent experiments. Twelve of the most susceptible and resistant accessions were selected based on the Tukey grouping of Lsmeans values of phenotyping experiments.

In order to easily access the roots and reduce the stress on the roots during the sampling, instead of jiffy substrate, plug trays filled with a mixture of sand-perlite (2/3 sand, 1/3 perlite), was used as a substrate for growth of germinated seeds. Germinated seedlings were transferred to plug trays and grown for 10 days in a phytotron with 25 °C day /23 °C night and a photoperiod of 16h.

The plug trays were kept on trays containing 300 ml of liquid Fahraeüs medium (Table S. 8) and were regularly irrigated. For the adaptation process, the trays were covered with cellophane; in the two first days.

10-days old plants were root inoculated as described before, after cutting the roots that were grown out of the plug trays bottom (Figure 32).

For RNA sampling roots and arial parts were harvested 0, 4, 24 and 96 hours after inoculation and mock inoculation; subsequently the samples were pooled in a susceptible and a resistant group for each time point. The harvested samples were frozen in liquid nitrogen and then transferred to -80 °C.

To confirm the success of the inoculation wilt symptoms were followed in additional unharvested plants.

For the sake of simplicity and to avoid mistakes, each condition of RNA sampling was given a number (Table S. 9).

Figure 32: State of 10-day old seedlings in plug tray (Alvéole) before inoculation.

2.4.2. RNA extraction

Total RNA was extracted was extracted manually with the TRIzol protocol. Frozen root samples were ground to a fine powder with a mortar and pestle under liquid nitrogen. Under the fume hood, 1 mL of TRIzol® (reference 15596026) was added to about 250 mg of ground tissue (on the ice while the samples were still frozen), and the samples were vortexed for 15 seconds to have a homogenous solution. Then in order to break down the nucleoprotein complexes, the samples were incubated for 15 minutes at 37° C. In the next step, 200 µL of chloroform were added to each sample and the tube was vortexed for 15 seconds to obtain a homogenous solution. These homogenous solutions were centrifuged for 15 minutes at 12,000 g at 4 °C and subsequently, the supernatant of each sample was transferred into new 1.5 ml microtubes that had previously been cooled on ice. Thereafter, 500 µL of isopropanol were added and the tubes were homogenized gently by inversion and left to incubate for 15 minutes on

ice. This step was followed by centrifugation for 20 minutes at 8000 g at 4 °C then the supernatant was removed. Since the roots are rich in polysaccharides in order to purify the RNA, the pellet was resuspended in 20 µL of a 2.5 M lithium chloride solution (stock solution consisting of 7.5 M $LiCl_2$ in 50 mM EDTA solvent, pH 8) and the samples were left overnight on ice in the refrigerator. This step was followed by centrifugation for 20 minutes at 12,000 g at 4 °C and then the supernatant was discarded. One mL of 70% ethanol was added to the pellet and the tubes were centrifuged for 10 minutes at 8000 g at 4 °C. Finally, the ethanol was removed and the pellets were dried for 30 minutes in air before being resuspended in 30 µL of DEPC (Diethyl Pyrocarbonate) treated water. The concentration and quality of extracted RNA was assessed with a nanodrop (NanoDrop nd-1000 Spectrophotometer) and samples were stored at -80 °C.

2.4.3. RNA Purification

Some samples which were extracted with TRIzol only in a first step had to be purified by Lithium chloride precipitation. To RNA in a volume of 30 µL, 15 µL of a Lithium chloride solution (7.5 M $LiCl_2$ in 50 mM EDTA pH8) was added and the samples were kept overnight at 4 °C on ice. This step was followed by centrifugation at 12000g for 20 min. The supernatant was discarded and the final step consisted of a washing step with cold 70% Ethanol as described above, before resuspending them in 30 µL of DEPC-treated water.
Finally, the quality of purified RNA was assessed with a nanodrop (NanoDrop ND-1000 Spectrophotometer), and samples stored at -80 °C.

2.4.4. cDNA synthesis

The ImProm-II ™ Reverse Transcription System kit (Promega, A3800) was used to perform the reverse transcription reaction and synthesis of cDNA.
Since secondary structures of RNA will lower the yield of cDNA synthesis, the aim in the first step is to relax the RNA strand and then allow for the hybridization of RNA

template and cDNA primer. To synthesize cDNA the oligo $(dT)_{15}$ was used as a cDNA primer.

On ice, 1µg of purified RNA and 0.5 µg (= 1µL) of oligo $(dT)_{15}$ were combined in Nuclease-Free Water in a final volume of 5µL for each reaction (Table S. 10, Table S. 11, Table S. 12). One positive control (1.2kb Kanamycin Positive Control RNA) and one negative control (No-Template) included in the kit were used to check the quality of cDNA synthesis (Table 12). These mixtures were incubated in a preheated 70 °C heat block (Geneamp PCR system 9700) for 5 minutes and then immediately chilled on ice for at least 5 minutes.

The reverse transcription reaction mixtures were prepared in 15 µL reaction volume by combining the components of the ImProm-II™ Reverse Transcription System in a sterile 1.5 ml microcentrifuge tube on ice (Table 13 Table 14).

The reverse transcription reaction was prepared as a master mix for all samples. They were vortexed softly to mix, and then were dispensed into the reaction tubes which contained 5µL of target RNA and the oligo $(dT)_{15}$.

The final step for complementary DNA (cDNA) synthesis was then carried out by incubating the samples at preheated 25 °C for 5 minutes (Annealing phase), and 42 °C for 55 minutes (Extension phase); this step was followed by 70 °C for 15 minutes to inactivate Reverse Transcriptase enzyme.

Table 12: Reaction mix for the positive and negative control of synthesis/combination of Target RNA and oligo $(dT)_{15}$.

Negative Control	volume (µL)		Positive control	volume (µL)
Experimental RNA (1µg/reaction)	0		1.2kb Kanamycin (1µg)	2
$Oligo(dT)_{15}$	1		$Oligo(dT)_{15}$	1
(0.5µg/reaction) (µL)			(0.5µg/reaction) (µL)	
Nuclease-Free Water	4		Nuclease-Free Water	2
Total (µL)	5		Total (µL)	5

Table 13: Reaction mix for the synthesis of complementary DNA for an Experimental reaction and Negative control.

Experimental Reaction	Con	volume (µL)		Negative Control	Con.	volume (µL)
Nuclease-Free Water (QSP 15µL)	-	5.5		Nuclease-Free Water (QSP 15µL)	-	6.5
ImProm-II™ 5X Reaction Buffer	5X	4		ImProm-II™ 5X Reaction Buffer	5X	4
MgCl2	3.75 mM	3		MgCl2	3.75 mM	3
dNTP Mix (final concentration 0.5mM each dNTP)	0.5mM	1		dNTP Mix (final concentration 0.5mM each dNTP)	0.5mM	1
Recombinant RNasin® Ribonuclease Inhibitor (optional)	1u/µL	0.5		Recombinant RNasin® Ribonuclease Inhibitor (optional)	1u/µL	0.5
ImProm-II™ Reverse Transcriptase	-	1		ImProm-II™ Reverse Transcriptase	-	-
Total	-	15		Total	-	15

Table 14: Reaction mix for the synthesis of complementary DNA for a Positive control.

Experimental Reaction	Con	volume (µL)
Nuclease-Free Water (QSP 15µL)	-	3.7
ImProm-II™ 5X Reaction Buffer	5X	4
MgCl2	6 mM	4.8
dNTP Mix (final concentration 0.5mM each dNTP)	0.5mM	1
Recombinant RNasin® Ribonuclease Inhibitor (optional)	1u/µL	0.5
ImProm-II™ Reverse Transcriptase	-	1.0
Total	-	15

2.4.5. Quantitative real-time PCR (qRT-PCR)

2.4.5.1. Primer efficiency of selected primers

The PCR primers efficiency is the pivotal criterium of the quantitative polymerase chain reaction (qPCR) assay performance. Inaccuracy in its estimation will lead to overestimation or underestimation of calculated fold changes (Svec et al. 2015). As a general rule, the efficiency of PCR primers for each set of newly designed primers, especially when $\Delta\Delta C_T$ method is used as a relative quantification approach for qPCR, should always be determined. In the $\Delta\Delta C_T$ method, it is an accepted assumption that the primers' efficiencies between the gene(s) of interest and the housekeeping gene(s) (endogenous control, reference gene) are in a similar range (generally between 90-110%) (Thornton and Basu 2011).

Theoretically, in each PCR cycle, the copy number of desired amplicons is doubled during the PCR exponential (logarithmic) phase, which would correspond to an efficiency of 100%.

The primer efficiency is generally determined through qPCR with a serial dilution of the cDNA generated from RNA this procedure is known as a standard curve.

In this study, 1.5 µL of cDNA from each condition were mixed, and dilutions of 50, 20, 8 and 2 ng. μL^{-1} were prepared from this mix and were used in the qRT-PCR assays with all primer pairs.

qRT-PCR reactions were performed in the QuantStudio™ 6 Flex Real-Time PCR System (Applied Biosystems). The EurobioGreen® mix qPCR 2X Lo-Rox Kit (Eurobio Scientific, Reference GAEMMX02L-8T) was used (Table 15). At least two technical repeats were performed on all samples. At the end of the PCR program, one cycle was added for the melting curve. The PCR program is shown in Table 16.

If the difference between the C_T of the two technical repeats was more than one unit, the qRT-PCR was repeated. The primer efficiency was calculated in excel as follows.

Table 15: qRT-PCR mix for primer efficiency and gene expression study.

Reagent	Concentration	Volume (µL)
EuribioGreen Mix	2x	5
Primer forward	10 µM	0.4
Primer Reverss	10 µM	0.4
water	-	1.2
cDNA	(50, 20,8,2) ng. μL^{-1}	3

Table 16: qRT-PCR program used for gene expression.

Number of cycles	Temperature	Time
1 cycle	95 °C	3 min
40 cycle	95 °C	15 sec
	60 °C	30 sec
1 cycle (Melting curve)	95 °C	15 sec
	60 °C	15 sec
	95 °C	15 sec

The average C_T values of the two replicates were calculated as well as the logarithm of each dilution. Subsequently, the logarithm values were plotted against the average C_T values in the scatter plot. Thereafter through excel a trendline and the equation corresponding to the chart were added (Figure S. 2). The shown equation by excel comprises the slope which is used to calculate the primer efficiency.

Equation 8 is used to calculate primmer efficiency. As a general rule, the primer efficiency is always presented as a percentage.

Equation 8: Primer Efficiency

$$\% \text{ Efficiency} = \left(10^{(-1/Slope)} - 1 \right) \times 100$$

Normally, the accepted slope is defined as (−3.6 ≥ slope ≥ −3.3) and approved primer efficiency is in a range of 90% - 110%. Theoretically primer efficiency of 90% - 110% implies that the polymerase enzyme is performing at full capacity and efficiency higher than 110% or less than 90% addresses the existence of PCR inhibitors in samples or unspecific amplification. However, the primer efficiency can be improved by some

modifications in annealing temperature or primer concentrations. By calculating the primers efficiency, primer pairs that showed acceptable efficiency were selected and used for the study of gene expression.

2.4.5.2. Analysis of gene expression

The qRT-PCR reactions with cDNA from roots were performed in the QuantStudio™ 6 Flex Real-Time PCR System (Applied Biosystems). The EurobioGreen® mix qPCR 2X Lo-Rox Kit (Eurobio Scientific, Reference GAEMMX02L-8T) was used with 10ng of cDNA per reaction (Table 15). All samples were subjected to two technical repeats. Two housekeeping genes, *Medtr2g008050* (Actin) and *Medtr4g097170* (H3L), were used as internal controls. The ΔC_T values were normalized against the harmonic mean of these two housekeeping genes. The qRT-PCR program is shown in (Table 16). The primers used in these qRT-PCRs are shown in Table 17.

Data analysis was performed with the Design & Analysis software (V.2.4.3) and ΔC_T, $\Delta\Delta C_T$ and fold change were calculated in the Excel program.

Finally, to verify whether the difference in gene expression levels in each time point between susceptible and resistant pools are statistically significant or not; the paired T-test was implemented on the $\Delta\Delta C_T$ of each repeat.

Table 17: Primers used for gene expression study.

Gene (v4.0)	sequence of forward primers (5'-> 3')	sequences of reverse primers (5 '-> 3')
MEDTR1g042280	CCTTCTTGGACCCAGTCTCG	CAGAAAACCCCGAGAGTGCA
MEDTR1g042160	ACTCGGAGCCTTACGTTCTT	TCCTAACTGGTCGACTGCAC
MEDTR4g023000	TCTCACGCTGCAGCAGTAAA	CCGAGACGTTGCTTCTCTGT
MEDTR8g075240	ATGCACCTGGTGTTCCCATT	CCTGGATGGTCGACGAAGAA
MEDTR8g075320	CGGTGTTCGCGGTATCGATA	GCATCAGCTTTTAGCCCAGC
MEDTR8g075340	GGGAGATTCTGCGAGAGTGG	GGCTTCTGCTCCAGGGTAAA
MEDTR8g075550	CCACGCGCTTATAGCTATGC	TGCCCAAATGTCCACTCCAA
MEDTR8g102470	TGTCACTCAATCGACGCTCC	TCTCCTCCGGCGAATATTGC
MEDTR1g087500	AACTGCTCCGTCCTTCGATG	ATAGCAGCATCGCGAGCTTT

IV - Results

IV.1.Characterization of Iranian *V. alfalfae*

1.1. Isolation of strains and primary selection of *Verticillium alfalfae*

Alfalfa plants (*Medicago sativa*) samples suspected of the *Verticillium* infection (Figure 33) were collected from different provinces and regions of Iran e.g., Arak, Hamedan, Urmia, Isfahan, Yazd, Karaj and Tehran during two prospections in Iran in 2017 and 2018. Fungal isolates were obtained on PDA medium from dried stems after surface sterilization and purified by successive subculturing.

Figure 33: Typical symptom of Verticillium wilt of an affected alfalfa plant in the fields in Iran.

A total of 94 pure isolates were obtained after the first isolation process. The color of some fungal cultures changed over time from white to milky yellow, gray and black.

To ensure purity of the cultures, monospore cultures were prepared from isolates. The same trend was observed even within monospore cultures (Figure 34).

The isolation continued by the visual screening of monospore cultures on Water Agar Medium, observation of the typical conidiophores led to the identification of 16 putative *Verticillium* isolates (Figure 35). As with initial isolates, monospore cultures of all Iranian *Verticillium* developed pigmentation on PDA medium, in contrast to the French strain V31.2.

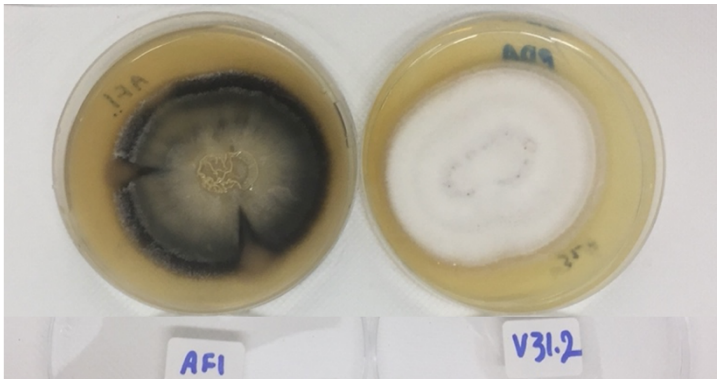

Figure 34: Phenotypic comparison of mycelium of Iranian (left) and French (right) *V. alfalfae* on PDA after 3 weeks.

Figure 35: Observation of *V. alfalfae* hyphae and conidiophores on the evacuated part of Water Agar media.

1.2. Molecular identification of fungal isolates

Sixteen putative *V. alfalfae* isolates were analyzed by PCR with the *V. alfalfae* specific primer (AlfF/AlfD1r) and *V. nonalfalfae* specific primer (NOF/NonUR). Amplification with AlfF/AlfD1r resulted in the expected size of 1060 bp for all *V. alfalfae* strains (Figure 36.A) and amplification with NOF/NonUR resulted in 1310 bp for *V. nonalfalfae* strain (Figure 36.B). The ITS universal primer (ITS1/ITS4), was used as a control for DNA quality, amplification resulted in a DNA band size around 541 bp for all samples (Figure 36.C).

Thus, the presence of *V. alfalfae* in alfalfa fields was confirmed for 3 regions of Iran (Figure 37). Seven isolates were selected among confirmed Iranian *V. alfalfae* (when isolates were obtained from very close areas, only one representative sample was selected); Table 18 shows the locations of sampling, the names given to these confirmed isolates and some other complementary information).

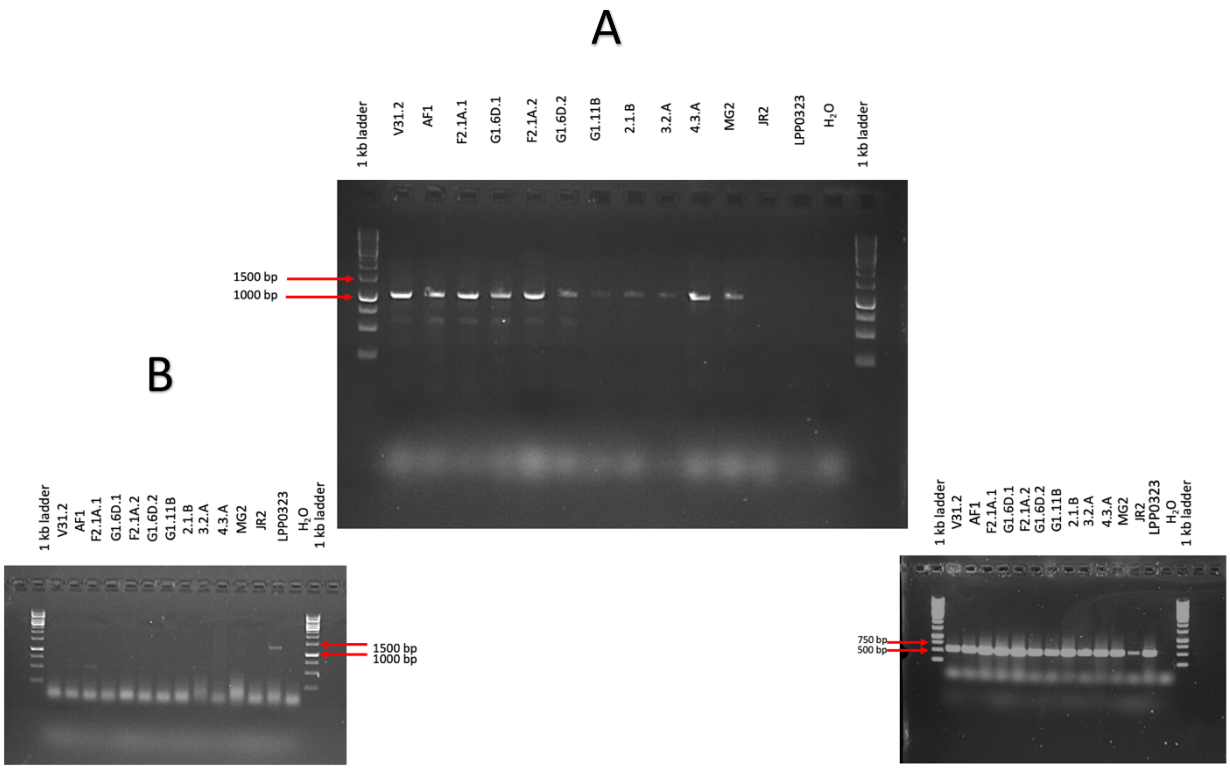

Figure 36: Polymerase chain reaction amplicons generated with Universal and species-specific primer pairs.

A: Amplicons generated with *V. alfalfae* specific primer (AlfF/AlfD1r), Annealing temperature: 62 °C, Expected Band Size: 1060 bp. B: Amplicons generated with the *V. nonalfalfae* specific primer (NOF/NonUR), Annealing temperature: 65 °C, Expected Band Size: 1310 bp. C: Amplicons generated with the ITS universal primer (ITS1/ITS4) Annealing temperature: 50 °C, Expected Band Size: 541 bp. The gel was visualized on a 1% (w/v) and 1.5% (w/v) agarose gel for ITS and the species-specific primer pairs respectively.

Figure 37: Provinces of Iran where diseased alfalfa plants were sampled.

The green stars show the provinces where the presence of *V. alfalfae* was confirmed by PCR while the red stars show the provinces where the sampled isolates were not confirmed as *V. alfalfae*.

Adapted from: Pešić et al., 2014.

Table 18: Names and origin of *V. alfalfae* isolates.

Sampling site (Province)	PCR amplification with *V. alfalfae*-specific primers	Name of Isolate	Selected for further studies
Arak (Iran)	+	2.1.B	+
		3.2.A	+
		AF1	+
		MG2	+
Hamedan (Iran)	+	4.3.A	+
Isfahan (Iran)	-	-	-
Karaj (Iran)	-	-	-
Tehran (Iran)	+	F2.1A.1	-
		F2.1A.2	+
		G1.11B	-
		G1.6D.1	+
		G1.6D.2	-
Urmia (Iran)	-	-	-
Yazd (Iran)	-	-	-
Occitania (France)	+	V31.2	+

1.3. Genotyping of *V. alfalfae* isolates

1.3.1. Designed SSR primers

In an attempt to search for molecular differences between the isolates (Iranian and French) a preliminary analysis with primers usually used for genotyping was performed. Seven primers for the amplification of microsatellites or Single Sequence Repeats (SSR) were designed based on the *V. alfalfae* VaMs. 102 genome. The sequences and properties of the designed primers are shown in the material and method section (Table 9).

.

In addition to these designed SSR primers, other primers described for differentiating between mating type of *Verticillium* strains or for other pathogenic fungi were used for genotyping. Table 9 shows the optimized temperatures for these primers.

Generally, amplification with all these primers did not reveal any differences between *V. alfalfae* isolates (Figure 38 - Figure 39). However, Primers Va1.23F/ Va1.23R, Va1.2'F3/ Va1.2'R3, VA1.25F/ VA1.25R, Va1.2F/ Va1.2R, Va1.24F/ VA1.24R, Va1.2'F5 / Va1.2'R5, Va1.2F(4)/Va1.2R(4), Vd M2F/ Vd M1R, ALF3/Mat1-1r, M13,(ATC)5 and (GAA)5 revealed specific amplification of *V. alfalfae* but not of *V. dahliae* strain JR2. It would be interesting to use them with more *V. alfalfae* strains and other *Verticillium* species in order to determine if they can be used as species-specific primers.

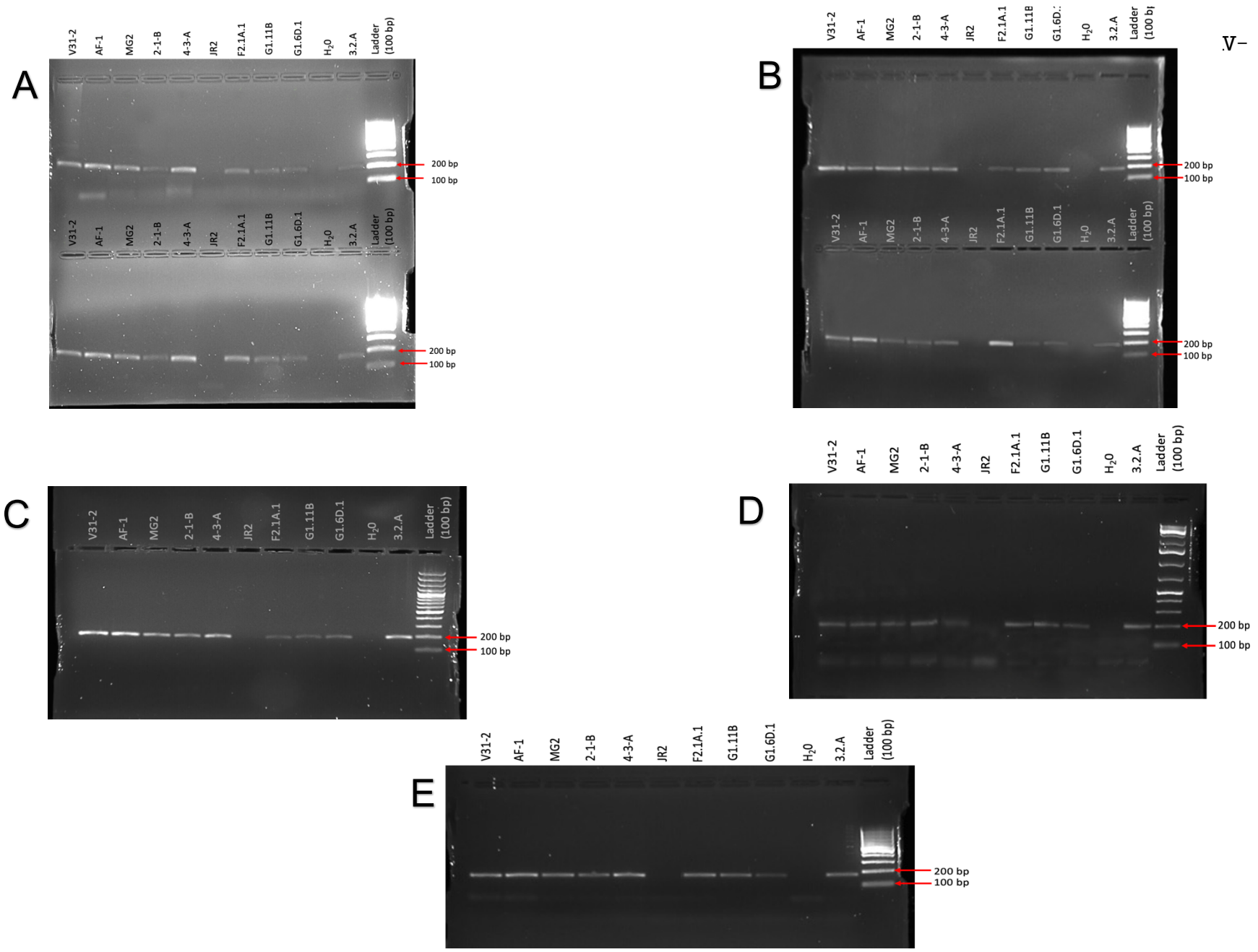

Figure 38: Electrophoresis results corresponding to *V. alfalfae* genotyping (The designed SSR Primes).

A : Top : Va1.23F/ Va1.23R(192 bp), Bottom : Va1.2'F3/ Va1.2'R3 (165 bp);B : Top : VA1.25F/ VA1.25R(193 bp), Bottom: Va1.2F/ Va1.2R(203bp) ; C : Va1.24F/ VA1.24R (192 bp); D : Va1.2'F5 / Va1.2'R5 (195 bp) ; E:) Va1.2F(4) / Va1.2R(4))-(169 bp)

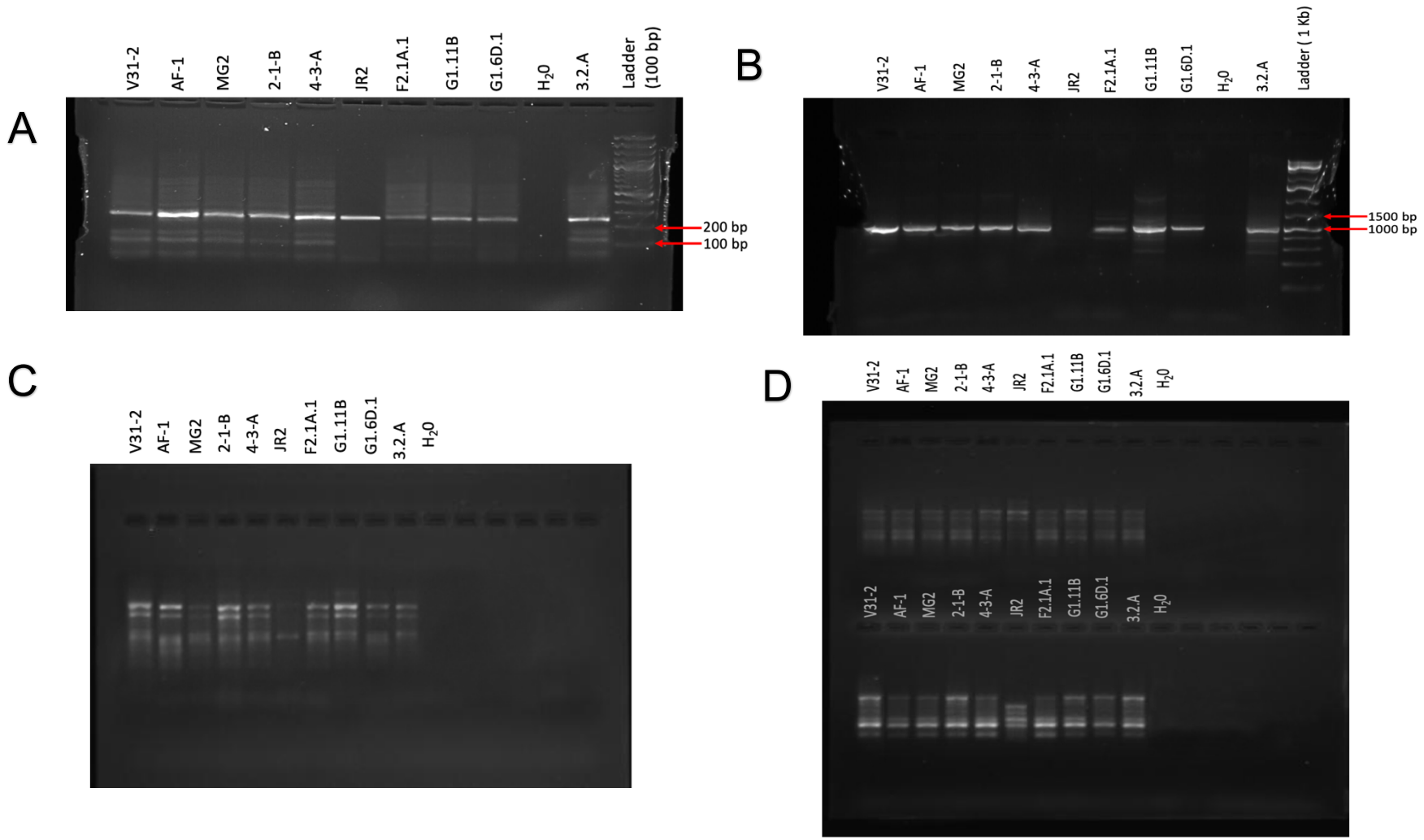

Figure 39: Electrophoresis results corresponding to *V. alfalfae* genotyping (The Primes were taken from other articles).

A: Vd M2F/ Vd M1R (247bp); B: ALF3/Mat1-1r (1116 bp); C: Top: M13; D: Top: $(ATC)_5$– Bottom: $(GAA)_5$.

1.4. Growth properties of *V. alfalfae* isolates

To investigate vegetative and reproductive features of the newly obtained *V. alfalfae* isolates, the 7 selected Iranian isolates and the French isolate V31.2 were characterized (Table 18). Two parameters were examined at 3 different temperatures (20 °C, 25 °C and 28 °C); hyphal growth and the amount of produced conidia after two weeks.

Radial growth of all Iranian *V. alfalfae* isolates and the French strain V.31-2 on PDA medium showed similar behavior for all isolates with linear growth for up to two weeks. Growth was best at 25 °C and very poor at 28 °C (Figure 40).

Statistical analysis by ANOVA shows a significant effect of both strain and temperature on growth rate (Table 19). Grouping by Lsmeans based on the Tukey test shows that the Iranian strains are all in one group and the French strain in a distinct group for vegetative growth (Figure 41), and that 25 °C is the best temperature for all isolates, followed by 20 °C; at 28 °C no differentiation was revealed within the strains. Compared to the French strain, the Iranian isolates grew less at all 3 temperatures.

Assessment of *in-vitro* sporulation also showed a significant effect of strain and temperature as well as a significant interaction strain × temperature as confirmed by ANOVA (Table 20). Again, Lsmeans grouping showed that except at 28 °C where no distinct difference between strains can be observed, the Iranian isolates are all in a group distinct from the French strain, with 25 °C as the best temperature for all (Figure 42). However, in contrast to hyphal growth where the French isolate had higher growth rates than the Iranian ones, sporulation of the Iranian isolates was superior to that of the French strain.

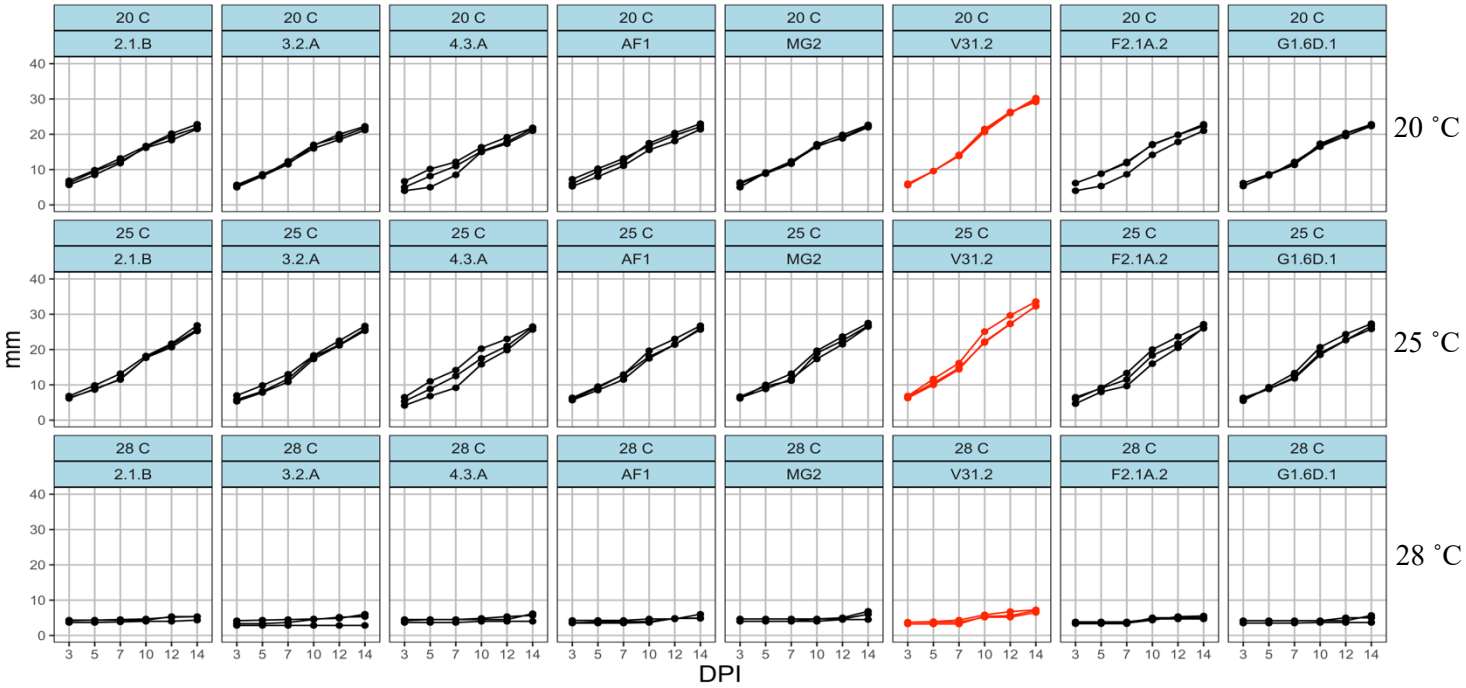

Figure 40: Radial growth of Iranian and French strains at three temperatures.

Fungal samples were cultured on PDA and grown in darkness. The growth was measured as radius during 14 days at specified intervals. The red curves represent the French isolate. Curves show mean values of 3 independent experiments, each with 3 Petri dishes.

Table 19: Analysis of variance of the effect of temperature and fungus strains on radial growth

Type III Analysis of Variance Table with Satterthwaite's method

	Sum Sq	Mean Sq	NumDF	DenDF	F value	Pr(>F)
Strain	2047	292.4	7	155.2	8.3372	1.254e-08 ***
Temperature	38688	19344.0	2	1584.2	551.5665	< 2.2e-16 ***
Strain:Temperature	686	49.0	14	1584.2	1.3965	0.1465

Signif. codes: 0 '***' 0.001 '**' 0.01 '*' 0.05 '.' 0.1 ' ' 1

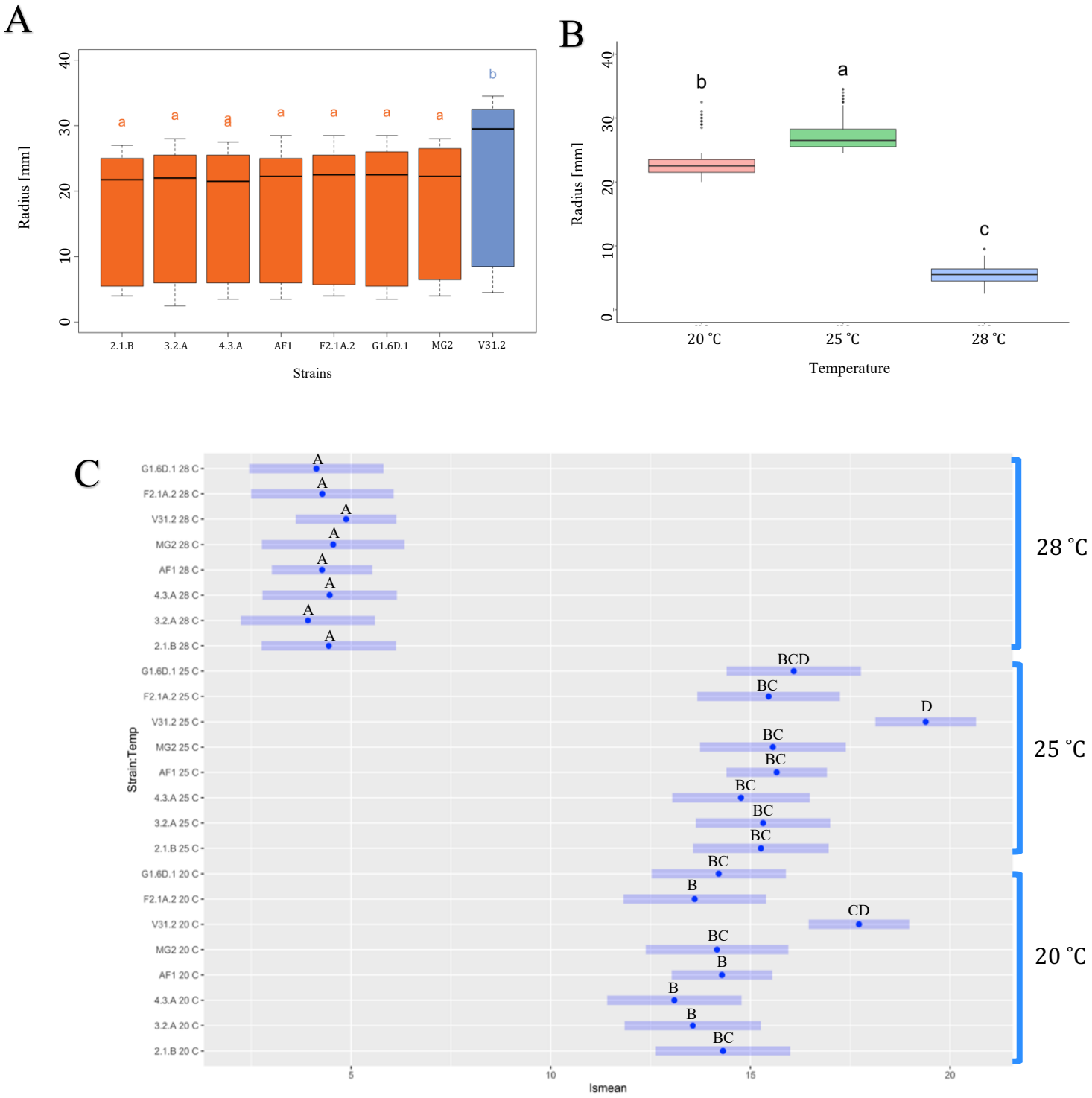

Figure 41: Radial growth of *V. alfalfae* strains at 20 °C, 25 °C and 28 °C after 14 days of growth on PDA, analyzed by Tukey's test.

A: Boxplot of strains' effect on radius. B: Boxplot of temperatures' effect on radius. The letters represent distinct groups based on the Tukey's test. C: Grouping of Lsmeans values of the fungal strains as a function of strain and temperature on radial growth, 95% confidence interval for their difference according to the factor level. The units are in millimeter.

Table 20: Analysis of variance of the effect of temperature and strain on sporulation.

Type III Analysis of Variance Table with Satterthwaite's method

	Sum Sq	Mean Sq	NumDF	DenDF	F value	Pr(>F)
Strain	4957	708	7	54.8	106.1	< 2e-16 ***
Temperature	17061	8531	2	13.2	1278.3	8.3e-16 ***
Strain: Temperature	2390	171	14	54.8	25.6	< 2e-16 ***

Signif. codes: 0 '***' 0.001 '**' 0.01 '*' 0.05 '.' 0.1 ' ' 1

Table 21: Spore production (million spores /mL, ±SE) of *V. alfalfae* at three temperatures.

Mean values are the means of 3 independent experiments each in triplicate.

Strain	Mean_20 °C	Mean_25 °C	Mean_28 °C
2.1.B	38.79 (±*1.00*)	56.69 (±*4.70*)	3.66 (±*0.12*)
3.2.A	36.63 (±*1.29*)	52.07 (±*2.09*)	3.12 (±*0.38*)
4.3.A	38.02 (±*0.21*)	51.98 (±*0.82*)	3.32 (±*0.20*)
AF1	40.10 (±*1.68*)	54.24 (±*1.74*)	3.17 (±*0.23*)
F2.1A.2	36.46 (±*1.96*)	53.62 (±*2.29*)	2.63 (±*0.31*)
G1.6D.1	38.33 (±*0.82*)	53.14 (±*0.46*)	3.09 (±*0.08*)
Mg2	37.80 (±*1.16*)	52.74 (±*0.53*)	3.23 (±*0.08*)
V31.2	13.19 (±*1.38*)	23.84 (±*1.04*)	2.57 (±*0.16*)

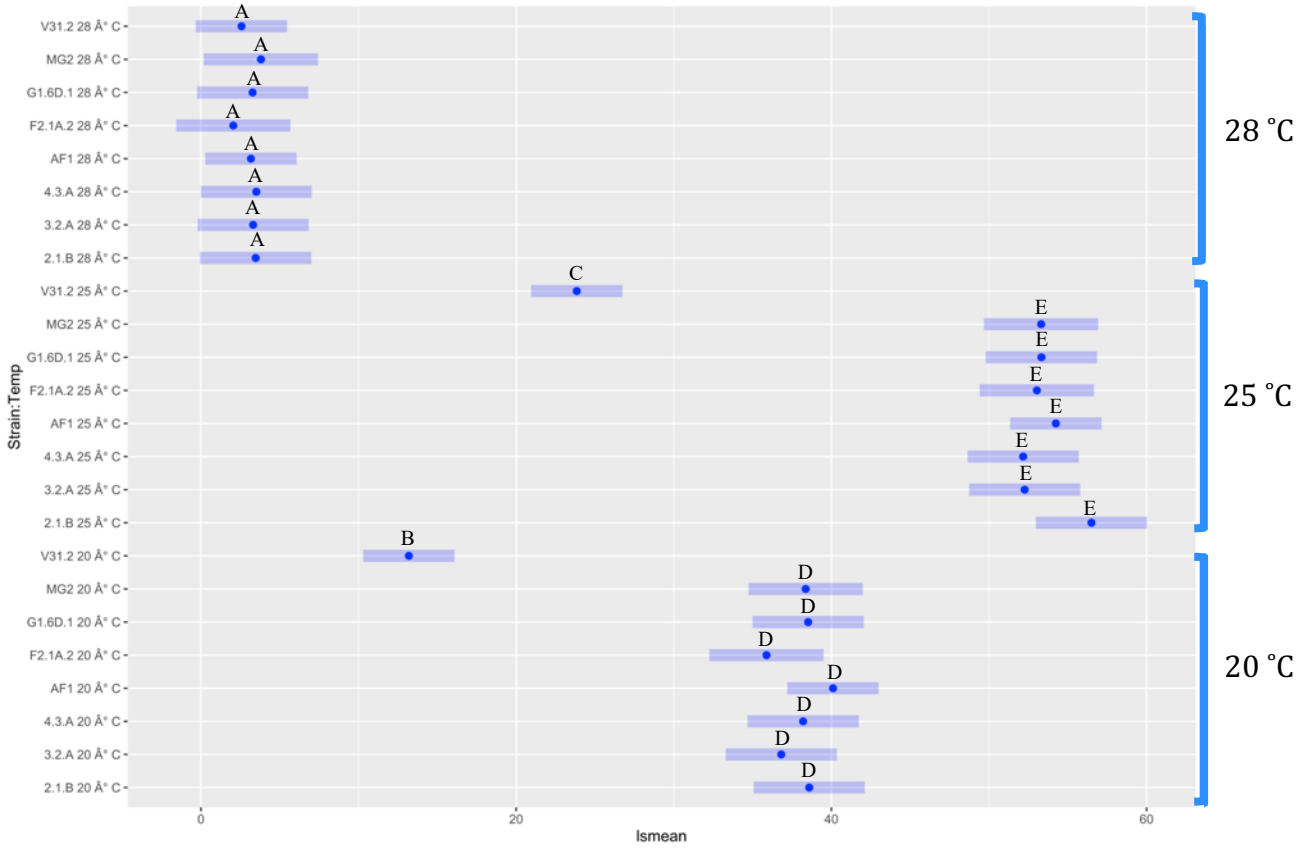

Figure 42: Sporulation of *V. alfalfae* strains at 20 ˚C,25 ˚C and 28 ˚C after 14 days of growth on PDA, analyzed by Tukey's test.

Grouping of Lsmeans values of the fungal strains as a function of strains and temperature on sporulation and 95% confidence interval for their difference according to the factor level. The units are in million spores per milliliter.

1.5. Pathogenicity test

A first experiment to check for the pathogenicity of 4 Iranian isolates and 3 other *V. alfalfae* selected from our lab collection was performed to select one Iranian isolates for further steps, with 16 *M. truncatula* accessions (Table 11) as described in M&M. Symptoms were scored regularly (Figure S. 1) and MSS and AUDPC were computed at the end of the experiments.

After correcting the data for block effects through the mixed linear model, the analysis of variance confirmed the effect of accessions and strains toward the AUDPC and MSS (Table 22- Table 23).

Table 22: Analysis of variance of the effect of fungal strain and *M. truncatula* accession on AUDPC.

Type III Analysis of Variance Table with Satterthwaite's method

	Sum Sq	Mean Sq	NumDF	DenDF	F value	Pr(>F)
Strain	0.0005903	0.00009838	6	132.28	8.3273	1.385e-08 ***
Accession	0.0099381	0.00062113	15	306.51	108.3559	< 2.2e-16 ***
Strain: Accession	0.0011615	0.00001263	90	306.51	2.246	0.094

Signif. codes: 0 ‘***’ 0.001 ‘**’ 0.01 ‘*’ 0.05 ‘.’ 0.1 ‘ ’ 1

Table 23: Analysis of variance of the effect of fungal strains and *M. truncatula* accessions on MSS.

Type III Analysis of Variance Table with Satterthwaite's method

	Sum Sq	Mean Sq	NumDF	DenDF	F value	Pr(>F)
Strain	3.953	0.6418	6	132.28	38.04	2.229e-15 ***
Accession	312.545	20.8363	15	306.51	162.2869	< 2.2e-16 ***
Strain: Accession	31.69	0.3444	90	306.51	1.1041	0.3659

Signif. codes: 0 ‘***’ 0.001 ‘**’ 0.01 ‘*’ 0.05 ‘.’ 0.1 ‘ ’ 1

The Tukey test grouping by Lsmeans based on the fungal strains revealed that all tested pathogens could be categorized into three discrete groups and intermediate groups of these three groups (Table 24 - Table 25).

Table 24: Lsmeans grouping of *V. alfalfae* strains corresponding to the AUDPC of 16 selected *M. truncatula* accessions.

Strain	lsmean	SE	df	lower.CL	upper.CL	.group
LUC	0,01121	0,000212	52,19046	0,010619	0,011801	1
4.3.A	0,012102	0,000314	52,19046	0,011226	0,012977	12
V31.2	0,012123	0,000314	52,19046	0,011247	0,012998	12
2.1.B	0,012346	0,000212	52,19046	0,011755	0,012937	2
Mg2	0,012662	0,000359	52,19046	0,011676	0,013647	23
VA107	0,013213	0,000323	52,19046	0,012313	0,014112	23
AF1	0,013692	0,000188	52,19046	0,013169	0,014216	3

Table 25: Lsmeans grouping of *V. alfalfae* strains corresponding to the MSS of 16 selected *M. truncatula* accessions.

Strain	lsmean	SE	df	lower.CL	upper.CL	.group
LUC	2,64131	0,035007	52,19046	2,543565	2,739055	1
VA107	2,712719	0,053502	52,19046	2,56396	2,861478	12
2.1.B	2,785529	0,035007	52,19046	2,687784	2,883274	123
V31.2	2,829774	0,051862	52,19046	2,68497	2,974578	23
Mg2	2,88602	0,059321	52,19046	2,723028	3,049012	23
AF1	2,916133	0,031016	52,19046	2,829531	3,002735	3
4.3.A	2,953844	0,051862	52,19046	2,80904	3,098648	3

These experiments confirmed that Iranian isolates are true pathogens of *M. truncatula,* and showed a slight divergence in the responses of the selected *M. truncatula* panel to the different isolates. It can be noted that the Iranian isolates are more aggressive in comparison to the other isolates.

The AF1 isolate which was collected from the Arak region where the first report of *V. alfalfae* in Iran was published (2004), was selected for further studies on the genetic control of *M. truncatula* response to an Iranian strain.

IV.2.Phenotypic response of *Medicago truncatula* to *Verticillium alfalfae*

2.1. Evaluation of the response of a *M. truncatula* biodiversity panel to Iranian isolate AF1

In order to link the phenotypic response of *M. truncatula* to AF1 for genome-wide association mapping, a panel of 242 *M. truncatula* accessions (Table S. 1) sequenced by the Medicago HapMap project was used. Ten-day old *M. truncatula* plants were root-inoculated with spores of *V. alfalfae* isolate AF1 and symptoms were scored regularly for 4 weeks. Appearance of symptoms was observed 7 -10 days after inoculation in susceptible *M. truncatula* accessions, highly susceptible lines reaching the ultimate score of 4 (dead plant) after 3 weeks. The three independent experiments (repeats), each organized in 4 independent blocks were performed and a total of 8,442 inoculated plants were evaluated.

The various *M. truncatula* accessions presented a continuous range of phenotypic variation in response to AF1 inoculation, from highly sensitive to highly resistant as exhibited by AUDPC and MSS values. This is typical for a Quantitative Disease Resistance (QDR).

2.1.1. Correction of breeding values through Augmented Block Design

Since each repeat involved four different blocks, as the first step, the blocks effect within each repeat had to be checked at the end of each repeat, before comparing the AUDPC and MSS values of different repeats. If there were statistically significant effects of the blocks then the block effects were estimated using the 4 check lines which were systematically present in each block (6 inoculated plants per each check line) and the AUDPC and MSS values of the other accession were corrected accordingly. Table 26 - Table 27 represents the approach to check for the blocks effect with the MSS values.

Table 26: Check the existence of block effect by the means of check line.

(Data is related to the MSS values of the blocks of the second repeat before correction)

MSS ~ Block + Accession

	Df	Sum Sq	Mean Sq	F value	Pr(>F)
Block	3	13.1	4.38	15.61	3.9e-05 ***
Accession	3	37.1	0.57	2.05	0.043 *
Residuals	17	4.8	0.280		

Signif. codes :	0 *** 0.001 ** 0.01 * 0.05 · 0.1	1			

MSS ~ Accession + Block

	Df	Sum Sq	Mean Sq	F value	Pr(>F)
Accession	3	48.1	0.620	2.21	0.029 *
Block	3	2.1	0.706	2.52	0.093 .
Residual	17	4.8	0.280		

Signif. Codes :	0 *** 0.001 ** 0.01 * 0.05 · 0.1	1			

Here, the check lines were just extracted and used to evaluate the block effects as they were presented systematically in all blocks which led to having a balanced dataset and avoiding the statistical barriers and misinterpretation which could be caused by unbalanced data. When the used statistical model (ANOVA model) was changed there was divergence in the outcome of the two models (Table 26) which technically is due to the partitioning of the sums of squares. It means there is a variability that can be attributed to different sources in the various predictors in the models. Theoretically, differences between blocks should not occur but in practice variations are often observed which are called Block effects. As long as the block effect is not calculated and the data is not corrected based on the block effect, different

experiments (repeat) cannot be compared. So, the block effects were estimated based on the check lines values and then the AUDPC and MSS values of other accession were adjusted based on this estimation and to confirm that the block effects were eliminated the same modeling and approach was followed with corrected values; after correcting for blocks effect the block must not be statistically significant (Table 27).

Table 27:Check the existence of block effect by the means of check line.

(Data is related to the MSS values of the blocks of the second repeat after correction)

MSS ~ Block + Accession

	Df	Sum Sq	Mean Sq	F value	Pr(>F)
Block	3	0.00	0.000	0.0	1
Accession	3	7.83	2.609	30.9	4.5e-05 ***
Residuals	9	0.76	0.084		

Signif. Codes : 0 *** 0.001 ** 0.01 * 0.05 · 0.1 1

MSS ~ Accession + Block

	Df	Sum Sq	Mean Sq	F value	Pr(>F)
Accession	3	7.83	2.609	30.9	4.5e-05 ***
Block	3	0.00	0.000	0.0	1
Residual	9	0.76	0.084		

Signif. Codes : 0 *** 0.001 ** 0.01 * 0.05 · 0.1 1

After calculation of corrected values of AUDPC and MSS (breeding values) (Figure 43A- Figure 44A), the Tukey test grouping based on Lsmeans values (least square means) as a function of accessions' response to inoculation (AUDP and MSS) was performed to reveal the existing diversity in the response panel (Figure 43B - Figure 44B).

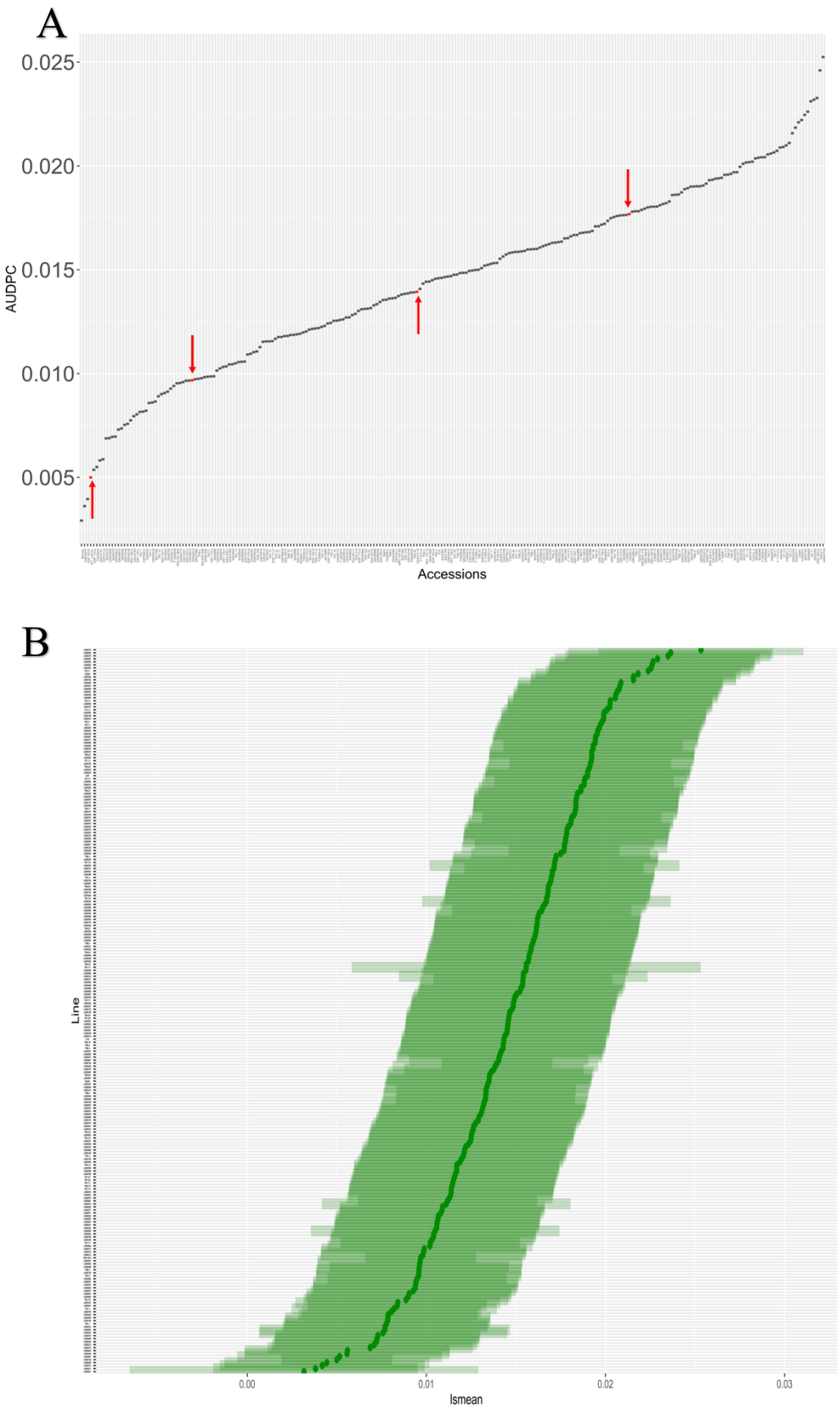

Figure 43: The dynamic variation among the panel for AUDPC.

The estimated AUDP values are adjusted through augmented block design. A: Boxplot of the mean values of three repeats of all 242 accessions. The red dots and arrows represent the check lines. B: Lsmeans value of AUDPC. The values are arranged in ascending order. For more information refer to the **Table S. 4**.

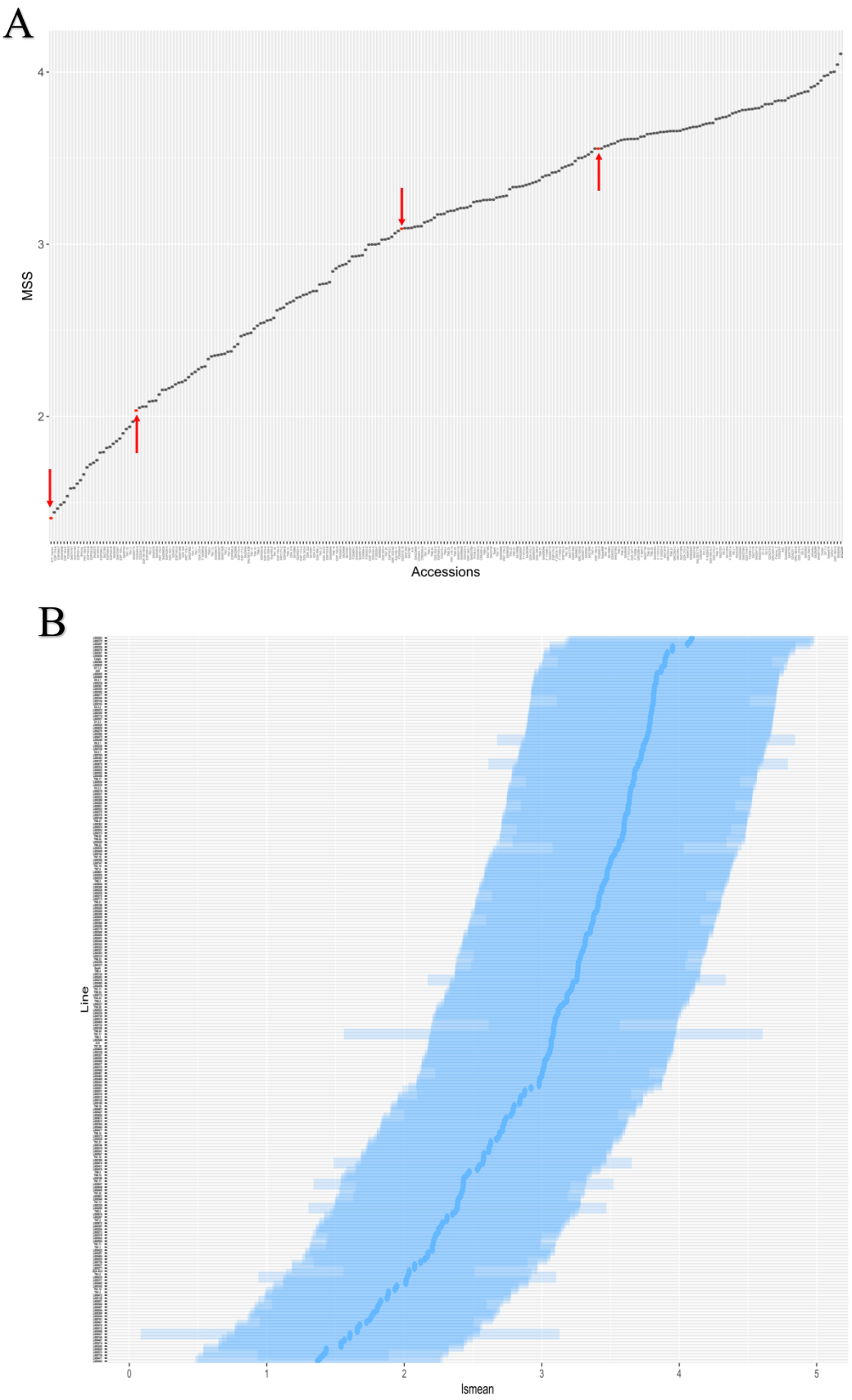

Figure 44: The dynamic variation among the panel for the MSS.

The estimated MSS values are adjusted through augmented block design. A: Boxplot of the mean values of three repeats of all 242 accessions. The red dots and arrows represent the check lines. B: Lsmeans value of MSS. The values are arranged in ascending order. For more information refer to the **Table S. 5**.

2.1.2. Correction of breeding values through the Mixed Liner Model (MLM)

In this approach, the breeding values (Adjusted AUDPC and MSS values) were not calculated at the end of each repeat. Here, all the raw data were put together and the Best Linear Unbiased Estimator (BLUEs) corresponding to the AUDPC or MSS were extracted through the linear mixed model (Figure 45A,Figure 46 A).

After extraction of BLUE values of AUDPC and MSS; to reveal the continuation of diversity in the response panel, the Tukey test grouping based on Lsmeans as a function of accessions' response to inoculation (such as the previous approach) was implemented (Figure 45B, Figure 46B).

In brief, most of genotypes (66.1 % and 89.3 % respectively) can be considered as susceptible, with AUDPC and MSS values of or above 0.0125 and 2 respectively.

Broad sense heritability (H^2) values for AUDPC and MSS were 0.719 and 0.724 respectively; the correlation between AUDPC and MSS was 0.96 (Figure 47).

Taken together, the results of phenotyping analysis with two different approaches show that the population and the phenotype scoring method are suitable to implement a Genome-wide association study in order to investigate the genetic architecture of *M. truncatula* response towards Iranian *V. alfalfae*.

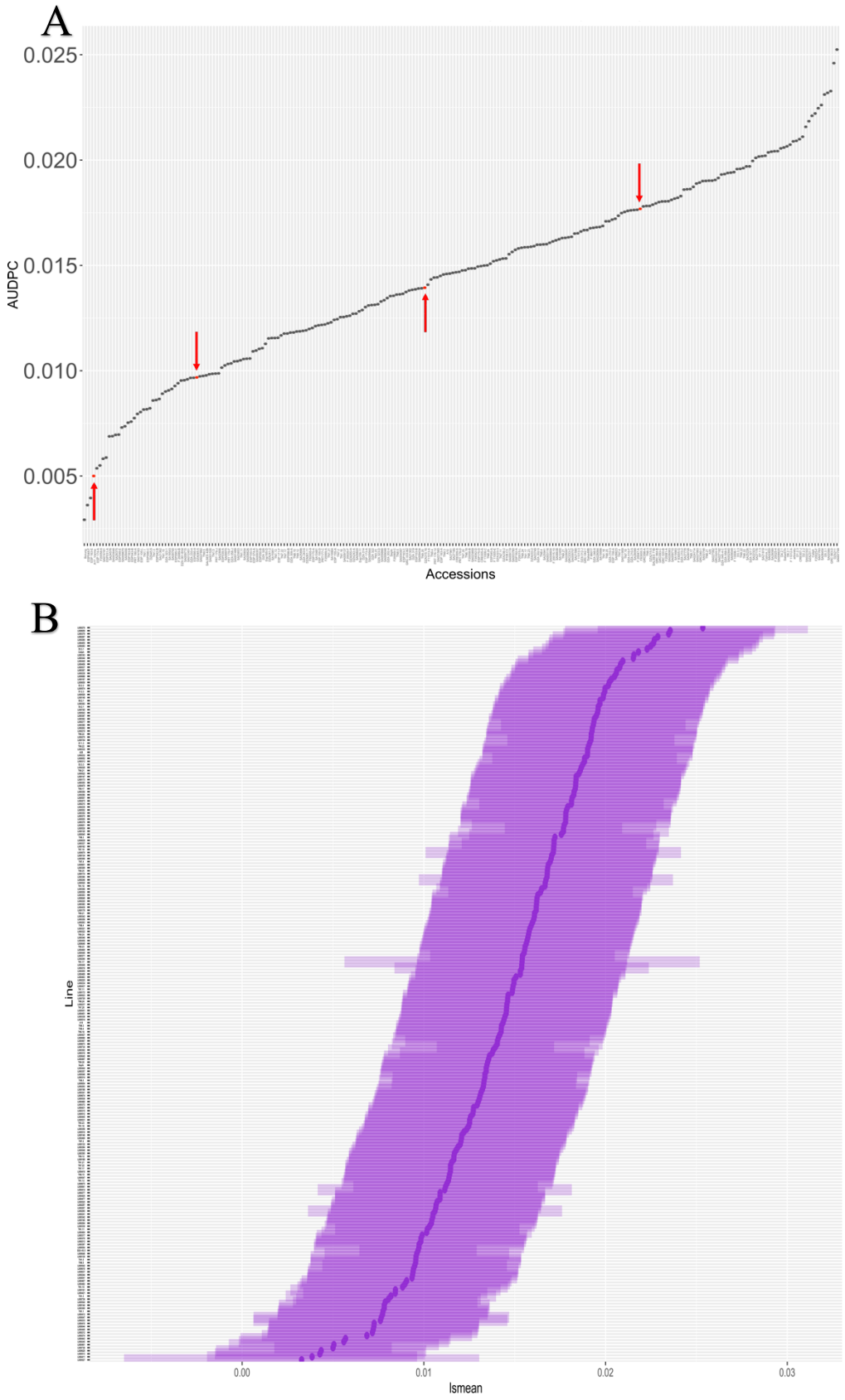

Figure 45: The dynamic variation among the panel for AUDPC.

The estimated AUDP values are adjusted through the mixed linear model. A: Boxplot of the mean values of three repeats of all 242 accessions. The red dots and arrows represent the check lines. B: Lsmeans value of AUDPC. The values are arranged in ascending order. For more information refer to the **Table S. 6**.

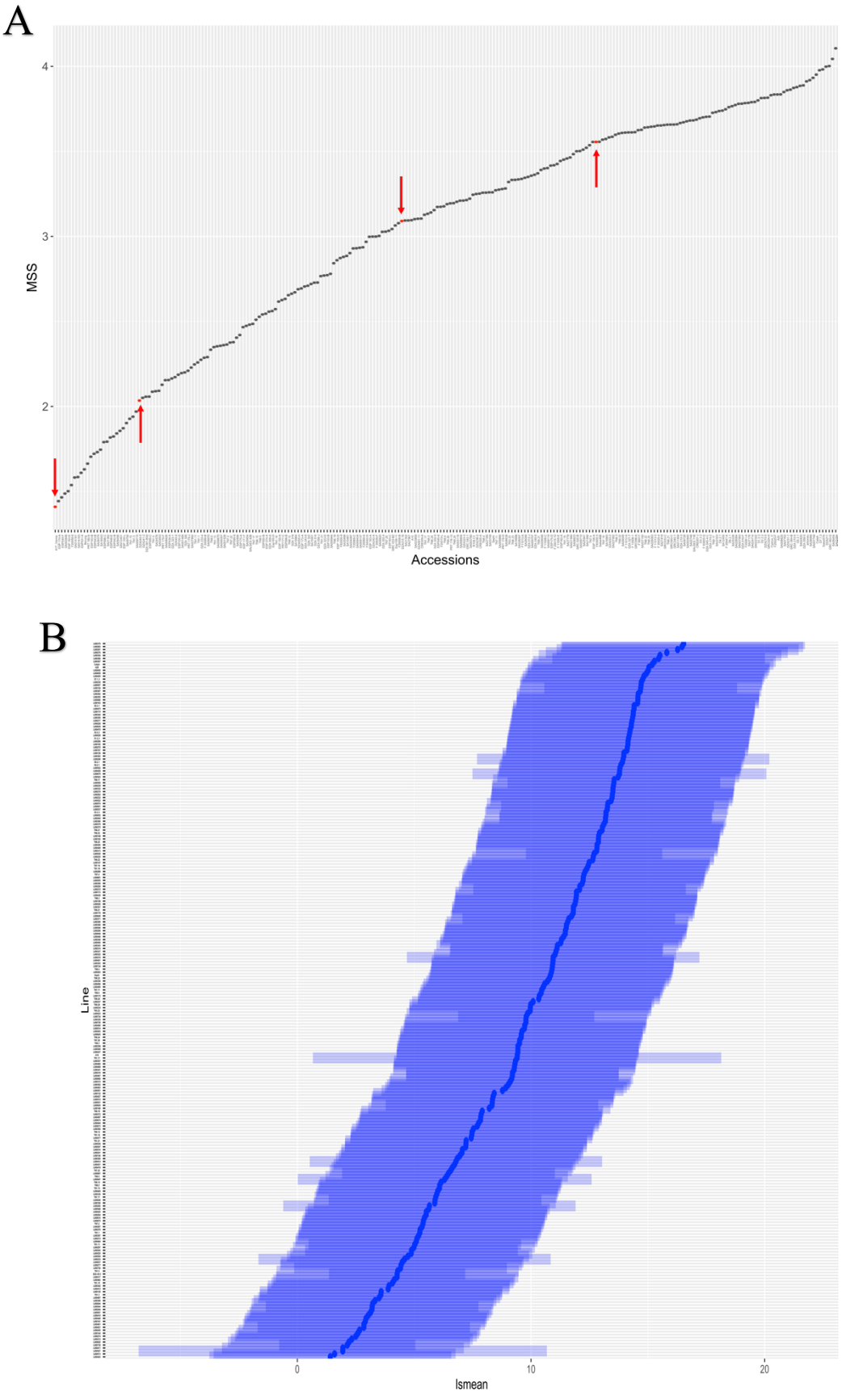

Figure 46:The dynamic variation among the panel for MSS.

The estimated MSS values are adjusted through the mixed linear model. A: Boxplot of the mean values of three repeats of all 242 accessions. The red dots and arrows represent the check lines. B: Lsmeans value of MSS. The values are arranged in ascending order. For more information refer to the **Table S. 7**.

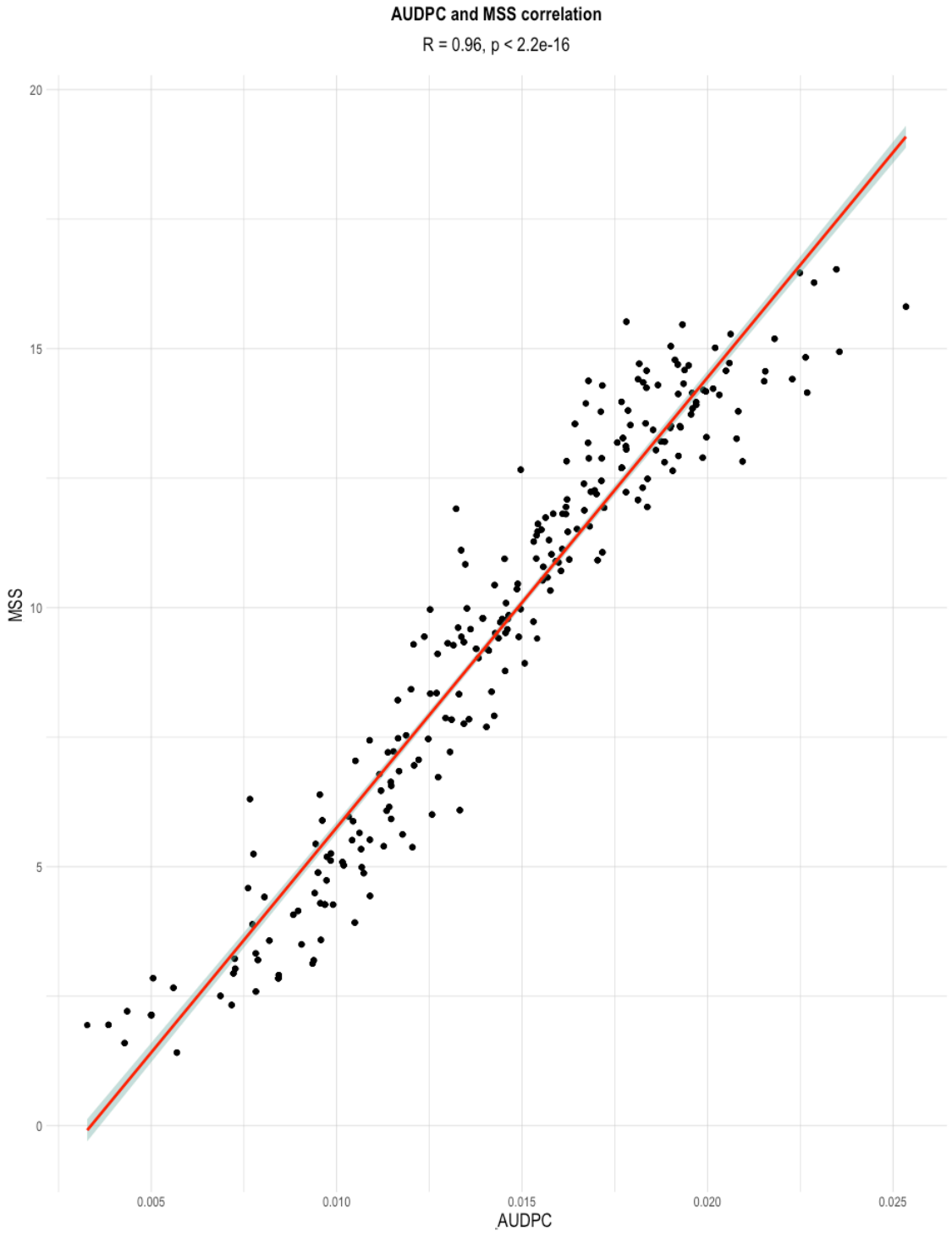

Figure 47: Correlation between AUDPC and MSS.

Scatterplot of the phenotypic values (Best linear unbiased estimators: BLUEs) AUDPC versus MSS. The linear regression line is shown in red.

2.2. Evaluation of the response of Iranian *Medicago* species to Iranian and French *V. alfalfae* isolates

To examine the response of Iranian *Medicago* species toward French and Iranian isolate a preliminary study was carried out at 25 °C.

Four Iranian *M. truncatula* and one *M. scutellata* (Table S. 2) were root inoculated with AF1 and V31-2 and symptoms were scored as described before.

For both AUDPC and MSS, statistical analysis by ANOVA revealed a highly significant effect of genotypes, in contrast to no effect of fungal strains (Table 28 and Table 29).

Table 28: Analysis of variance of the effect of Iranian *Medicago* accessions and fungal strains on AUDPC.

	Df	Sum Sq	Mean Sq	F value	Pr(>F)
Strain	1	0.00000171	1.7130e-06	1.7866	0.252299
Accessions	4	0.00049284	1.2321e-04	128.47	0.000178 ***
Residuals	4	0.00000384	9.5900e-07		

Signif. codes: 0 ‘***’ 0.001 ‘**’ 0.01 ‘*’ 0.05 ‘.’ 0.1 ‘ ’ 1

Table 29: Analysis of variance of the effect of Iranian *Medicago* accessions and fungal strains on MSS.

	Df	Sum Sq	Mean Sq	F value	Pr(>F)
Strain	1	0.2250	0.2250	3.8925	0.119764
Accessions	4	14.0487	3.5122	60.7614	0.000778 ***
Residuals	4	0.2312	0.0578		

Signif. codes: 0 ‘***’ 0.001 ‘**’ 0.01 ‘*’ 0.05 ‘.’ 0.1 ‘ ’ 1

Based on Lsmeans grouping, the Iranian Lines can be categorized into three distinct groups and one intermediate by AUDPC (Table 30) and only into two groups by MSS (Table 31).

Table 30: Lsmeans Grouping of response of Iranian *Medicago* accessions (AUDPC) to inoculation with French and Iranian *V. alfalfae* strains

Genotype	lsmean	SE	df	lower.CL	upper.CL	.group
1724	0,002128	0,000692	4	-0,00104	0,005297	1
7600	0,017386	0,000692	4	0,014216	0,020555	2
7321	0,018064	0,000692	4	0,014894	0,021233	23
Scu	0,019291	0,000692	4	0,016122	0,022461	23
7543	0,022098	0,000692	4	0,018929	0,025268	3

Table 31: Lsmeans Grouping of response of Iranian *Medicago* accessions (MSS) to inoculation with French and Iranian *V. alfalfae* strains.

Genotype	lsmean	SE	df	lower.CL	upper.CL	.group
1724	0,888889	0,170004	4	0,110772	1,667006	1
7321	3,6875	0,170004	4	2,909383	4,465617	2
7600	3,722222	0,170004	4	2,944105	4,500339	2
7543	3,9375	0,170004	4	3,159383	4,715617	2
Scu	4	0,170004	4	3,221883	4,778117	2

This preliminary study proved that the Iranian *Medicago* species are genetically diffe3rent with regard to their susceptibility to *V. alfalfae.* Furthermore, the same trend was observed with both Iranian and French V. alfalfae (Figure 48).

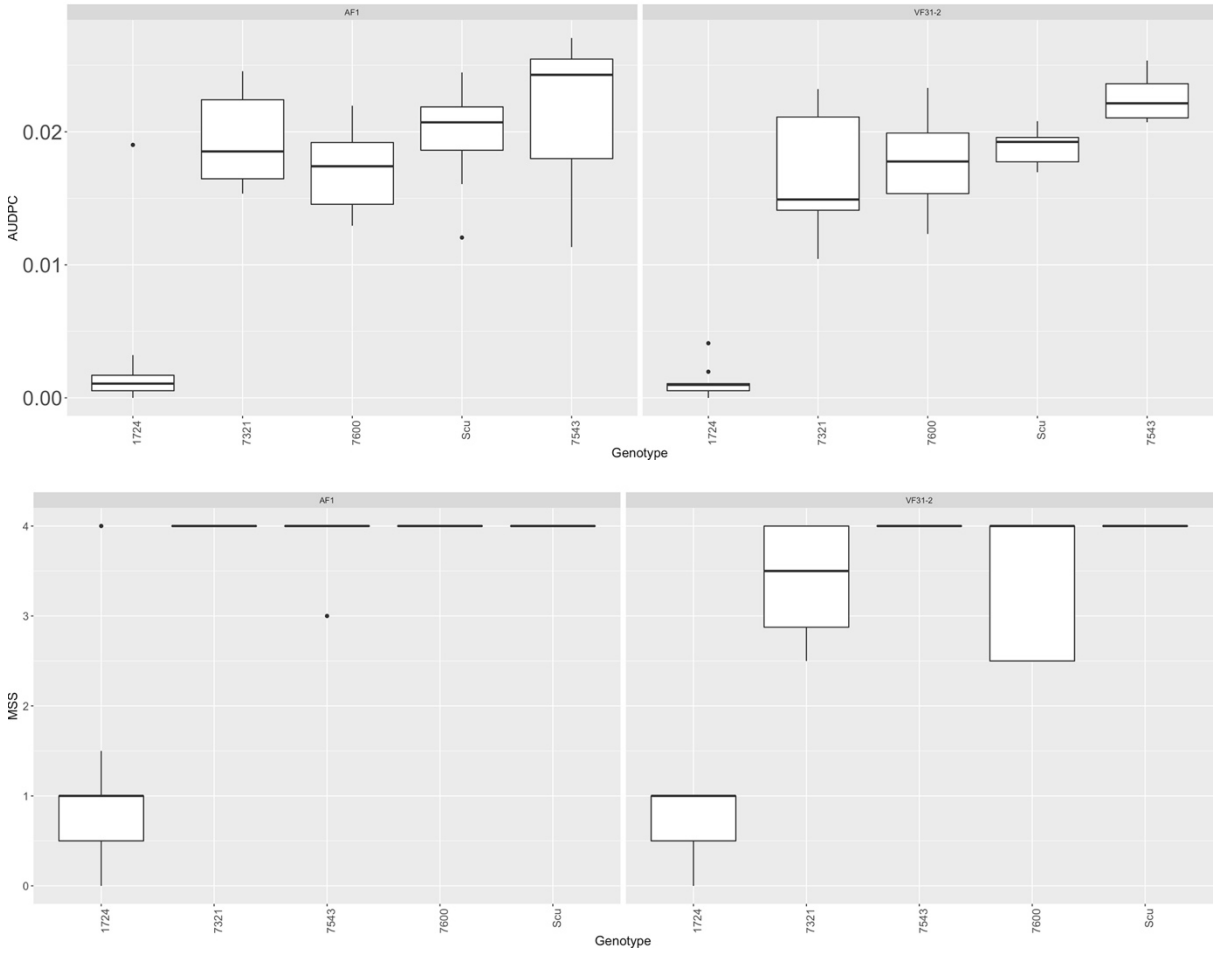

Figure 48: The response of Iranian *Medicago* accession toward French and Iranian *V. alfalfae* inoculum.

Up: AUDPC Box plot. Bottom MSS Box plot. The values correspond to the mean values of different individuals of each accession in only one repeat.

IV.3.Genome-wide association study

3.1. Genome-wide Association mapping

The continuous variability in the response panel towards *V. alfalfae* AF1 encouraged to implement a Genome-wide association mapping (GWAS) in order to detect *loci* related to *M. truncatula* resistance against the Iranian strain. The GWAS was undertaken using 5,671,743 high density markers of single nucleotide polymorphism (SNP). Five GWAS statistical models were used for both approaches (correction based on augmented block design or mixed linear model): Two Generalized Linear Models (GLM) including GLM without population structure (naive model) and GLM with population structure (GLM fixed effect model or GLM-Q-model) and also three Mixed Linear Models (MLM) including MLM with kinship (K-Model), MLM with population structure matrix (Q-Model) and K-Q Model. To correct for the multiple comparisons problem and reduce type II error of models' outcome Bonferroni multiple testing correction and False Discovery Rate (FDR) ($\alpha = 0.05$) were estimated and then the Q-Q plot was plotted for each model separately. The Q-Q plots of each statistical model were compared and the best-fitted model for each trait was selected; finally, the selected statistical models of two approaches were compared together and the more precise approach was selected and its results were used in the subsequent steps.

3.1.1. Breeding values adjusted through Augmented Block Design

Figure 49 and Figure 50 present the Q-Q plots derived from the five statistical models for AUDPC and MSS, respectively when the initial breeding values were corrected based on the check lines through augmented block design. According to the Q-Q plots the two GLM models represent a systematic divergence from the expected uniform distribution (red bisector). This indicates that they were not able to correct for population stratification (Q matrix) in the case of naive model or cryptic relatedness within SNPs (K matrix) in the case of both models. However, in the case of the three

MLMs, the same phenomenon (a systematic divergence) was observed for the Q Model (concerning the AUDPC), K Model and K+ Q Model.

In addition, some degree of overcorrection for population structure and cryptic relatedness within SNPs was observed in upper parts of the plots. This was more and less true for both AUDPC and MSS. Altogether, based on these results the best-fitted statistical model for AUDPC and MSS values that were adjusted through augmented block design was the Q-Model.

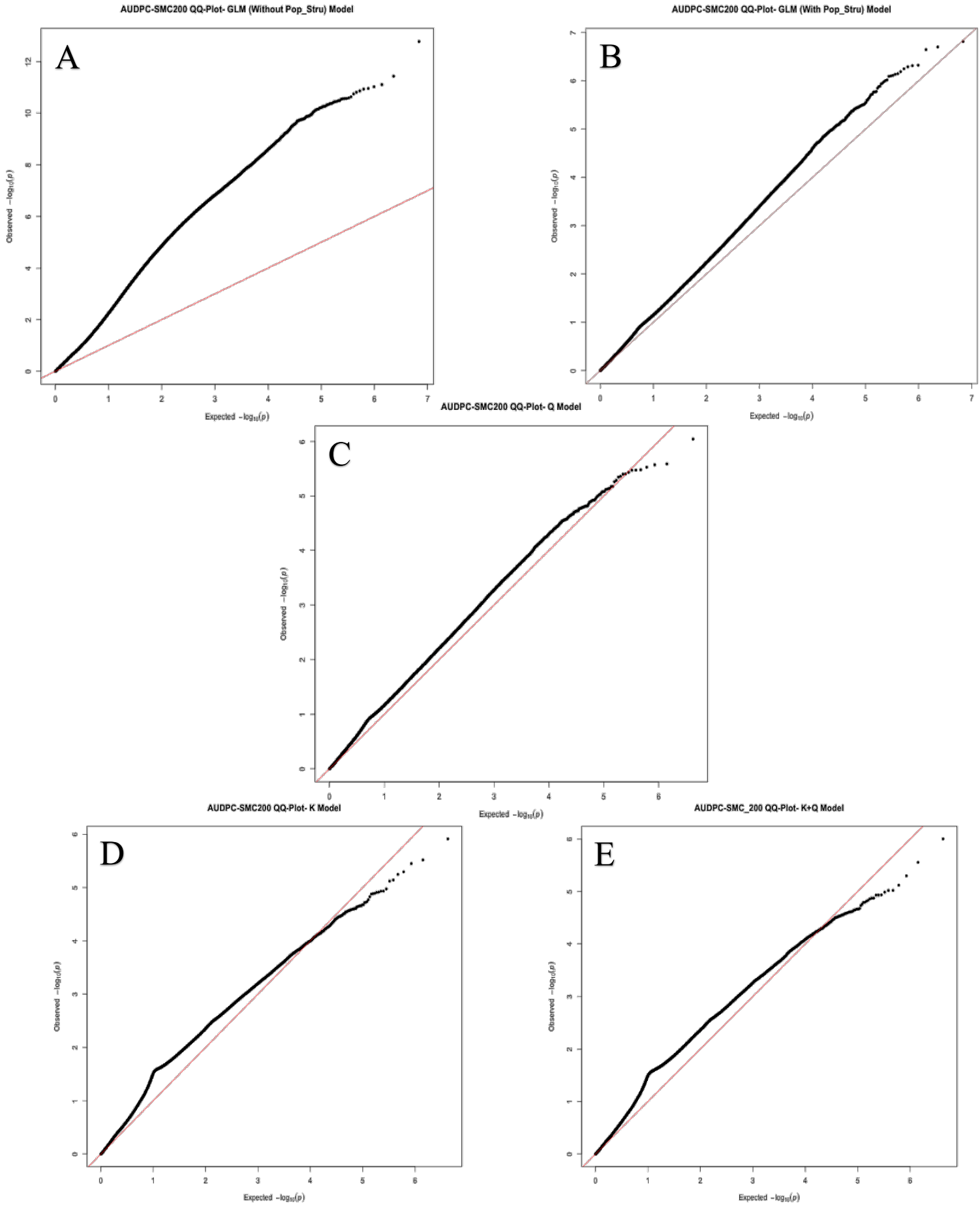

Figure 49: Q-Q plots of GWAS analyses on AUDPC with GLM and MLMs statistical models.

A: GLM without population matrix (naïve model); B: GLM including population matrix (GLM-Q model); C: MLM (Q Model); D: MLM (K Model); E: MLM (K+Q Model). Each point represents the observed value of the P-value as a function of its theoretical value for an SNP; The more the points overlap the bisector (red line), the more efficient the model is. MLM: Mixed Linear Model, GLM: Generalized Linear Model. SMC200 refers to the site minimum count in the tassel program that was set to the 200. The initial breeding values are adjusted based on check lines through augmented block design.

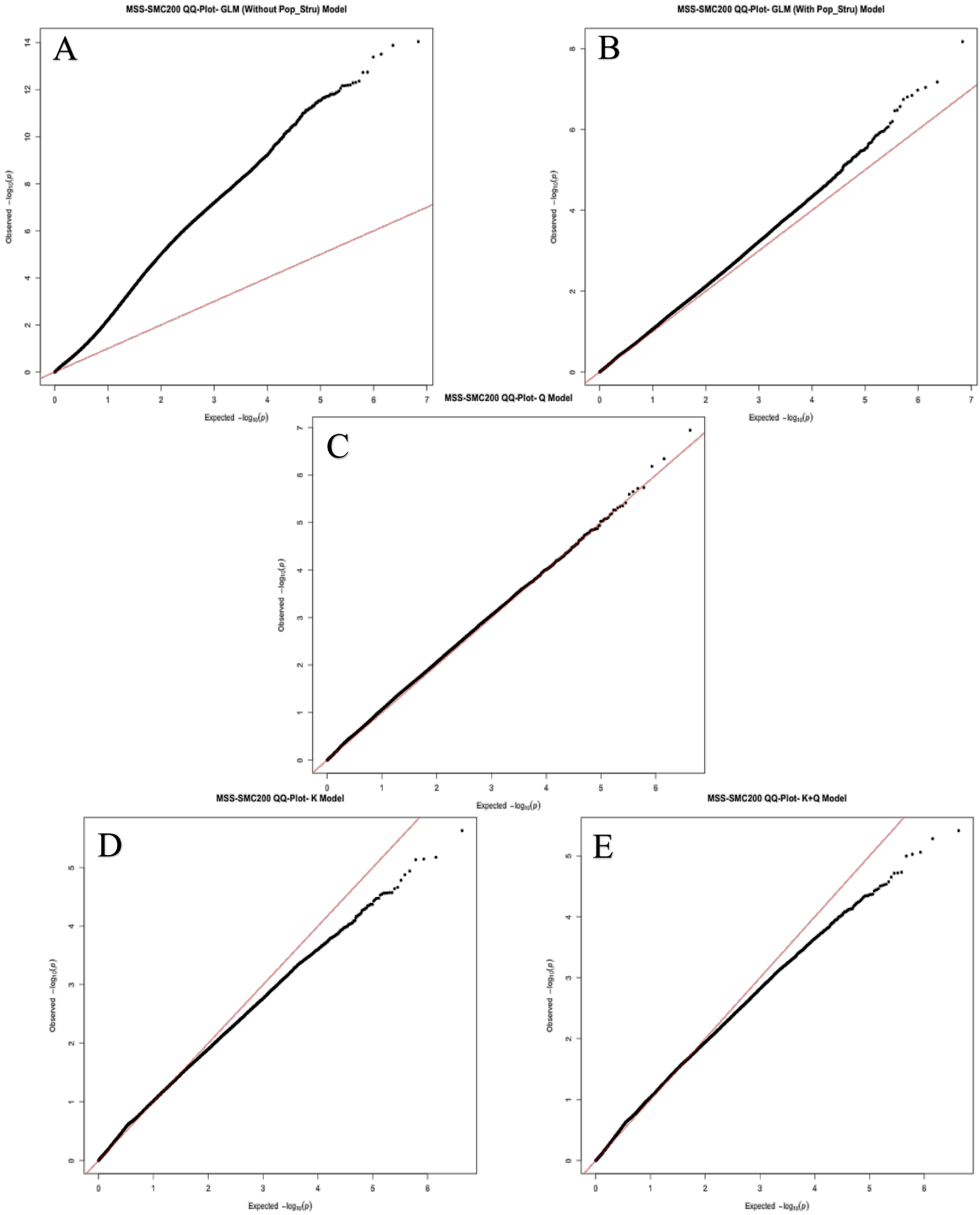

Figure 50: Q-Q plots of GWAS analyses on MSS with GLM and MLMs statistical models.

A: GLM without population matrix (naive model); B: GLM including population matrix (GLM-Q model); C: MLM (Q Model), D: MLM (K Model); E: MLM (K+Q Model). Each point represents the observed value of the P-value as a function of its theoretical value for an SNP; The more the points overlap the bisector (red line), the more efficient the model is. MLM: Mixed Linear Model, GLM: Generalized Linear Model. SMC200 refers to the site minimum count in the tassel program that was set to the 200. The initial breeding values are adjusted based on check lines through augmented block design.

3.1.2. Breeding values adjusted through the MLM

Figure 51 - Figure 52 present the Q-Q plots derived from different statistical models with AUDPC and MSS, respectively, where the initial breeding values were adjusted through the mixed linear model.

Based on the Q-Q plots it can be said that more and less the same trend was observed as when the initial breeding values were adjusted based on augmented block design. The GLM models (naive Model and fixed effects model (Q-model)) illustrate a systematic divergence from the expected uniform distribution (red bisector) which indicates that these models also were not able to correct neither for population stratification (Q matrix) (in case of GLM without population structure) nor cryptic relatedness within SNPs (K matrix) (for both GLM models). However, in the case of the MLMs, the same scenario happened (a systematic divergence) in some parts of the Q-Q plots, and also some extent of overcorrection for population structure and cryptic relatedness within SNPs in the upper parts of the plots. Generally, through a comparison of different statistical models, it can be concluded that the MLM Q-Model is the best-fitted statistical model for both AUDPC and MSS whose values are adjusted through the MLM. Although, it should be considered that the presence of some false positives or false negatives are not unlikely for both approaches and should be further investigated through gene expression analysis.

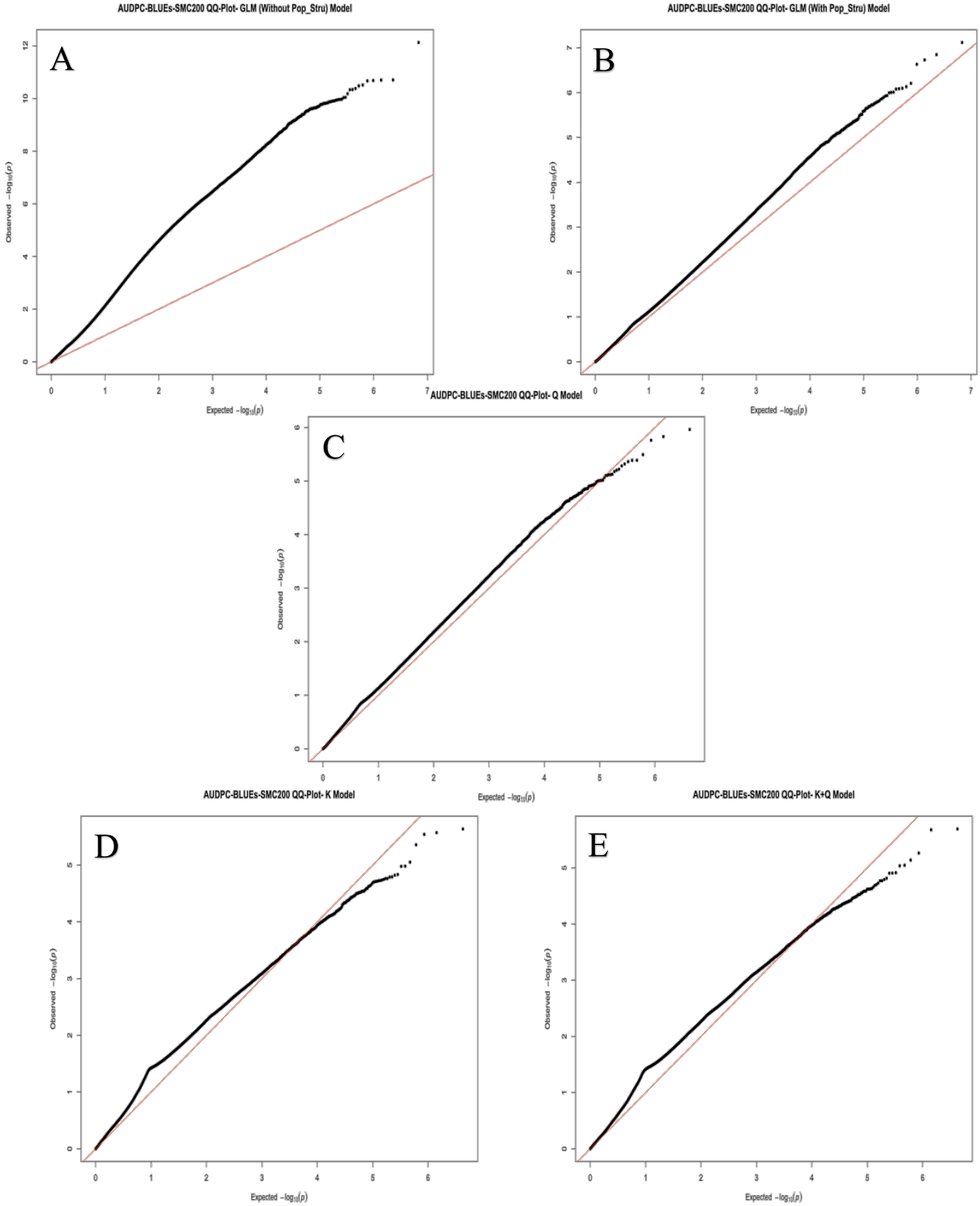

Figure 51: Q-Q plots of GWAS analyses on AUDPC with GLM and MLMs statistical models.

A: GLM without population matrix (naive model); B: GLM including population matrix (GLM-Q model); C: MLM (Q Model); D: MLM (K Model; E: MLM (K+Q Model). Each point represents the observed value of the P-value as a function of its theoretical value for an SNP; The more the points overlap the bisector (red line), the more efficient the model is. MLM: Mixed Linear Model, GLM: Generalized Linear Model. BLUE: the Best Linear Unbiased estimator. SMC200 refers to the site minimum count in the tassel program that was set to the 200.The initial breeding values are adjusted based on the mixed linear model (MLM) design.

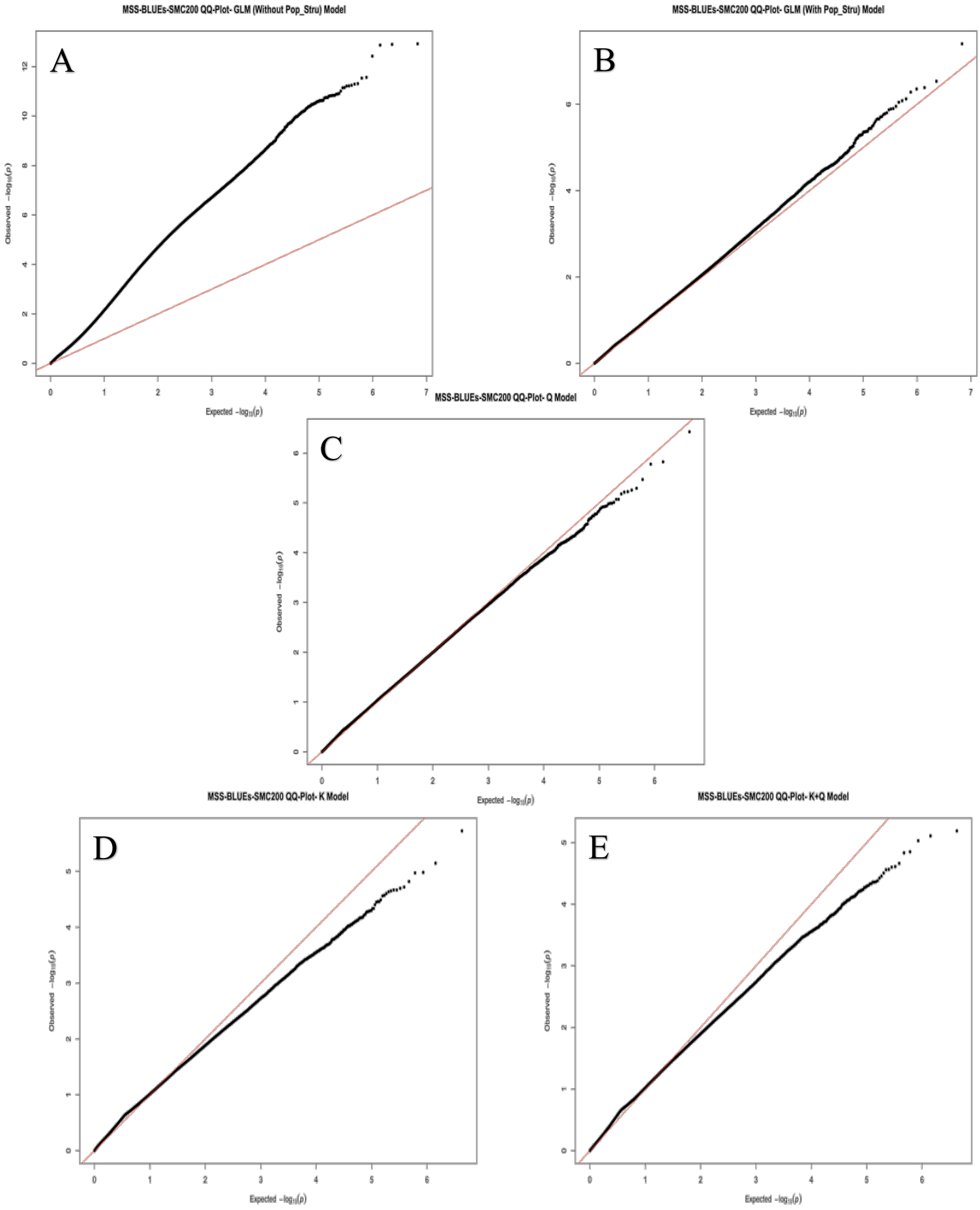

Figure 52: Q-Q plots of GWAS analyses on MSS with GLM and MLMs statistical models.

A: GLM without population matrix (naive model); B: GLM including population matrix (GLM-Q model); C: MLM (Q Model); D: MLM (K Model); E: MLM (K+Q Model). Each point represents the observed value of the P-value as a function of its theoretical value for an SNP; The more the points overlap the bisector (red line), the more efficient the model is. MLM: Mixed Linear Model, GLM: Generalized Linear Model. BLUE: the Best Linear Unbiased estimator. SMC200 refers to the site minimum count in the tassel program that was set to the 200. The initial breeding values are adjusted based on the mixed linear model (MLM) design.

3.1.3. Comparison of Q Model derived from two approaches and selection of the most appropriate model

Although in both approaches, the Q model seems to be the best-fitted one, due to the limitations, it was very important to focus only on the results of one approach. Hence, the results of these two approaches were compared and the best-fitted model was selected for further studies. Figure 53 clarifies the Q-Q plot corresponding to the two approaches and the traits.

In the case of AUDPC (Figure 53A1-A2), although more and less the same trend is observed in the two approaches, the one in which the initial AUDPC values were derived from MLM, has less divergence between observed and expected (red bisector) values.

Considering MSS (Figure 53B1-B2); while some overcorrection is presented in the upper right part of the plot where the initial MSS values were estimated through MLM, the overlap is generally better between observed and expected (red bisector) values.

All of this indicates the superiority of the MLM approach over the block augmented design approach. Hence, this approach was used for further steps.

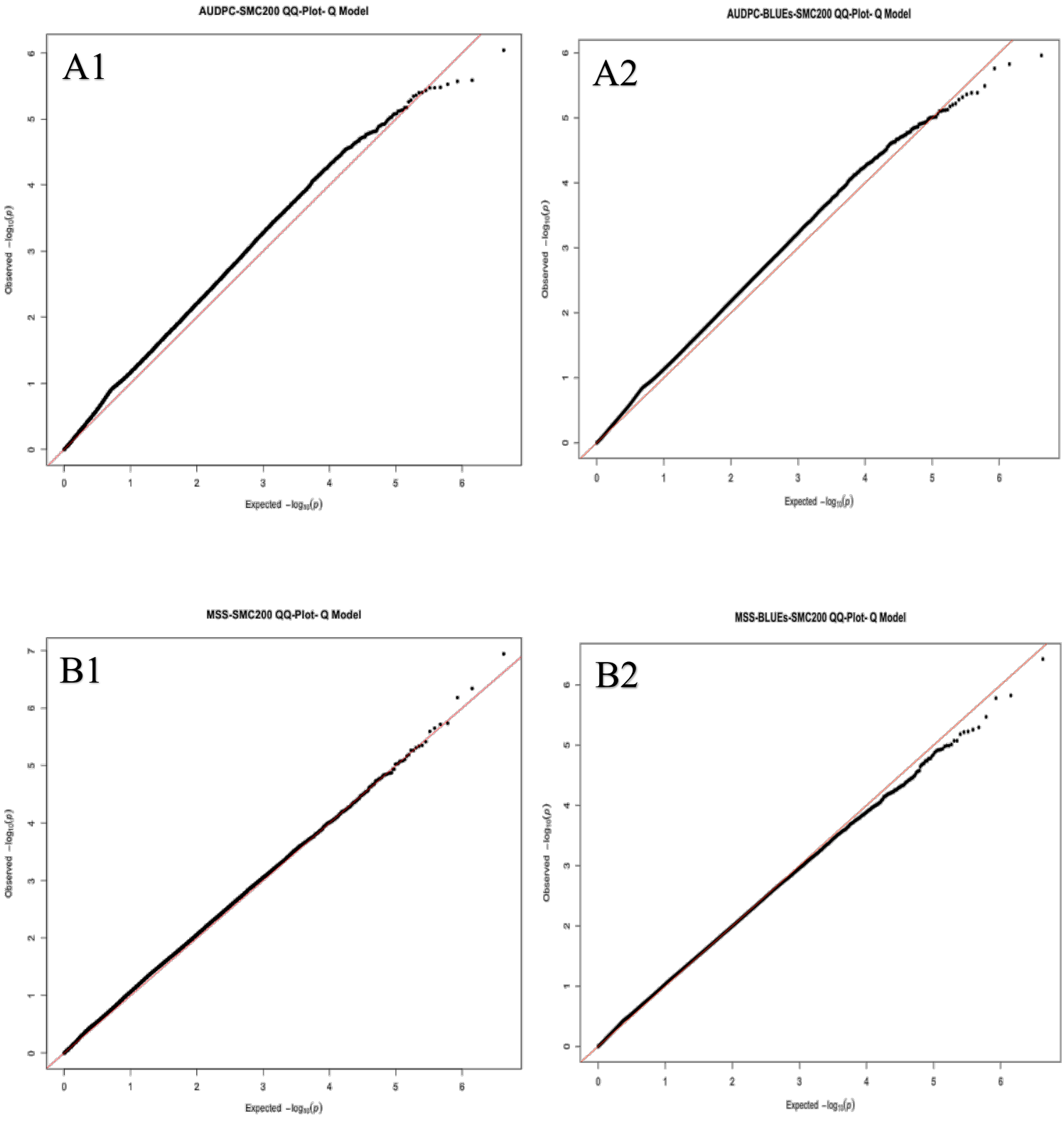

Figure 53: Q statistical model derived from two approaches.

A: AUDPC, B: MSS, A1: The AUDPC initial breeding values were adjusted through augmented block design, A2: The AUDPC initial breeding values were adjusted through MLM, B1: The MSS initial breeding values were adjusted through augmented block design, B2: The MSS initial breeding values were adjusted through MLM.

3.1.4. Identification of *loci* associated to resistance against *V. alfalfae* AF1

Following the selection of the best-fitted model, the Manhattan plot was computed to illustrate the association of SNPs with AUDPC and MSS. To select the significant associated SNPs, Bonferroni and False Discovery Rate (FDR) were considered as the preliminary threshold, and were plotted alongside with the suggestive line proposed through the qqman R package (D. Turner 2018) (Figure 54).

Bonferroni seemed to be too stringent as just one SNP for MSS appeared statistically significant based on this threshold, while the FDR threshold was less stringent and revealed more statistically significant SNPs. The suggestive line which was very close to the FDR, was selected as the main threshold for selecting the significant candidate SNPs in order not to miss any probable candidate genes (Figure 54).

Analysis of the association between AUDPC (Figure 54A), MSS (Figure 54B), and SNPs revealed several strongly associated loci.

Filtering with the SNPs association score equal to or greater than 5 (based on the suggestive line) ended up in the identification of 24 and 14 significant SNPs respectively for the parameters AUDPC and MSS on 7 and 6 Linkage groups (LG) as listed in Table 32 and Table 33. Among them, 8 SNPs were common to AUDPC and MSS, with chromosome number 8 containing 5 of these common significant SNPs while chromosomes number 1, 4 and 7 contain only one common SNP each.

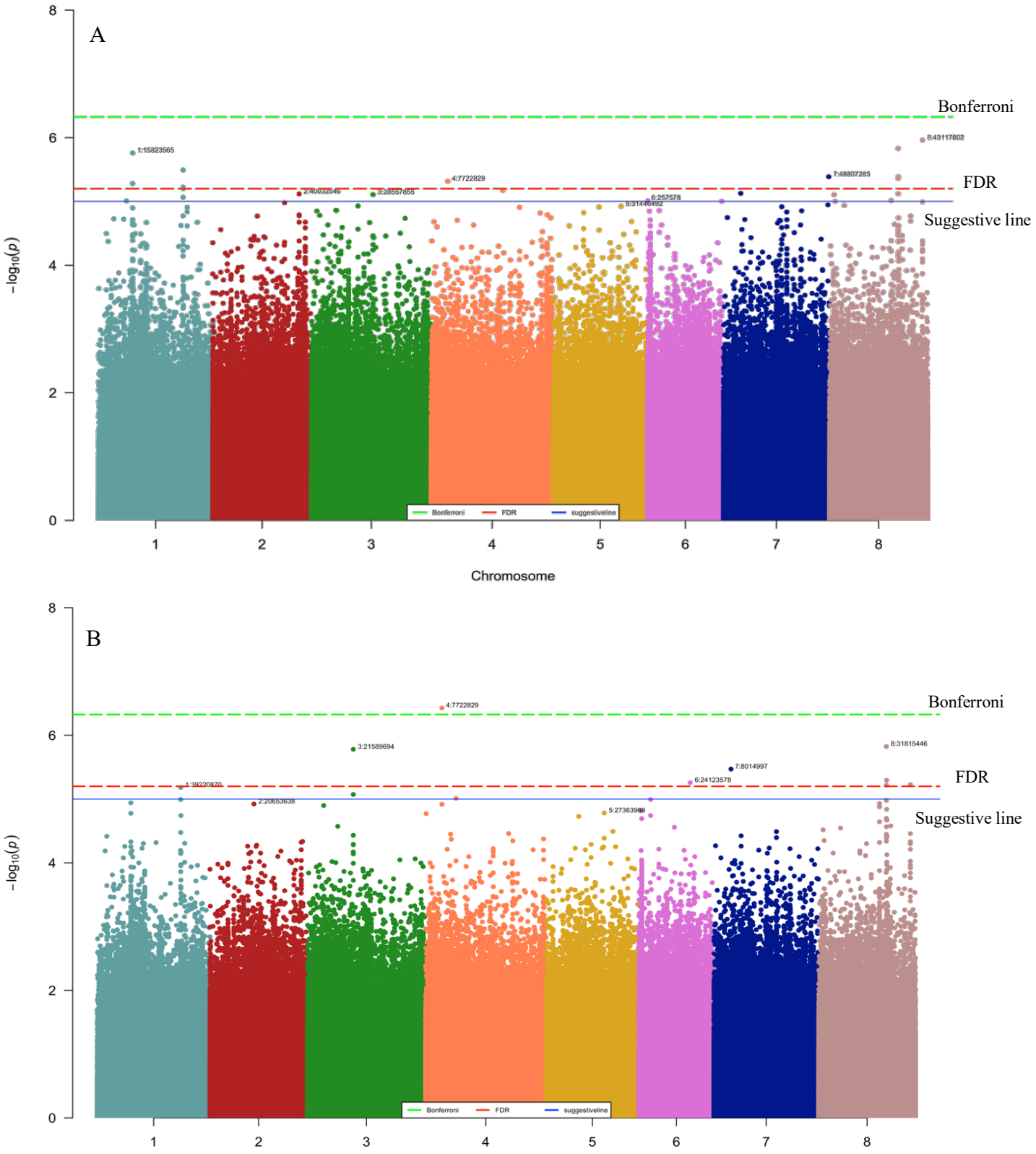

Figure 54:Manhattan plot of the GWAS analysis of the response to *Verticillium alfalfae* AF1.

A: AUDPC, B: MSS. The green dash line represents the Bonferroni threshold, the red dash line the FDR threshold and the blue solid line the suggestive line of the qqman R package. AUDPC and MSS phenotypes were evaluated in 242 accessions of the MtHapMap collection. Association genetic analysis was performed using a Mixed linear model -Q Model. Each point represents the probability that the SNP is related to the studied phenotype. The X-axis represents the P-value of each SNP in genomic order by chromosome and SNPs position on the chromosome while the Y-axis represents the association score that is calculated as -log10[p-value] for each SNP.

Table 32: Candidate SNPs linked to resistance to *Verticillium alfalfae* AF1 through AUDPC as identified by GWAS in 242 *M. truncatula* accessions.

SNPs (Locus) with an association score equal or greater than 5 are listed. The score of each of the SNPs corresponds to [-log10 (P-value)] and was obtained according to a mixed linear model Q-Model. The SNPs in common with MSS are written in bold.

Marker	Chr	Position	F	P-Values	Add_effect	Add_F	Add_p	Score
1:12964012	1	12964012	12,298	9,74E-06	0,0015	7,234	0,00781575	5,0114
1:15800708	1	15800708	13,116	5,23E-06	-0,0019	22,205	5,22E-06	5,2817
1:15823565	1	15823565	14,294	1,73E-06	-0,0031	19,255	1,94E-05	5,7614
1:39220870	**1**	**39220870**	**13,527**	**3,22E-06**	**-0,0018**	**19,847**	**1,43E-05**	**5,4922**
1:39222678	1	39222678	12,852	6,01E-06	0,0021	25,047	1,31E-06	5,2210
1:39226123	1	39226123	12,399	8,62E-06	-0,0021	20,818	9,00E-06	5,0643
1:39333665	1	39333665	12,764	6,29E-06	0,0022	22,984	3,29E-06	5,2012
2:33302078	2	33302078	13,134	4,60E-06	-0,0031	26,165	7,73E-07	5,3375
2:40032546	2	40032546	12,522	7,62E-06	0,0017	14,301	0,00020683	5,1179
3:28557855	3	28557855	12,523	7,81E-06	-0,0015	9,873	0,00194763	5,1073
4:7722829	**4**	**7722829**	**13,112**	**4,81E-06**	**-0,0025**	**26,059**	**8,33E-07**	**5,3180**
4:33221889	4	33221889	12,688	6,65E-06	-0,0043	24,553	1,58E-06	5,1769
6:257578	6	257578	12,412	9,66E-06	0,0032	22,977	3,69E-06	5,0152
6:34475434	6	34475434	12,313	9,89E-06	0,0048	22,962	3,50E-06	5,0049
7:8014997	**7**	**8014997**	**12,591**	**7,47E-06**	**-0,0020**	**21,642**	**6,24E-06**	**5,1268**
7:48807285	7	48807285	13,391	4,10E-06	-0,0031	17,304	5,13E-05	5,3871
8:2106964	8	2106964	12,560	7,87E-06	-0,0020	18,726	2,51E-05	5,1043
8:2597013	8	2597013	12,384	9,89E-06	-0,0024	20,817	9,93E-06	5,0048
8:28608045	**8**	**28608045**	**12,353**	**9,62E-06**	**-0,0018**	**20,838**	**9,42E-06**	**5,0167**
8:31815446	**8**	**31815446**	**14,445**	**1,48E-06**	**0,0033**	**28,847**	**2,33E-07**	**5,8292**
8:31823520	8	31823520	13,188	4,35E-06	0,0027	24,456	1,67E-06	5,3616
8:31847916	**8**	**31847916**	**12,752**	**7,59E-06**	**0,0034**	**25,459**	**1,27E-06**	**5,1197**
8:31944993	**8**	**31944993**	**13,229**	**4,11E-06**	**0,0024**	**26,417**	**6,68E-07**	**5,3860**
8:43117802	**8**	**43117802**	**14,761**	**1,09E-06**	**0,0046**	**22,605**	**3,91E-06**	**5,9610**

Table 33: Candidate SNPs linked to resistance to *Verticillium alfalfae* AF1 through MSS as identified by GWAS in 242 *M. truncatula* accessions.

SNPs (Locus) with an association score equal or greater than 5 are listed. The score of each of the SNPs corresponds to [-log10 (P-value)] and was obtained according to a mixed linear model Q-Model. The SNPs in common with AUDPC are written in bold.

Marker	Chr	Position	F	P-Values	Add_effect	Add_F	Add_p	score
1:39220870	**1**	**39220870**	**12,715**	**6,57E-06**	**-1,6560**	**20,242**	**1,19E-05**	**5,1823**
3:21589694	3	21589694	14,394	1,66E-06	-1,7515	27,438	4,70E-07	5,7799
3:21589926	3	21589926	12,404	8,46E-06	-1,6009	23,911	2,10E-06	5,0725
3:21589932	3	21589932	12,404	8,46E-06	1,6009	23,911	2,10E-06	5,0725
4:7722829	**4**	**7722829**	**16,080**	**3,73E-07**	**-2,5560**	**32,161**	**5,53E-08**	**6,4281**
4:14324686	4	14324686	12,364	9,74E-06	2,7186	24,277	1,98E-06	5,0113
6:24123578	6	24123578	12,887	5,54E-06	-1,4013	25,771	8,94E-07	5,2565
7:8014997	**7**	**8014997**	**13,493**	**3,39E-06**	**-1,8777**	**23,419**	**2,74E-06**	**5,4700**
8:28608045	**8**	**28608045**	**12,324**	**9,87E-06**	**-1,7208**	**22,749**	**3,89E-06**	**5,0057**
8:28608060	8	28608060	12,462	8,71E-06	1,7043	24,888	1,46E-06	5,0599
8:31815446	**8**	**31815446**	**14,434**	**1,50E-06**	**3,0202**	**28,809**	**2,37E-07**	**5,8250**
8:31847916	**8**	**31847916**	**13,014**	**6,07E-06**	**3,0694**	**25,971**	**1,02E-06**	**5,2171**
8:31944993	**8**	**31944993**	**12,992**	**5,07E-06**	**2,1183**	**25,922**	**8,38E-07**	**5,2951**
8:43117802	**8**	**43117802**	**12,826**	**5,93E-06**	**3,7437**	**18,392**	**2,85E-05**	**5,2267**

3.1.5. Selection of candidate genes and primer design

The regions 10 kb upstream and downstream of selected significant SNPs were explored through the Jbrowser site (Buels et al. 2016). Genes which were located within these areas - 79 and 43 genes for AUDPC and MSS respectively - were considered as possible candidate genes (Table S. 14).

To reduce this number for further studies, additional criteria were applied. First, they should be directly or indirectly involved in resistance mechanisms based on gene annotation. This criterion resulted in selection of 52 and 27 possible candidate genes responsible for AUDPC and MSS. Second, the selected genes should be common between AUDPC and MSS. This resulted in 21 candidates (Figure 55).

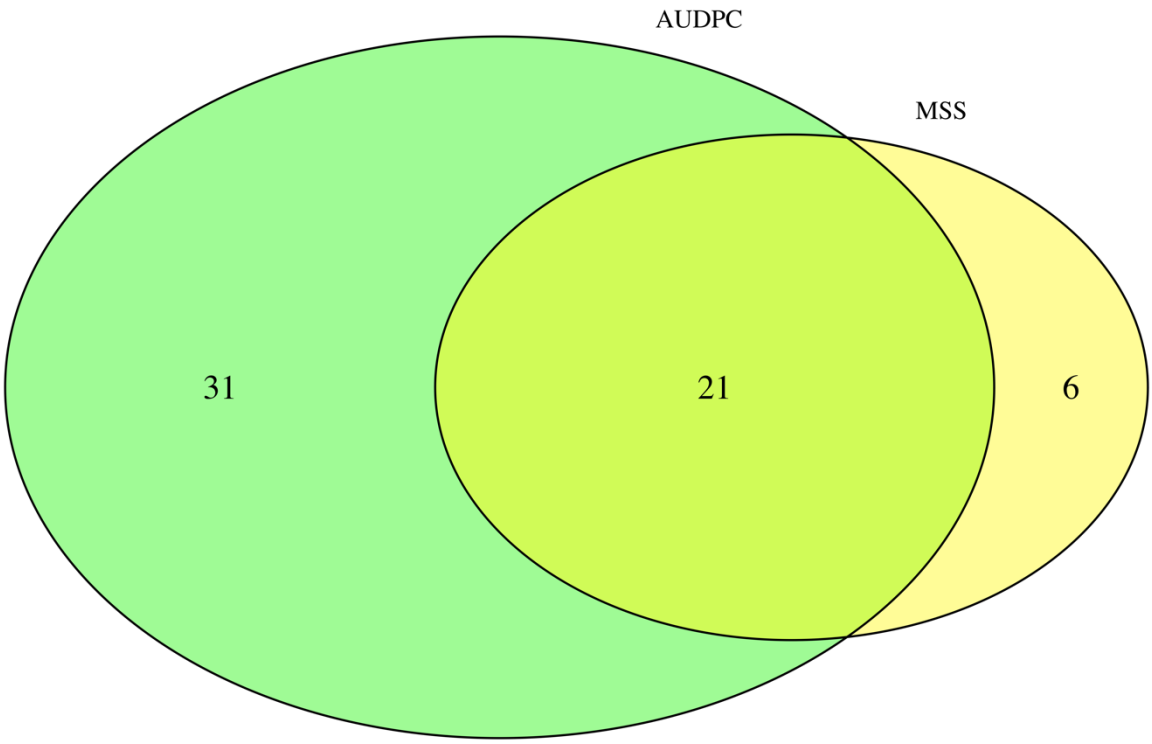

Figure 55: Number of selected candidate genes in response to *V. alfalfae* AF1 as determined by GWAS within the AUDPC and MSS.

Out of these 21 genes, 17 genes related to SNP with lowest P-values or/and having the most prominent function in resistance mechanisms based on gene annotation were selected as the final candidate genes.

The full sequence of selected candidate genes was obtained through (http://www.medicagohapmap.org/fgb2/gbrowse/mt40/). Primers for Quantitative PCR (qRT-PCR) were designed using the primer3plus web interface for primer3 (Primer3Plus Version: 2.4.2, https://primer3plus.com/cgi-bin/dev/primer3plus.cgi). Subsequently, 10 different primer pairs per gene, were designed base on exon-exon junction (except for gene "*MEDTR3g054420*" for which no exon-exon primer was found). After checking for primers' stability and specific amplification through blast with the A17 genome 16 different primer pairs (one pair per each gene) which met all criteria, were selected (Table S. 13).

IV.4.Gene expression

4.1. Expression of candidate genes in *M. truncatula* roots inoculated with AF1

For gene expression studies, root inoculations were performed not in Jiffy substrate as for the phenotyping experiments, but in plug trays which allow easier access to roots for harvesting and reduce the stress on the roots during sampling.

Based on the Tukey grouping of Lsmeans values derived from the phenotyping experiments, 12 of the most susceptible and resistant accessions were selected for this study (Table 34). Three independent experiments were carried out for the gene expression study. To investigate the probable effect of plug trays on the inoculation and also to trace the success of the inoculation in the gene expression study, the evaluation of wilt symptoms in unharvested plants for 28 days was included in the gene expression study. The results confirmed the same trend in response to inoculation between the phenotyping process (where the jiffy was used as substrate) and gene expression study (where the plug tray was used as substrate) (Figure 56).

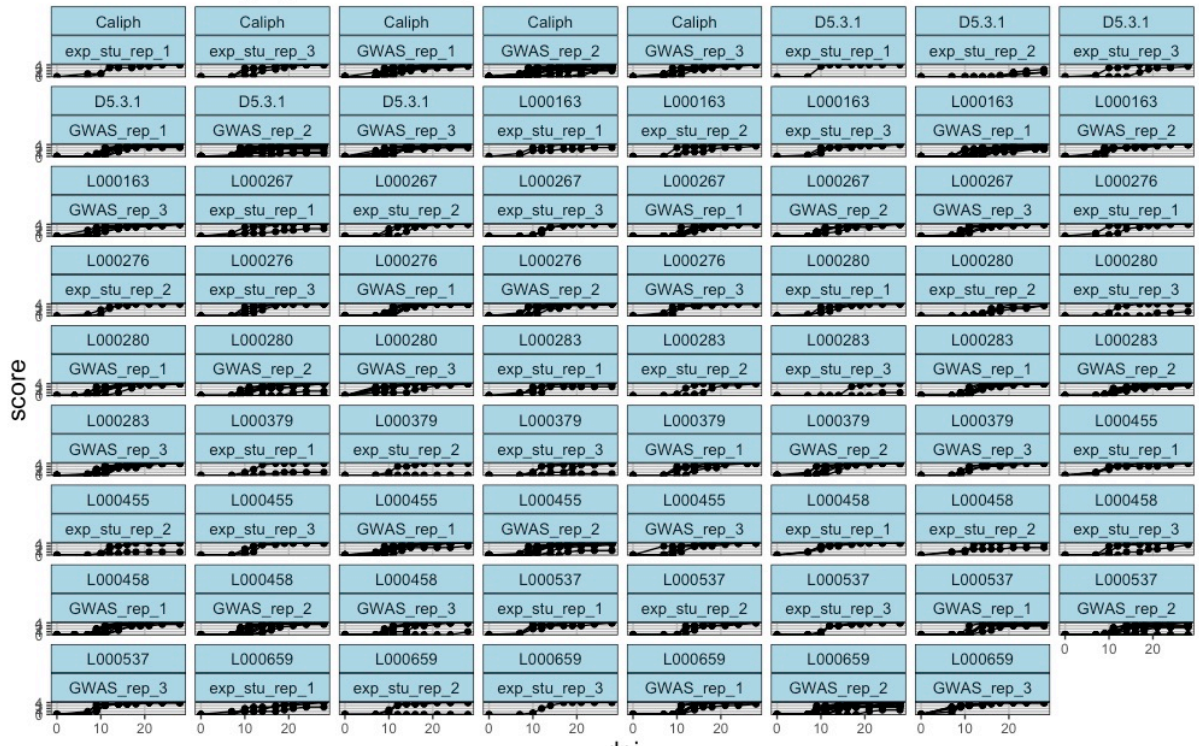

Figure 56: Comparison of the trend of *M. truncatula* accession to the Iranian *V. alfalfae* (AF1) inoculation when jiffy and plug trays are used as substrate.

For RNA sampling roots and arial parts were harvested at 0, 4 h (as very early time), 24 h (as early time) and 96 h (as later time) after inoculation. To mask the genetic variation of individual accessions the samples were pooled in a susceptible and a resistant group for each time point.

Table 34: Accessions selected for gene expression analysis.

ID	Line	Country of Origin	BLUEs_AUDPC	BLUEs_MSS	Response to AF1
HM173	L000411	Spain	0,003847	1,378796	Resistant
HM058	L000513	Spain	0,00428	1,431084	Resistant
HM128	L000620	France, Corsica	0,004348	1,416628	Resistant
HM101	L000738	Unknown	0,005001	1,409722	Resistant
HM117	L000401	Spain	0,005049	1,549689	Resistant
HM044	L000245	Jordan	0,005598	1,543006	Resistant
HM092	L000443	Spain	0,00569	1,37275	Resistant
HM068	L000274	Portugal	0,006866	1,550761	Resistant
HM205	L000212	Portugal	0,007169	1,662605	Resistant
HM123	L000440	Spain	0,007215	1,649124	Resistant
HM141	L000044	Tunis	0,007248	1,800373	Resistant
HM118	L000410	Spain	0,007265	1,66644	Resistant
HM059	L000449	France	0,020947	3,541393	Susceptible
HM165	L000344	Algeria	0,021528	3,803844	Susceptible
HM001	L000163	Syria	0,021559	3,811832	Susceptible
HM207	Caliph	Unknown	0,021808	3,889299	Susceptible
HM284	D5.3.1	Syria	0,022285	3,817523	Susceptible
HM138	L000283	Libya	0,022491	4,090339	Susceptible
HM127	L000455	France, Corsica	0,022646	3,840099	Susceptible
HM192	L000280	Tunis	0,022688	3,762328	Susceptible
HM134	L000267	Greece	0,022874	4,050639	Susceptible
HM062	L000379	Greece	0,023474	4,085681	Susceptible
HM116	L000659	Algeria	0,023557	3,875298	Susceptible
HM069	L000276	Tunis	0,025352	3,95402	Susceptible

4.1.1. Primer efficiency of selected primers

The efficiency of each pair of designed primer was assayed and calculated through a standard curve method. Since there was no prior knowledge about the expression of genes, all cDNAs derived from different sampling times and conditions were mixed and the primer efficiency was assayed through the standard curve and with a series of dilution (Figure S. 2).

Out of 16 primer pairs, 9 qualified thus for further qRT-PCR, which represents 56.25% of the success in the primer design phase (Table 35).

Table 35: Efficiency of designed primers.

Primer Name (Gene V.4.0)	GenBank	Functional annotation	R^2	Slope	% Efficiency	Selected pair
MEDTR1g042280	AES60208.2	Casein kinase I-like protein	0,998	-3,600	89,55	+
MEDTR1g042160	AES60195.1	MATH domain protein	0,992	-3,293	101,21	+
MEDTR1g087880	AES61721.2	P-loop nucleoside triphosphate hydrolase superfamily protein	0,996	-2,046	208,1	-
MEDTR4g023000	AES87221.1	Glycoside hydrolase family 1 protein	0,990	-3,299	100,99	+
MEDTR7g024390	AES78087.1	Heat shock cognate 70 kDa protein	0,988	-0,32	115919,34	-
MEDTR8g075240	AET03747.1	Rho-like GTP-binding protein	0,999	-3,561	90,91	+
MEDTR8g075260	AET03749.1	TPR superfamily protein	0,906	-1,788	262,42	-
MEDTR8g075310	AET03754.2	IAA-amino acid hydrolase ILR1-like protein	0,846	-1,035	824,32	-
MEDTR8g075320	AET03755.1	Proteasome subunit alpha type-7-A protein	0,992	-3,299	115,500	+
MEDTR8g075330	AET03756.1	Glycoside hydrolase family 38 protein	0,796	-7,328	36,92	-
MEDTR8g075340	AET03757.1	Osmosensor histidine kinase	0,986	-3,25	103,07	+
MEDTR8g075510	KEH20376.1	Pathogenesis-related thaumatin family protein	0,973	-2,131	194,49	-
MEDTR8g075550	AET03777.1	Pathogenesis-related thaumatin family protein	0,981	-3,292	101,32	+
MEDTR8g102470	KEH21334.1	6-phosphogluconate dehydrogenase NAD-binding domain protein	0,990	-3,299	100,96	+
MEDTR1g087510	AES61694.1	Hypothetical protein *MTR_1g087510*	0,975	-2,620	140,77	-
MEDTR1g087500	AES61693.1	Hypothetical protein *MTR_1g087500*	0,996	-3,604	89,43	+

4.1.2. Study and analysis of the gene expression of candidate genes in roots of *Medicago truncatula*

A first observation is that all selected genes were expressed in *M. truncatula* roots. A second observation is that they were also all induced by inoculation at some moment of the time course and induction was higher in resistant plants.

Four different expression patterns were detected and can be categorized as follows:

1. The first group contains the genes *MEDTR4g023000* (glycoside hydrolase family 1 protein), *MEDTR8g075340* (osmosensor histidine kinase) and *MEDTR8g102470* (3-hydroxyisobutyrate dehydrogenase-like 1 /6-phosphogluconate dehydrogenase NAD-binding domain protein). They represented very early induction at 4 hours post-inoculation (hpi) in both susceptible and resistant plants which decreased thereafter. The expression returned very quickly to basic level in susceptible plants. The induction of *MEDTR4g023000* lasted till 96 hpi that of *MEDTR8g075340* and *MEDTR8g102470* lasted till 24 hpi in resistant plants (Figure 57).

A

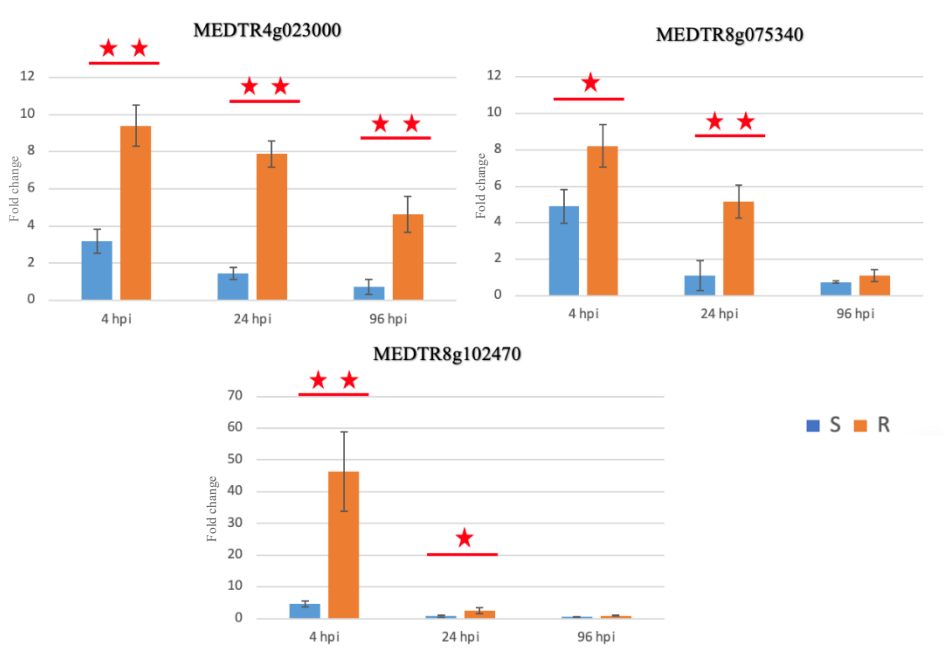

B

Gene Name	Description		4 H	24 H	4 DPI
MEDTR4g023000	Glycoside hydrolase family 1 protein	P-values derived from t-test of mean comparisons of susceptible pool versus resistant one	0,002628	0,001692	0,006969
MEDTR8g075340	Osmosensor histidine kinase		0,02081	0,001682	0,2103
MEDTR8g102470	6-phosphogluconate dehydrogenase NAD-binding domain protein		0,001471	0,01249	0,2099

Figure 57:A: Gene expression in *M. truncatula* roots determined by qRT-PCR.

A: Fold change of expression in inoculated roots versus mock-inoculated roots at 4, 24, and 96 hpi. Susceptible plant pools are shown in blue, resistant plan pools in orange. The X-axis represents hours post inoculation (hpi) and Y-axis represents Fold change. The red stars represent the significance levels derived from T-test P-values. B: P-values derived from the T-test comparisons within each susceptible and resistant pool at different time points.

2. The second group contains the genes *MEDTR1g042280* (casein kinase I-like protein), *MEDTR1g042160* (MATH domain protein) and *MEDTR1g087500* (hypothetical protein). They also exhibited very early induction at four hpi in both susceptible and resistant plants which was higher in resistant plants, but compared to genes of the first group their maximum induction was at 24 hpi. In this group the induction lasted till 96 hpi in resistant plants (Figure 58).

A

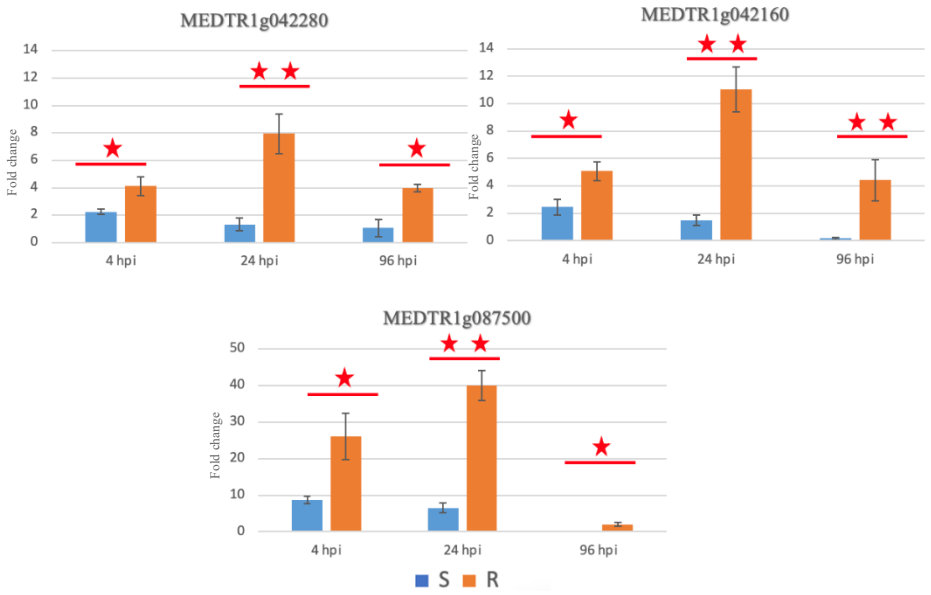

B

Gene Name	Description		4 H	24 H	4 DPI
MEDTR1g042280	casein kinase I-like protein	P-values derived from t-test of mean comparisons of susceptible pool versus resistant one	0,01459	0,002692	0,0175
MEDTR1g042160	MATH domain protein		0,03673	0,007174	0,00196
MEDTR1g087500	hypothetical protein		0,03788	0,00284	0,02941

Figure 58: Gene expression in *M. truncatula* roots determined by qRT-PCR.

A: Fold change of expression in inoculated roots versus mock-inoculated roots at 4, 24, and 96 hpi. Susceptible plant pools are shown in blue, resistant plan pools in orange. The X-axis represents hours post inoculation (hpi) and Y-axis represents Fold change. The red stars represent the significance levels derived from T-test P-values. B: P-values derived from the T-test comparisons within each susceptible and resistant pool at different time points.

3. The third group contains only one gene, *MEDTR8g075240* (Rho-like GTP-binding protein) and exhibited an early induction at 4 hpi in resistant plants which increased until 96 hpi whereas in susceptible plants only a weak induction at 24h was observed. (Figure 59).

A

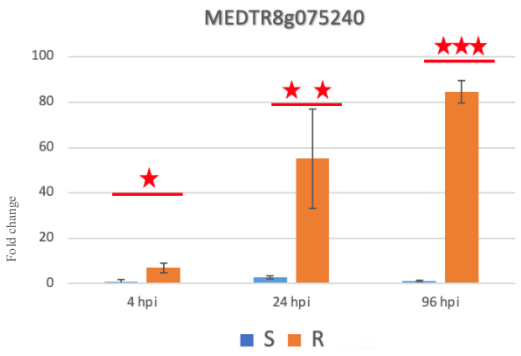

B

Gene Name	Description		4 H	24 H	4 DPI
MEDTR8g075240	Rho-like GTP-binding protein	P-values derived from t-test of mean comparisons of susceptible pool versus resistant one	0,03335	0,005369	0,0009976

Figure 59: A: Gene expression in *M. truncatula* roots determined by qRT-PCR.

A: Fold change of expression in inoculated roots versus mock-inoculated roots at 4, 24, and 96 hpi. Susceptible plant pools are shown in blue, resistant plan pools in orange. The X-axis represents hours post inoculation (hpi) and Y-axis represents Fold change. The red stars represent the significance levels derived from T-test P-values. B: P-values derived from the T-test comparisons within each susceptible and resistant pool at different time points.

4. The fourth group containing the genes *MEDTR8g075320* (proteasome subunit alpha type-7-A protein) and *MEDTR8g075550* (pathogenesis-related thaumatin family protein) exhibited strong induction at 24 hpi which decreased thereafter in resistant plants. In this group, the highest induction was observed at 24 hpi. (Figure 60).

A

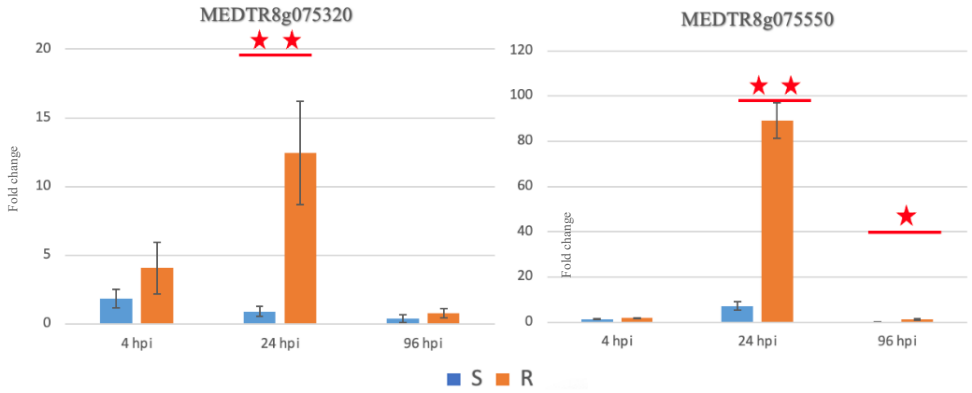

B

Gene Name	Description		4 H	24 H	4 DPI
MEDTR8g075320	proteasome subunit alpha type-7-A protein	P-values derived from t-test of mean comparisons of susceptible pool versus resistant one	0,08346	0,004908	0,4177
MEDTR8g075550	pathogenesis-related thaumatin family protein		0,07434	0,004228	0,03435

Figure 60: A: Gene expression in *M. truncatula* roots determined by qRT-PCR.

A: Fold change of expression in inoculated roots versus mock-inoculated roots at 4, 24, and 96 hpi. Susceptible plant pools are shown in blue, resistant plan pools in orange. The X-axis represents hours post inoculation (hpi) and Y-axis represents Fold change. The red stars represent the significance levels derived from T-test P-values. B: P-values derived from the T-test comparisons within each susceptible and resistant pool at different time points.

V - Discussion

In order to study the response of *M. truncatula* to two potential threats - temperature increase and introduction of a new strain of *V. alfalfae* - we used an isolate obtained through field trips to Iran. The first report of *V. alfalfae* in Iran was published in 2004 by Ghalandar *et.al*. who detected the pathogen in alfalfa fields of the Markazi Province. Thirteen years after this publication, our samples from different parts of Iran show that this disease has spread since then to various areas of the Markazi and neighboring Hamedan provinces and to the Teheran region. Since alfalfa culture in Iran depends on irrigation, it can be supposed that the pathogen spread has been favoured by irrigation systems, as has been reported for *V. dahliae* on olive tree (Jiménez-Díaz et al. 2011; López-Escudero and Mercado-Blanco 2011). Seed companies in Iran and neighboring countries should thus include tolerance to *verticillium* wilt in future alfalfa breeding programs and survey alfalfa producing regions for occurrence of this disease. Fungal isolates from symptomatic alfalfa in three other provinces (West Azerbaijan, Isfahan and Yazd) were not confirmed as *V. alfalfae*, but this does not preclude the existence of the pathogen in these regions. As suggested by their pink mycelium on PDA medium, some isolates were probably *Fusarium* species, but we did not attempt to identify them further.

Unlike the French strain, Iranian isolates developed black pigmentation after longer growth on PDA. Also, the temperature seems to affect the formation of black pigmentation; it occurred more frequently at 25 °C. Although, we did not study this issue sufficiently to statistically support this observation, it is consistent with the results reported by Xu *et. al* (2019) that noted this discoloration on the PDA media (especially more common at 25 °C) and believed that this phenomenon is in link to the existence of resting mycelium. In addition, in some older literature (Heale and Isaac 1965; I. Isaac and MacGarvie 1966; I Isaac 1949), the authors report their observations on the effect of temperature, light, and age of culture on the formation of black resting bodies in the *verticillium* genus. However, due to the taxonomic division of *Verticillium* at that time, they made no mention of *V. alfalfae* in their reports.

By hyphal growth and sporulation, all Iranian isolates are in one statistical group as opposed to the French isolate. A negative correlation between hyphal growth and sporulation was observed for all strains. This has also been reported earlier for other fungal species such as *Aspergillus Niger* (Muller 1956), *V. agaricinum* and

Schizosaccharomyces pombe (McKoy and Trinci 1987) and *Ascochyta rabiei* (Mahiout et al. 2015).

We could not reveal any genetic differences between the French and Iranian isolates through a preliminary study with some molecular markers. This relies probably on the fact that no sexual reproduction has been reported for this fungus, although mating type genes are present in its genome. For this reason, genetic variability of the species is expected to be limited. However, the phenotypic divergence strongly suggests that *V. alfalfae* in Iran belongs to a different genotype. An Iranian strain should thus have the potential to reveal different genetic control of resistance in *M. truncatula*, compared to the plant's response to the French strain.

The Iranian isolate AFI was chosen for subsequent studies based on pathogenicity results showing a slightly higher aggressiveness towards the selected diversity panel and also because it was collected from the Arak region (the same region where the first report of *V. alfalfae* in Iran was published (Ghalandar et al. 2004)).

A preliminary study of Iranian *Medicago* species showed that among the 4 *M. truncatula* accessions there is one resistance accession towards both French and Iranian isolates. Due to the low number of seeds and time constraints, we could not conduct this study on fixed lines, but due to the autogamous production of *M. truncatula,* we are confident that the obtained results are significant. However, we are fully aware of the need to reconduct the study in the form of an appropriate experimental design with several repeats.

The continuous distribution of AUDPC and MSS scores through the panel of *M. truncatula* accessions suggested that resistance to the Iranian strain of *V. alfalfae* is controlled in a polygenic manner. The broad sense heritability (H^2) calculated values for both traits (AUDPC=0.719, MSS=0.724) suggests that their variability is linked to a combination of genetic and environmental factors with a significant share of genetic variance.

Taken together, the range of phenotypic variation of response to the pathogen and high heritability indicated that population and traits are suitable for studying the architecture of resistance through genome-wide association mapping.

Genome wide association study (GWAS) was used to investigate the genetic architecture of *M. truncatula* resistance towards the Iranian *V. alfalfae* isolate. Genome wide association mapping evaluates the statistical significance of the association between quantitative differences of a particular phenotype and specific genetic polymorphisms in a set of genetically distinct individuals (Ogura and Busch 2015). A first important step of GWAS is to select an appropriate statistical model which eliminates false positives and copes with spurious associations due to familial relatedness, population structure (Balding 2006; M. Wang et al. 2012; Yu and Buckler 2006) and population admixture (M. Chen et al. 2014; Gay et al. 2020).

Among all statistical models, although the *MLM Q-model* showed some overcorrection for confounding effects of population, it addressed a better-fitted model in comparison to other models. Also, among the two approaches, the one whose breeding values were adjusted through the MLM was more precise as confirmed by the Q-Q plot (the more overlap points presented between observed and expected p-values); since this approach corrected the data based on the all involved accession while the correction in the augmented block approach was done just base on the mean of four check lines. Hence, the MLM Q-model whose breeding values were corrected through MLM was used for the following steps.

A GWAS of the response of the association panel to the French *Verticillium* isolate V31-2 at 20 °C in a previous work led to the identification of 34 candidate genes (Mazurier 2018), while our present study with the Iranian *Verticillium* isolate AF1 at 25 °C identified 92 candidate genes, with only one gene (*Medtr1g042160*) in common corresponding to about 1% overlap between the two studies. Due to the high number of candidate genes and the small contribution of each *locus* to resistance; it did not seem reasonable to go further for functional studies. In addition, since two variables (temperature and pathogen strain) have been changed, it is not possible to separate their effects on the outcome of the interaction between *M. truncatula* and *V. alfalfae.*

Also, we should note that this study did not reveal neither common SNPs nor common genes in LD with detected QTLs from previous studies with LR3, LR4, LR5 (Ben et al. 2013) populations and also with LPP0323 (Negahi et al. 2014). However, the results show that such combined effects can completely change the genetic signatures of plant disease resistance and should be a warning to breeders and institutions that control exchange of plant material.

In order to select candidate genes putatively involved in the resistance response to *V. alfalfae* strain AF1, the areas 10 kb upstream and downstream of all significant SNPs were analyzed, based on data on linkage disequilibrium and recombination rates described for *M. truncatula* in a previous study (Branca et al. 2011). Chromosome 8 shows the highest number of genes putatively involved in resistance towards AF1 with 31 and 17 genes for AUDPC and MSS respectively.

By qPCR the expression of all 9 selected candidate genes in *M. truncatula* roots was confirmed. Although the responses were very diverse, it was possible to classify them into four different groups by their time course. Interestingly these genes revealed the higher expression and more relative durability in the resistant accessions; however, at some time points; they expressed in the susceptible accessions as well while no significant difference could be found within two pools such as genes *MEDTR8g075340*, *MEDTR8g102470* (Figure 57) or genes *MEDTR8g075320*, *MEDTR8g075550* (Figure 60).

Expression of these 9 genes from *loci* on chromosomes 1, 4, 7 and 8 was studied in roots of susceptible and resistant plants after root inoculation.

These candidate genes were selected based on their functional annotation, to focus on responses related to signaling and defense in stress resistance.

Kinases through phosphorylation of their targets participate in many signaling pathways, as do GTP-binding proteins. Genes encoding a casein kinase 1 like protein and a osmosensor histidine kinase, and a Rho-like GTP binding protein were induced at 4 hpi in *M. truncatula* roots inoculated with AF1, to a higher level in resistant plants compared to susceptible ones, in agreement with their putative roles in phytohormone signaling and defense against biotic stress (Yin et al. 2015; H. Zhao et al. 2020; Pham et al. 2012; N. Li et al. 2019; Klessig, Choi, and Dempsey 2018).

Ubiquitination is also an important part of signaling pathways in response to pathogens (Marino, Peeters, and Rivas 2012). Genes encoding a MATH domain protein and a proteasome subunit alpha type-7-A protein were induced at 4 hpi, to a higher level in resistant plants compared to susceptible ones. Genes for MATH domain proteins were also reported to be induced during pathogen attack in rice (Kushwaha et al. 2016).

Other proteins participate more directly to defense such as the pathogenesis-related proteins to which belong thaumatin and glycoside hydrolases (Ali et al. 2018). The induction of the gene encoding the thaumatin family protein was later than that of the

eight other genes, which is consistent with a role as defense protein, whereas the gene encoding glycoside hydrolase family 1 protein had it is highest induction at 4hpi which indicates a possible signaling involvement of this protein.

Finally, the genes encoding a 6-phosphogluconate dehydrogenase NAD-binding domain protein / probable 3-hydroxyisobutyrate dehydrogenase-like 1 protein and a hypothetical protein cover primary metabolism and unknown functions. They were also induced in roots by AF1 inoculation, early and stronger in resistant plants, indicating their putative involvement in the plants' resistance response.

About the hypothetical protein; *MTR_1g087500* (*Medtr1g087500*) encodes this hypothetical protein in *M. truncatula*. Sequence analysis through NCBI blast showed a predicted cell wall protein of *Lupinus angustifolius* with 80% identities and very low e-Value (2e-135) which this e-Value addresses there is an exact match between these two sequences. This gene showed strong upregulation in the pool of resistant plants in 4 and 24-hours post inoculation around 26- and 40-fold, respectively.

So, although we are aware of the need for further studies on this gene, the results suggest that this gene and by extension a putative cell wall protein has a role in resistance.

Taken together, the expression patterns of these genes, *i.e.,* strong induction in resistant plants vs. weak induction in susceptible plants, support the claim that the *loci* identified by GWAS have significant contributions to resistance. This is in agreement with the general observation described by Beckman & Robert (1995) that resistant plants have early recognition along with an effective response to a pathogen, which helps them overcome this stress condition, whereas susceptible plants have weak or delayed detection as well as ineffective responses.

Since the nine genes studied here represent only a small part of the many putative candidate genes underlying the *loci*, identified by GWAS, their respective contributions would be small and functional studies by over- or under-expressing the gene cannot be expected to provide relevant insights into the mechanisms of resistance.

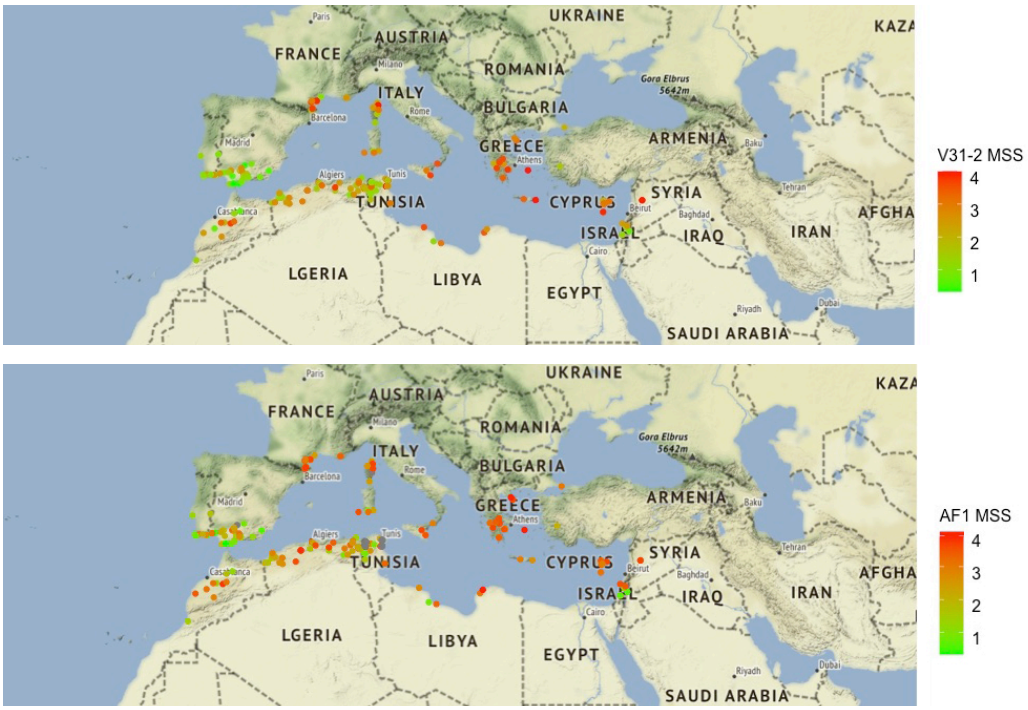

Figure 61: Comparison of the response of 242 *M. truncatula* accession to Iranian *V. alfalfae* (AF1) strain and French *V. alfalfae* (V31-2) strain.

Geographical distribution of the 242 accessions of *Medicago truncatula* whose origin is documented and whose response to Verticillium alfalfae V31-2 and AF-1 has been evaluated. Each accession is represented by a point whose color varies according to the MSS corrected after inoculation by V31-2 and AF-1.

Another aspect of our study was to test if the geographical distribution of resistance to *V. alfalfae*, as described by Gentzbittel *et la.* (2019) would change with a new strain and a higher temperature. Indeed, the WhoGEM approach showed that susceptibility is dominant in accessions from the eastern regions and resistance was highest in accessions from western regions of the Mediterranean basin. In addition, we hypothesized that the susceptibility response would be increasing at a higher temperature as the fungal growth analysis and pathogenicity tests confirmed, 25 °C as the optimum temperature for growth and sporulation and favoured higher symptom scores (also reported by Sbeiti, (2016)). More and less, we had the same outcome (accumulation of resistant accessions on the west and susceptible on the east part of Mediterranean). However, increase in the temperature, promotes the susceptibility (as it was expected) but again the same trend is observed (accumulation of resistant accessions in the western regions and susceptible in the eastern part of Mediterranean basin) (Figure 61). We should not be unaware that pathogenicity tests have shown that the AF1 strain is more pathogenic than the French strain (V31-2), but given the available information, it is not possible to determine and quantify the strain's effect on

this susceptible response. However, the results of this study confirm the previous hypothesis, in other words, the obtained results from this study do not give any reason to disprove the previous hypothesis, so it can be said that resistance to *V. alfalfae* among Mediterranean accessions is structured. However, we emphasize in order to dispel the doubts and confirm the accuracy of the obtained results, two other studies (although with a smaller number of accessions) should be carried out; one with V31-2 at 25 °C and the other with AF1 at 20 °C. If these experiments confirm our results, the question that can be raised is where is the origin of *V. alfalfae*?

VI - Conclusion and Perspectives

Control of plant root pathogens such as *Verticillium alfalfae* is very difficult. Since agronomic practices such as rotation and biological control are very costly while having only very limited effects and have not much efficacy at all, also, the application of fungicides is very harmful to the environment, so, genetic improvement of crop species that are exposed to this pathogen is the only effective strategy. Such a strategy should take into account that due to climate change; the temperatures will increase and that global trade favours the introduction of new pathogens.

With this scenario as background, the resistance of *Medicago truncatula* toward an Iranian strain of *Verticillium alfalfae* was studied, at higher temperature than standard inoculation assays. The high density of SNP markers in *M. truncatula* made it possible to perform a genome wide association study in order to study the genetic control of resistance toward *V. alfalfae*.

V. alfalfae isolates were obtained from alfalfa fields in Iran were indeed different from the French isolate used in previous studies, and resistance to one of these isolates was associated to 30 loci that were not detected before under previous conditions.

VI.1.Iranian *Verticillium alfalfae* isolates merit further studies

Phenotype, growth characteristics and aggressiveness of the Iranian isolates were different from those traits observed in the French isolate.

For further studies we suggest to perform the full genome sequencing of Iranian isolates and *V. alfalfae* samples from other collections, to be able to make a comparison with the reference strain sequence. Plotting the phylogenetic tree will be helpful to visualize the genetic diversity within the species, and maybe could indicate the origin or Iranian strains (native or introduced from abroad only recently?) These sequence data might also be helpful to find and develop strain-specific molecular markers useful for the control of plant material.

In addition, the aggressiveness of Iranian *V. alfalfae* isolates and *V. alfalfae* isolates from other collections should be studied on Iranian *M. truncatula* accessions and on commercial alfalfa cultivars. This could reveal additional sources of resistance.

VI.2.HapMap, an international project without any representative from the center of biodiversity of Alfalfa

MtHapMap is an international repository that so far has collected 339 different species of the Medicago genus around the world and gathered valuable genomic information of this species. However, this successful project has neglected a key point.

Iran is the center of Medicago biodiversity and even the name of the species Medicago is derived from the ancient name of Iran. Yet, this valuable collection suffers from the absence of any representative accessions from the Medicago Biodiversity center.

Only 9 accessions from Turkey (the closest country to Iran) are included in the HapMap collection, while only 4 of them belong to *M. truncatula*.

Now that we have collected 4 accessions of *M. truncatula* and one *M. scutellata* from Iran, we are fully prepared to provide them to the MtHapMap project and we also are willing to assist in sequencing and extracting genomic data, to enrich the dataset in this collection. We also propose to explore Iran to find more accessions of Medicago to further enrich this collection.

VI.3. The use of a new strain and higher temperature does not profoundly change the distribution pattern of susceptible and resistant accessions

A previous study on the distribution of genomic admixture has shown that resistance to the French isolate V31-2 was associated to populations in the western part of the Mediterranean region (Gentzbittel et al. 2019). Our work revealed that despite changing two parameters (strain and temperature), the distribution was essentially the

same. This somehow refutes the hypothesis that resistance to the French strain was due to co-evolution between host plant and pathogen. However, should *V. alfalfae* have been introduced recently to Iran by trade from western countries, the initial hypothesis could still stand. Hence, genomic data and a phylogenetic tree of *Verticillium* strains (preceding chapter) are necessary in order to get a clearer picture of the relationships.

VI.4.New loci are associated to resistance towards Iranian *V. alfalfae* at 25 °C

Although the geographical distribution of resistant genotypes has not really changed, resistance under the conditions of the present study involves a higher number of loci, which are all different from the loci identified previously (Mazurier 2018). It is difficult at this stage to separate the effects of temperature and of strain, and to perform GWAS with the same collection of *M. truncatula* lines, with the Iranian strain at lower temperature would be too tedious. A different way to tackle this question could be the study of expression of candidate genes.

These genes confirmed the involvement of loci in resistance since their expression was induced by inoculation, and to a stronger extent in resistant plants. The same expression studies should be made under the following conditions:

Inoculation with the Iranian isolate at 20 °C, and inoculation with the French isolate at 25 °C. Comparison of the expression patterns under these different conditions might indicate if a given locus is influenced more or less by temperature or by strain or by both.

VI.5.New functions of genes under resistance loci

The results of this study revealed the contribution of some hypothetical proteins in resistance toward *V. alfalfae* such as the gene *MTR_1g087500*. As there is not much information neither about these hypothetical proteins in *M. truncatula* nor their

homologous genes in other species; we suggest to study the expression of genes under the identified loci encoding other hypothetical protein. The time course of their expression and the tissular localization of their expression could give a hint to their function.

VI.6. Breeders and institutions could benefit from the results of this study

Eventually, as the purpose of this study is to identify the presence of resistance genes to *V. alfalfae* disease, the knowledge retained from this study should be transferred to cultivated alfalfa. Based on a comparison of the alleles of candidate genes in resistant and susceptible genotypes it might be possible to develop molecular markers for alfalfa breeding. Since we detected differences in the expression pattern, promoter sequences might be a good target, or transcription factors binding to these promoters. Homologs of the *M. truncatula* candidate genes should then be identified in alfalfa and their expression or sequence polymorphism studied in some resistant and susceptible varieties, to confirm their usefulness.

However, in the light of our findings that strain and environmental conditions may change the localization of QTLs completely, breeding programs should test a wider range of conditions and isolates in order to increase the food security of human beings.

VII - Annex

Table S. 1: Accessions used in GWAS

	ID	Line	Population	Origin	Category
1	HM001	L000163	SA022322	Syria	CC8
2	HM002	L000174	SA028064	Cyprus	CC8
3	HM003	L000544	ESP 105-L	Spain	CC8
4	HM004	L000736	DZA45.6	Algeria	CC8
5	HM005	L000734	DZA315.16	Algeria	CC8
6	HM006	L000530	F83005.5	France	CC8
7	HM007	L000651	SALSES 71B	France	CC8
8	HM008	L000368	DZA 012-J	Algeria	CC8
9	HM009	L000555	GRC 020-B	Greece	CC16
10	HM010	L000154	SA024714	Italy	CC16
11	HM011	L000543	DZA 327-7	Algeria	CC16
12	HM012	L000239	SA026063	Morocco	CC16
13	HM013	L000648	SALSES 42B	France	CC16
14	HM014	L000542	DZA 233-4	Algeria	CC16
15	HM015	L000550	F 11013-3	France	CC16
16	HM016	L000049	SA009707	Tunis	CC16
17	HM017	A10	A10	Unknown	RIL.Parent
18	HM018	A20	A20	Unknown	RIL.Parent
19	HM019	L000527	Borung	Unknown	RIL.Parent
20	HM020	TN1.11	TN1.11	Tunis	RIL.Parent
21	HM021	TN1.21	TN1.21	Tunis	RIL.Parent
22	HM022	TN3.23	TN3.23	Tunis	RIL.Parent
23	HM023	TN6.18	TN6.18	Tunis	RIL.Parent
24	HM024	TN8.3	TN8.3	Tunis	RIL.Parent
25	HM025	TN9.22	TN9.22	Tunis	RIL.Parent
26	HM026	L000450	F 11008-C	France	RIL.Parent/CC96
27	HM027	L000531	F83005-9	France	RIL.Parent/CC144
28	HM028	L000342	DZA241-2	Algeria	RIL.Parent/CC144
29	HM029	L000729	R108.C3	Unknown	M. tricycla
30	HM031	L000545	ESP 158-A	Spain	CC32
31	HM032	L000549	F 11005-E	France	CC32
32	HM033	L000552	F 20047-A	France, Corsica	CC32
33	HM034	L000554	F 20089-B	France, Corsica	CC32
34	HM035	L000679	F 66017	France	CC32
35	HM036	L000337	GRC 042-1	Greece	CC32
36	HM037	L000557	GRC 064-B	Greece	CC32
37	HM038	L000369	PRT 180-A	Portugal	CC32

	ID	Line	Population	Origin	Category
38	HM039	L000263	SA003116	Israel	CC32
39	HM040	L000321	SA003780	Italy	CC32
40	HM041	L000198	SA009048	Libya	CC32
41	HM042	L000290	SA009119	Turkey	CC32
42	HM043	L000310	SA009944	Tunis	CC32
43	HM044	L000245	SA014161	Jordan	CC32
44	HM045	L000144	SA014163	Jordan	CC32
45	HM046	L000213	SA027882	Morocco	CC32
46	HM047	L000654	DZA 014	Algeria	CC64
47	HM048	L000475	DZA 016-F	Algeria	CC64
48	HM049	L000360	DZA 058-5	Algeria	CC64
49	HM050	L000477	DZA 058-J	Algeria	CC64
50	HM051	L000357	DZA 202-4	Algeria	CC64
51	HM052	L000639	DZA 210-3	Algeria	CC64
52	HM053	L000601	DZA 246-6	Algeria	CC64
53	HM054	L000395	DZA 309-A	Algeria	CC64
54	HM055	L000675	DZA 326	Algeria	CC64
55	HM056	L000416	ESP 074-A	Spain	CC64
56	HM057	L000512	ESP 155-D	Spain	CC64
57	HM058	L000513	ESP 163-E	Spain	CC64
58	HM059	L000449	F 11012-A	France	CC64
59	HM060	L000520	F 20015-10	France, Corsica	CC64
60	HM061	L000645	GRC 033-B2	Greece	CC64
61	HM062	L000379	GRC 063-D	Greece	CC64
62	HM063	L000525	PRT 176-F	Portugal	CC64
63	HM064	L000371	PRT 178-D	Portugal	CC64
64	HM065	L000370	PRT 179-J	Portugal	CC64
65	HM066	L000204	SA001489	Israel	CC64
66	HM067	L000265	SA001526	Algeria	CC64
67	HM068	L000274	SA003648	Portugal	CC64
68	HM069	L000276	SA007749	Tunis	CC64
69	HM070	L000307	SA008625	Morocco	CC64
70	HM071	L000297	SA008626	Morocco	CC64
71	HM072	L000061	SA009357	Algeria	CC64
72	HM073	L000052	SA009710	Tunis	CC64
73	HM074	L000314	SA009866	Algeria	CC64
74	HM075	L000130	SA012451	Italy	CC64
75	HM076	L000234	SA023859	Tunis	CC64
76	HM077	L000232	SA027062	Greece	CC64
77	HM078	L000228	SA027063	Greece	CC64
78	HM079	L000362	DZA 045-4-C	Algeria	CC96

	ID	Line	Population	Origin	Category
79	HM080	L000637	DZA 061-B3d	Algeria	CC96
80	HM081	L000356	DZA 202-5	Algeria	CC96
81	HM082	L000355	DZA 210-2	Algeria	CC96
82	HM083	L000354	DZA 210-5	Algeria	CC96
83	HM084	L000394	DZA 243-6	Algeria	CC96
84	HM085	L000673	DZA 319	Algeria	CC96
85	HM086	L000674	DZA 322	Algeria	CC96
86	HM087	L000397	DZA 323-1	Algeria	CC96
87	HM088	L000497	DZA 323-D	Algeria	CC96
88	HM089	L000431	ESP 155-A	Spain	CC96
89	HM090	L000437	ESP 163-A	Spain	CC96
90	HM091	L000548	ESP 171-F	Spain	CC96
91	HM092	L000443	ESP 174-A	Spain	CC96
92	HM093	L000444	ESP 173-A	Spain	CC96
93	HM094	L000574	F 13006-1	France	CC96
94	HM095	L000458	F 20025-4	France, Corsica	CC96
95	HM096	L000460	F 20026-F	France, Corsica	CC96
96	HM097	L000522	F 83005-G	France	CC96
97	HM098	L000523	PRT 176-12	Portugal	CC96
98	HM099	L000202	SA002840	Cyprus	CC96
99	HM101	L000738	A17_Varma	Unknown	Unknown
100	HM103	L000302	SA004087	Tunis	CC96
101	HM104	L000303	SA008604	Algeria	CC96
102	HM105	L000293	SA009137	Algeria	CC96
103	HM106	L000060	SA009434	Tunis	CC96
104	HM107	L000047	SA009670	Algeria	CC96
105	HM108	L000317	SA009715	Tunis	CC96
106	HM109	L000126	SA011959	Israel	CC96
107	HM110	L000225	SA021560	Libya	CC96
108	HM111	L000219	SA027192	Italy	CC96
109	HM112	L000178	SA028097	Cyprus	CC96
110	HM113	L000537	CRE007-J	Greece, Crete	CC144
111	HM114	L000338	CRE009-A	Greece, Crete	CC144
112	HM115	L000529	Cyprus_C	Cyprus	CC144
113	HM116	L000659	DZA211	Algeria	CC144
114	HM117	L000401	ESP031-A	Spain	CC144
115	HM118	L000410	ESP043-B	Spain	CC144
116	HM119	L000414	ESP050-B	Spain	CC144
117	HM120	L000482	ESP095-C	Spain	CC144
118	HM122	L000546	Esp159-11	Spain	CC144
119	HM123	L000440	ESP163-B	Spain	CC144

	ID	Line	Population	Origin	Category
120	HM124	L000547	Esp165-D	Spain	CC144
121	HM125	L000445	ESP175-A	Spain	CC144
122	HM126	L000456	F20015-L	France, Corsica	CC144
123	HM127	L000455	F20025-F	France, Corsica	CC144
124	HM128	L000620	F20058-6	France, Corsica	CC144
125	HM129	L000468	F20069-A	France, Corsica	CC144
126	HM130	L000467	F20069-C	France, Corsica	CC144
127	HM131	L000551	F34042-D	France	CC144
128	HM132	L000376	GRC093-C	Greece	CC144
129	HM133	L000375	GRC098-A	Greece	CC144
130	HM134	L000267	SA02084	Greece	CC144
131	HM135	L000332	SA02748	Israel	CC144
132	HM136	L000270	SA02820	Turkey	CC144
133	HM137	L000322	SA03749	Israel	CC144
134	HM138	L000283	SA08454	Libya	CC144
135	HM139	L000306	SA08623	Morocco	CC144
136	HM140	L000286	SA09049	Libya	CC144
137	HM141	L000044	SA09456	Tunis	CC144
138	HM142	L000315	SA09820	Libya	CC144
139	HM143	L000132	SA10481	Tunis	CC144
140	HM144	L000241	SA15951	Portugal, Madeira	CC144
141	HM145	L000146	SA19964	Turkey	CC144
142	HM146	L000237	SA21302	Libya	CC144
143	HM147	L000161	SA21362	Libya	CC144
144	HM148	L000162	SA21590	Libya	CC144
145	HM149	L000148	SA21819	Cyprus	CC144
146	HM150	L000238	SA22323	Syria	CC144
147	HM151	L000165	SA25226	Italy	CC144
148	HM152	L000166	SA25654	Morocco	CC144
149	HM153	L000168	SA25898	Italy	CC144
150	HM154	L000173	SA27778	Morocco	CC144
151	HM155	L000216	SA27961	Morocco	CC144
152	HM156	L000217	SA28089	Cyprus	CC144
153	HM157	L000215	SA28099	Cyprus	CC144
154	HM158	L000649	Salse46B	France	CC144
155	HM159	L000680	arboretu	France	CC192
156	HM160	L000340	CRE005-A	Greece, Crete	CC192
157	HM161	L000365	DZA033-2	Algeria	CC192
158	HM162	L000538	DZA055-H	Algeria	CC192
159	HM163	L000358	DZA061-11	Algeria	CC192
160	HM164	L000350	DZA215-5	Algeria	CC192

	ID	Line	Population	Origin	Category
161	HM165	L000344	DZA231-1	Algeria	CC192
162	HM166	L000343	DZA236-2	Algeria	CC192
163	HM167	L000341	DZA242-A	Algeria	CC192
164	HM168	L000400	DZA323-3	Algeria	CC192
165	HM169	L000404	ESP039-A	Spain	CC192
166	HM170	L000407	ESP042-B	Spain	CC192
167	HM171	L000409	ESP045-A	Spain	CC192
168	HM172	L000412	ESP048-E	Spain	CC192
169	HM173	L000411	ESP048-F	Spain	CC192
170	HM174	L000610	ESP095-9	Spain	CC192
171	HM175	L000510	ESP098-B	Spain	CC192
172	HM176	L000421	ESP098-C	Spain	CC192
173	HM177	L000425	ESP100-G	Spain	CC192
174	HM178	L000427	ESP103-B	Spain	CC192
175	HM179	L000438	ESP162-A	Spain	CC192
176	HM180	L000514	ESP163-C	Spain	CC192
177	HM181	L000448	ESP175-D	Spain	CC192
178	HM182	L000451	F11013-A	France	CC192
179	HM184	L000463	F20058-B	France, Corsica	CC192
180	HM185	L000470	F20081-A	France, Corsica	CC192
181	HM186	L000387	GRC024-H	Greece	CC192
182	HM187	L000386	GRC033-C	Greece	CC192
183	HM188	L000383	GRC040-1	Greece	CC192
184	HM189	L000372	PRT177-C	Portugal	CC192
185	HM190	L000330	SA02806	Portugal	CC192
186	HM191	L000277	SA03653	Portugal	CC192
187	HM192	L000280	SA07763	Tunis	CC192
188	HM193	L000309	SA08638	Morocco	CC192
189	HM194	L000057	SA09700	Tunis	CC192
190	HM195	L000313	SA09728	Tunis	CC192
191	HM196	L000207	SA09970	Tunis	CC192
192	HM197	L000246	SA12455	Italy	CC192
193	HM198	L000244	SA18543	Tunis	CC192
194	HM199	L000147	SA19983	Cyprus	CC192
195	HM200	L000134	SA19998	Cyprus	CC192
196	HM201	L000233	SA24576	Morocco	CC192
197	HM202	L000226	SA25941	Italy	CC192
198	HM203	L000167	SA27176	Greece	CC192
199	HM204	L000172	SA27185	Italy	CC192
200	HM205	L000212	SA28375	Portugal	CC192
201	HM206	L000650	Salse57A	France	CC192

	ID	Line	Population	Origin	Category
202	HM207	Caliph	Caliph	Unknown	Unknown
203	HM209	Sephi	Sephi	Unknown	Unknown
204	HM210	TN1.1	TN1.1	Tunis	Tunisian lines
205	HM211	TN1.17	TN1.17	Tunis	Tunisian lines
206	HM212	TN1.3	TN1.3	Tunis	Tunisian lines
207	HM213	TN7.11	TN7.11	Tunis	Tunisian lines
208	HM215	TN7.17	TN7.17	Tunis	Tunisian lines
209	HM217	TN7.19	TN7.19	Tunis	Tunisian lines
210	HM218	TN7.2	TN7.2	Tunis	Tunisian lines
211	HM219	TN7.20	TN7.20	Tunis	Tunisian lines
212	HM220	TN7.22	TN7.22	Tunis	Tunisian lines
213	HM222	TN7.4	TN7.4	Tunis	Tunisian lines
214	HM223	TN8.15	TN8.15	Tunis	Tunisian lines
215	HM224	TN8.21	TN8.21	Tunis	Tunisian lines
216	HM225	TN8.22	TN8.22	Tunis	Tunisian lines
217	HM226	TN8.23	TN8.23	Tunis	Tunisian lines
218	HM227	TN8.24	TN8.24	Tunis	Tunisian lines
219	HM228	TN8.25	TN8.25	Tunis	Tunisian lines
220	HM230	TN8.4	TN8.4	Tunis	Tunisian lines
221	HM231	TN8.5	TN8.5	Tunis	Tunisian lines
222	HM232	TN9.12	TN9.12	Tunis	Tunisian lines
223	HM234	TN9.17	TN9.17	Tunis	Tunisian lines
224	HM235	TN9.20	TN9.20	Tunis	Tunisian lines
225	HM236	TN9.21	TN9.21	Tunis	Tunisian lines
226	HM237	TN9.24	TN9.24	Tunis	Tunisian lines
227	HM238	TN9.5	TN9.5	Tunis	Tunisian lines
228	HM239	TN1.5	TN1.5	Tunis	Tunisian lines
229	HM240	TN1.13	TN1.13	Tunis	Tunisian lines
230	HM241	TN1.15	TN1.15	Tunis	Tunisian lines
231	HM242	TN1.16	TN1.16	Tunis	Tunisian lines
232	HM243	TN1.18	TN1.18	Tunis	Tunisian lines
233	HM244	TN9.3	TN9.3	Tunis	Tunisian lines
234	HM245	TN9.4	TN9.4	Tunis	Tunisian lines
235	HM280	D1.2.3	D1.2.3	Syria	Damas lines
236	HM281	D2.2.2	D2.2.2	Syria	Damas lines
237	HM282	D3.3.3	D3.3.3	Syria	Damas lines
238	HM283	D4.2.1	D4.2.1	Syria	Damas lines
239	HM284	D5.3.1	D5.3.1	Syria	Damas lines
240	HM285	D6.2.1	D6.2.1	Syria	Damas lines
241	HM286	D7.1.3	D7.1.3	Syria	Damas lines
242	Unknown	DZA 45.5	DZA045-5	Algeria	CC8

Table S. 2: Iranian Medicago species used in this study.

Medicago species	Accession Numbers	Province	City	Height	Latitude	Longitude
M. truncatula	1724	Golestan	Gorgan	70	-	-
	7321	Qom	Qom	-	-	-
	7543	Golestan	Minoo dasht	420	37/54/00	55/56/00
	7600	Golestan	Minoo dasht	300	37/48/00	55/58/00
M. Scutellata	Scu	-	-	-	-	-

Table S. 3: Composition of Genomic DNA Extraction Buffer.

Product	Stock concentration	Quantity for 100 mL of extraction buffer
CTAB	-	2g
NaCl	5 M	28 mL
Tris-HCl	1 M pH8	10 mL
EDTA (Ethylenediamine tetraacetic acid)	0,5 M pH8	4 mL
H_2O	-	57,5 mL
Add 0.5 mL of Beta-mercaptoethanol just before extraction		

Table S. 4: The estimated AUDPC values are adjusted through augmented block design.

The values are arranged in ascending order.

	Line	AUDPC Lsmean	SE	lower.CL	upper.CL
1	L000527	-5,8251071	0,20094262	-6,574681	-5,0755332
2	L000411	-5,6252044	0,11752851	-6,0637577	-5,1866511
3	L000513	-5,5779727	0,11757855	-6,0167139	-5,1392314
4	L000738	-5,3352006	0,0621505	-5,568995	-5,1014062
5	L000620	-5,3174464	0,11765851	-5,7564888	-4,878404
6	L000401	-5,2094572	0,11757141	-5,6481721	-4,7707423
7	L000443	-5,208762	0,11757855	-5,6475032	-4,7700208
8	L000233	-5,0590232	0,14291705	-5,5921821	-4,5258644
9	L000047	-5,0170187	0,14370506	-5,553132	-4,4809055
10	L000274	-5,0100034	0,11766288	-5,4490623	-4,5709445
11	L000212	-4,9596943	0,11758145	-5,3984465	-4,5209421
12	TN1.1	-4,9452549	0,11775665	-5,3846664	-4,5058433
13	L000440	-4,9408504	0,11761453	-5,3797272	-4,5019736
14	L000410	-4,9386737	0,11761453	-5,3775505	-4,4997969
15	L000412	-4,9325101	0,11759416	-5,3713102	-4,4937101
16	L000044	-4,9215521	0,11761212	-5,3604198	-4,4826844
17	L000369	-4,8595254	0,11788363	-5,299416	-4,4196347
18	L000544	-4,8505596	0,10265442	-5,2337762	-4,467343
19	L000144	-4,8346848	0,11791736	-5,2747029	-4,3946668
20	L000736	-4,8195158	0,10265442	-5,2027324	-4,4362992
21	L000421	-4,7941597	0,10245666	-5,1766278	-4,4116916
22	TN1.3	-4,7899996	0,11775665	-5,2294111	-4,3505881
23	L000245	-4,7707865	0,14307954	-5,3045536	-4,2370194
24	L000161	-4,7622864	0,1176468	-5,2012846	-4,3232883
25	TN1.15	-4,7400209	0,11768798	-5,179174	-4,3008677
26	L000407	-4,7334723	0,11757018	-5,1721821	-4,2947624
27	L000482	-4,6997198	0,11761453	-5,1385966	-4,260843
28	L000244	-4,6876398	0,1175896	-5,126423	-4,2488566
29	L000554	-4,6874465	0,11757855	-5,1261878	-4,2487053
30	L000057	-4,680958	0,11758145	-5,1197102	-4,2422057
31	TN9.5	-4,6779236	0,11776936	-5,1173831	-4,2384641
32	L000397	-4,6667021	0,11757348	-5,1054249	-4,2279794
33	L000637	-4,664628	0,11791736	-5,104646	-4,22461
34	L000542	-4,6596227	0,10265442	-5,0428393	-4,2764062
35	TN1.5	-4,6569081	0,11771814	-5,0961747	-4,2176415
36	L000204	-4,6567161	0,11766288	-5,095775	-4,2176572
37	L000610	-4,6559971	0,11753831	-5,0945879	-4,2174063

	Line	AUDPC Lsmean	SE	lower.CL	upper.CL
38	DZA 45.5	-4,6490358	0,0621505	-4,8828302	-4,4152414
39	L000130	-4,6483442	0,11792021	-5,0883731	-4,2083152
40	L000370	-4,6454577	0,11792021	-5,0854866	-4,2054287
41	L000213	-4,6384035	0,1175757	-5,0771344	-4,1996727
42	L000648	-4,637092	0,10265442	-5,0203086	-4,2538754
43	L000317	-4,6278471	0,11780921	-5,067458	-4,1882362
44	L000404	-4,619032	0,11761674	-5,057917	-4,180147
45	L000330	-4,6036982	0,11757018	-5,0424081	-4,1649883
46	TN1.11	-4,5966386	0,10254844	-4,9794537	-4,2138234
47	L000297	-4,5813198	0,1175757	-5,0200506	-4,1425889
48	L000265	-4,5767762	0,14298675	-5,1101958	-4,0433566
49	L000166	-4,5660684	0,11761212	-5,0049361	-4,1272007
50	L000207	-4,5602493	0,11763154	-4,99919	-4,1213086
51	L000425	-4,5572803	0,1175896	-4,9960635	-4,1184971
52	L000241	-4,5558659	0,11762794	-4,9947932	-4,1169385
53	L000477	-4,54939	0,11756503	-4,9880805	-4,1106996
54	L000525	-4,548735	0,11763154	-4,9876757	-4,1097943
55	L000342	-4,5404015	0,11762794	-4,9793288	-4,1014741
56	L000277	-4,5394684	0,11757018	-4,9781782	-4,1007585
57	L000168	-4,5375807	0,1176468	-4,9765789	-4,0985826
58	L000547	-4,5214207	0,1175757	-4,9601516	-4,0826898
59	L000414	-4,5119709	0,14301773	-5,0455065	-3,9784353
60	L000061	-4,5092303	0,10265282	-4,8924401	-4,1260205
61	L000416	-4,5014356	0,11756503	-4,940126	-4,0627451
62	L000675	-4,4890991	0,11793146	-4,9291707	-4,0490276
63	TN1.13	-4,4885525	0,11776936	-4,928012	-4,049093
64	L000395	-4,4857108	0,11791736	-4,9257288	-4,0456927
65	TN7.22	-4,4835025	0,11776936	-4,922962	-4,044043
66	TN7.17	-4,4789967	0,11771814	-4,9182633	-4,0397301
67	TN8.15	-4,4699209	0,11775665	-4,9093324	-4,0305094
68	TN9.12	-4,4626354	0,11776936	-4,9020949	-4,0231759
69	L000468	-4,4610031	0,11765683	-4,9000393	-4,021967
70	TN1.21	-4,4598751	0,11751411	-4,8983748	-4,0213755
71	L000548	-4,4591349	0,11758145	-4,8978871	-4,0203826
72	L000132	-4,4496624	0,11761212	-4,8885301	-4,0107947
73	L000510	-4,441306	0,11757018	-4,8800159	-4,0025961
74	L000394	-4,4350904	0,11792021	-4,8751194	-3,9950614
75	TN1.16	-4,4330479	0,11768798	-4,872201	-3,9938947
76	L000146	-4,4304969	0,11759799	-4,8693115	-3,9916823
77	TN7.2	-4,421992	0,11775665	-4,8614035	-3,9825805
78	L000358	-4,4047087	0,11757018	-4,8434186	-3,9659989

	Line	AUDPC Lsmean	SE	lower.CL	upper.CL
79	L000531	-4,399384	0,11754906	-4,8380147	-3,9607533
80	L000372	-4,3902337	0,11759416	-4,8290337	-3,9514336
81	L000445	-4,389935	0,11754906	-4,8285657	-3,9513043
82	L000512	-4,3850796	0,11756503	-4,8237701	-3,9463891
83	TN3.23	-4,3832012	0,11751532	-4,8217051	-3,9446972
84	L000431	-4,3806312	0,11757855	-4,8193724	-3,94189
85	L000341	-4,3764091	0,11757018	-4,815119	-3,9376992
86	L000315	-4,3682412	0,11761674	-4,8071262	-3,9293562
87	L000460	-4,3546852	0,11763154	-4,7936259	-3,9157444
88	L000654	-4,3498907	0,10260826	-4,7329324	-3,9668491
89	L000674	-4,348439	0,11792021	-4,788468	-3,90841
90	L000538	-4,3481387	0,11757018	-4,7868486	-3,9094289
91	L000198	-4,348057	0,11791736	-4,788075	-3,908039
92	L000310	-4,3478832	0,1026524	-4,7310916	-3,9646748
93	TN8.5	-4,3447966	0,11771814	-4,7840632	-3,90553
94	L000314	-4,3398782	0,10264159	-4,7230455	-3,956711
95	L000293	-4,3394829	0,11757348	-4,7782057	-3,9007602
96	Sephi	-4,3271136	0,11768798	-4,7662667	-3,8879605
97	L000546	-4,3250421	0,11754906	-4,7636728	-3,8864114
98	L000444	-4,3201991	0,11763154	-4,7591398	-3,8812584
99	L000497	-4,3170738	0,11763154	-4,7560145	-3,8781331
100	L000427	-4,31626	0,1175896	-4,7550433	-3,8774768
101	TN9.20	-4,3162198	0,11775665	-4,7556314	-3,8768083
102	L000338	-4,311249	0,11759799	-4,7500636	-3,8724344
103	L000357	-4,306051	0,11792021	-4,74608	-3,866022
104	L000645	-4,2942541	0,11791736	-4,7342722	-3,8542361
105	L000302	-4,2885083	0,11793146	-4,7285799	-3,8484368
106	L000734	-4,286999	0,0621505	-4,5207934	-4,0532046
107	L000321	-4,2847982	0,11793146	-4,7248698	-3,8447267
108	L000467	-4,2808954	0,10256426	-4,6637701	-3,8980207
109	TN9.4	-4,2766081	0,11768798	-4,7157612	-3,837455
110	L000225	-4,2746644	0,11755641	-4,7133227	-3,8360061
111	L000673	-4,2686672	0,11793146	-4,7087388	-3,8285957
112	L000060	-4,2659124	0,11793146	-4,7059839	-3,8258409
113	TN6.18	-4,262162	0,11755988	-4,7008339	-3,8234902
114	TN9.3	-4,2592643	0,11771814	-4,6985309	-3,8199977
115	L000551	-4,2546206	0,11761453	-4,6934974	-3,8157438
116	L000514	-4,2536849	0,11759416	-4,692485	-3,8148848
117	L000451	-4,2482222	0,11757018	-4,686932	-3,8095123
118	TN8.24	-4,2425972	0,11775665	-4,6820088	-3,8031857
119	L000523	-4,2418769	0,11758145	-4,6806291	-3,8031247

	Line	AUDPC Lsmean	SE	lower.CL	upper.CL
120	L000237	-4,2416549	0,11759416	-4,6804549	-3,8028548
121	A10	-4,2379191	0,11753831	-4,6765099	-3,7993283
122	TN7.20	-4,2375836	0,11776936	-4,6770431	-3,7981241
123	L000437	-4,2332644	0,11763154	-4,6722051	-3,7943237
124	L000729	-4,2276509	0,11751411	-4,6661505	-3,7891513
125	L000234	-4,2258116	0,1175757	-4,6645424	-3,7870807
126	L000463	-4,2131835	0,11752851	-4,6517368	-3,7746302
127	TN7.11	-4,2130547	0,11775665	-4,6524663	-3,7736432
128	L000450	-4,2085296	0,11757855	-4,6472708	-3,7697883
129	L000172	-4,2060313	0,11758145	-4,6447835	-3,7672791
130	L000290	-4,1994456	0,11761212	-4,6383133	-3,7605779
131	L000456	-4,1970484	0,11765683	-4,6360845	-3,7580122
132	L000216	-4,1961627	0,14307871	-4,7299268	-3,6623985
133	L000409	-4,1956312	0,11752851	-4,6341845	-3,7570779
134	L000371	-4,1880788	0,1026424	-4,5712498	-3,8049078
135	TN1.17	-4,1864174	0,20100063	-4,9362075	-3,4366272
136	L000448	-4,1823142	0,11757018	-4,6210241	-3,7436043
137	L000178	-4,1822003	0,11791736	-4,6222183	-3,7421823
138	L000322	-4,1801241	0,11765683	-4,6191602	-3,7410879
139	L000340	-4,1733688	0,11759416	-4,6121689	-3,7345687
140	L000400	-4,1732009	0,1175896	-4,6119841	-3,7344177
141	TN8.23	-4,1724352	0,11771814	-4,6117019	-3,7331686
142	L000549	-4,1696962	0,11757855	-4,6084375	-3,730955
143	L000649	-4,1663744	0,11762794	-4,6053018	-3,7274471
144	TN9.24	-4,1652964	0,11768798	-4,6044495	-3,7261432
145	TN8.4	-4,1552586	0,11768798	-4,5944117	-3,7161054
146	L000438	-4,1515697	0,11757018	-4,5902795	-3,7128598
147	L000226	-4,1460359	0,11758145	-4,5847881	-3,7072837
148	L000343	-4,1404411	0,11759416	-4,5792411	-3,701641
149	TN9.21	-4,1386606	0,11776936	-4,5781201	-3,6992011
150	L000263	-4,1356793	0,11766288	-4,5747382	-3,6966204
151	L000356	-4,1289752	0,11788363	-4,5688658	-3,6890845
152	L000365	-4,125774	0,1175896	-4,5645572	-3,6869908
153	L000049	-4,1248163	0,11791736	-4,5648343	-3,6847982
154	L000520	-4,1246671	0,11756503	-4,5633575	-3,6859766
155	L000306	-4,1238121	0,11759799	-4,5626267	-3,6849975
156	L000303	-4,1213104	0,11793146	-4,5613819	-3,6812389
157	L000550	-4,1172814	0,10262687	-4,5003935	-3,7341694
158	L000246	-4,1155972	0,14298075	-4,6489944	-3,5822001
159	TN8.25	-4,1082126	0,11771814	-4,5474792	-3,668946
160	TN1.18	-4,1074659	0,11776936	-4,5469254	-3,6680064

	Line	AUDPC Lsmean	SE	lower.CL	upper.CL
161	L000386	-4,1021355	0,11757018	-4,5408454	-3,6634257
162	L000368	-4,1020552	0,11791736	-4,5420732	-3,6620372
163	L000309	-4,0891679	0,11761687	-4,5280538	-3,6502821
164	L000134	-4,0861216	0,11758145	-4,5248739	-3,6473694
165	L000601	-4,0860835	0,11788363	-4,5259741	-3,6461928
166	TN7.19	-4,085654	0,11775665	-4,5250655	-3,6462425
167	TN7.4	-4,085191	0,11775665	-4,5246025	-3,6457795
168	L000174	-4,0835278	0,11792021	-4,5235568	-3,6434989
169	TN8.3	-4,0735013	0,11751532	-4,5120053	-3,6349973
170	L000162	-4,0674027	0,11751372	-4,5059005	-3,6289048
171	L000679	-4,0603913	0,14370506	-4,5965045	-3,524278
172	L000215	-4,0603474	0,10256426	-4,4432221	-3,6774727
173	L000639	-4,0587498	0,11788363	-4,4986405	-3,6188592
174	L000337	-4,0575202	0,10264552	-4,4407026	-3,6743379
175	L000545	-4,0504155	0,10248953	-4,4330078	-3,6678232
176	L000375	-4,0491826	0,11761674	-4,4880676	-3,6102976
177	L000376	-4,0448186	0,11759799	-4,4836332	-3,606004
178	L000126	-4,0419885	0,11793146	-4,48206	-3,601917
179	L000530	-4,0417236	0,0621505	-4,275518	-3,8079292
180	L000651	-4,0356275	0,10265442	-4,4188441	-3,6524109
181	L000286	-4,0319736	0,11765851	-4,471016	-3,5929311
182	L000555	-4,0313067	0,11753831	-4,4698975	-3,5927159
183	L000552	-4,0254892	0,11758145	-4,4642415	-3,586737
184	L000354	-4,0244869	0,11793146	-4,4645584	-3,5844154
185	L000475	-4,0201442	0,11756503	-4,4588346	-3,5814537
186	L000239	-4,018615	0,11791736	-4,458633	-3,578597
187	TN9.17	-4,0170723	0,11771814	-4,456339	-3,5778057
188	L000202	-4,0141317	0,11761212	-4,4529994	-3,575264
189	L000173	-4,0099321	0,1176468	-4,4489302	-3,570934
190	L000557	-4,0057933	0,11758145	-4,4445455	-3,5670411
191	L000350	-4,0055725	0,11757018	-4,4442824	-3,5668627
192	L000355	-4,000419	0,11788363	-4,4403096	-3,5605283
193	D3.3.3	-3,9988033	0,11757141	-4,4375182	-3,5600885
194	L000522	-3,9968544	0,11757855	-4,4355956	-3,5581131
195	L000470	-3,9955694	0,1175896	-4,4343526	-3,5567861
196	TN8.21	-3,9951834	0,11775665	-4,4345949	-3,5557718
197	L000147	-3,9921949	0,11758145	-4,4309471	-3,5534427
198	L000052	-3,9842233	0,1026424	-4,3673943	-3,6010523
199	L000228	-3,9819658	0,1176468	-4,4209639	-3,5429677
200	D7.1.3	-3,98106	0,11762794	-4,4199874	-3,5421327
201	L000313	-3,9786942	0,11752851	-4,4172476	-3,5401409

	Line	AUDPC Lsmean	SE	lower.CL	upper.CL
202	L000217	-3,9776171	0,11762794	-4,4165444	-3,5386897
203	L000219	-3,9774408	0,1175757	-4,4161716	-3,5387099
204	L000332	-3,9730409	0,11761674	-4,4119259	-3,5341559
205	TN9.22	-3,9723952	0,11755988	-4,411067	-3,5337234
206	L000270	-3,9720871	0,11765851	-4,4111295	-3,5330446
207	TN8.22	-3,969033	0,11775665	-4,4084445	-3,5296215
208	A20	-3,9687336	0,11753877	-4,4073263	-3,5301409
209	D4.2.1	-3,9663803	0,11767025	-4,4054672	-3,5272935
210	L000232	-3,9651523	0,11766288	-4,4042113	-3,5260934
211	L000154	-3,9521207	0,09237088	-4,2971372	-3,6071042
212	L000362	-3,9518658	0,11788363	-4,3917565	-3,5119752
213	D6.2.1	-3,9469344	0,11767025	-4,3860212	-3,5078476
214	L000165	-3,9463981	0,11761212	-4,3852658	-3,5075303
215	L000360	-3,9443457	0,1026464	-4,327531	-3,5611604
216	L000383	-3,9397144	0,11759416	-4,3785145	-3,5009144
217	L000543	-3,9377755	0,11753858	-4,3763671	-3,4991838
218	D1.2.3	-3,9369785	0,11767025	-4,3760654	-3,4978917
219	L000387	-3,9324456	0,11757358	-4,3711685	-3,4937228
220	L000148	-3,9304444	0,11761453	-4,3693212	-3,4915676
221	D2.2.2	-3,927781	0,11767025	-4,3668679	-3,4886942
222	L000529	-3,9205615	0,11761453	-4,3594383	-3,4816847
223	L000650	-3,9171028	0,11748166	-4,3554803	-3,4787253
224	L000574	-3,9144218	0,11756503	-4,3531123	-3,4757313
225	L000680	-3,9088256	0,11748166	-4,347203	-3,4704481
226	L000537	-3,8993242	0,11759799	-4,3381388	-3,4605096
227	L000167	-3,8936838	0,11758145	-4,332436	-3,4549316
228	L000449	-3,8874923	0,11758145	-4,3262445	-3,4487401
229	L000238	-3,8843805	0,11761687	-4,3232664	-3,4454947
230	L000307	-3,8819362	0,11793146	-4,3220077	-3,4418647
231	L000458	-3,8660926	0,11763154	-4,3050334	-3,4271519
232	L000344	-3,8430618	0,11761453	-4,2819386	-3,404185
233	L000163	-3,8427491	0,11792021	-4,2827781	-3,4027202
234	Caliph	-3,8416119	0,11771814	-4,2808785	-3,4023452
235	D5.3.1	-3,8289045	0,11757141	-4,2676194	-3,3901897
236	L000280	-3,8014804	0,11752851	-4,2400337	-3,3629271
237	L000283	-3,7987904	0,11765683	-4,2378265	-3,3597543
238	L000659	-3,7853664	0,11762794	-4,2242937	-3,346439
239	L000455	-3,7788049	0,11757358	-4,2175278	-3,340082
240	L000267	-3,7778045	0,11761453	-4,2166813	-3,3389276
241	L000379	-3,7455769	0,11793146	-4,1856485	-3,3055054
242	L000276	-3,6773473	0,1175757	-4,1160781	-3,2386164

Table S. 5: The estimated MSS values are adjusted through augmented block design.

The values are arranged in ascending order.

	Line	MSS Lsmean	SE	lower.CL	upper.CL
1	L000443	1,37052815	0,23893255	0,47894236	2,26211394
2	L000411	1,38801985	0,23884186	0,49677467	2,27926504
3	L000738	1,40972222	0,1265503	0,93344279	1,88600165
4	L000513	1,42886149	0,23893255	0,5372757	2,32044728
5	L000620	1,43235566	0,23909631	0,54015305	2,32455827
6	L000245	1,54092994	0,2390832	0,64877722	2,43308266
7	L000274	1,54122503	0,2391136	0,64895731	2,43349275
8	L000401	1,56444498	0,23892698	0,67287918	2,45601077
9	L000144	1,60383929	0,23963331	0,70961273	2,49806586
10	L000527	1,60609378	0,40815258	0,08358786	3,12859971
11	L000440	1,65849379	0,2390072	0,76662671	2,55036086
12	L000212	1,65850971	0,23894705	0,76686929	2,55015014
13	L000410	1,6758098	0,2390072	0,78394273	2,56767688
14	L000421	1,7263677	0,20826311	0,94889046	2,50384493
15	L000161	1,75162334	0,2390832	0,85947062	2,64377606
16	L000244	1,76305696	0,23896649	0,87134269	2,65477123
17	L000369	1,77728253	0,23956694	0,88330667	2,6712584
18	L000044	1,8001706	0,23901011	0,90829267	2,69204853
19	L000407	1,80598138	0,23892679	0,91441711	2,69754566
20	L000544	1,81833238	0,20866683	1,03932719	2,59733756
21	L000057	1,82935276	0,23894705	0,93771233	2,72099319
22	L000130	1,87541762	0,23964183	0,98115855	2,76967668
23	L000412	1,88227353	0,23897578	0,990525	2,77402207
24	TN1.3	1,885084	0,23930342	0,99210255	2,77806546
25	TN1.15	1,93270744	0,23916717	1,04023859	2,8251763
26	L000342	1,94539206	0,23904221	1,05339311	2,83739101
27	L000482	2,01193202	0,2390072	1,12006494	2,90379909
28	L000317	2,01291176	0,23941519	1,11950639	2,90631712
29	L000233	2,02173203	0,29036438	0,93851736	3,1049467
30	TN1.5	2,03187045	0,2392287	1,13917014	2,92457077
31	DZA 45.5	2,03472222	0,1265503	1,55844279	2,51100165
32	L000277	2,0744999	0,23892679	1,18293563	2,96606418
33	L000637	2,07606152	0,23963331	1,18183495	2,97028808
34	L000736	2,11882841	0,20866683	1,33982322	2,89783359
35	L000525	2,14924492	0,23904037	1,25725323	3,04123661
36	L000404	2,16962409	0,23901962	1,27771062	3,06153756
37	L000297	2,17319466	0,23893587	1,28159575	3,06479358

	Line	MSS Lsmean	SE	lower.CL	upper.CL
38	L000425	2,2038939	0,23896649	1,31217963	3,09560817
39	TN1.1	2,20389713	0,23930342	1,31091568	3,09687859
40	TN1.11	2,20935777	0,20845046	1,4311721	2,98754345
41	L000554	2,21358371	0,23893255	1,32199792	3,1051695
42	L000542	2,22099187	0,20866683	1,44198668	2,99999706
43	L000370	2,22898905	0,23964183	1,33472998	3,12324811
44	L000213	2,24726874	0,23893587	1,35566982	3,13886766
45	L000204	2,24955836	0,2391136	1,35729064	3,14182609
46	L000397	2,26845433	0,23892536	1,37689437	3,16001429
47	L000675	2,27896116	0,23966487	1,38461502	3,1733073
48	TN7.2	2,30932643	0,23930342	1,41634497	3,20230788
49	L000207	2,31206543	0,23904037	1,42007375	3,20405712
50	L000610	2,3517104	0,23886196	1,46038828	3,24303251
51	TN9.5	2,37356357	0,23933329	1,48046935	3,26665778
52	L000265	2,38677924	0,29049009	1,30309425	3,47046423
53	L000330	2,3869999	0,23892679	1,49543563	3,27856418
54	TN1.13	2,38891445	0,23933329	1,49582023	3,28200866
55	L000548	2,3933582	0,23894705	1,50171777	3,28499863
56	L000061	2,40985146	0,20866352	1,63086025	3,18884267
57	TN7.22	2,41570016	0,23933329	1,52260595	3,30879437
58	L000445	2,42495413	0,23888389	1,53355066	3,3163576
59	L000648	2,42749262	0,20866683	1,64848743	3,20649781
60	L000047	2,43020963	0,29197373	1,34096056	3,5194587
61	TN7.17	2,43105689	0,2392287	1,53835658	3,32375721
62	L000166	2,43274636	0,23901011	1,54086843	3,32462429
63	TN8.15	2,45528602	0,23930342	1,56230457	3,34826748
64	TN8.5	2,47259084	0,2392287	1,57989053	3,36529116
65	L000416	2,53240503	0,23890498	1,64092279	3,42388727
66	L000431	2,54376048	0,23893255	1,65217469	3,43534627
67	L000414	2,57055389	0,2905696	1,48657117	3,65453661
68	L000395	2,57606152	0,23963331	1,68183495	3,47028808
69	TN1.16	2,57759704	0,23916717	1,68512819	3,4700659
70	L000547	2,5799407	0,23893587	1,68834178	3,47153961
71	L000241	2,61485871	0,23904221	1,72285976	3,50685766
72	L000510	2,61490394	0,23892679	1,72333967	3,50646822
73	L000146	2,62545451	0,23898141	1,73368451	3,5172245
74	TN1.21	2,62919052	0,23881061	1,73806185	3,52031919
75	L000538	2,67172212	0,23892679	1,78015785	3,5632864
76	L000372	2,69028034	0,23897578	1,7985318	3,58202887
77	TN9.12	2,69421748	0,23933329	1,80112326	3,58731169
78	L000477	2,71560609	0,23890498	1,82412385	3,60708833

	Line	MSS Lsmean	SE	lower.CL	upper.CL
79	L000444	2,71575896	0,23904037	1,82376727	3,60775065
80	L000394	2,72435942	0,23964183	1,83010035	3,61861848
81	L000674	2,72883642	0,23964183	1,83457735	3,62309549
82	L000673	2,74165957	0,23966487	1,84731344	3,63600571
83	L000654	2,77573624	0,20857051	1,99709594	3,55437655
84	L000427	2,78933161	0,23896649	1,89761734	3,68104588
85	L000497	2,79161366	0,23904037	1,89962197	3,68360535
86	TN6.18	2,79985103	0,2389061	1,90836311	3,69133895
87	L000168	2,83815216	0,2390832	1,94599944	3,73030488
88	L000132	2,84407115	0,23901011	1,95219321	3,73594908
89	L000512	2,84669074	0,23890498	1,9552085	3,73817299
90	L000310	2,87285145	0,2086627	2,0938629	3,65184001
91	L000531	2,87746736	0,23888389	1,98606389	3,76887083
92	L000551	2,92213015	0,2390072	2,03026308	3,81399722
93	L000302	2,98054846	0,23966487	2,08620233	3,8748946
94	L000341	2,98142207	0,23892679	2,08985779	3,87298634
95	L000468	2,98487668	0,23910167	2,09265384	3,87709952
96	L000463	3,00026039	0,23884186	2,1090152	3,89150557
97	L000467	3,0030811	0,20848145	2,22477869	3,78138351
98	L000060	3,00911989	0,23966487	2,11477376	3,90346603
99	L000315	3,01687684	0,23901962	2,12496337	3,90879031
100	L000437	3,01946914	0,23904037	2,12747745	3,91146083
101	L000460	3,02067349	0,23904037	2,1286818	3,91266518
102	L000293	3,03730354	0,23892536	2,14574358	3,9288635
103	L000357	3,04565571	0,23964183	2,15139664	3,93991478
104	L000338	3,05909031	0,23898141	2,16732032	3,95086031
105	L000645	3,06217263	0,23963331	2,16794606	3,95639919
106	TN7.20	3,0678827	0,23933329	2,17478849	3,96097691
107	A10	3,06877389	0,23886196	2,17745178	3,960096
108	L000546	3,06913403	0,23888389	2,17773056	3,9605375
109	TN9.3	3,07834026	0,2392287	2,18563994	3,97104058
110	TN1.17	3,08366567	0,40827066	1,56071944	4,6066119
111	TN8.24	3,08584158	0,23930342	2,19286012	3,97882304
112	L000358	3,08640466	0,23892679	2,19484039	3,97796894
113	L000734	3,09027778	0,1265503	2,61399835	3,56655721
114	L000409	3,09580373	0,23884186	2,20455855	3,98704892
115	L000514	3,09777678	0,23897578	2,20602824	3,98952531
116	L000729	3,10770359	0,23881061	2,21657492	3,99883226
117	L000234	3,12020321	0,23893587	2,22860429	4,01180213
118	L000523	3,12126363	0,23894705	2,2296232	4,01290406
119	TN9.20	3,13491565	0,23930342	2,2419342	4,02789711

	Line	MSS Lsmean	SE	lower.CL	upper.CL
120	L000237	3,15806718	0,23897578	2,26631865	4,04981572
121	TN9.4	3,18199519	0,23916717	2,28952634	4,07446405
122	TN3.23	3,18298532	0,23881511	2,29184014	4,0741305
123	L000172	3,18426729	0,23894705	2,29262686	4,07590772
124	TN9.24	3,20074519	0,23916717	2,30827634	4,09321405
125	TN7.11	3,21639713	0,23930342	2,32341568	4,10937859
126	L000456	3,22289792	0,23910167	2,33067507	4,11512076
127	L000400	3,22778668	0,23896649	2,33607241	4,11950095
128	L000216	3,25503882	0,29069409	2,17058954	4,33948811
129	L000263	3,25696577	0,2391136	2,36469805	4,14923349
130	L000134	3,25959197	0,23894705	2,36795154	4,15123239
131	TN8.4	3,26212987	0,23916717	2,36966102	4,15459873
132	Sephi	3,2644026	0,23916717	2,37193375	4,15687145
133	L000337	3,26499842	0,20864769	2,48606673	4,04393012
134	L000356	3,26802327	0,23956694	2,37404741	4,16199914
135	TN8.23	3,27745958	0,2392287	2,38475927	4,1701599
136	L000314	3,28308666	0,20864058	2,50418226	4,06199106
137	L000303	3,2888818	0,23966487	2,39453566	4,18322793
138	L000321	3,30078656	0,23966487	2,40644042	4,19513269
139	L000322	3,3079536	0,23910167	2,41573076	4,20017644
140	L000343	3,31421196	0,23897578	2,42246343	4,2059605
141	L000340	3,31625621	0,23897578	2,42450768	4,20800475
142	L000451	3,32053165	0,23892679	2,42896737	4,21209592
143	L000450	3,32608371	0,23893255	2,43449792	4,2176695
144	L000549	3,35310391	0,23893255	2,46151812	4,2446897
145	L000178	3,35383929	0,23963331	2,45961273	4,24806586
146	L000290	3,36048529	0,23901011	2,46860735	4,25236322
147	L000368	3,3686012	0,23963331	2,47437463	4,26282776
148	L000371	3,37476244	0,20863693	2,59587042	4,15365447
149	L000049	3,37566469	0,23963331	2,48143813	4,26989125
150	L000309	3,3813164	0,23902228	2,48939217	4,27324064
151	L000448	3,39871643	0,23892679	2,50715215	4,2902807
152	L000520	3,4054209	0,23890498	2,51393866	4,29690315
153	L000198	3,40939485	0,23963331	2,51516829	4,30362141
154	TN9.21	3,41086472	0,23933329	2,5177705	4,30395893
155	L000173	3,41656125	0,2390832	2,52440853	4,30871397
156	L000215	3,41835888	0,20848145	2,64005647	4,19666129
157	L000438	3,42588879	0,23892679	2,53432452	4,31745307
158	L000226	3,43704507	0,23894705	2,54540464	4,3286855
159	L000306	3,43793647	0,23898141	2,54616648	4,32970646
160	L000649	3,45082552	0,23904221	2,55882657	4,34282447

	Line	MSS Lsmean	SE	lower.CL	upper.CL
161	TN8.3	3,46069726	0,23881511	2,56955208	4,35184244
162	L000225	3,47343469	0,23889755	2,58197985	4,36488953
163	L000555	3,47432944	0,23886196	2,58300733	4,36565155
164	L000601	3,47595978	0,23956694	2,58198391	4,36993564
165	TN7.4	3,48140435	0,23930342	2,58842289	4,37438581
166	TN1.18	3,49116312	0,23933329	2,59806891	4,38425734
167	L000147	3,49975874	0,23894705	2,60811832	4,39139917
168	L000286	3,50314829	0,23909631	2,61094568	4,39535091
169	TN7.19	3,51387188	0,23930342	2,62089042	4,40685334
170	L000162	3,53061058	0,2388037	2,6395085	4,42171267
171	L000449	3,53729759	0,23894705	2,64565717	4,42893802
172	L000530	3,55555556	0,1265503	3,07927612	4,03183499
173	TN9.22	3,56216535	0,2389061	2,67067743	4,45365327
174	L000545	3,56555798	0,20832315	2,78785375	4,3432622
175	TN8.22	3,58502459	0,23930342	2,69204313	4,47800604
176	TN8.25	3,58705971	0,2392287	2,69435939	4,47976002
177	L000313	3,59366698	0,23884186	2,7024218	4,48491217
178	L000052	3,59812554	0,20863693	2,81923351	4,37701756
179	L000574	3,59860272	0,23890498	2,70712048	4,49008496
180	L000365	3,5992763	0,23896649	2,70756203	4,49099057
181	TN8.21	3,60225572	0,23930342	2,70927426	4,49523718
182	L000148	3,60630523	0,2390072	2,71443816	4,49817231
183	L000376	3,61174599	0,23898141	2,719976	4,50351599
184	L000375	3,62699589	0,23901962	2,73508242	4,51890935
185	L000522	3,62700964	0,23893255	2,73542385	4,51859542
186	L000651	3,62857105	0,20866683	2,84956587	4,40757624
187	L000202	3,63552414	0,23901011	2,7436462	4,52740207
188	L000386	3,63712616	0,23892679	2,74556189	4,52869044
189	L000232	3,63905775	0,2391136	2,74679003	4,53132548
190	L000537	3,64096677	0,23898141	2,74919678	4,53273676
191	L000219	3,64541689	0,23893587	2,75381797	4,5370158
192	D3.3.3	3,64922758	0,23892698	2,75766179	4,54079338
193	L000239	3,66356152	0,23963331	2,76933495	4,55778808
194	L000550	3,66394275	0,20861048	2,88515128	4,44273422
195	TN9.17	3,67210244	0,2392287	2,77940213	4,56480276
196	L000458	3,67345127	0,23904037	2,78145958	4,56544295
197	L000552	3,67443823	0,23894705	2,7827978	4,56607866
198	L000543	3,67963351	0,23886239	2,78831011	4,57095691
199	L000332	3,69544827	0,23901962	2,8035348	4,58736174
200	L000679	3,70104296	0,29197373	2,61179389	4,79029204
201	L000167	3,71204507	0,23894705	2,82040464	4,6036855

	Line	MSS Lsmean	SE	lower.CL	upper.CL
202	L000383	3,72246112	0,23897578	2,83071259	4,61420966
203	L000165	3,72441303	0,23901011	2,83253509	4,61629096
204	D4.2.1	3,72646689	0,23912882	2,83414148	4,6187923
205	L000126	3,73795587	0,23966487	2,84360973	4,63230201
206	L000228	3,73815216	0,2390832	2,84599944	4,63030488
207	D6.2.1	3,74938355	0,23912882	2,85705814	4,64170896
208	L000246	3,75876286	0,2904884	2,67508424	4,84244147
209	L000475	3,76745794	0,23890498	2,8759757	4,65894018
210	L000280	3,7715516	0,23884186	2,88030641	4,66279678
211	L000270	3,77976057	0,23909631	2,88755796	4,67196318
212	L000639	3,78024549	0,23956694	2,88626963	4,67422136
213	L000529	3,78436791	0,2390072	2,89250084	4,67623499
214	D1.2.3	3,78905217	0,23912882	2,89672676	4,68137758
215	L000557	3,78982285	0,23894705	2,89818242	4,68146327
216	L000174	3,79148905	0,23964183	2,89722998	4,68574811
217	L000350	3,79672212	0,23892679	2,90515785	4,6882864
218	L000470	3,8008636	0,23896649	2,90914933	4,69257787
219	D2.2.2	3,80255816	0,23912882	2,91023275	4,69488357
220	L000163	3,8095446	0,23964183	2,91528553	4,70380367
221	L000154	3,81212211	0,18780186	3,11060086	4,51364335
222	L000344	3,81321407	0,2390072	2,92134699	4,70508114
223	L000217	3,8134539	0,23904221	2,92145495	4,70545285
224	L000362	3,81663438	0,23956694	2,92265852	4,71061025
225	L000355	3,81802327	0,23956694	2,92404741	4,71199914
226	L000387	3,82037316	0,23893039	2,92879484	4,71195149
227	L000238	3,83039048	0,23902228	2,93846624	4,72231471
228	D5.3.1	3,83227911	0,23892698	2,94071332	4,72384491
229	L000680	3,83441276	0,2387465	2,94352546	4,72530006
230	L000455	3,8391863	0,23893039	2,94760797	4,73076462
231	A20	3,8680134	0,23886295	2,97668724	4,75933957
232	D7.1.3	3,87171296	0,23904221	2,97971401	4,76371192
233	L000659	3,89289919	0,23904221	3,00090023	4,78489814
234	L000360	3,89606958	0,2086484	3,117136	4,67500316
235	Caliph	3,89661743	0,2392287	3,00391712	4,78931775
236	L000650	3,90490939	0,2387465	3,01402209	4,7957967
237	L000307	3,9138818	0,23966487	3,01953566	4,80822793
238	L000276	3,95097244	0,23893587	3,05937352	4,84257136
239	L000354	3,95197703	0,23966487	3,0576309	4,84632317
240	L000267	4,06000894	0,2390072	3,16814186	4,95187601
241	L000379	4,08054846	0,23966487	3,18620233	4,9748946
242	L000283	4,09224847	0,23910167	3,20002563	4,98447131

Table S. 6: The estimated AUDPC values are adjusted through Mixed Linear Model.

The values are arranged in ascending order.

	Line	AUDPC Lsmean	SE	lower.CL	upper.CL
1	L000527	0,003272502	0,00261965	-0,0065	0,013045
2	L000411	0,003846547	0,00154718	-0,001931	0,009625
3	L000513	0,00428002	0,00154778	-0,0015	0,01006
4	L000620	0,004348327	0,00154889	-0,001436	0,010133
5	L000738	0,00500124	0,00084857	0,001774	0,008229
6	L000401	0,00504879	0,00154775	-0,000731	0,010829
7	L000245	0,005598412	0,00154879	-0,000186	0,011382
8	L000443	0,005689907	0,00154778	-9,03E-05	0,01147
9	L000274	0,006865962	0,001549	0,001081	0,012651
10	L000212	0,007168931	0,00154788	0,001388	0,01295
11	L000440	0,007215376	0,00154828	0,001433	0,012997
12	L000044	0,007248351	0,0015483	0,001466	0,013031
13	L000410	0,007264657	0,00154828	0,001483	0,013047
14	L000233	0,007609475	0,00187239	0,000622	0,014597
15	L000047	0,007661472	0,0018833	0,000633	0,01469
16	L000412	0,007727306	0,00154807	0,001946	0,013509
17	TN1.1	0,007755319	0,00155027	0,001966	0,013545
18	L000369	0,00781794	0,00155207	0,002022	0,013614
19	L000144	0,007820907	0,00155253	0,002023	0,013619
20	L000544	0,007874716	0,00135775	0,002798	0,012951
21	L000736	0,008052286	0,00135775	0,002976	0,013129
22	TN1.3	0,008184387	0,00155027	0,002395	0,013974
23	L000421	0,008427171	0,00135502	0,003361	0,013493
24	L000161	0,008437119	0,00154879	0,002653	0,014221
25	TN1.15	0,008832162	0,00154935	0,003046	0,014618
26	L000482	0,008959995	0,00154828	0,003178	0,014742
27	L000407	0,00905363	0,00154774	0,003274	0,014834
28	L000057	0,009348936	0,00154788	0,003568	0,01513
29	L000244	0,009380469	0,00154802	0,003599	0,015162
30	L000637	0,009406259	0,00155253	0,003608	0,015204
31	L000610	0,00943206	0,00154733	0,003654	0,015211
32	L000542	0,009495267	0,00135775	0,004419	0,014572
33	TN9.5	0,009545285	0,00155047	0,003755	0,015336
34	TN1.5	0,009559241	0,00154976	0,003772	0,015347
35	L000130	0,00957275	0,00155259	0,003774	0,015371
36	L000648	0,009613909	0,00135775	0,004538	0,01469
37	DZA 45.5	0,0096813	0,00084857	0,006454	0,012909

	Line	AUDPC Lsmean	SE	lower.CL	upper.CL
38	L000554	0,009726862	0,00154778	0,003947	0,015507
39	L000397	0,009737429	0,00154775	0,003957	0,015518
40	L000213	0,009836903	0,00154781	0,004057	0,015617
41	L000370	0,009844186	0,00155259	0,004046	0,015643
42	L000317	0,009903674	0,00155106	0,004111	0,015696
43	L000404	0,01015551	0,00154836	0,004373	0,015938
44	TN1.11	0,010189849	0,00135628	0,005119	0,015261
45	L000330	0,010318511	0,00154774	0,004538	0,016099
46	L000204	0,010415565	0,001549	0,004631	0,0162
47	L000166	0,010441315	0,0015483	0,004659	0,016224
48	L000342	0,010487589	0,00154852	0,004705	0,016271
49	L000241	0,01050616	0,00154852	0,004723	0,016289
50	L000265	0,010614379	0,00187321	0,003624	0,017605
51	L000207	0,010658722	0,0015485	0,004876	0,016442
52	L000297	0,010674488	0,00154781	0,004894	0,016455
53	L000525	0,010730614	0,0015485	0,004948	0,016514
54	L000477	0,010887496	0,0015476	0,005108	0,016667
55	L000425	0,010893592	0,00154802	0,005112	0,016675
56	L000277	0,010896884	0,00154774	0,005117	0,016677
57	L000414	0,011150603	0,00187374	0,004158	0,018143
58	L000061	0,011194136	0,00135772	0,006118	0,01627
59	L000675	0,011268425	0,00155275	0,005469	0,017067
60	TN1.13	0,011346232	0,00155047	0,005556	0,017137
61	L000547	0,011380624	0,00154781	0,0056	0,017161
62	TN8.15	0,011414215	0,00155027	0,005625	0,017204
63	L000416	0,011459704	0,0015476	0,00568	0,017239
64	TN7.17	0,011469289	0,00154976	0,005682	0,017257
65	TN7.22	0,011470169	0,00155047	0,00568	0,017261
66	TN1.21	0,011532288	0,00154698	0,005755	0,01731
67	L000168	0,011647958	0,00154879	0,005864	0,017432
68	TN9.12	0,011654336	0,00155047	0,005864	0,017445
69	L000395	0,011681805	0,00155253	0,005884	0,01748
70	L000548	0,011777098	0,00154788	0,005997	0,017558
71	L000394	0,011872542	0,00155259	0,006074	0,017671
72	L000132	0,012004628	0,0015483	0,006222	0,017787
73	TN7.2	0,012042161	0,00155027	0,006253	0,017832
74	L000468	0,012072466	0,00154892	0,006288	0,017857
75	L000146	0,012088825	0,00154811	0,006307	0,01787
76	L000510	0,012209971	0,00154774	0,00643	0,01799
77	L000358	0,012362871	0,00154774	0,006583	0,018143
78	TN1.16	0,012468546	0,00154935	0,006682	0,018255

	Line	AUDPC Lsmean	SE	lower.CL	upper.CL
79	TN3.23	0,012518954	0,00154701	0,006742	0,018296
80	L000531	0,012523714	0,00154746	0,006745	0,018303
81	L000445	0,012571829	0,00154746	0,006793	0,018351
82	L000512	0,01269461	0,0015476	0,006915	0,018474
83	L000315	0,012721008	0,00154836	0,006939	0,018503
84	L000431	0,012738	0,00154778	0,006958	0,018518
85	L000372	0,0129365	0,00154807	0,007155	0,018718
86	L000460	0,012992802	0,0015485	0,00721	0,018776
87	L000538	0,013056961	0,00154774	0,007277	0,018837
88	L000674	0,013098413	0,00155259	0,0073	0,018897
89	L000341	0,013147484	0,00154774	0,007367	0,018928
90	L000198	0,013219504	0,00155253	0,007421	0,019018
91	L000293	0,013275198	0,00154775	0,007495	0,019055
92	L000654	0,013298895	0,0013571	0,008225	0,018373
93	TN8.5	0,013320524	0,00154976	0,007533	0,019108
94	L000314	0,013357913	0,00135756	0,008282	0,018434
95	L000546	0,013362291	0,00154746	0,007583	0,019141
96	L000357	0,013429751	0,00155259	0,007631	0,019228
97	L000444	0,013429909	0,0015485	0,007647	0,019213
98	Sephi	0,013469207	0,00154935	0,007683	0,019255
99	TN9.20	0,013511909	0,00155027	0,007722	0,019301
100	L000497	0,013567081	0,0015485	0,007784	0,01935
101	L000645	0,013609384	0,00155253	0,007811	0,019407
102	L000310	0,013760964	0,00135771	0,008685	0,018837
103	L000302	0,013825256	0,00155275	0,008026	0,019624
104	L000734	0,013939732	0,00084857	0,010712	0,017167
105	L000673	0,01403855	0,00155275	0,00824	0,019837
106	L000467	0,014050545	0,00135649	0,008979	0,019122
107	L000060	0,014102042	0,00155275	0,008303	0,019901
108	L000427	0,014177011	0,00154802	0,008396	0,019958
109	TN6.18	0,014248202	0,00154762	0,008469	0,020028
110	TN9.4	0,014258393	0,00154935	0,008472	0,020045
111	TN9.3	0,014273638	0,00154976	0,008486	0,020061
112	A10	0,014361926	0,00154733	0,008583	0,02014
113	L000514	0,014412239	0,00154807	0,008631	0,020194
114	L000338	0,014464599	0,00154811	0,008683	0,020246
115	L000451	0,014527459	0,00154774	0,008747	0,020308
116	L000551	0,014541675	0,00154828	0,00876	0,020324
117	TN7.20	0,014553113	0,00155047	0,008763	0,020343
118	L000237	0,014566972	0,00154807	0,008786	0,020348
119	TN8.24	0,014602772	0,00155027	0,008813	0,020392

	Line	AUDPC Lsmean	SE	lower.CL	upper.CL
120	L000729	0,014614304	0,00154698	0,008837	0,020392
121	L000523	0,014636749	0,00154788	0,008856	0,020417
122	L000172	0,014861108	0,00154788	0,009081	0,020642
123	TN7.11	0,014880815	0,00155027	0,009091	0,02067
124	L000437	0,014909402	0,0015485	0,009126	0,020692
125	L000234	0,014960682	0,00154781	0,00918	0,020741
126	L000225	0,014961853	0,00154755	0,009182	0,020741
127	L000463	0,015069199	0,00154718	0,009291	0,020847
128	L000409	0,015307431	0,00154718	0,009529	0,021085
129	L000450	0,015312923	0,00154778	0,009533	0,021093
130	L000216	0,015381722	0,00187458	0,008386	0,022377
131	L000448	0,015388159	0,00154774	0,009608	0,021168
132	TN1.17	0,015404913	0,00262045	0,00563	0,02518
133	L000290	0,015418563	0,0015483	0,009636	0,021201
134	L000371	0,015426143	0,00135755	0,010351	0,020502
135	L000549	0,015520287	0,00154778	0,00974	0,021301
136	L000400	0,015551325	0,00154802	0,00977	0,021332
137	TN8.23	0,015571718	0,00154976	0,009784	0,021359
138	L000649	0,015634066	0,00154852	0,009851	0,021417
139	L000456	0,01568323	0,00154892	0,009899	0,021468
140	L000340	0,01572527	0,00154807	0,009944	0,021507
141	TN9.24	0,015762557	0,00154935	0,009976	0,021549
142	L000322	0,015791712	0,00154892	0,010007	0,021576
143	L000321	0,015838295	0,00155275	0,010039	0,021637
144	TN8.4	0,015909037	0,00154935	0,010123	0,021695
145	L000263	0,015981372	0,001549	0,010197	0,021766
146	L000356	0,01604876	0,00155207	0,010252	0,021845
147	L000343	0,016083122	0,00154807	0,010302	0,021864
148	TN9.21	0,016092054	0,00155047	0,010302	0,021882
149	L000178	0,016180813	0,00155253	0,010383	0,021979
150	L000438	0,016183095	0,00154774	0,010403	0,021963
151	L000365	0,016198855	0,00154802	0,010418	0,02198
152	L000226	0,016211802	0,00154788	0,010431	0,021992
153	L000049	0,016230416	0,00155253	0,010432	0,022029
154	L000303	0,016272677	0,00155275	0,010474	0,022072
155	L000550	0,016424152	0,00135737	0,011349	0,021499
156	L000368	0,016481833	0,00155253	0,010684	0,02228
157	TN1.18	0,016666137	0,00155047	0,010876	0,022456
158	L000520	0,016679162	0,0015476	0,0109	0,022459
159	L000246	0,016718195	0,0018732	0,009728	0,023708
160	L000386	0,016778107	0,00154774	0,010998	0,022558

	Line	AUDPC Lsmean	SE	lower.CL	upper.CL
161	L000174	0,01678987	0,00155259	0,010992	0,022588
162	TN8.25	0,016798633	0,00154976	0,011011	0,022586
163	L000309	0,016819853	0,00154839	0,011037	0,022602
164	L000601	0,016852804	0,00155207	0,011056	0,022649
165	TN7.4	0,016954808	0,00155027	0,011165	0,022744
166	L000306	0,017006342	0,00154811	0,011225	0,022788
167	L000134	0,017036201	0,00154788	0,011256	0,022817
168	L000679	0,017122782	0,0018833	0,010095	0,024151
169	TN7.19	0,017138211	0,00155027	0,011349	0,022928
170	L000162	0,017147722	0,00154693	0,011371	0,022925
171	L000337	0,017163287	0,00135761	0,012087	0,022239
172	L000639	0,0171645	0,00155207	0,011368	0,022961
173	TN8.3	0,017211326	0,00154701	0,011434	0,022989
174	L000545	0,017565966	0,00135543	0,012498	0,022634
175	L000126	0,01768182	0,00155275	0,011883	0,023481
176	L000530	0,017684772	0,00084857	0,014457	0,020912
177	L000651	0,01771857	0,00135775	0,012642	0,022795
178	L000376	0,017797442	0,00154811	0,012016	0,023579
179	L000555	0,01780134	0,00154733	0,012023	0,02358
180	L000375	0,017810081	0,00154836	0,012028	0,023592
181	L000354	0,017812926	0,00155275	0,012014	0,023612
182	L000552	0,017854927	0,00154788	0,012074	0,023636
183	L000239	0,017919404	0,00155253	0,012121	0,023718
184	L000215	0,018122966	0,00135649	0,013051	0,023195
185	L000475	0,01812774	0,0015476	0,012348	0,023907
186	L000557	0,018158396	0,00154788	0,012378	0,023939
187	L000286	0,018250861	0,00154889	0,012466	0,024035
188	L000350	0,018266593	0,00154774	0,012487	0,024047
189	TN9.17	0,018330274	0,00154976	0,012543	0,024118
190	L000470	0,018352982	0,00154802	0,012572	0,024134
191	L000355	0,018358284	0,00155207	0,012562	0,024155
192	L000173	0,018376893	0,00154879	0,012593	0,024161
193	L000147	0,018382946	0,00154788	0,012602	0,024164
194	L000522	0,018532169	0,00154778	0,012752	0,024312
195	TN8.21	0,018609283	0,00155027	0,01282	0,024399
196	L000228	0,018663512	0,00154879	0,012879	0,024448
197	D3.3.3	0,018746481	0,00154775	0,012966	0,024527
198	L000313	0,018841276	0,00154718	0,013063	0,024619
199	L000052	0,018845006	0,00135755	0,013769	0,023921
200	L000232	0,018998015	0,001549	0,013213	0,024783
201	A20	0,019008592	0,00154734	0,01323	0,024787

	Line	AUDPC Lsmean	SE	lower.CL	upper.CL
202	L000332	0,019012462	0,00154836	0,01323	0,024795
203	TN9.22	0,019060135	0,00154762	0,01328	0,02484
204	D7.1.3	0,01912191	0,00154852	0,013339	0,024905
205	L000154	0,019194812	0,00122712	0,0146	0,023789
206	L000270	0,019209902	0,00154889	0,013426	0,024994
207	TN8.22	0,01921595	0,00155027	0,013426	0,025006
208	L000219	0,019256546	0,00154781	0,013476	0,025037
209	L000202	0,019274731	0,0015483	0,013493	0,025057
210	L000360	0,019325344	0,00135761	0,01425	0,024401
211	L000217	0,019354637	0,00154852	0,013572	0,025138
212	L000362	0,019381349	0,00155207	0,013585	0,025178
213	L000387	0,01949225	0,00154777	0,013712	0,025272
214	L000543	0,019555623	0,00154733	0,013777	0,025334
215	L000165	0,019585247	0,0015483	0,013803	0,025367
216	D4.2.1	0,019596434	0,00154911	0,013811	0,025382
217	L000383	0,019692091	0,00154807	0,013911	0,025473
218	D6.2.1	0,019693975	0,00154911	0,013909	0,025479
219	L000148	0,019868846	0,00154828	0,014087	0,025651
220	L000529	0,019888432	0,00154828	0,014106	0,025671
221	D1.2.3	0,019955584	0,00154911	0,01417	0,025741
222	L000574	0,019970288	0,0015476	0,014191	0,02575
223	D2.2.2	0,020150112	0,00154911	0,014365	0,025935
224	L000650	0,020204341	0,00154655	0,014429	0,02598
225	L000167	0,020318678	0,00154788	0,014538	0,026099
226	L000680	0,02049722	0,00154655	0,014722	0,026273
227	L000238	0,020588867	0,00154839	0,014806	0,026371
228	L000307	0,020622605	0,00155275	0,014824	0,026422
229	L000537	0,020783714	0,00154811	0,015002	0,026565
230	L000458	0,020828757	0,0015485	0,015046	0,026612
231	L000449	0,020946606	0,00154788	0,015166	0,026727
232	L000344	0,021528199	0,00154828	0,015746	0,02731
233	L000163	0,02155872	0,00155259	0,01576	0,027357
234	Caliph	0,021807821	0,00154976	0,01602	0,027596
235	D5.3.1	0,022285452	0,00154775	0,016505	0,028066
236	L000283	0,022490945	0,00154892	0,016706	0,028275
237	L000455	0,022645749	0,00154777	0,016866	0,028426
238	L000280	0,022688206	0,00154718	0,01691	0,028466
239	L000267	0,022873948	0,00154828	0,017092	0,028656
240	L000379	0,023474066	0,00155275	0,017675	0,029273
241	L000659	0,023556766	0,00154852	0,017774	0,02934
242	L000276	0,025351536	0,00154781	0,019571	0,031132

Table S. 7: The estimated MSS values are adjusted through Mixed Linear Model.

The values are arranged in ascending order.

	Line	MSS Lsmean	SE	lower.CL	upper.CL
1	L000443	1,372750174	0,24286	0,465666	2,279835
2	L000411	1,378795871	0,24277	0,472064	2,285528
3	L000738	1,409722222	0,1337	0,900431	1,919013
4	L000620	1,41662796	0,24303	0,508889	2,324367
5	L000513	1,431083508	0,24286	0,523999	2,338168
6	L000245	1,543005697	0,24302	0,635324	2,450687
7	L000401	1,549689036	0,24286	0,642616	2,456762
8	L000274	1,550761219	0,24305	0,642953	2,458569
9	L000144	1,608000263	0,24361	0,698105	2,517895
10	L000527	1,622511018	0,41056	0,090966	3,154056
11	L000440	1,649123544	0,24294	0,741739	2,556508
12	L000212	1,66260483	0,24287	0,755462	2,569748
13	L000410	1,666439561	0,24294	0,759055	2,573824
14	L000421	1,723554023	0,21273	0,928025	2,519083
15	L000161	1,753699097	0,24302	0,846018	2,66138
16	L000244	1,76316651	0,2429	0,85594	2,670393
17	L000369	1,788903933	0,24353	0,87928	2,698527
18	L000407	1,799602258	0,24285	0,892539	2,706666
19	L000044	1,800373264	0,24294	0,892979	2,707768
20	L000544	1,817955038	0,21316	1,020812	2,615099
21	L000057	1,833447876	0,24287	0,926305	2,740591
22	L000130	1,877705492	0,24362	0,967772	2,787639
23	TN1.3	1,879639064	0,24325	0,971086	2,788192
24	L000412	1,884157808	0,2429	0,976901	2,791415
25	L000342	1,927791268	0,24298	1,020267	2,835316
26	TN1.15	1,928234264	0,24311	1,020219	2,836249
27	L000482	2,002561772	0,24294	1,095177	2,909946
28	L000233	2,012764643	0,29363	0,916999	3,10853
29	L000317	2,023917764	0,24338	1,114889	2,932947
30	TN1.5	2,024552418	0,24317	1,116295	2,93281
31	DZA 45.5	2,034722222	0,1337	1,525431	2,544013
32	L000277	2,068120777	0,24285	1,161057	2,975184
33	L000637	2,080222485	0,24361	1,170327	2,990118
34	L000736	2,11845107	0,21316	1,321308	2,915595
35	L000525	2,160800467	0,24297	1,253287	3,068314
36	L000404	2,161225607	0,24295	1,253796	3,068656
37	L000297	2,176242181	0,24286	1,269138	3,083347

	Line	MSS Lsmean	SE	lower.CL	upper.CL
38	TN1.1	2,198452195	0,24325	1,289899	3,107005
39	L000425	2,204003451	0,2429	1,296777	3,11123
40	TN1.11	2,208776151	0,21293	1,412503	3,005049
41	L000554	2,21580573	0,24286	1,308721	3,12289
42	L000542	2,220614531	0,21316	1,423471	3,017758
43	L000370	2,23127692	0,24362	1,321344	3,14121
44	L000213	2,250316255	0,24286	1,343212	3,157421
45	L000204	2,259094552	0,24305	1,351287	3,166902
46	L000675	2,28409389	0,24364	1,374066	3,194122
47	L000397	2,288273285	0,24285	1,381204	3,195342
48	TN7.2	2,303881488	0,24325	1,395329	3,212434
49	L000207	2,32362098	0,24297	1,416108	3,231134
50	L000610	2,355452677	0,24279	1,448627	3,262278
51	TN9.5	2,375579062	0,24328	1,466904	3,284254
52	L000330	2,380620777	0,24285	1,473557	3,287684
53	TN1.13	2,390929939	0,24328	1,482255	3,299605
54	L000265	2,394298759	0,29376	1,298048	3,49055
55	L000548	2,397453315	0,24287	1,49031	3,304596
56	TN7.22	2,417715654	0,24328	1,509041	3,32639
57	L000061	2,417805315	0,21315	1,620685	3,214925
58	TN7.17	2,42373886	0,24317	1,515481	3,331996
59	L000445	2,423993556	0,24281	1,517093	3,330894
60	L000648	2,427115285	0,21316	1,629972	3,224259
61	L000166	2,432949021	0,24294	1,525554	3,340344
62	L000047	2,438510026	0,29534	1,336304	3,540716
63	TN8.15	2,449841084	0,24325	1,541288	3,358394
64	TN8.5	2,465272809	0,24317	1,557015	3,37353
65	L000416	2,537471906	0,24283	1,630494	3,444449
66	L000431	2,545982498	0,24286	1,638898	3,453067
67	TN1.16	2,573123865	0,24311	1,665109	3,481139
68	L000414	2,578161209	0,29384	1,481599	3,674724
69	L000395	2,580222485	0,24361	1,670327	3,490118
70	L000547	2,582988213	0,24286	1,675884	3,490093
71	L000241	2,597257913	0,24298	1,689734	3,504782
72	L000510	2,608524817	0,24285	1,701461	3,515588
73	L000146	2,614211168	0,24291	1,706929	3,521493
74	TN1.21	2,615482179	0,24273	1,708862	3,522102
75	L000538	2,665342999	0,24285	1,75828	3,572406
76	L000372	2,692164616	0,2429	1,784908	3,599421
77	TN9.12	2,69623297	0,24328	1,787558	3,604908
78	L000477	2,720672964	0,24283	1,813695	3,62765

	Line	MSS Lsmean	SE	lower.CL	upper.CL
79	L000394	2,726647291	0,24362	1,816714	3,636581
80	L000444	2,727314509	0,24297	1,819801	3,634828
81	L000674	2,731124295	0,24362	1,821191	3,641058
82	L000673	2,746792302	0,24364	1,836764	3,656821
83	L000654	2,77646652	0,21306	1,97971	3,573223
84	L000427	2,789441161	0,2429	1,882214	3,696668
85	TN6.18	2,793603119	0,24284	1,886606	3,7006
86	L000497	2,803169209	0,24297	1,895656	3,710682
87	L000168	2,840227919	0,24302	1,932547	3,747909
88	L000132	2,844273808	0,24294	1,936879	3,751668
89	L000512	2,85175762	0,24283	1,94478	3,758735
90	L000310	2,87431055	0,21315	2,077191	3,67143
91	L000531	2,876506784	0,24281	1,969606	3,783407
92	L000551	2,912759907	0,24294	2,005375	3,820144
93	L000341	2,97504294	0,24285	2,06798	3,882106
94	L000468	2,982966867	0,24304	2,075206	3,890728
95	L000302	2,985681191	0,24364	2,075653	3,895709
96	L000463	2,991036408	0,24277	2,084304	3,897769
97	L000467	3,007842792	0,21296	2,21145	3,804236
98	L000315	3,008478354	0,24295	2,101048	3,915908
99	L000060	3,01425262	0,24364	2,104224	3,924281
100	L000437	3,031024687	0,24297	2,123512	3,938538
101	L000460	3,032229039	0,24297	2,124716	3,939742
102	L000338	3,047846977	0,24291	2,140565	3,955129
103	L000357	3,047943587	0,24362	2,13801	3,957877
104	TN1.17	3,055031498	0,41069	1,523013	4,58705
105	L000293	3,057122491	0,24285	2,150054	3,964191
106	L000645	3,066333596	0,24361	2,156438	3,976229
107	L000546	3,06817345	0,24281	2,161273	3,975074
108	TN7.20	3,069898193	0,24328	2,161224	3,978573
109	TN9.3	3,071022225	0,24317	2,162765	3,97928
110	A10	3,072516169	0,24279	2,165691	3,979342
111	L000358	3,080025539	0,24285	2,172962	3,987089
112	TN8.24	3,08039664	0,24325	2,171844	3,988949
113	L000409	3,086579754	0,24277	2,179847	3,993312
114	L000734	3,090277778	0,1337	2,580987	3,599569
115	L000729	3,093995251	0,24273	2,187376	4,000615
116	L000514	3,099661055	0,2429	2,192404	4,006918
117	L000234	3,123250728	0,24286	2,216146	4,030355
118	L000523	3,125358743	0,24287	2,218216	4,032502
119	TN9.20	3,129470714	0,24325	2,220918	4,038024

	Line	MSS Lsmean	SE	lower.CL	upper.CL
120	L000237	3,159951459	0,2429	2,252695	4,067208
121	TN3.23	3,167403884	0,24274	2,260771	4,074037
122	TN9.4	3,177522013	0,24311	2,269507	4,085537
123	L000172	3,188362406	0,24287	2,281219	4,095505
124	TN9.24	3,196272013	0,24311	2,288257	4,104287
125	TN7.11	3,210952195	0,24325	2,302399	4,119505
126	L000456	3,220988105	0,24304	2,313227	4,128749
127	L000400	3,227896225	0,2429	2,320669	4,135123
128	TN8.4	3,257656693	0,24311	2,349642	4,165672
129	L000216	3,259389629	0,29397	2,162331	4,356448
130	Sephi	3,25992942	0,24311	2,351914	4,167944
131	L000134	3,263687081	0,24287	2,356544	4,17083
132	L000263	3,26650196	0,24305	2,358694	4,17431
133	TN8.23	3,270141551	0,24317	2,361884	4,178399
134	L000337	3,2743132	0,21314	2,477254	4,071373
135	L000356	3,279644673	0,24353	2,370021	4,189268
136	L000314	3,288906873	0,21313	2,491878	4,085935
137	L000303	3,294014525	0,24364	2,383986	4,204043
138	L000321	3,305919287	0,24364	2,395891	4,215948
139	L000322	3,30604379	0,24304	2,398283	4,213805
140	L000451	3,314152523	0,24285	2,407089	4,221216
141	L000343	3,31609624	0,2429	2,40884	4,223353
142	L000340	3,318140492	0,2429	2,410884	4,225397
143	L000450	3,32830573	0,24286	2,421221	4,23539
144	L000549	3,355325932	0,24286	2,448241	4,262411
145	L000178	3,358000263	0,24361	2,448105	4,267895
146	L000290	3,360687949	0,24294	2,453293	4,268083
147	L000368	3,372762167	0,24361	2,462867	4,282657
148	L000049	3,379825659	0,24361	2,46993	4,289721
149	L000371	3,384806039	0,21313	2,587782	4,18183
150	L000309	3,389689352	0,24296	2,482241	4,297138
151	L000448	3,392337301	0,24285	2,485274	4,299401
152	L000520	3,410487779	0,24283	2,50351	4,317465
153	TN9.21	3,412880211	0,24328	2,504206	4,321555
154	L000198	3,413555818	0,24361	2,503661	4,323451
155	L000173	3,41863701	0,24302	2,510956	4,326318
156	L000438	3,419509666	0,24285	2,512446	4,326573
157	L000215	3,42312057	0,21296	2,626727	4,219514
158	L000306	3,426693131	0,24291	2,519411	4,333975
159	L000649	3,433224724	0,24298	2,5257	4,340749
160	L000226	3,441140183	0,24287	2,533997	4,348283

	Line	MSS Lsmean	SE	lower.CL	upper.CL
161	TN8.3	3,445115824	0,24274	2,538483	4,351749
162	TN7.4	3,47595941	0,24325	2,567407	4,384512
163	L000555	3,478071724	0,24279	2,571246	4,384897
164	L000225	3,485793206	0,24282	2,578839	4,392747
165	L000286	3,487420593	0,24303	2,579681	4,39516
166	L000601	3,487581181	0,24353	2,577958	4,397205
167	TN1.18	3,493178617	0,24328	2,584504	4,401853
168	L000147	3,503853858	0,24287	2,596711	4,410997
169	TN7.19	3,508426943	0,24325	2,599874	4,41698
170	L000162	3,541096008	0,24273	2,634509	4,447683
171	L000449	3,541392709	0,24287	2,63425	4,448536
172	L000530	3,555555556	0,1337	3,046265	4,064846
173	TN9.22	3,555917439	0,24284	2,64892	4,462915
174	L000545	3,578328945	0,21279	2,782562	4,374096
175	TN8.22	3,579579646	0,24325	2,671027	4,488132
176	TN8.25	3,579741673	0,24317	2,671484	4,487999
177	L000313	3,584443002	0,24277	2,677711	4,491175
178	TN8.21	3,596810781	0,24325	2,688258	4,505364
179	L000148	3,596934991	0,24294	2,689551	4,504319
180	L000365	3,599385846	0,2429	2,692159	4,506613
181	L000376	3,600502654	0,24291	2,693221	4,507785
182	L000574	3,603669597	0,24283	2,696692	4,510647
183	L000052	3,608169134	0,21313	2,811145	4,405193
184	L000375	3,618597402	0,24295	2,711167	4,526027
185	L000651	3,628193717	0,21316	2,83105	4,425337
186	L000522	3,629231656	0,24286	2,722147	4,536316
187	L000537	3,629723434	0,24291	2,722441	4,537006
188	L000386	3,630747039	0,24285	2,723684	4,53781
189	D3.3.3	3,634471645	0,24286	2,727398	4,541545
190	L000202	3,635726799	0,24294	2,728332	4,543121
191	L000219	3,648464403	0,24286	2,74136	4,555569
192	L000232	3,648593942	0,24305	2,740786	4,556402
193	TN9.17	3,664784408	0,24317	2,756527	4,573042
194	L000239	3,667722485	0,24361	2,757827	4,577618
195	L000550	3,67056556	0,2131	2,873651	4,46748
196	L000552	3,678533346	0,24287	2,77139	4,585676
197	L000458	3,685006816	0,24297	2,777494	4,59252
198	L000332	3,687049783	0,24295	2,77962	4,59448
199	L000543	3,692709319	0,24279	2,785886	4,599533
200	L000679	3,70934336	0,29534	2,607138	4,811549
201	L000167	3,716140183	0,24287	2,808997	4,623283

	Line	MSS Lsmean	SE	lower.CL	upper.CL
202	D4.2.1	3,718199619	0,24307	2,810327	4,626073
203	L000383	3,724345398	0,2429	2,817089	4,631602
204	L000165	3,724615688	0,24294	2,817221	4,63201
205	L000228	3,740227919	0,24302	2,832547	4,647909
206	D6.2.1	3,741116286	0,24307	2,833243	4,648989
207	L000126	3,743088599	0,24364	2,83306	4,653117
208	L000246	3,751923013	0,29375	2,65568	4,848166
209	L000280	3,762327617	0,24277	2,855595	4,66906
210	L000270	3,76403287	0,24303	2,856293	4,671772
211	L000475	3,772524816	0,24283	2,865547	4,679502
212	L000529	3,774997669	0,24294	2,867613	4,682382
213	D1.2.3	3,780784902	0,24307	2,872912	4,688658
214	L000350	3,790342999	0,24285	2,88328	4,697406
215	L000639	3,791866896	0,24353	2,882243	4,70149
216	L000174	3,79377692	0,24362	2,883844	4,70371
217	L000557	3,793917961	0,24287	2,886775	4,701061
218	D2.2.2	3,794290889	0,24307	2,886418	4,702164
219	L000217	3,795853108	0,24298	2,888329	4,703377
220	L000470	3,800973148	0,2429	2,893746	4,7082
221	L000344	3,803843823	0,24294	2,896459	4,711228
222	L000163	3,811832476	0,24362	2,901899	4,721766
223	D5.3.1	3,817523174	0,24286	2,91045	4,724596
224	L000154	3,818482392	0,19275	3,096545	4,54042
225	L000387	3,821285682	0,24286	2,914202	4,728369
226	L000680	3,821676179	0,24267	2,915311	4,728041
227	L000362	3,828255784	0,24353	2,918632	4,737879
228	L000355	3,829644673	0,24353	2,920021	4,739268
229	L000238	3,838763426	0,24296	2,931315	4,746212
230	L000455	3,840098813	0,24286	2,933016	4,747182
231	D7.1.3	3,854112169	0,24298	2,946588	4,761637
232	A20	3,874600537	0,24279	2,967768	4,781433
233	L000659	3,875298391	0,24298	2,967774	4,782823
234	Caliph	3,8892994	0,24317	2,981042	4,797557
235	L000650	3,892172812	0,24267	2,985808	4,798538
236	L000360	3,903294618	0,21314	3,106238	4,700351
237	L000307	3,919014525	0,24364	3,008986	4,829043
238	L000276	3,954019959	0,24286	3,046915	4,861125
239	L000354	3,957109763	0,24364	3,047082	4,867138
240	L000267	4,050638695	0,24294	3,143254	4,958023
241	L000379	4,085681191	0,24364	3,175653	4,995709
242	L000283	4,090338661	0,24304	3,182578	4,9981

Table S. 8: Composition of the Fahraeüs medium

Product	Molecular weight (g/mol)	Quantity of product for 100mL of stock solution (g)	Stock solution concentration (mM)		Volume to add for 1L of solution (µL)
Micro elements					
$MnCl_2$ $4H_20$	197,91	0,01	0,01	10000 X	100
$CuSO_4 \cdot 5H_20$	249,69	0,01	4,01	10000 X	100
$ZnCl_2$	136,28	0,01	7,34	10000 X	100
H_3BO_4	61,84	0,01	16,17	10000 X	100
$Na_2MoO_4 \cdot 2H_20$	241,98	0,01	4,13	10000 X	100
Macro elements					
$CaCl_2 \cdot 2H_20$	147,03	13,20	898	1000 X	1000
$MgSO_4 \cdot 7H_20$	246,5	12	488	1000 X	1000
KH_2P0_4	136,09	10	735	1000 X	1000
Na_2HPO_4 $2H_20$	177,99	7,5	421	500 X	2000
Ferric Ammonium Citrate	16,5 – 18,5% fer	0,5	0,5%	1000 X	1000

- The nitrogen source of this solution is added in the form of ammonium sulphate (NH42SO4) at 0.33 g/L. The pH of the solution is adjusted to 7.5 before autoclaving.
- For a liquid Fahraeüs medium, calcium chloride ($CaCl_2$) is added after autoclaving to avoid any precipitation.

Table S. 9: Coding corresponding to each RNA extraction conditions

	1	2	3	4	5	6	7	8	9	10	11	12	13	14
Condition	0 H- S	0 H-R	4 H-S-M	4 H-S-I	4 H-R-M	4 H-R-I	24 H-S-M	24 H-S-I	24 H-R-M	24 H-R-I	96 H-S-M	96 H-S-I	96 H-R-M	96 H-R-I
Rep 1 (A)	A1	A2	A3	A4	A5	A6	A7	A8	A9	A10	A11	A12	A13	A14
Rep 2 (B)	B1	B2	B3	B4	B5	B6	B7	B8	B9	B10	B11	B12	B13	B14
Rep 3 (C)	C1	C2	C3	C4	C5	C6	C7	C8	C9	C10	C11	C12	C13	C14

S: Susceptible, R: Resistance, M: Mock inoculated, I: inoculated, 0 H: Zero Hour, 4 H: 4 Hour, 24 H: 24 Hour, 96 H: 96 Hour post inoculation.

Table S. 10: Reaction mix for the synthesis/combination of Target RNA and oligo $(dT)_{15}$ for samples of repeat 1.

	1	2	3	4	5	6	7	8	9	10	11	12	13	14
Condition	0 H- S	0 H-R	4 H-S-M	4 H-S-I	4 H-R-M	4 H-R-I	24 H-S-M	24 H-S-I	24 H-R-M	24 H-R-I	96 H-S-M	96 H-S-I	96 H-R-M	96 H-R-I
Repeat 1	A1	A2	A3	A4	A5	A6	A7	A8	A9	A10	A11	A12	A13	A14
Experimental RNA (µL) (1µg/reaction)	1.1	1.3	1.5	0,8	1,0	1,7	0.9	1.8	0.7	.13	0.9	1.3	1.0	1.0
$Oligo(dT)_{15}$ (0.5µg/reaction) (µL)	1	1	1	1	1	1	1	1	1	1	1	1	1	1
Nuclease-Free Water(µL)	2.9	2.7	2.5	3.2	3.0	2.3	3.1	2.2	3.3	2.7	3.1	2.7	3.0	3.0
Total (µL)	5	5	5	5	5	5	5	5	5	5	5	5	5	5

S: Susceptible, R: Resistance, M: Mock inoculated, I: inoculated, 0 H: Zero Hour, 4 H: 4 Hour, 24 H: 24 Hour, 96 H: 96 Hour post inoculation.

Table S. 11: Reaction mix for the synthesis/combination of Target RNA and oligo $(dT)_{15}$ for samples of repeat 2.

	1	2	3	4	5	6	7	8	9	10	11	12	13	14
Condition	0 H- S	0 H-R	4 H-S-M	4 H-S-I	4 H-R-M	4 H-R-I	24 H-S-M	24 H-S-I	24 H-R-M	24 H-R-I	96 H-S-M	96 H-S-I	96 H-R-M	96 H-R-I
Repeat 2	B1	B2	B3	B4	B5	B6	B7	B8	B9	B10	B11	B12	B13	B14
Experimental RNA (µL) (1µg/reaction)	0.6	1.3	1.0	0.9	0,6	1,0	1.0	3.4	1.5	1.1	2.5	0.5	0.6	0.7
$Oligo(dT)_{15}$ (0.5µg/reaction) (µL)	1	1	1	1	1	1	1	1	1	1	1	1	1	1
Nuclease-Free Water	3.4	2.7	3.0	3.1	3.4	3.0	3.0	0.6	2.5	2.9	1.5	3.5	3.4	3.3
Total (µL)	5	5	5	5	5	5	5	5	5	5	5	5	5	5

Susceptible, R: Resistance, M: Mock inoculated, I: inoculated, 0 H: Zero Hour, 4 H: 4 Hour, 24 H: 24 Hour, 96 H: 96 Hour post inoculation

Table S. 12: Reaction mix for the synthesis/combination of Target RNA and oligo $(dT)_{15}$ for samples of repeat 3.

	1	2	3	4	5	6	7	8	9	10	11	12	13	14
Condition	0 H- S	0 H-R	4 H-S-M	4 H-S-I	4 H-R-M	4 H-R-I	24 H-S-M	24 H-S-I	24 H-R-M	24 H-R-I	96 H-S-M	96 H-S-I	96 H-R-M	96 H-R-I
Repeat 3	C1	C2	C3	C4	C5	C6	C7	C8	C9	C10	C11	C12	C13	C14
Experimental RNA (µL) (1µg/reaction)	1.3	2.2	1.3	1.2	2.3	2.4	1.8	0.9	1.2	1.4	2.2	3.3	1.0	1.4
$Oligo(dT)_{15}$ (0.5µg/reaction) (µL)	1	1	1	1	1	1	1	1	1	1	1	1	1	1
Nuclease-Free Water	2.7	1.8	2.7	2.8	1.7	1.6	2.2	3.1	2.8	2.6	1.8	0.7	3.0	2.6
Total (µL)	5	5	5	5	5	5	5	5	5	5	5	5	5	5

S: Susceptible, R: Resistance, M: Mock inoculated, I: inoculated, 0 H: Zero Hour, 4 H: 4 Hour, 24 H: 24 Hour, 96 H: 96 Hour post inoculation.

Table S. 13: The properties of designed qRT-PCR primers for candidate genes responsible for resistance towards Iranian *V. alfalfae* AF1.

Gene	Direction	Sequence	Tm	GC	Penalty	Product Size	Penalty	Alignment
MEDTR1g042280	Left Primer	CCTTCTTGGACCCAGTCTCG	59.8 C	60.0 %	0.248	127 bp	0.498	100%
	Right Primer	CAGAAAACCCCGAGAGTGCA	60.2 C	55.0 %	0.250	127 bp	0.498	100%
MEDTR1g042160	Left Primer	ACTCGGAGCCTTACGTTCTT	58.7 C	50.0 %	1.255	86 bp	1.857	100%
	Right Primer	TCCTAACTGGTCGACTGCAC	59.4 C	55.0 %	0.602	86 bp	1.857	100%
MEDTR1g087880	Left Primer	GGGGCAGATGTCAAAGAGCT	60.0 C	55.0 %	0.035	130 bp	0.073	100%
	Right Primer	ACCGTTCACTAGCTGCTGTC	60.0 C	55.0 %	0.038	130 bp	0.073	100%
MEDTR4g023000	Left Primer	TCTCACGCTGCAGCAGTAAA	60.0 C	50.0 %	0.033	135 bp	0.072	100%
	Right Primer	CCGAGACGTTGCTTCTCTGT	60.0 C	55.0 %	0.039	135 bp	0.072	100%
MEDTR7g024390	Left Primer	TCAGGTTGCGATGAACCCTG	60.3 C	55.0 %	0.322	136 bp	0.501	100%
	Right Primer	TGGCTTTTCACCAGGACCAG	60.2 C	55.0 %	0.179	136 bp	0.501	100%
MEDTR8g075240	Left Primer	ATGCACCTGGTGTTCCCATT	59.9 C	50.0 %	0.115	82 bp	0.646	100%
	Right Primer	CCTGGATGGTCGACGAAGAA	59.5 C	55.0 %	0.531	82 bp	0.646	100%
MEDTR8g075260	Left Primer	TGGTGTTCCCAGAACTCGTT	59.2 C	50.0 %	0.835	143 bp	1.076	100%
	Right Primer	TTATCGCCGCCCAAAACAAC	59.8 C	50.0 %	0.241	143 bp	1.076	100%
MEDTR8g075310	Left Primer	CATGTGGCGATGCTTCTTGG	59.9 C	55.0 %	0.100	108 bp	0.637	100%
	Right Primer	ACCTGTGCCTTTTTCCTCGG	60.5 C	55.0 %	0.537	108 bp	0.637	100%
MEDTR8g075320	Left Primer	CGGTGTTCGCGGTATCGATA	60.0 C	55.0 %	0.041	141 bp	0.143	100%
	Right Primer	GCATCAGCTTTTAGCCCAGC	59.9 C	55.0 %	0.102	141 bp	0.143	100%
MEDTR8g075330	Left Primer	CATTGACATCGGACCGGGAA	60.1 C	55.0 %	0.108	140 bp	0.222	100%
	Right Primer	TGTCACCCTCACTAGAGCCA	59.9 C	55.0 %	0.114	140 bp	0.222	100%
MEDTR8g075340	Left Primer	GGGAGATTCTGCGAGAGTGG	59.9 C	60.0 %	0.104	150 bp	0.432	100%
	Right Primer	GGCTTCTGCTCCAGGGTAAA	59.7 C	55.0 %	0.328	150 bp	0.432	100%

Gene	Direction	Sequence	Tm	GC	Penalty	Product Size	Penalty	Alignment
MEDTR8g075510	Left Primer	ACTTGTACTGCTGCGGATGA	59.4 C	50.0 %	0.608	90 bp	1.969	100%
	Right Primer	TGATCCTGGCTTTGACTCCA	58.6 C	50.0 %	1.361	90 bp	1.969	100%
MEDTR8g075550	Left Primer	CCACGCGCTTATAGCTATGC	59.3 C	55.0 %	0.716	150 bp	0.903	100%
	Right Primer	TGCCCAAATGTCCACTCCAA	59.8 C	50.0 %	0.187	150 bp	0.903	100%
MEDTR8g102470	Left Primer	TGTCACTCAATCGACGCTCC	60.1 C	55.0 %	0.109	80 bp	0.143	100%
	Right Primer	TCTCCTCCGGCGAATATTGC	60.0 C	55.0 %	0.034	80 bp	0.143	100%
MEDTR1g087500	Left Primer	TGGAATCTCCAGCAAGGTCTG	59.7 C	52.4 %	1.280	102 bp	1.391	100%
	Right Primer	CGCAAAACCTTGAGTCGTCG	60.1 C	55.0 %	0.111	102 bp	1.391	100%
MEDTR1g087510	Left Primer	AACTGCTCCGTCCTTCGATG	60.1 C	55.0 %	0.109	82	0.640	100%
	Right Primer	ATAGCAGCATCGCGAGCTTT	60.5 C	50.0 %	0.532	82	0.640	100%
MEDTR3g054420	Left Primer	No exon-exon primer was found.						
	Right Primer							

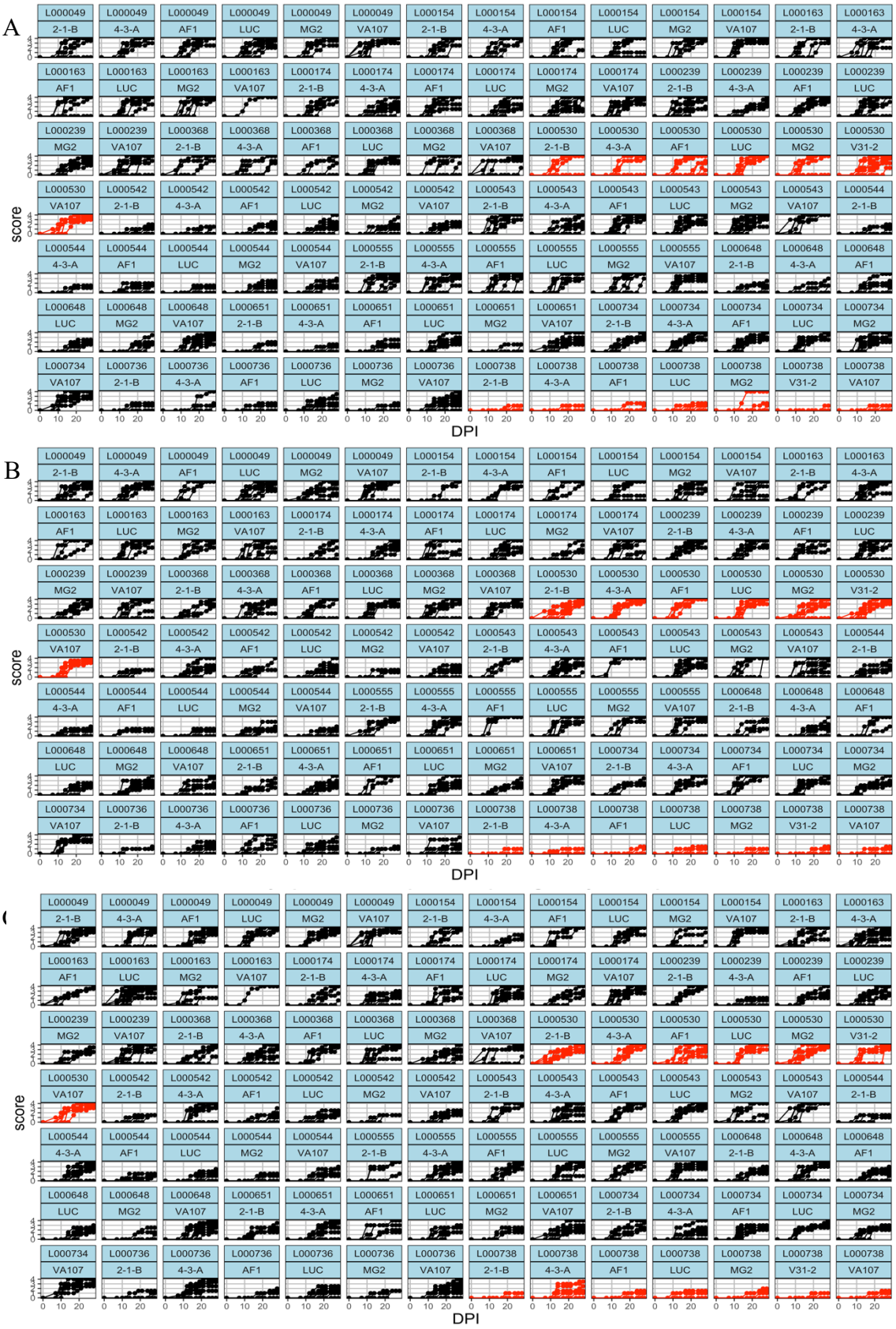

Figure S. 1: Development of wilt symptoms in a subset of 16 *M. truncatula* accessions inoculated with seven *V. alfalfae* isolates for pathogenicity test.

Symptoms are scored on a scale of 0 to 4 (Ben *et. al*.-2013) for 28 days after inoculation (dpi). Data are Raw data. Each curve represents the evolution of the plant's symptoms. Red curves represent the check lines used to evaluate block effects and correct the raw values. A: First repeat, B: Second repeat, C: Third repeat.

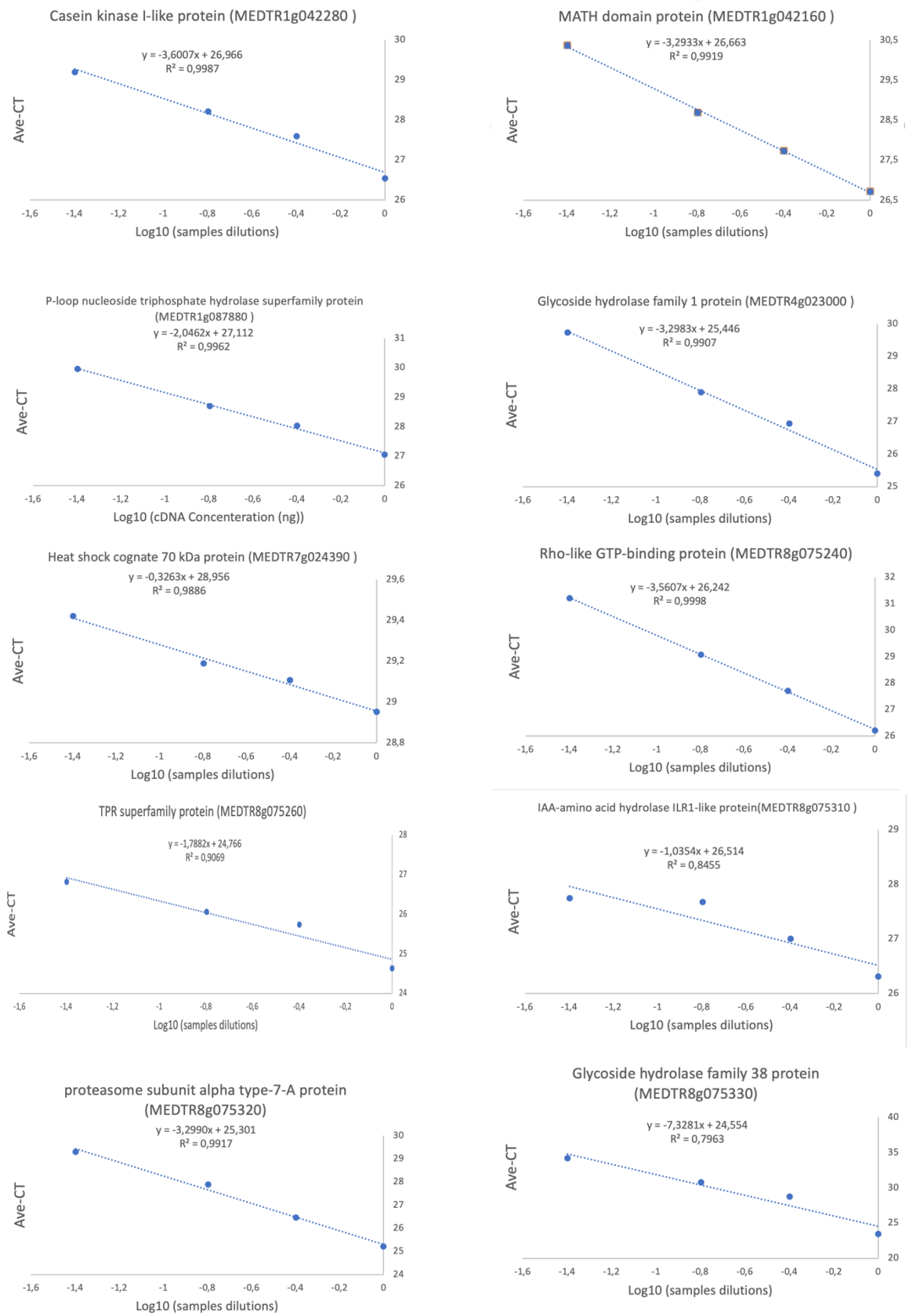

Figure S.2: Standard curve of the designed primer pair for gene expression analysis of 24 selected *M. truncatula* toward the AF1 **inoculation.**

The X axis represents the logarithm 10 of samples dilutions, The Y axis represents the mean values of two C_T values.

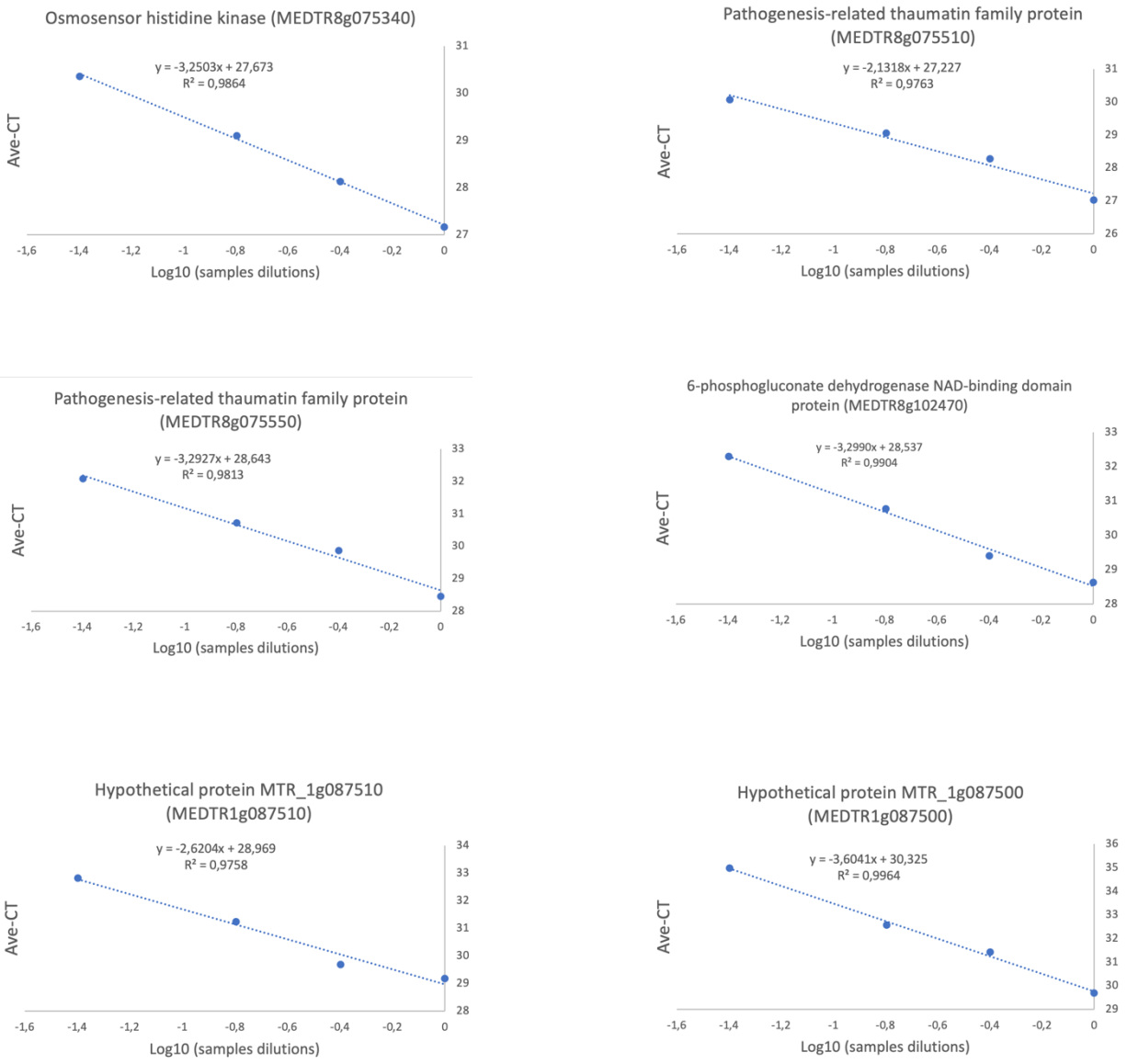

Figure S. 2: Standard curve of the designed primer pair for gene expression analysis of 24 selected *M. truncatula* toward the AF1 **inoculation.**

The X axis represents the logarithm 10 of samples dilutions, The Y axis represents the mean values of two C_T values.

Table S. 14: ***Verticillium alfalfae*** AF1 **resistance genes were identified by genetic association analysis with 242 accesses to the MtHapMap collection.**

This lists, for each chromosome (Chr), the genes located in a 10 Kb region of upstream or downstream of the SNP(s) (Locus) having an equal or higher association score of 5 for each studied trait (AUDPC, MSS). The association score of each SNP corresponds to [-log10 (P-value)]and is obtained for each SNP based on the mixed linear model Q model including the structure of the population and the identity kinship matrix. The gene whose name is written in bold format is the gene that was overlapped with a previous study in the response of *M truncatula* to the *V. alfalfae* French strain(V31-2) (Mazurier *et. al*, 2018).

Chr	Locus	Trait	Score	Gene	Position of gene	Annotation	Gene Length (bp)
1	12 964 012	AUDPC	5,0113637	*Medtr1g035570*	chr1:12954107..12956283 (+ strand)	B3 DNA-binding domain protein	2,177
		AUDPC	5,0113637	*Medtr1g035580*	chr1:12962762..12964258 (+ strand)	Cytochrome P450 family protein	1,497
		AUDPC	5,0113637	*Medtr1g035590*	chr1:12967573..12969327 (- strand)	Hypothetical protein	1,755
	15 800 708	AUDPC	5,28168349	*Medtr1g042280*	chr1:15791912..15798057 (+ strand)	Casein kinase I-like protein	6,146
		AUDPC	5,28168349	*Medtr1g042260*	chr1:15800210..15800555 (- strand)	Hypothetical protein	346
		AUDPC	5,28168349	*Medtr1g042230*	chr1:15807642..15807824 (- strand)	Hypothetical protein	183
	15 823 565	AUDPC	5,76136032	*Medtr1g042200*	chr1:15813194..15814126 (- strand)	Nodule Cysteine-Rich (NCR) secreted peptide	933
		AUDPC	5,76136032	*Medtr1g042160*	chr1:15824709..15827639 (+ strand)	**MATH domain protein**	2,931
		AUDPC	5,76136032	*Medtr1g042410*	chr1:15829827..15834137 (- strand)	Hypothetical protein	4,311
	39 220 870	AUDPC	5,94217176	*Medtr1g087510*	chr1:39209847..39210906 (+ strand)	Hypothetical protein	1,06
		AUDPC	5,94217176	*Medtr1g087500*	chr1:39213341..39217313 (- strand)	Hypothetical protein	3,973
		AUDPC	5,94217176	*Medtr1g087480*	chr1:39219270..39220811 (+ strand)	Hypothetical protein	1,542
		AUDPC	5,94217176	*Medtr1g087470*	chr1:39221382..39222320 (- strand)	myb-CC type transfactor, lheqle motif protein	939
		AUDPC	5,94217176	*Medtr1g087440*	chr1:39228819..39238060 (+ strand)	CTP synthase-like protein	9,242
		MSS	5,18232261	*Medtr1g087510*	chr1:39209847..39210906 (+ strand)	Hypothetical protein	1,06
		MSS	5,18232261	*Medtr1g087500*	chr1:39213341..39217313 (- strand)	Hypothetical protein	3,973
		MSS	5,18232261	*Medtr1g087480*	chr1:39219270..39220811 (+ strand)	Hypothetical protein	1,542

Chr	Locus	Trait	Score	Gene	Position of gene	Annotation	Gene Length (bp)
		MSS	5,18232261	*Medtr1g087470*	chr1:39221382..39222320 (- strand)	myb-CC type transfactor, lheqle motif protein	939
		MSS	5,18232261	*Medtr1g087440*	chr1:39228819..39238060 (+ strand)	CTP synthase-like protein	9,242
	39 222 678	AUDPC	5,2209544	*Medtr1g087500*	chr1:39213341..39217313 (- strand)	Hypothetical protein	3,973
		AUDPC	5,2209544	*Medtr1g087480*	chr1:39219270..39220811 (+ strand)	Hypothetical protein	1,542
		AUDPC	5,2209544	*Medtr1g087440*	chr1:39228819..39238060 (+ strand)	CTP synthase-like protein	9,242
	39 226 123	AUDPC	5,06430868	*Medtr1g087470*	chr1:39221382..39222320 (- strand)	myb-CC type transfactor, lheqle motif protein	939
	39 333 665	AUDPC	5,20124047	*Medtr1g087870*	chr1:39334321..39335188 (- strand)	Hypothetical protein	868
		AUDPC	5,20124047	*Medtr1g087880*	chr1:39338160..39344460 (+ strand)	P-loop nucleoside triphosphate hydrolase superfamily protein	6,301
2	33 302 078	AUDPC	5,33745675	*Medtr2g085170*	chr2:33286444..33292940 (+ strand)	DUF616 family protein	6,497
		AUDPC	5,33745675	*Medtr2g085160*	chr2:33296899..33300046 (+ strand)	UDP-sugar transporter-like protein	3,148
		AUDPC	5,33745675	*Medtr2g085110*	chr2:33311559..33312182 (+ strand)	Hypothetical protein	624
	40 032 546	AUDPC	5,11787751	*Medtr2g093840*	chr2:40026869..40030806 (+ strand)	Carboxyl-terminal peptidase	3,938
		AUDPC	5,11787751	*Medtr2g093960*	chr2:40039886..40042385 (+ strand)	C2H2-type zinc finger protein	2,5
3	21 589 694	MSS	5,77990148	*Medtr3g054370*	chr3:21579372..21580016 (- strand)	LBP/BPI/CETP family, amine-terminal domain protein	645
		MSS	5,77990148	*Medtr3g054380*	chr3:21584416..21584972 (- strand)	Histone H4 domain protein	557
		MSS	5,77990148	*Medtr3g054400*	chr3:21589785..21592985 (- strand)	pre-mRNA-splicing factor ATP-dependent RNA helicase PRP16	3,201
		MSS	5,77990148	*Medtr3g054410*	chr3:21595772..21596200 (+ strand)	NADH-quinone oxidoreductase, chain I	429
		MSS	5,77990148	*Medtr3g054420*	chr3:21597527..21598634 (- strand)	Flavin containing amine oxidase	1,108

Chr	Locus	Trait	Score	Gene	Position of gene	Annotation	Gene Length (bp)
		MSS	5,77990148	*Medtr3g054960*	chr3:21599470..21602209 (- strand)	Oxysterol-binding protein, putative	2,74
	21 589 926	MSS	5,07253021	*Medtr3g054400*	chr3:21589785..21592985 (- strand)	pre-mRNA-splicing factor ATP-dependent RNA helicase PRP16	3,201
		MSS	5,07253021	*Medtr3g054960*	chr3:21599470..21602209 (- strand)	Oxysterol-binding protein, putative	2,74
	21 589 932	MSS	5,07253021	*Medtr3g054370*	chr3:21579372..21580016 (- strand)	LBP/BPI/CETP family, amine-terminal domain protein	645
		MSS	5,07253021	*Medtr3g054420*	chr3:21597527..21598634 (- strand)	Flavin containing amine oxidase	1,108
	28 557 855	AUDPC	5,10734345	*Medtr3g063070*	chr3:28542831..28547875 (- strand)	TRAM, LAG1 and CLN8 (TLC) lipid-sensing domain protein	5,045
		AUDPC	5,10734345	*Medtr3g063080*	chr3:28551005..28551570 (- strand)	Nodule Cysteine-Rich (NCR) secreted peptide	566
		AUDPC	5,10734345	*Medtr3g063090*	chr3:28555542..28555852 (- strand)	Nodule Cysteine-Rich (NCR) secreted peptide	311
		AUDPC	5,10734345	*Medtr3g063110*	chr3:28563081..28563968 (+ strand)	Deoxyuridine 5'-triphosphate nucleotidohydrolase	888
		AUDPC	5,10734345	*Medtr3g063120*	chr3:28566348..28568344 (- strand)	(3S)-linalool/(E)-nerolidol/(E,E)-geranyl linalool synthase	1,997
4	7 722 829	AUDPC	5,3180167	*Medtr4g022930*	chr4:7713902..7714295 (- strand)	NBS-LRR disease resistance protein	394
		AUDPC	5,3180167	*Medtr4g022940*	chr4:7714382..7714630 (- strand)	Hypothetical protein	249
		AUDPC	5,3180167	*Medtr4g022950*	chr4:7716004..7717366 (- strand)	NBS-LRR resistance protein	1,363
		AUDPC	5,3180167	*Medtr4g022960*	chr4:7719854..7722924 (- strand)	NBS-LRR type disease resistance protein	3,071
		AUDPC	5,3180167	*Medtr4g023000*	chr4:7727432..7733212 (+ strand)	Glycoside hydrolase family 1 protein	5,781

Chr	Locus	Trait	Score	Gene	Position of gene	Annotation	Gene Length (bp)
		MSS	6,4280652	*Medtr4g022930*	chr4:7713902..7714295 (- strand)	NBS-LRR disease resistance protein	394
		MSS	6,4280652	*Medtr4g022940*	chr4:7714382..7714630 (- strand)	Hypothetical protein	249
		MSS	6,4280652	*Medtr4g022950*	chr4:7716004..7717366 (- strand)	NBS-LRR resistance protein	1,363
		MSS	6,4280652	*Medtr4g022960*	chr4:7719854..7722924 (- strand)	NBS-LRR type disease resistance protein	3,071
		MSS	6,4280652	*Medtr4g023000*	chr4:7727432..7733212 (+ strand)	Glycoside hydrolase family 1 protein	5,781
	14 324 686	MSS	5,01133441	*Medtr4g040170*	chr4:14333831..14334031 (- strand)	WEB family plant protein	201
	33 221 889	AUDPC	5,17693464	*Medtr4g085040*	chr4:33226801..33227987 (- strand)	RNA recognition motif, a.k.a. RRM, RBD protein	1,187
		AUDPC	5,17693464	*Medtr4g085050*	chr4:33232123..33232359 (- strand)	Hypothetical protein	237
6	257 578	AUDPC	5,01522401	*Medtr6g004360*	chr6:251033..251452 (- strand)	Leguminosin group486 secreted peptide	420
		AUDPC	5,01522401	*Medtr6g004370*	chr6:253048..253822 (- strand)	Hypothetical protein	775
		AUDPC	5,01522401	*Medtr6g004380*	chr6:255372..255809 (- strand)	Leguminosin group486 secreted peptide	438
		AUDPC	5,01522401	*Medtr6g004390*	chr6:258027..258629 (- strand)	Hypothetical protein	603
		AUDPC	5,01522401	*Medtr6g004400*	chr6:259538..265898 (- strand)	tRNA pseudouridine synthase B	6,361
		AUDPC	5,01522401	*Medtr6g004420*	chr6:269237..271638 (+ strand)	Hypothetical protein	2,402
		AUDPC	5,01522401	*Medtr6g004430*	chr6:272083..276122 (- strand)	GHMP kinase ATP-binding protein, putative	4,04
	24 123 578	MSS	5,25652662	*Medtr6g065120*	chr6:24112211..24113617 (+ strand)	Carboxylesterase	1,407
		MSS	5,25652662	*Medtr6g065130*	chr6:24114473..24115590 (- strand)	Hypothetical protein	1,118
		MSS	5,25652662	*Medtr6g065150*	chr6:24123153..24123555 (- strand)	PPR domain protein	403
		MSS	5,25652662	*Medtr6g065160*	chr6:24123887..24124878 (- strand)	Hypothetical protein	992

Chr	Locus	Trait	Score	Gene	Position of gene	Annotation	Gene Length (bp)
		MSS	5,25652662	*Medtr6g065170*	chr6:24126811..24130941 (- strand)	cell differentiation RCD1-like protein	4,131
		MSS	5,25652662	*Medtr6g065190*	chr6:24133813..24137605 (- strand)	PPR repeat protein	3,793
	34 475 434	AUDPC	5,00485795	*Medtr6g091590*	chr6:34476546..34479076 (+ strand)	Hypothetical protein	2,531
		AUDPC	5,00485795	*Medtr6g091600*	chr6:34480457..34482218 (+ strand)	pollen Ole e I family allergens	1,762
		AUDPC	5,00485795	*Medtr6g091605*	chr6:34485056..34485354 (+ strand)	Late nodulin	299
7	8 014 997	AUDPC	5,12679405	*Medtr7g024373*	chr7:8008805..8012520 (+ strand)	Hypothetical protein	3,716
		AUDPC	5,12679405	*Medtr7g024360*	chr7:8001360..8001545 (- strand)	Transmembrane protein, putative	186
		AUDPC	5,12679405	*Medtr7g024350*	chr7:7996153..7999666 (+ strand)	DUF3317 family protein	3,514
		AUDPC	5,12679405	*Medtr7g024390*	chr7:8016048..8019129 (+ strand)	Heat shock cognate 70 kDa protein	3,082
		AUDPC	5,12679405	*Medtr7g024420*	chr7:8022686..8026281 (- strand)	Glycosyl hydrolase family 10 protein	3,596
		MSS	5,47004782	*Medtr7g024373*	chr7:8008805..8012520 (+ strand)	Hypothetical protein	3,716
		MSS	5,47004782	*Medtr7g024390*	chr7:8016048..8019129 (+ strand)	Heat shock cognate 70 kDa protein	3,082
		MSS	5,47004782	*Medtr7g024420*	chr7:8022686..8026281 (- strand)	Glycosyl hydrolase family 10 protein	3,596
	48 807 285	AUDPC	5,38705364	*Medtr7g117620*	chr7:48789283..48796112 (+ strand)	Ankyrin repeat protein	6,83
8	2 106 964	AUDPC	5,10427439	*Medtr8g009270*	chr8:2096904..2097968 (- strand)	Transmembrane protein, putative	1,065
		AUDPC	5,10427439	*Medtr8g009280*	chr8:2101157..2105141 (+ strand)	GroES chaperonin	3,985
		AUDPC	5,10427439	*Medtr8g009290*	chr8:2106435..2111759 (- strand)	Pigment defective 320 protein, putative	5,325
		AUDPC	5,10427439	*Medtr8g009295*	chr8:2112924..2113151 (- strand)	Hypothetical protein	228

Chr	Locus	Trait	Score	Gene	Position of gene	Annotation	Gene Length (bp)
		AUDPC	5,10427439	*Medtr8g009300*	chr8:2117013..2117798 (+ strand)	plant invertase/pectin methylesterase inhibitor	786
	2 597 013	AUDPC	5,00479687	*Medtr8g010160*	chr8:2583935..2588108 (- strand)	ABI3-interacting protein	4,174
		AUDPC	5,00479687	*Medtr8g010170*	chr8:2590280..2595983 (- strand)	ABI3-interacting protein	5,704
		AUDPC	5,00479687	*Medtr8g010180*	chr8:2604129..2608095 (+ strand)	LRR receptor-like kinase	3,967
		AUDPC	5,00479687	*Medtr8g010200*	chr8:2609370..2610443 (- strand)	RALF-like protein	1,074
		AUDPC	5,00479687	*Medtr8g010220*	chr8:2612652..2614243 (- strand)	Transmembrane protein, putative	1,592
	28 608 045	AUDPC	5,01674637	*Medtr8g068530*	chr8:28597194..28600951 (- strand)	U-box kinase family protein	3,758
		AUDPC	5,01674637	*Medtr8g068540*	chr8:28603243..28606770 (+ strand)	LRR receptor-like kinase family protein	3,528
		AUDPC	5,01674637	*Medtr8g068550*	chr8:28607635..28613301 (- strand)	Nucleobase-ascorbate transporter-like protein	5,667
		AUDPC	5,01674637	*Medtr8g068560*	chr8:28616562..28617450 (- strand)	Hypothetical protein	889
		MSS	5,0056968	*Medtr8g068530*	chr8:28597194..28600951 (- strand)	U-box kinase family protein	3,758
		MSS	5,0056968	*Medtr8g068560*	chr8:28616562..28617450 (- strand)	Hypothetical protein	889
	28 608 060	MSS	5,05989693	*Medtr8g068530*	chr8:28597194..28600951 (- strand)	U-box kinase family protein	3,758
		MSS	5,05989693	*Medtr8g068540*	chr8:28603243..28606770 (+ strand)	LRR receptor-like kinase family protein	3,528
		MSS	5,05989693	*Medtr8g068550*	chr8:28607635..28613301 (- strand)	Nucleobase-ascorbate transporter-like protein	5,667
		MSS	5,05989693	*Medtr8g068560*	chr8:28616562..28617450 (- strand)	Hypothetical protein	889
	31 815 446	AUDPC	5,82915717	*Medtr8g075240*	chr8:31801964..31806400 (+ strand)	Rho-like GTP-binding protein	4,437
		AUDPC	5,82915717	*Medtr8g075250*	chr8:31809006..31815514 (+ strand)	Cell cycle checkpoint protein RAD17, putative	6,509
		AUDPC	5,82915717	*Medtr8g075260*	chr8:31815891..31818432 (- strand)	TPR superfamily protein	2,542

Chr	Locus	Trait	Score	Gene	Position of gene	Annotation	Gene Length (bp)
		AUDPC	5,82915717	*Medtr8g075280*	chr8:31824623..31830186 (+ strand)	Transmembrane protein, putative	5,564
		MSS	5,82501829	*Medtr8g075240*	chr8:31801964..31806400 (+ strand)	Rho-like GTP-binding protein	4,437
		MSS	5,82501829	*Medtr8g075250*	chr8:31809006..31815514 (+ strand)	Cell cycle checkpoint protein RAD17, putative	6,509
		MSS	5,82501829	*Medtr8g075260*	chr8:31815891..31818432 (- strand)	TPR superfamily protein	2,542
		MSS	5,82501829	*Medtr8g075280*	chr8:31824623..31830186 (+ strand)	Transmembrane protein, putative	5,564
	31 823 520	AUDPC	5,3615769	*Medtr8g075290*	chr8:31832998..31834861 (- strand)	Hypothetical protein	1,864
		AUDPC	5,3615769	*Medtr8g075300*	chr8:31836166..31836442 (+ strand)	Hypothetical protein	277
		AUDPC	5,3615769	*Medtr8g075310*	chr8:31836958..31839826 (- strand)	IAA-amino acid hydrolase ILR1-like protein	2,869
		AUDPC	5,3615769	*Medtr8g075320*	chr8:31840594..31843234 (- strand)	Proteasome subunit alpha type-7-A protein	2,641
	31 847 916	AUDPC	5,11974577	*Medtr8g075330*	chr8:31848061..31856341 (+ strand)	Glycoside hydrolase family 38 protein	8,281
		AUDPC	5,11974577	*Medtr8g075340*	chr8:31858278..31864631 (- strand)	Osmosensor histidine kinase	6,354
		AUDPC	5,11974577	*Medtr8g075350*	chr8:31867632..31871181 (- strand)	Senescence/Dehydration-associated-like protein	3,55
		MSS	5,21714976	*Medtr8g075310*	chr8:31836958..31839826 (- strand)	IAA-amino acid hydrolase ILR1-like protein	2,869
		MSS	5,21714976	*Medtr8g075320*	chr8:31840594..31843234 (- strand)	Proteasome subunit alpha type-7-A protein	2,641
		MSS	5,21714976	*Medtr8g075330*	chr8:31848061..31856341 (+ strand)	Glycoside hydrolase family 38 protein	8,281
		MSS	5,21714976	*Medtr8g075340*	chr8:31858278..31864631 (- strand)	Osmosensor histidine kinase	6,354
	31 944 993	AUDPC	5,3859965	*Medtr8g075510*	chr8:31934282..31936698 (- strand)	Pathogenesis-related thaumatin family protein	2,417

Chr	Locus	Trait	Score	Gene	Position of gene	Annotation	Gene Length (bp)
		AUDPC	5,3859965	*Medtr8g075550*	chr8:31943948..31946277 (- strand)	Pathogenesis-related thaumatin family protein	2,33
		MSS	5,29510439	*Medtr8g075510*	chr8:31934282..31936698 (- strand)	Pathogenesis-related thaumatin family protein	2,417
		MSS	5,29510439	*Medtr8g075550*	chr8:31943948..31946277 (- strand)	Pathogenesis-related thaumatin family protein	2,33
	43 117 802	AUDPC	5,96098274	*Medtr8g102460*	chr8:43122066..43126983 (+ strand)	Hexokinase	4,918
		AUDPC	5,96098274	*Medtr8g102467*	chr8:43130682..43131324 (+ strand)	Transmembrane protein, putative	643
		AUDPC	5,96098274	*Medtr8g102470*	chr8:43130205..43132889 (- strand)	6-phosphogluconate dehydrogenase NAD-binding domain protein	2,685
		AUDPC	5,96098274	*Medtr8g102480*	chr8:43135772..43137978 (+ strand)	tRNA/rRNA methyltransferase (SpoU) family protein	2,207
		MSS	5,22668701	*Medtr8g102460*	chr8:43122066..43126983 (+ strand)	Hexokinase	4,918
		MSS	5,22668701	*Medtr8g102467*	chr8:43130682..43131324 (+ strand)	Transmembrane protein, putative	643
		MSS	5,22668701	*Medtr8g102470*	chr8:43130205..43132889 (- strand)	6-phosphogluconate dehydrogenase NAD-binding domain protein	2,685

VIII - Bibliography

Abdurakhmonov, Ibrokhim Y., and Abdusattor Abdukarimov. 2008. “Application of Association Mapping to Understanding the Genetic Diversity of Plant Germplasm Resources.” *International Journal of Plant Genomics* 2008 (February 2008). https://doi.org/10.1155/2008/574927.

Adhikari, Laxman, Shiva O. Makaju, Orville M. Lindstrom, and Ali M. Missaoui. 2021. “Mapping Freezing Tolerance QTL in Alfalfa: Based on Indoor Phenotyping.” *BMC Plant Biology* 21 (1): 1–13. https://doi.org/10.1186/s12870-021-03182-4.

Affouard, A, A Joly, J Lombardo, J Champ, H Goeau, and P Bonnet. 2020. “Pl@ntNet Automatically Identified Occurrences. Version 1.2. Pl@ntNet.” Pl@ntNet. 2020. https://doi.org/10.15468/mma2ec.

Agrios, George. 2005. *Plant Pathology-5th Edition*. Burlington: Elsevier Academic Press.

Ahmed, Lina Qadir, Jean-Louis Durand, and Abraham J. Escobar-Gutiérrez. 2019. “ Genetic Diversity of Alfalfa (Medicago Sativa) in Response to Temperature during Germination .” *Seed Science and Technology*. https://doi.org/10.15258/sst.2019.47.3.10.

Ahuja, Ishita, Ralph Kissen, and Atle M. Bones. 2012. “Phytoalexins in Defense against Pathogens.” *Trends in Plant Science* 17 (2): 73–90. https://doi.org/10.1016/j.tplants.2011.11.002.

Ainsworth, G. C., and Alfred S. Sussman. 2013. *The Fungal Population: An Advanced Treatise*. Edited by Elsevier. Elsevier. https://doi.org/10.1016/C2013-0-11991-5.

Al-Maskri, Ahmed Yahya, Muhammad Sajjad, and Sultan Habibullah Khan. 2012. “Association Mapping: A Step Forward to Discovering New Alleles for Crop Improvement.” *International Journal of Agriculture and Biology* 14 (1): 153–60. https://doi.org/10.13140/2.1.1925.9524.

Ali, Sajad, Bashir Ahmad Ganai, Azra N. Kamili, Ajaz Ali Bhat, Zahoor Ahmad Mir, Javaid Akhter Bhat, Anshika Tyagi, et al. 2018. “Pathogenesis-Related Proteins and Peptides as Promising Tools for Engineering Plants with Multiple Stress Tolerance.” *Microbiological Research* 212–213 (March): 29–37. https://doi.org/10.1016/j.micres.2018.04.008.

Allen, Tom. 2012. “The Principles of Plant Pathology: The Disease Triangle and Influence of the Environment.” Mississippi Crop Situation. 2012. https://www.mississippi-crops.com/2012/08/31/the-principles-of-plant-pathology-the-disease-triangle-and-influence-of-the-environment/.

Alonso, Jose M., and Anna N. Stepanova. 2004. “The Ethylene Signaling Pathway.” *Science* 306 (5701): 1513–15. https://doi.org/10.1126/science.1104812.

Amano, Masashi, Kazuhiro Toyoda, Yuki Ichinose, Tetsuji Yamada, and Tomonori Shiraishi. 1997. “Association between Ion Fluxes and Defense Responses in Pea and Cowpea Tissues.” *Plant and Cell Physiology* 38 (6): 698–706. https://doi.org/10.1093/oxfordjournals.pcp.a029223.

Amos, W, E Driscoll, and J I Hoffman. 2011. “Candidate Genes versus Genome-Wide Associations: Which Are Better for Detecting Genetic Susceptibility to Infectious Disease?” *Proceedings of the Royal Society B: Biological Sciences* 278 (1709): 1183–88. https://doi.org/10.1098/rspb.2010.1920.

Aranzana, María José, Sung Kim, Keyan Zhao, Erica Bakker, Matthew Horton, Katrin Jakob, Clare Lister, et al. 2005. “Genome-Wide Association Mapping in Arabidopsis Identifies Previously Known Flowering Time and Pathogen Resistance Genes.” *PLoS Genetics* 1 (5): 0531–39. https://doi.org/10.1371/journal.pgen.0010060.

Arrones, Andrea, Santiago Vilanova, Mariola Plazas, Giulio Mangino, Laura Pascual, María José Díez, Jaime Prohens, and Pietro Gramazio. 2020. “The Dawn of the Age of Multi-Parent Magic Populations in Plant Breeding: Novel Powerful next-Generation Resources for Genetic Analysis and Selection of Recombinant Elite Material.” *Biology* 9 (8): 1–25. https://doi.org/10.3390/biology9080229.

Atallah, Z. K., J. Bae, S. H. Jansky, D. I. Rouse, and W. R Stevenson. 2007. “Multiplex Real-Time Quantitative PCR to Detect and Quantify Verticillium Dahliae Colonization in Potato Lines That Differ in Response to Verticillium Wilt.” *Phytopathology*® 97 (7): 865–72. https://doi.org/10.1094/PHYTO-97-7-0865.

Atallah, Z. K., Ryan J. Hayes, and Krishna V. Subbarao. 2011. “Fifteen Years of Verticillium Wilt of Lettuce in America’s Salad Bowl: A Tale of Immigration, Subjugation, and Abatement.” *Plant Disease* 95 (7): 784–92. https://doi.org/10.1094/PDIS-01-11-0075.

Aylor, Donald E. 1986. “A Framework for Examining Inter-Regional Aerial Transport

of Fungal Spores." *Agricultural and Forest Meteorology* 38 (4): 263–88. https://doi.org/10.1016/0168-1923(86)90017-1.

Balding, David J. 2006. "A Tutorial on Statistical Methods for Population Association Studies." *Nature Reviews Genetics* 7 (10): 781–91. https://doi.org/10.1038/nrg1916.

Bandillo, Nonoy, Chitra Raghavan, Pauline Muyco, Ma Anna Lynn Sevilla, Irish T Lobina, Christine Dilla-Ermita, Chih-Wei Tung, et al. 2013. "Multi-Parent Advanced Generation Inter-Cross (MAGIC) Populations in Rice: Progress and Potential for Genetics Research and Breeding." *Rice* 6 (1): 11. https://doi.org/10.1186/1939-8433-6-11.

Barbara, Dez J. D.J., and Emily Clewes. 2003. "Plant Pathogenic Verticillium Species: How Many of Them Are There?" *Molecular Plant Pathology* 4 (4): 297–305. https://doi.org/10.1046/j.1364-3703.2003.00172.x.

Barendse, William. 2011. "The Effect of Measurement Error of Phenotypes on Genome Wide Association Studies." *BMC Genomics* 12. https://doi.org/10.1186/1471-2164-12-232.

Barker, David G., Sylvie Bianchi, François Blondon, Yvette Dattée, Gérard Duc, Sadi Essad, Pascal Flament, et al. 1990. "Medicago Truncatula, a Model Plant for Studying the Molecular Genetics of TheRhizobium-Legume Symbiosis." *Plant Molecular Biology Reporter* 8 (1): 40–49. https://doi.org/10.1007/BF02668879.

Bartoli, Claudia, and Fabrice Roux. 2017. "Genome-Wide Association Studies In Plant Pathosystems: Toward an Ecological Genomics Approach." *Frontiers in Plant Science* 8 (May). https://doi.org/10.3389/fpls.2017.00763.

Basak, Merve, Bulent Uzun, and Engin Yol. 2019. "Genetic Diversity and Population Structure of the Mediterranean Sesame Core Collection with Use of Genome-Wide SNPs Developed by Double Digest RAD-Seq." *PLoS ONE* 14 (10). https://doi.org/10.1371/journal.pone.0223757.

Beckman, C. H., and E. M. Roberts. 1995. "On the Nature and Genetic Basis for Resistanc and Tolerance to Fngal Wild Diseases of Plants." *Adv. Bot. Res.* 21: 35–77.

Ben, Cécile, Maoulida Toueni, Sara Montanari, Marie-Claire Tardin, Magalie Fervel, Azam Negahi, Laure Saint-Pierre, et al. 2013. "Natural Diversity in the Model Legume Medicago Truncatula Allows Identifying Distinct Genetic Mechanisms Conferring Partial Resistance to Verticillium Wilt." *Journal of Experimental*

Botany 64 (1): 317–32. https://doi.org/10.1093/jxb/ers337.

Bernardo-Cravo, Adriana P., Dirk S. Schmeller, Antonis Chatzinotas, Vance T. Vredenburg, and Adeline Loyau. 2020. “Environmental Factors and Host Microbiomes Shape Host–Pathogen Dynamics.” *Trends in Parasitology* 36 (7): 616–33. https://doi.org/10.1016/j.pt.2020.04.010.

Bigeard, Jean, Jean Colcombet, and Heribert Hirt. 2015. “Signaling Mechanisms in Pattern-Triggered Immunity (PTI).” *Molecular Plant* 8 (4): 521–39. https://doi.org/10.1016/j.molp.2014.12.022.

Bilello, Stanley. 2016. *21st Century Homestead: Nitrogen-Fixing Crops - Stanley Bilello - Google Books*. Lulu.com. https://books.google.fr/books?id=yZc_DQAAQBAJ&pg=PA1&lpg=PA1&dq=called+alfalfa+in+Latin+medica,+a+name+that+referred+to+the+Medes&source=bl&ots=REMjl5LpMP&sig=ACfU3U3Rp1vPfOIK3JbRX0YtZAS8kEzEKQ&hl=en&sa=X&ved=2ahUKEwiQktGE1broAhX-A2MBHZXGAa8Q6AEwA3oECAoQA.

Bishop, C.D., and R.M. Cooper. 1983. “An Ultrastructural Study of Root Invasion in Three Vascular Wilt Diseases.” *Physiological Plant Pathology* 22 (1): 15-IN13. https://doi.org/10.1016/s0048-4059(83)81034-0.

BLACKHURST, FRANCES M. 1963. “Induction of Verticillium Wilt Disease Symptoms in Detached Shoots of Resistant and of Susceptible Tomato Plants.” *Annals of Applied Biology* 52 (1): 79–88. https://doi.org/10.1111/j.1744-7348.1963.tb03729.x.

Blatt, Michael R., Alexander Grabov, Jane Brearley, Kim Hammond-Kosack, and Jonathan D.G. Jones. 1999. “K+ Channels of Cf-9 Transgenic Tobacco Guard Cells as Targets for Cladosporium Fulvum Avr9 Elicitor-Dependent Signal Transduction.” *Plant Journal* 19 (4): 453–62. https://doi.org/10.1046/j.1365-313X.1999.00534.x.

Boller, Thomas, and Georg Felix. 2009. “A Renaissance of Elicitors: Perception of Microbe-Associated Molecular Patterns and Danger Signals by Pattern-Recognition Receptors.” *Annual Review of Plant Biology* 60: 379–407. https://doi.org/10.1146/annurev.arplant.57.032905.105346.

Bowen, J. k., C. h. Mesarich, V. g. M. Bus, R. m. Beresford, K. m. Plummer, and M. d. Templeton. 2011. “Venturia Inaequalis: The Causal Agent of Apple Scab.” *Molecular Plant Pathology* 12 (2): 105–22. https://doi.org/10.1111/j.1364-3703.2010.00656.x.

Bradbury, Peter J., Zhiwu Zhang, Dallas E. Kroon, Terry M. Casstevens, Yogesh Ramdoss, and Edward S. Buckler. 2007. “TASSEL: Software for Association Mapping of Complex Traits in Diverse Samples.” *Bioinformatics* 23 (19): 2633–35. https://doi.org/10.1093/bioinformatics/btm308.

Branca, A., T. D. Paape, P. Zhou, R. Briskine, A. D. Farmer, J. Mudge, A. K. Bharti, et al. 2011. “Whole-Genome Nucleotide Diversity, Recombination, and Linkage Disequilibrium in the Model Legume Medicago Truncatula.” *Proceedings of the National Academy of Sciences of the United States of America* 108 (42). https://doi.org/10.1073/pnas.1104032108.

Bredow, Melissa, and Jacqueline Monaghan. 2019. “Regulation of Plant Immune Signaling by Calcium-Dependent Protein Kinases.” *Molecular Plant-Microbe Interactions*® 32 (1): 6–19. https://doi.org/10.1094/MPMI-09-18-0267-FI.

Bruce S. Weir. 1996. “Genetic Data Analysis II.” *Genetical Research* 68 (2): 187–187. https://doi.org/10.1017/s0016672300034121.

Bu, Bingwu, Dewen Qiu, Hongmei Zeng, Lihua Guo, Jingjing Yuan, and Xiufen Yang. 2014. “A Fungal Protein Elicitor PevD1 Induces Verticillium Wilt Resistance in Cotton.” *Plant Cell Reports* 33 (3): 461–70. https://doi.org/10.1007/s00299-013-1546-7.

Buels, Robert, Eric Yao, Colin M. Diesh, Richard D. Hayes, Monica Munoz-Torres, Gregg Helt, David M. Goodstein, et al. 2016. “JBrowse: A Dynamic Web Platform for Genome Visualization and Analysis.” *Genome Biology* 17 (1): 66. https://doi.org/10.1186/s13059-016-0924-1.

Bush, William S., and Jason H. Moore. 2012. “Chapter 11: Genome-Wide Association Studies.” *PLoS Computational Biology* 8 (12). https://doi.org/10.1371/journal.pcbi.1002822.

Calabrese, Barbara. 2019. “Linkage Disequilibrium.” In *Encyclopedia of Bioinformatics and Computational Biology*, 763–65. Elsevier. https://doi.org/10.1016/B978-0-12-809633-8.20234-3.

Capstaff, Nicola M., and Anthony J. Miller. 2018. “Improving the Yield and Nutritional Quality of Forage Crops.” *Frontiers in Plant Science* 9 (April): 535. https://doi.org/10.3389/fpls.2018.00535.

Čarná, Mária, Vladimír Repka, Petr Skůpa, and Ernest Šturdík. 2014. “Auxins in Defense Strategies.” *Biologia* 69 (10): 1255–63. https://doi.org/10.2478/s11756-014-0431-3.

Casadevall, Arturo, and Liise Anne Pirofski. 1999. “Host-Pathogen Interactions: Redefining the Basic Concepts of Virulence and Pathogenicity.” *Infection and Immunity* 67 (8): 3703–13. https://doi.org/10.1007/s13592-015-0412-8.

Casler, Michael D., and Daniel J. Undersander. 2018. “Identification of Temperate Pasture Grasses and Legumes.” In *Horse Pasture Management*, 11–35. Elsevier. https://doi.org/10.1016/B978-0-12-812919-7.00002-0.

Catalano, D.N., C.C. Sheaffer, A.M. Grev, M.L. Schultz, and K.L. Martinson. 2015. “122 Forage Nutritive Value, Yield, and Preference of Legumes under Horse Grazing.” *Journal of Equine Veterinary Science* 35 (5): 435. https://doi.org/10.1016/j.jevs.2015.03.133.

Cavanagh, Colin R., Shiaoman Chao, Shichen Wang, Bevan Emma Huang, Stuart Stephen, Seifollah Kiani, Kerrie Forrest, et al. 2013. “Genome-Wide Comparative Diversity Uncovers Multiple Targets of Selection for Improvement in Hexaploid Wheat Landraces and Cultivars.” *Proceedings of the National Academy of Sciences of the United States of America* 110 (20): 8057–62. https://doi.org/10.1073/pnas.1217133110.

Chen, Mengjie, Can Yang, Cong Li, Lin Hou, Xiaowei Chen, and Hongyu Zhao. 2014. “Admixture Mapping Analysis in the Context of GWAS with GAW18 Data.” *BMC Proceedings*. Vol. 8. https://doi.org/10.1186/1753-6561-8-S1-S3.

Chen, Raymond E., and Jeremy Thorner. 2007. “Function and Regulation in MAPK Signaling Pathways.” *Biochimica et Biophysica Acta* 1773 (8): 1311–40. http://www.ncbi.nlm.nih.gov/pmc/articles/PMC2031910/%5Cnhttp://www.ncbi.nlm.nih.gov/pmc/articles/PMC2031910/pdf/nihms-28620.pdf.

Cheng, Cheng, Xiquan Gao, Baomin Feng, Jen Sheen, Libo Shan, and Ping He. 2013. “Plant Immune Response to Pathogens Differs with Changing Temperatures.” *Nature Communications* 4 (1): 2530. https://doi.org/10.1038/ncomms3530.

Chini, Andrea, Alessio Cimmino, Marco Masi, Pierluigi Reveglia, Paola Nocera, Roberto Solano, and Antonio Evidente. 2018. “The Fungal Phytotoxin Lasiojasmonate A Activates the Plant Jasmonic Acid Pathway.” *Journal of Experimental Botany* 69 (12): 3095–3102. https://doi.org/10.1093/jxb/ery114.

Chisholm, Stephen T., Gitta Coaker, Brad Day, and Brian J. Staskawicz. 2006. “Host-Microbe Interactions: Shaping the Evolution of the Plant Immune Response.” *Cell* 124 (4): 803–14. https://doi.org/10.1016/j.cell.2006.02.008.

Chitarra, Gilma S, Tjakko Abee, Frank M Rombouts, Maarten A Posthumus, and Jan Dijksterhuis. 2004. “Germination of Penicillium Paneum Conidia Is Regulated by 1-Octen-3-Ol, a Volatile Self-Inhibitor” 70 (5): 2823–29. https://doi.org/10.1128/AEM.70.5.2823.

Choi, Hong Kyu, Jeong Hwan Mun, Dong Jin Kim, Hongyan Zhu, Jong Min Baek, Joanne Mudge, Bruce Roe, et al. 2004. “Estimating Genome Conservation between Crop and Model Legume Species.” *Proceedings of the National Academy of Sciences of the United States of America* 101 (43): 15289–94. https://doi.org/10.1073/pnas.0402251101.

Closkey, Robert T . M ’, and Brian Fieldwick. 2004. “The Receptor for the Fungal Elicitor Ethylene-Inducing.” *The Plant Cell* 56 (1): 119–29. https://doi.org/10.1105/tpc.022475.The.

D. Turner, Stephen. 2018. “Qqman: An R Package for Visualizing GWAS Results Using Q-Q and Manhattan Plots.” *Journal of Open Source Software* 3 (25): 731. https://doi.org/10.21105/joss.00731.

Delaunois, Bertrand, Philippe Jeandet, Christophe ClÃ©ment, Fabienne Baillieul, StÃ©phan Dorey, and Sylvain Cordelier. 2014. “Uncovering Plant-Pathogen Crosstalk through Apoplastic Proteomic Studies.” *Frontiers in Plant Science* 5 (JUN): 1–18. https://doi.org/10.3389/fpls.2014.00249.

Dell’Acqua, Matteo, Daniel M. Gatti, Giorgio Pea, Federica Cattonaro, Frederik Coppens, Gabriele Magris, Aye L. Hlaing, et al. 2015. “Genetic Properties of the MAGIC Maize Population: A New Platform for High Definition QTL Mapping in Zea Mays.” *Genome Biology* 16 (1): 1–23. https://doi.org/10.1186/s13059-015-0716-z.

Devaiah, Ballachanda N., Athikkattuvalasu S. Karthikeyan, and Kashchandra G. Raghothama. 2007. “WRKY75 Transcription Factor Is a Modulator of Phosphate Acquisition and Root Development in Arabidopsis.” *Plant Physiology* 143 (4): 1789–1801. https://doi.org/10.1104/pp.106.093971.

Devine, Carrick, and Michael Dikeman. 2014. *Encyclopedia of Meat Sciences*. Edited by Elsevier. 2nd ed. https://books.google.fr/books?id=vL9dAwAAQBAJ&pg=RA1-PA401&lpg=RA1-PA401&dq=Some+mold+chlamydospores,+conidia,+and+vegetative+cells+are+known+to+retain+viability+more+than+22+years,+while+spores+may+retain+viability+for+more+than+30+years.&source=bl&ots=G.

Dietzel, Kristin, Denis Valle, Noah Fierer, Jana M. U'ren, and Albert Barberán. 2019. "Geographical Distribution of Fungal Plant Pathogens in Dust across the United States." *Frontiers in Ecology and Evolution* 7 (AUG): 1–8. https://doi.org/10.3389/fevo.2019.00304.

Ding, Zhong Jie, Jing Ying Yan, Xiao Yan Xu, Gui Xin Li, and Shao Jian Zheng. 2013. "WRKY46 Functions as a Transcriptional Repressor of ALMT1, Regulating Aluminum-Induced Malate Secretion in Arabidopsis." *Plant Journal* 76 (5): 825–35. https://doi.org/10.1111/tpj.12337.

Djami-Tchatchou, Arnaud T., Gregory A. Harrison, Chris P. Harper, Renhou Wang, Michael J. Prigge, Mark Estelle, and Barbara N. Kunkel. 2020. "Dual Role of Auxin in Regulating Plant Defense and Bacterial Virulence Gene Expression During Pseudomonas Syringae PtoDC3000 Pathogenesis." *Molecular Plant-Microbe Interactions*® 33 (8): 1059–71. https://doi.org/10.1094/MPMI-02-20-0047-R.

Dong, J., C. Chen, and Z. Chen. 2003. "Expression Profiles of the ArabidopsisWRKY Gene Superfamily during Plant Defense Response," 21–37. https://doi.org/10.1023/A:1020780022549.

Dufresne, Marie, and Anne E. Osbourn. 2001. "Definition of Tissue-Specific and General Requirements for Plant Infection in a Phytopathogenic Fungus." *Molecular Plant-Microbe Interactions*® 14 (3): 300–307. https://doi.org/10.1094/MPMI.2001.14.3.300.

Durrant, W.E., and X. Dong. 2004. "SYSTEMIC ACQUIRED RESISTANCE." *Annual Review of Phytopathology* 42 (1): 185–209. https://doi.org/10.1146/annurev.phyto.42.040803.140421.

Enebak, Scott A. 2012. "Soil Fumigation: The Critical Use Exemption, Quarantine Pre-Shipment Rules, Re-Registration Decision and Their Effect on the 2012 Growing Season." In *National Proceedings: Forest and C; J. R. Pinto; and L. E. Riley; Tech. Coords. USDA Forest Service; Fort Collins; Co.*, 26–30.

Fahleson, Jan, Ulf Lagercrantz, Qiong Hu, Lisa Ann Steventon, and Christina Dixelius. 2003. "Estimation of Genetic Variation among Verticillium Isolates Using AFLP Analysis." *European Journal of Plant Pathology* 109 (4): 361–71. https://doi.org/10.1023/A:1023534005538.

Ferguson, Brett J., Arief Indrasumunar, Satomi Hayashi, Meng Han Lin, Yu Hsiang Lin, Dugald E. Reid, and Peter M. Gresshoff. 2010. "Molecular Analysis of

Legume Nodule Development and Autoregulation.” *Journal of Integrative Plant Biology*. John Wiley & Sons, Ltd. https://doi.org/10.1111/j.1744-7909.2010.00899.x.

Ferreira, Jorge, Monica Cornacchione, Xuan Liu, and Donald Suarez. 2015. “Nutrient Composition, Forage Parameters, and Antioxidant Capacity of Alfalfa (Medicago Sativa, L.) in Response to Saline Irrigation Water.” *Agriculture* 5 (3): 577–97. https://doi.org/10.3390/agriculture5030577.

Fisher, R. A. 1935. “The Logic of Inductive Inference.” *Journal of the Royal Statistical Society* 98 (1): 39–82. http://www.jstor.org/stable/2342435.

Flint-Garcia, Sherry A., Jeffry M. Thornsberry, and Edward S. Buckler. 2003. “Structure of Linkage Disequilibrium in Plants.” *Annual Review of Plant Biology* 54 (1): 357–74. https://doi.org/10.1146/annurev.arplant.54.031902.134907.

Foissac, Sylvain, Jerome Gouzy, Stephane Rombauts, Catherine Mathe, Joelle Amselem, Lieven Sterck, Yves de Peer, Pierre Rouze, and Thomas Schiex. 2008. “Genome Annotation in Plants and Fungi: EuGene as a Model Platform.” *Current Bioinformatics* 3 (2): 87–97. https://doi.org/10.2174/157489308784340702.

Fradin, Emilie F., and Bart P. H. J. Thomma. 2006. “Physiology and Molecular Aspects of Verticillium Wilt Diseases Caused by V. Dahliae and V. Albo-Atrum.” *Molecular Plant Pathology* 7 (2): 71–86. https://doi.org/10.1111/j.1364-3703.2006.00323.x.

Fragoso, Christopher A., Maria Moreno, Zuoheng Wang, Christopher Heffelfinger, Lady J. Arbelaez, John A. Aguirre, Natalia Franco, et al. 2017. “Genetic Architecture of a Rice Nested Association Mapping Population.” *G3: Genes, Genomes, Genetics* 7 (6): 1913–26. https://doi.org/10.1534/g3.117.041608.

Francl, L. J. 2001. “The..Disease Triangle: A Plant Pathological Paradigm Revisited.” *The Plant Health Instructor*. https://doi.org/10.1094/PHI-T-2001-0517-01.

Frugoli, Julia, and Jeanne Harris. 2001. “Medicago Truncatula on the Move!” *The Plant Cell* 13 (3): 458–63. https://doi.org/10.1105/tpc.13.3.458.

Galagan, James E, Sarah E Calvo, Katherine A Borkovich, Eric U Selker, Nick D Read, David Jaffe, William FitzHugh, et al. 2003. “The Genome Sequence of the Filamentous Fungus Neurospora Crassa.” *Nature* 422 (6934): 859–68. https://doi.org/10.1038/nature01554.

Gao, Qing Ming, Shifeng Zhu, Pradeep Kachroo, and Aardra Kachroo. 2015. “Signal

Regulators of Systemic Acquired Resistance." *Frontiers in Plant Science* 6 (APR): 1–12. https://doi.org/10.3389/fpls.2015.00228.

Gao, Xiquan, Kevin Cox Jr., and Ping He. 2014. "Functions of Calcium-Dependent Protein Kinases in Plant Innate Immunity." *Plants* 3 (1): 160–76. https://doi.org/10.3390/plants3010160.

Garmier, Marie, Laurent Gentzbittel, Jiangqi Wen, Kirankumar S. Mysore, and Pascal Ratet. 2017. "Medicago Truncatula : Genetic and Genomic Resources." *Current Protocols in Plant Biology* 2 (December): 318–49. https://doi.org/10.1002/cppb.20058.

Garris, Amanda J., Thomas H. Tai, Jason Coburn, Steve Kresovich, and Susan McCouch. 2005. "Genetic Structure and Diversity in Oryza Sativa L." *Genetics* 169 (3): 1631–38. https://doi.org/10.1534/genetics.104.035642.

Gashaw, Mekuanint. 2016. "Review on Biomass Yield Dynamics and Nutritional Quality of Alfalfa (Medicago Sativa) Journal Of Harmonized Research (JOHR) Journal Of Harmonized Research in Applied Sciences," no. February.

Gaut, Brandon S., and Anthony D. Long. 2003. "The Lowdown on Linkage Disequilibrium." *The Plant Cell* 15 (7): 1502–6. https://doi.org/10.1105/tpc.150730.

Gay, Nicole R., Michael Gloudemans, Margaret L. Antonio, Nathan S. Abell, Brunilda Balliu, Yoson Park, Alicia R. Martin, et al. 2020. "Impact of Admixture and Ancestry on EQTL Analysis and GWAS Colocalization in GTEx." *Genome Biology* 21 (1): 233. https://doi.org/10.1186/s13059-020-02113-0.

Geiringer, Hilda. 1944. "On the Probability Theory of Linkage in Mendelian Heredity." *The Annals of Mathematical Statistics* 15 (1): 25–57. https://doi.org/10.1214/aoms/1177731313.

Gentzbittel, Laurent, Cécile Ben, Mélanie Mazurier, Min-Gyoung Shin, Todd Lorenz, Martina Rickauer, Paul Marjoram, Sergey V. Nuzhdin, and Tatiana V. Tatarinova. 2019. "WhoGEM: An Admixture-Based Prediction Machine Accurately Predicts Quantitative Functional Traits in Plants." *Genome Biology* 20 (1): 106. https://doi.org/10.1186/s13059-019-1697-0.

Ghalandar, M., E. Clewes, D. J. Barbara, R. Zare, and A. Heydari. 2004. "Verticillium Wilt (Verticillium Albo-Atrum) on Medicago Sativa (Alfalfa) in Iran." *Plant Pathology* 53 (6): 812–812. https://doi.org/10.1111/j.1365-3059.2004.01081.x.

Gholami, Azra, Nathan De Geyter, Jacob Pollier, Sofie Goormachtig, and Alain

Goossens. 2014. “Natural Product Biosynthesis in Medicago Species.” *Natural Product Reports* 31 (3): 356. https://doi.org/10.1039/c3np70104b.

Glass, N. L., and G. C. Donaldson. 1995. “Development of Primer Sets Designed for Use with the PCR to Amplify Conserved Genes from Filamentous Ascomycetes.” *Applied and Environmental Microbiology* 61 (4): 1323–30. https://doi.org/10.1128/aem.61.4.1323-1330.1995.

Gorelick, Root, and Manfred D. Laubichler. 2004. “Decomposing Multilocus Linkage Disequilibrium.” *Genetics* 166 (3): 1581–83. https://doi.org/10.1534/genetics.166.3.1581.

Graham, Peter H, and Carroll P Vance. 2003. “Update on Legume Utilization Legumes : Importance and Constraints to Greater Use.” *Plant Physiology* 131 (March): 872–77. https://doi.org/10.1104/pp.017004.872.

Grunewald, Wim, Giel van Noorden, Gert Van Isterdael, Tom Beeckman, Godelieve Gheysen, and Ulrike Mathesius. 2009. “Manipulation of Auxin Transport in Plant Roots during Rhizobium Symbiosis and Nematode Parasitism.” *The Plant Cell* 21 (9): 2553–62. https://doi.org/10.1105/tpc.109.069617.

Guest, D.I. 2017. *Plant Pathology, Principles*. *Encyclopedia of Applied Plant Sciences*. Elsevier. https://doi.org/10.1016/B978-0-12-394807-6.00056-3.

Gultekin, Yunus, Shelby J. Filley, Mary A. Smallman, David B. Hannaway, and Serkan Ates. 2021. “Pasture Production, Persistence of Legumes and Lamb Growth in Summer-Dry Hill Pastures.” *Grass and Forage Science* 76 (1): 159–72. https://doi.org/10.1111/gfs.12497.

Guo, Sun Wei. 1997. “Linkage Disequilibrium Measures for Fine-Scale Mapping: A Comparison.” *Human Heredity* 47 (6): 301–14. https://doi.org/10.1159/000154430.

Gupta, Pushpendra K., Pawan L. Kulwal, and Vandana Jaiswal. 2014. *Association Mapping in Crop Plants: Opportunities and Challenges*. *Advances in Genetics*. Vol. 85. Elsevier. https://doi.org/10.1016/B978-0-12-800271-1.00002-0.

Gupta, Pushpendra K., Sachin Rustgi, and Pawan L. Kulwal. 2005. “Linkage Disequilibrium and Association Studies in Higher Plants: Present Status and Future Prospects.” *Plant Molecular Biology* 57 (4): 461–85. https://doi.org/10.1007/s11103-005-0257-z.

Hamel, Louis Philippe, Marie Claude Nicole, Sébastien Duplessis, and Brian E. Ellis. 2012. “Mitogen-Activated Protein Kinase Signaling in Plant-Interacting Fungi:

Distinct Messages from Conserved Messengers.” *Plant Cell* 24 (4): 1327–51. https://doi.org/10.1105/tpc.112.096156.

Hampton, R.E., S.D. Wullschleger, and D.M. Oosterhuis. 1990. “Impact of Verticillium Wilt on Net Photosynthesis, Respiration and Photorespiration in Field-Grown Cotton (Gossypium Hirsutum L.).” *Physiological and Molecular Plant Pathology* 37 (4): 271–80. https://doi.org/10.1016/0885-5765(90)90076-A.

Hawksworth, DL, and PW Talboys. 1970. “Descriptions of Plant Pathogenic Fungi and Bacteria No. 256.” *Commonwealth Mycological Institute,Kew, Surrey, UK*.

Haynes, Kathleen G., and D. Peter Weingartner. 2004. “The Use of Area under the Disease Progress Curve to Assess Resistance to Late Blight in Potato Germplasm.” *American Journal of Potato Research* 81 (2): 137–41. https://doi.org/10.1007/BF02853611.

Heale, J B, and I Isaac. 1965. “Environmental Factors in the Production of Dark Resting Structures in Verticillium Albo-Atrum, V. Dahliae and V. Tricorpus.” *Transactions of the British Mycological Society* 48 (1): 39–50. https://doi.org/10.1016/s0007-1536(65)80005-5.

Hedrick, Philip W. 1987. “Gametic Disequilibrium Measures: Proceed With Caution.” *Genetics* 117 (2): 331–41. https://doi.org/10.1093/genetics/117.2.331.

Hernandez, C M, J Crossa, and A Castillo. 1993. “The Area under the Function: An Index for Selecting Desirable Genotypes.” *Theoretical and Applied Genetics: International Journal of Plant Breeding Research* 87 (4): 409–15. https://doi.org/10.1007/BF00215085.

Herrera-Vásquez, Ariel, Paula Salinas, and Loreto Holuigue. 2015. “Salicylic Acid and Reactive Oxygen Species Interplay in the Transcriptional Control of Defense Genes Expression.” *Frontiers in Plant Science* 6 (MAR): 1–9. https://doi.org/10.3389/fpls.2015.00171.

Hoffman, Gabriel E. 2013. “Correcting for Population Structure and Kinship Using the Linear Mixed Model: Theory and Extensions.” *PLoS ONE* 8 (10). https://doi.org/10.1371/journal.pone.0075707.

Hu, Jianlin, Chaocheng Guo, Bo Wang, Jiaqing Ye, Meng Liu, Zhikun Wu, Yingjie Xiao, et al. 2018. “Genetic Properties of a Nested Association Mapping Population Constructed With Semi-Winter and Spring Oilseed Rapes.” *Frontiers in Plant Science* 9 (November): 1–14. https://doi.org/10.3389/fpls.2018.01740.

Huang, H. C. 2003. “Verticillium Wilt of Alfalfa: Epidemiology and Control Strategies.”

Canadian Journal of Plant Pathology 25 (4): 328–38. https://doi.org/10.1080/07060660309507088.

Huang, Honglin, Farhan Ullah, Dao Xiu Zhou, Ming Yi, and Yu Zhao. 2019. "Mechanisms of ROS Regulation of Plant Development and Stress Responses." *Frontiers in Plant Science* 10 (June): 1–10. https://doi.org/10.3389/fpls.2019.00800.

Inderbitzin, Patrik, Richard M. Bostock, R. Michael Davis, Toshiyuki Usami, Harold W. Platt, and Krishna V. Subbarao. 2011. "Phylogenetics and Taxonomy of the Fungal Vascular Wilt Pathogen Verticillium, with the Descriptions of Five New Species." Edited by Alexander Idnurm. *PLoS ONE* 6 (12): e28341. https://doi.org/10.1371/journal.pone.0028341.

Inderbitzin, Patrik, R. Michael Davis, Richard M. Bostock, and Krishna V. Subbarao. 2013. "Identification and Differentiation of Verticillium Species and V. Longisporum Lineages by Simplex and Multiplex PCR Assays." *PLoS ONE* 8 (6). https://doi.org/10.1371/journal.pone.0065990.

Inderbitzin, Patrik, and Krishna V. Subbarao. 2014. "*Verticillium* Systematics and Evolution: How Confusion Impedes Verticillium Wilt Management and How to Resolve It." *Phytopathology* 104 (6): 564–74. https://doi.org/10.1094/PHYTO-11-13-0315-IA.

Ingvarsson, P??r K., and Nathaniel R. Street. 2011. "Association Genetics of Complex Traits in Plants." *New Phytologist* 189 (4): 909–22. https://doi.org/10.1111/j.1469-8137.2010.03593.x.

Isaac, I., and Q. MacGarvie. 1966. "Dormancy and Germination of Resting Structures of Verticillium Spp." *Transactions of the British Mycological Society* 49 (4): 669-IN16. https://doi.org/10.1016/S0007-1536(66)80017-7.

Isaac, I. 1949. "A Comparative Study of Pathogenic Isolates of Verticillium ." *Trans Br Mycol Soc* 32.

Isaac, Ivor. 1953. "A Further Comparative Study of Pathogenic Isolates of Verticillium: V. Nubilum Pethybr. and V. Tricorpus Sp.Nov." *Transactions of the British Mycological Society* 36 (3): 180-IN2. https://doi.org/10.1016/S0007-1536(53)80002-1.

Jalmi, Siddhi K., and Alok K. Sinha. 2015. "ROS Mediated MAPK Signaling in Abiotic and Biotic Stress- Striking Similarities and Differences." *Frontiers in Plant Science* 6 (September): 1–9. https://doi.org/10.3389/fpls.2015.00769.

Jeger, M. J., and S. L.H. Viljanen-Rollinson. 2001. “The Use of the Area under the Disease-Progress Curve (AUDPC) to Assess Quantitative Disease Resistance in Crop Cultivars.” *Theoretical and Applied Genetics* 102 (1): 32–40. https://doi.org/10.1007/s001220051615.

Jennings, H. S. 1917. “The Numerical Results of Diverse Systems of Breeding, with Respect to Two Pairs of Char- Acters, Linked or Independent, with Special Relation to the Effects of Linkage.” *Genetics* 2 (97): 1714–23. https://linkinghub.elsevier.com/retrieve/pii/S016895250202557X.

Jensen, Erik S., Mark B. Peoples, and Henrik Hauggaard-Nielsen. 2010. “Faba Bean in Cropping Systems.” *Field Crops Research*. Elsevier B.V. https://doi.org/10.1016/j.fcr.2009.10.008.

Jiang, Cong, Xue Zhang, Huiquan Liu, and Jin-Rong Xu. 2018. “Mitogen-Activated Protein Kinase Signaling in Plant Pathogenic Fungi.” https://doi.org/10.1371/journal.ppat.1006875.

Jiménez-Díaz, Rafael M., Conceptión Olivares-García, Blanca B. Landa, María Del Mar Jiménez-Gasco, and Juan A. Navas-Cortés. 2011. “Region-Wide Analysis of Genetic Diversity in Verticillium Dahliae Populations Infecting Olive in Southern Spain and Agricultural Factors Influencing the Distribution and Prevalence of Vegetative Compatibility Groups and Pathotypes.” *Phytopathology* 101 (3): 304–15. https://doi.org/10.1094/PHYTO-07-10-0176.

Jiménez-Galindo, José Cruz, Rosa Ana Malvar, Ana Butrón, Rogelio Santiago, Luis Fernando Samayoa, Marlon Caicedo, and Bernardo Ordás. 2019. “Mapping of Resistance to Corn Borers in a MAGIC Population of Maize.” *BMC Plant Biology* 19 (1): 1–17. https://doi.org/10.1186/s12870-019-2052-z.

Jones, Jonathan D.G., and Jeffery L. Dangl. 2006. “The Plant Immune System.” *Nature*. https://doi.org/10.1038/nature05286.

Jong, Joke C. De, Barbara J. McCormack, Nicholas Smirnoff, and Nicholas J. Talbot. 1997. “Glycerol Generates Turgor in Rice Blast.” *Nature*. https://doi.org/10.1038/38418.

Jonge, R. de, Melvin D. Bolton, Anja Kombrink, G. C. M. van den Berg, Koste A. Yadeta, and B. P. H. J. Thomma. 2013. “Extensive Chromosomal Reshuffling Drives Evolution of Virulence in an Asexual Pathogen.” *Genome Research* 23 (8): 1271–82. https://doi.org/10.1101/gr.152660.112.

Jwa, Nam-Soo, and Byung Kook Hwang. 2017. “Convergent Evolution of Pathogen

Effectors toward Reactive Oxygen Species Signaling Networks in Plants." *Frontiers in Plant Science* 8 (September): 1–12. https://doi.org/10.3389/fpls.2017.01687.

Kámán-Tóth, Evelin, Tamás Dankó, Gábor Gullner, Zoltán Bozsó, László Palkovics, and Miklós Pogány. 2019. "Contribution of Cell Wall Peroxidase- and NADPH Oxidase-derived Reactive Oxygen Species to Alternaria Brassicicola -induced Oxidative Burst in Arabidopsis." *Molecular Plant Pathology* 20 (4): 485–99. https://doi.org/10.1111/mpp.12769.

Kamaté, K., I. D. Rodriguez-Llorente, M. Scholte, P. Durand, P. Ratet, E. Kondorosi, A. Kondorosi, and T. H. Trinh. 2000. "Transformation of Floral Organs with GFP in Medicago Truncatula." *Plant Cell Reports* 19 (7): 647–53. https://doi.org/10.1007/s002999900168.

Kang, Yun, Minguye Li, Senjuti Sinharoy, and Jerome Verdier. 2016. "A Snapshot of Functional Genetic Studies in Medicago Truncatula." *Frontiers in Plant Science* 7 (AUG2016). https://doi.org/10.3389/fpls.2016.01175.

Kankanala, Prasanna, Raja Sekhar Nandety, and Kirankumar S. Mysore. 2019. "Genomics of Plant Disease Resistance in Legumes." *Frontiers in Plant Science* 10 (October): 1–20. https://doi.org/10.3389/fpls.2019.01345.

Kazan, Kemal, and John M. Manners. 2009. "Linking Development to Defense: Auxin in Plant-Pathogen Interactions." *Trends in Plant Science* 14 (7): 373–82. https://doi.org/10.1016/j.tplants.2009.04.005.

Khoshraftar, Shima, Stacy Hung, Sadia Khan, Yunchen Gong, Vibha Tyagi, John Parkinson, Mohini Sain, Alan M. Moses, and Dinesh Christendat. 2013. "Sequencing and Annotation of the Ophiostoma Ulmi Genome." *BMC Genomics* 14 (1). https://doi.org/10.1186/1471-2164-14-162.

Klessig, Daniel F., Hyong Woo Choi, and D'Maris Amick Dempsey. 2018. "Systemic Acquired Resistance and Salicylic Acid: Past, Present, and Future." *Molecular Plant-Microbe Interactions* 31 (9): 871–88. https://doi.org/10.1094/MPMI-03-18-0067-CR.

Klosterman, Steven J., Krishna V. Subbarao, Seogchan Kang, Paola Veronese, Scott E. Gold, Bart P.H.J. H. J. Thomma, Zehua Chen, et al. 2011. "Comparative Genomics Yields Insights into Niche Adaptation of Plant Vascular Wilt Pathogens." Edited by Jeffery L. Dangl. *PLoS Pathogens* 7 (7): e1002137.

https://doi.org/10.1371/journal.ppat.1002137.

Kombrink, Anja, and Bart P. H. J. Thomma. 2013. “LysM Effectors: Secreted Proteins Supporting Fungal Life.” Edited by Joseph Heitman. *PLoS Pathogens* 9 (12): e1003769. https://doi.org/10.1371/journal.ppat.1003769.

Kong, Xiangpei, Chunlei Zhang, Huihui Zheng, Min Sun, Feng Zhang, Mengyue Zhang, Fuhao Cui, et al. 2020. “Antagonistic Interaction between Auxin and SA Signaling Pathways Regulates Bacterial Infection through Lateral Root in Arabidopsis.” *Cell Reports* 32 (8): 108060. https://doi.org/10.1016/j.celrep.2020.108060.

Köpke, Ulrich, and Thomas Nemecek. 2010. “Ecological Services of Faba Bean.” *Field Crops Research*. Elsevier. https://doi.org/10.1016/j.fcr.2009.10.012.

Kulikova, Olga, Gustavo Gualtieri, René Geurts, Dong Jin Kim, Douglas Cook, Thierry Huguet, J. Hans De Jong, Paul F. Fransz, and Ton Bisseling. 2001. “Integration of the FISH Pachytene and Genetic Maps of Medicago Truncatula.” *Plant Journal* 27 (1): 49–58. https://doi.org/10.1046/j.1365-313X.2001.01057.x.

Kumar, Ujjawal, Singh Kushwaha, Vikas Mangal, Anil Kumar Bairwa, and Narendra Kumar Singh Sneha Adhikari, Tabassum Ahmed, Pallavi Bhat, Ankit Yadav, Narendra Dhaka, Deepak Raj Prajapati, Amit Kumar Gaur, Ranjana Tamta, Indra Deo. 2017. “Association Mapping , Principles and Techniques.” *Journal of Biological and Environmental Engineering* 2 (1): 1–9.

Kunkel, Barbara N., and David M. Brooks. 2002. “Cross Talk between Signaling Pathways in Pathogen Defense.” *Current Opinion in Plant Biology* 5 (4): 325–31. https://doi.org/10.1016/S1369-5266(02)00275-3.

Kushwaha, Hemant R., Rohit Joshi, Ashwani Pareek, and Sneh L. Singla-Pareek. 2016. “MATH-Domain Family Shows Response toward Abiotic Stress in Arabidopsis and Rice.” *Frontiers in Plant Science* 7 (June): 923. https://doi.org/10.3389/fpls.2016.00923.

Kuznetsova, Alexandra, Per B. Brockhoff, and Rune H. B. Christensen. 2017. “LmerTest Package: Tests in Linear Mixed Effects Models.” *Journal of Statistical Software* 82 (13). https://doi.org/10.18637/jss.v082.i13.

Land, C. J., K. S. Lawrence, C. H. Burmester, and B. Meyer. 2017. “Cultivar, Irrigation, and Soil Contribution to the Enhancement of Verticillium Wilt Disease in Cotton.” *Crop Protection* 96: 1–6. https://doi.org/10.1016/j.cropro.2017.01.002.

Latati, Mourad, Adnane Bargaz, Baroudi Belarbi, Mohamed Lazali, Samia Benlahrech, Siham Tellah, Ghiles Kaci, Jean Jacques Drevon, and Sidi Mohamed Ounane. 2016. “The Intercropping Common Bean with Maize Improves the Rhizobial Efficiency, Resource Use and Grain Yield under Low Phosphorus Availability.” *European Journal of Agronomy*. Elsevier B.V. https://doi.org/10.1016/j.eja.2015.09.015.

Latunde-Dada, Akinwunmi O. 2001. “Colletotrichum : Tales of Forcible Entry, Stealth, Transient Confinement and Breakout.” *Molecular Plant Pathology* 2 (4): 187–98. https://doi.org/10.1046/j.1464-6722.2001.00069.x.

Lecourieux, David, Raoul Ranjeva, and Alain Pugin. 2006. “Calcium in Plant Defence-signalling Pathways.” *New Phytologist* 171 (2): 249–69. https://doi.org/10.1111/j.1469-8137.2006.01777.x.

Lee, Nancy, Cletus A. D’Souza, and James W. Kronstad. 2003. “Of Smuts, Blasts, Mildews, and Blights: CAMP Signaling in Phytopathogenic Fungi.” *Annual Review of Phytopathology* 41: 399–427. https://doi.org/10.1146/annurev.phyto.41.052002.095728.

Lemke, R. L., Z. Zhong, C. A. Campbell, and R. Zentner. 2007. “Can Pulse Crops Play a Role in Mitigating Greenhouse Gases from North American Agriculture?” In *Agronomy Journal*, 99:1719–25. American Society of Agronomy. https://doi.org/10.2134/agronj2006.0327s.

Lenth, Russell V. 2016. “Least-Squares Means: The R Package Lsmeans.” *Journal of Statistical Software* 69 (1). https://doi.org/10.18637/jss.v069.i01.

Lenth, Russell V., Paul Buerkner, Iago Giné-Vázquez, Maxime Herve, Maarten Jung, Jonathon Love, Fernando Miguez, Hannes Riebl, and Henrik Singmann. 2021. “Emmeans: Estimated Marginal Means, Aka Least-Squares Means.” https://cran.r-project.org/package=emmeans.

Lenth, Russell V. 2013. “Using the Lsmeans Package.” *CRAN R Project* 50 (60): 70.

Lewis, Gwilym, Brian Schrire, Barbara Mackinder, and Mike Lock. 2005. *Legumes of the World*. Edited by Gwilym Lewis, Brian Schrire, Barbara Mackinder, and Mike Lock. The Royal Botanic Gardens, Kew.

Lewontin, R. C. 1988. “On Measures of Gametic Disequilibrium.” *Genetics* 120 (3): 849–52.

Lewontin, R C. 1964. “THE INTERACTION OF SELECTION AND LINKAGE. II. OPTIMUM MODELS.” *Genetics* 50 (4): 757–82.

https://doi.org/10.1093/genetics/50.4.757.

Lewontin, Richard. 1974. *The Genetic Basis of Evolutionary Change*. New York, Columbia University Press, 1974: New York, Columbia University Press, 1974. papers2://publication/uuid/109090E5-E88A-4B56-8A35-DE9789DB2D5E.

Li, Ning, Xiao Han, Dan Feng, Deyi Yuan, and Li Jun Huang. 2019. “Signaling Crosstalk between Salicylic Acid and Ethylene/Jasmonate in Plant Defense: Do We Understand What They Are Whispering?” *International Journal of Molecular Sciences* 20 (3). https://doi.org/10.3390/ijms20030671.

Li, Yang, Guanghui Wang, Jin Rong Xu, and Cong Jiang. 2016. “Penetration Peg Formation and Invasive Hyphae Development Require Stage-Specific Activation of MoGTI1 in Magnaporthe Oryzae.” *Molecular Plant-Microbe Interactions* 29 (1): 36–45. https://doi.org/10.1094/MPMI-06-15-0142-R.

Liszkay, Anja, Barbara Kenk, and Peter Schopfer. 2003. “Evidence for the Involvement of Cell Wall Peroxidase in the Generation of Hydroxyl Radicals Mediating Extension Growth.” *Planta* 217 (4): 658–67. https://doi.org/10.1007/s00425-003-1028-1.

Liu, Fang, Yi Xiao, Xing Lai Ji, Ke Qin Zhang, and Cheng Gang Zou. 2017. “The CAMP-PKA Pathway-Mediated Fat Mobilization Is Required for Cold Tolerance in C. Elegans.” *Scientific Reports* 7 (1): 1–10. https://doi.org/10.1038/s41598-017-00630-w.

Liu, Po Pu, Saikat Bhattacharjee, Daniel F. Klessig, and Peter Moffett. 2010. “Systemic Acquired Resistance Is Induced by R Gene-Mediated Responses Independent of Cell Death.” *Molecular Plant Pathology* 11 (1): 155–60. https://doi.org/10.1111/j.1364-3703.2009.00564.x.

Liu, Wei, Zhi Hong Xu, Da Luo, and Hong Wei Xue. 2003. “Roles of OsCKI1, a Rice Casein Kinase I, in Root Development and Plant Hormone Sensitivity.” *Plant Journal* 36 (2): 189–202. https://doi.org/10.1046/j.1365-313X.2003.01866.x.

Liu, Z.J., and J.F. Cordes. 2004. “DNA Marker Technologies and Their Applications in Aquaculture Genetics.” *Aquaculture* 238 (1–4): 1–37. https://doi.org/10.1016/j.aquaculture.2004.05.027.

LOON, L.C. VAN, and E.A. VAN STRIEN. 1999. “The Families of Pathogenesis-Related Proteins, Their Activities, and Comparative Analysis of PR-1 Type Proteins.” *Physiological and Molecular Plant Pathology* 55 (2): 85–97. https://doi.org/10.1006/pmpp.1999.0213.

López-Escudero, Francisco Javier, and Jesús Mercado-Blanco. 2011. “Verticillium Wilt of Olive: A Case Study to Implement an Integrated Strategy to Control a Soil-Borne Pathogen.” *Plant and Soil* 344 (1–2): 1–50. https://doi.org/10.1007/s11104-010-0629-2.

Lötjönen, Sanna, and Markku Ollikainen. 2017. “Does Crop Rotation with Legumes Provide an Efficient Means to Reduce Nutrient Loads and GHG Emissions?” *Review of Agricultural, Food and Environmental Studies* 98 (4): 283–312. https://doi.org/10.1007/s41130-018-0063-z.

Luo, Jingyun, Chengcheng Wei, Haijun Liu, Shikun Cheng, Yingjie Xiao, Xiaqing Wang, Jianbing Yan, and Jianxiao Liu. 2020. “MaizeCUBIC: A Comprehensive Variation Database for a Maize Synthetic Population.” *Database : The Journal of Biological Databases and Curation* 2020 (January): 44. https://doi.org/10.1093/database/baaa044.

Mackay, Ian, and Wayne Powell. 2007. “Methods for Linkage Disequilibrium Mapping in Crops.” *Trends in Plant Science* 12 (2): 57–63. https://doi.org/10.1016/j.tplants.2006.12.001.

Mahiout, Djamel. 2017. “Contribution à La Caractérisation de Ascochyta Rabiei (Pass.) Labr., Agent Causal de l’anthracnose Du Pois Chiche (Cicer Arietinum L.) et Étude de Son Interaction Avec Medicago Truncatula Gaertn.” *Thèse*. Université Abd El Hamid Ibn Badis de Mostaganem.

Mahiout, Djamel, Boubekeur Seddik Bendahmane, Youcef Benkada Mokhtar, and Martina Rickauer. 2015. “Physiological Characterisation of Ascochyta Rabiei (Pass.) Lab. Isolated from Diseased Chickpea Fields in Six Regions of Northwestern Algeria.” *American-Eurasian J. Agric. & Environ. Sci* 15 (6): 1136–46. https://doi.org/10.5829/idosi.aejaes.2015.15.6.94125.

Manchia, M, J Cullis, G Turecki, G A Rouleau, and R Uher. 2013. “The Impact of Phenotypic and Genetic Heterogeneity on Results of Genome Wide Association Studies of Complex Diseases.” *PLoS ONE* 8 (10): 76295. https://doi.org/10.1371/journal.pone.0076295.

Manfred Schwab. 2011. *Encyclopedia of Cancer*. Edited by Manfred Schwab. *Encyclopedia of Cancer*. Vol. 16. Berlin, Heidelberg: Springer Berlin Heidelberg. https://doi.org/10.1007/978-3-642-16483-5.

Mannaa, Mohamed, and Young Su Seo. 2021. “Plants under the Attack of Allies: Moving towards the Plant Pathobiome Paradigm.” *Plants*.

https://doi.org/10.3390/plants10010125.

Marees, Andries T., Hilde de Kluiver, Sven Stringer, Florence Vorspan, Emmanuel Curis, Cynthia Marie-Claire, and Eske M. Derks. 2018. “A Tutorial on Conducting Genome-Wide Association Studies: Quality Control and Statistical Analysis.” *International Journal of Methods in Psychiatric Research* 27 (2): 1–10. https://doi.org/10.1016/j.taml.2017.02.002.

Marino, Daniel, Nemo Peeters, and Susana Rivas. 2012. “Ubiquitination during Plant Immune Signaling.” *Plant Physiology* 160 (1): 15–27. https://doi.org/10.1104/pp.112.199281.

Matta, A., and L. C P Kerling. 1964. “Verticillium Albo-Atrum as a Parasite of Senecio Vulgaris.” *Netherlands Journal of Plant Pathology* 70 (1): 27–32. https://doi.org/10.1007/BF02102384.

Mazaheri, Mona, Marlies Heckwolf, Brieanne Vaillancourt, Joseph L. Gage, Brett Burdo, Sven Heckwolf, Kerrie Barry, et al. 2019. “Genome-Wide Association Analysis of Stalk Biomass and Anatomical Traits in Maize.” *BMC Plant Biology* 19 (1): 1–17. https://doi.org/10.1186/s12870-019-1653-x.

Mazurier, MÉLANIE. 2018. “Biodiversity and Adaptation to Root Pathogen Verticillium Alfalfae at Medicago Truncatula. Importance of Micro-Evolution (Doctoral Dissertation Thesis).” Université Toulouse 3 Paul Sabatier. https://tel.archives-ouvertes.fr/OMP-ECOLAB-TEL/tel-01927066v1.

McKoy, Judith F., and A.P.J. Trinci. 1987. “Sporulation of Verticillium Agaricinum and Schizosaccharomyces Pombe in Batch and Chemostat Culture.” *Transactions of the British Mycological Society* 88 (3): 299–307. https://doi.org/10.1016/s0007-1536(87)80002-5.

Mendiburu, Felipe de, and Muhammad Yaseen. 2017. “Agricolae: Statistical Procedures for Agricultural Research.”

Mikaili, P, and J Shayegh. 2011. “Medicago Sativa: A Historical Ethnopharmacology and Etymological Study of the Alfalfa.” *Research Opinions in Animal & Veterinary Sciences* 1 (9): 614–18. www.roavs.com.

Mishra, Sonal, Swati Upadhyay, and Rakesh K. Shukla. 2017. “The Role of Strigolactones and Their Potential Cross-Talk under Hostile Ecological Conditions in Plants.” *Frontiers in Physiology* 7 (JAN): 1–7. https://doi.org/10.3389/fphys.2016.00691.

MOL, L., K. SCHOLTE, and J. VOS. 1995. “Effects of Crop Rotation and Removal of

Crop Debris on the Soil Population of Two Isolates of Verticillium Dahliae." *Plant Pathology* 44 (6): 1070–74. https://doi.org/10.1111/j.1365-3059.1995.tb02666.x.

Moreau, Delphine. 2006. "Morphology, Development and Plant Architecture of M. Truncatula." *Recherche*, no. November: 1–6.

Moroz, Natalia, Karen R. Fritch, Matthew J. Marcec, Diwaker Tripathi, Andrei Smertenko, and Kiwamu Tanaka. 2017. "Extracellular Alkalinization as a Defense Response in Potato Cells." *Frontiers in Plant Science* 8 (January): 1–11. https://doi.org/10.3389/fpls.2017.00032.

Morton, Newton E. 2005. "Review Series Linkage Disequilibrium Maps and Association Mapping." *Conflict* 115 (6). https://doi.org/10.1172/JCI25032.The.

Mott, Richard, Christopher J. Talbot, Maria G. Turri, Allan C. Collins, and Jonathan Flint. 2000. "A Method for Fine Mapping Quantitative Trait Loci in Outbred Animal Stocks." *Proceedings of the National Academy of Sciences of the United States of America* 97 (23): 12649–54. https://doi.org/10.1073/pnas.230304397.

Mukhtar, M. Shahid, Maggie E. McCormack, Cristiana T. Argueso, and Karolina M. Pajerowska-Mukhtar. 2016. "Pathogen Tactics to Manipulate Plant Cell Death." *Current Biology* 26 (13): R608–19. https://doi.org/10.1016/j.cub.2016.02.051.

Muller, Walter H. 1956. "Influence of Temperature on Growth and Sporulation of Certain Fungi." *Botanical Gazette* 117 (4): 336–43. http://www.jstor.org/stable/2473142.

Mur, Luis A. J., Paul Kenton, Amanda J Lloyd, Helen Ougham, and Elena Prats. 2008. "The Hypersensitive Response; the Centenary Is upon Us but How Much Do We Know?" *Journal of Experimental Botany* 59 (3): 501–20. https://doi.org/10.1093/jxb/erm239.

Myles, Sean, Jason Peiffer, Patrick J. Brown, Elhan S. Ersoz, Zhiwu Zhang, Denise E. Costich, and Edwards S Buckler. 2009. "Association Mapping: Critical Considerations Shift from Genotyping to Experimental Design." *The Plant Cell* 21 (8): 2194–2202. https://doi.org/10.1105/tpc.109.068437.

"National Alfalfa & Forage Alliance." 2019. NAFA. 2019. https://www.alfalfa.org/.

Navarro, Lionel, Cyril Zipfel, Owen Rowland, Ingo Keller, Silke Robatzek, Thomas Boller, and Jonathan D.G. Jones. 2004. "The Transcriptional Innate Immune Response to Flg22. Interplay and Overlap with Avr Gene-Dependent Defense Responses and Bacterial Pathogenesis." *Plant Physiology* 135 (2): 1113–28. https://doi.org/10.1104/pp.103.036749.

Naveed, Zunaira Afzal, Xiangying Wei, Jianjun Chen, Hira Mubeen, and Gul Shad Ali. 2020. “The PTI to ETI Continuum in Phytophthora-Plant Interactions.” *Frontiers in Plant Science* 11 (December). https://doi.org/10.3389/fpls.2020.593905.

Negahi, A., C. Ben, L. Gentzbittel, P. Maury, A. R. Nabipour, A. Ebrahimi, A. Sarrafi, and M. Rickauer. 2014. “Quantitative Trait Loci Associated with Resistance to a Potato Isolate of Verticillium Albo-Atrum in Medicago Truncatula.” *Plant Pathology* 63 (2): 308–15. https://doi.org/10.1111/ppa.12100.

Negahi, A., A. Sarrafi, A. Ebrahimi, P. Maury, J. M. Prospéri, C. Ben, and M. Rickauer. 2013. “Genetic Variability of Tolerance to Verticillium Albo-Atrum and Verticillium Dahliae in Medicago Truncatula.” *European Journal of Plant Pathology* 136 (1): 135–43. https://doi.org/10.1007/s10658-012-0148-5.

Nicholson, Ralph L., and Lynn Epstein. 1991. “Adhesion of Fungi to the Plant Surface.” *The Fungal Spore and Disease Initiation in Plants and Animals*, 3–23. https://doi.org/10.1007/978-1-4899-2635-7_1.

Nicholson, Ralph L., Hirofumi Yoshioka, Naoto Yamaoka, and Hitoshi Kunoh. 1988. “Preparation of the Infection Court ByErysiphe Graminis.” *Experimental Mycology* 12 (4): 336–49. https://doi.org/10.1016/0147-5975(88)90025-4.

Niki, Tomoya, Ichiro Mitsuhara, Shigemi Seo, Norihiro Ohtsubo, and Yuko Ohashi. 1998. “Antagonistic Effect of Salicylic Acid and Jasmonic Acid on the Expression of Pathogenesis-Related (PR) Protein Genes in Wounded Mature Tobacco Leaves.” *Plant and Cell Physiology* 39 (5): 500–507. https://doi.org/10.1093/oxfordjournals.pcp.a029397.

Nirmala, Jayaveeramuthu, Tom Drader, Paulraj K. Lawrence, Chuntao Yin, Scot Hulbert, Camille M. Steber, Brian J. Steffenson, Les J. Szabo, Diter Von Wettstein, and Andris Kleinhofs. 2011. “Concerted Action of Two Avirulent Spore Effectors Activates Reaction to Puccinia Graminis 1 (Rpg1)-Mediated Cereal Stem Rust Resistance.” *Proceedings of the National Academy of Sciences of the United States of America* 108 (35): 14676–81. https://doi.org/10.1073/pnas.1111771108.

Nishad, Resna, Talaat Ahmed, Vattakandy Jasin Rahman, and Abdul Kareem. 2020. “Modulation of Plant Defense System in Response to Microbial Interactions.” *Frontiers in Microbiology* 11 (July): 1–13. https://doi.org/10.3389/fmicb.2020.01298.

Novakazi, Fluturë, Lene Krusell, Jens Jensen, Jihad Orabi, Ahmed Jahoor, Therése Bengtsson, and on behalf of the PPP Barley Consortium. 2020. “You Had Me at ‘MAGIC’!: Four Barley MAGIC Populations Reveal Novel Resistance QTL for Powdery Mildew.” *Genes* 11 (12): 1512. https://doi.org/10.3390/genes11121512.

Nürnberger, T. 1999. “Signal Perception in Plant Pathogen Defense.” *Cellular and Molecular Life Sciences* 55 (2): 167–82. https://doi.org/10.1007/s000180050283.

Nürnberger, Thorsten, and Frédéric Brunner. 2002. “Innate Immunity in Plants and Animals: Emerging Parallels between the Recognition of General Elicitors and Pathogen-Associated Molecular Patterns.” *Current Opinion in Plant Biology* 5 (4): 318–24. https://doi.org/10.1016/S1369-5266(02)00265-0.

Nurnberger, Thorsten, Frederic Brunner, Birgit Kemmerling, and Lizelle Piater. 2004. “Innate Immunity in Plants and Animals: Striking Similarities and Obvious Differences.” *Immunological Reviews* 198 (1): 249–66. https://doi.org/10.1111/j.0105-2896.2004.0119.x.

Nürnberger, Thorsten, and Dierk Scheel. 2001. “Signal Transmission in the Plant Immune Response.” *Trends in Plant Science* 6 (8): 372–79. https://doi.org/10.1016/S1360-1385(01)02019-2.

O’Brien, Jose A., Arsalan Daudi, Vernon S Butt, and G. Paul Bolwell. 2012. “Reactive Oxygen Species and Their Role in Plant Defence and Cell Wall Metabolism.” *Planta* 236 (3): 765–79. https://doi.org/10.1007/s00425-012-1696-9.

Ogura, Takehiko, and Wolfgang Busch. 2015. “From Phenotypes to Causal Sequences: Using Genome Wide Association Studies to Dissect the Sequence Basis for Variation of Plant Development.” *Current Opinion in Plant Biology* 23: 98–108. https://doi.org/10.1016/j.pbi.2014.11.008.

Okada, Kazunori, Hiroshi Abe, and Gen Ichiro Arimura. 2015. “Jasmonates Induce Both Defense Responses and Communication in Monocotyledonous and Dicotyledonous Plants.” *Plant and Cell Physiology* 56 (1): 16–27. https://doi.org/10.1093/pcp/pcu158.

Oome, Stan, Tom M. Raaymakers, Adriana Cabral, Simon Samwel, Hannah Böhm, Isabell Albert, Thorsten Nürnberger, and Guido Van Den Ackerveken. 2014. “Nep1-like Proteins from Three Kingdoms of Life Act as a Microbe-Associated Molecular Pattern in Arabidopsis.” *Proceedings of the National Academy of Sciences of the United States of America* 111 (47): 16955–60.

https://doi.org/10.1073/pnas.1410031111.

Ozaki, Kouichi, Yozo Ohnishi, Aritoshi Iida, Akihiko Sekine, Ryo Yamada, Tatsuhiko Tsunoda, Hiroshi Sato, et al. 2002. “Functional SNPs in the Lymphotoxin-α Gene That Are Associated with Susceptibility to Myocardial Infarction.” https://doi.org/10.1038/ng1047.

Papaioannou, Ioannis A., Eleftherios K. Ligoxigakis, Demetrios J. Vakalounakis, Emmanouil A. Markakis, and Milton A. Typas. 2013. “Phytopathogenic, Morphological, Genetic and Molecular Characterization of a Verticillium Dahliae Population from Crete, Greece.” *European Journal of Plant Pathology* 136 (3): 577–96. https://doi.org/10.1007/s10658-013-0189-4.

Patnala, Radhika, Judith Clements, and Jyotsna Batra. 2013. “Candidate Gene Association Studies: A Comprehensive Guide to Useful in Silico Tools.” *BMC Genetics* 14. https://doi.org/10.1186/1471-2156-14-39.

Pavan, Stefano, Chiara Delvento, Luigi Ricciardi, Concetta Lotti, Elena Ciani, and Nunzio D’Agostino. 2020. “Recommendations for Choosing the Genotyping Method and Best Practices for Quality Control in Crop Genome-Wide Association Studies.” *Frontiers in Genetics*. Frontiers Media S.A. https://doi.org/10.3389/fgene.2020.00447.

Pegg, G. F., and B L. Brady. 2002. *Verticillium Wilts*. Edited by Beryl Ledsom Brady. Illustrate. CABI Pub., CAB International, Wallingford, Oxon OX10 8DE, UK. 552. https://books.google.fr/books/about/Verticillium_Wilts.html?id=Ks4tbrkiR8cC&redir_esc=y.

Pennycooke, Joyce C., Hongmei Cheng, and Eric J. Stockinger. 2008. “Comparative Genomic Sequence and Expression Analyses of Medicago Truncatula and Alfalfa Subspecies Falcata Cold-Acclimation-Specific Genes.” *Plant Physiology* 146 (3): 1242–54. https://doi.org/10.1104/pp.107.108779.

Pešić, Vladimir, Harry Smit, and Alireza Saboori. 2014. “Checklist of the Water Mites (Acari, Hydrachnidia) of Iran: Second Supplement and Description of One New Species.” *Ecologica Montenegrina* 1 (1): 30–48. https://doi.org/10.37828/em.2014.1.6.

Pham, Jasmine, Jasmine Liu, Mark H. Bennett, John W. Mansfield, and Radhika Desikan. 2012. “Arabidopsis Histidine Kinase 5 Regulates Salt Sensitivity and Resistance against Bacterial and Fungal Infection.” *New Phytologist* 194 (1): 168–80. https://doi.org/10.1111/j.1469-8137.2011.04033.x.

Phuong, Le Thi, Aprilia Nur Fitrianti, Mai Thanh Luan, Hidenori Matsui, Yoshiteru Noutoshi, Mikihiro Yamamoto, Yuki Ichinose, Tomonori Shiraishi, and Kazuhiro Toyoda. 2020. “Antagonism between SA- and JA-Signaling Conditioned by Saccharin in Arabidopsis Thaliana Renders Resistance to a Specific Pathogen.” *Journal of General Plant Pathology* 86 (2): 86–99. https://doi.org/10.1007/s10327-019-00899-x.

Popp, J. D., W. P. McCaughey, R. D.H. Cohen, T. A. McAllister, and W. Majak. 2000. “Enhancing Pasture Productivity with Alfalfa: A Review.” *Canadian Journal of Plant Science* 80 (3): 513–19. https://doi.org/10.4141/P99-049.

Porras-Hurtado, Liliana, Yarimar Ruiz, Carla Santos, Christopher Phillips, Ángel Carracedo, and Maria V. Lareu. 2013. “An Overview of STRUCTURE: Applications, Parameter Settings, and Supporting Software.” *Frontiers in Genetics* 4 (MAY): 1–13. https://doi.org/10.3389/fgene.2013.00098.

Priestley, J.H. 1922. “PHYSIOLOGICAL STUDIES IN PLANT ANATOMY.” *New Phytologist* 21 (2): 58–61. https://doi.org/10.1111/j.1469-8137.1922.tb07588.x.

Prioritization, Candidate Gene. 2020. “Genetic Basis of Maize Resistance to Multiple Insect Mapping and Candidate Gene Prioritization.”

Pusztahelyi, Tünde. 2018. “Chitin and Chitin-Related Compounds in Plant–Fungal Interactions.” *Mycology*. https://doi.org/10.1080/21501203.2018.1473299.

Qian, Hui Rong, and Shuguang Huang. 2005. “Comparison of False Discovery Rate Methods in Identifying Genes with Differential Expression.” *Genomics* 86 (4): 495–503. https://doi.org/10.1016/j.ygeno.2005.06.007.

Quiros, Carlos F., and Gary R. Bauchan. 2015. “The Genus Medicago and the Origin of the Medicago Sativa Comp.” In , 93–124. https://doi.org/10.2134/agronmonogr29.c3.

R Core Team. 2020. “R: A Language and Environment for Statistical Computing. R Foundation for Statistical Computing.” Vienna; Austria: R Foundation for Statistical Computing. http://www.r-project.org/.

Radišek, Sebastjan, Jernej Jakše, and Branka Javornik. 2006. “Genetic Variability and Virulence among Verticillium Albo-Atrum Isolates from Hop.” *European Journal of Plant Pathology* 116 (4): 301–14. https://doi.org/10.1007/s10658-006-9061-0.

Rajput, L. S., Sharma Taru, P. Madhusudhan, Kumar Sanjeev, and P. Sinha. 2019. “Role of Various Signaling Pathways for Glycerol Synthesis in Appessoria of

Magnaporthe Oryzae under Climate Change Scenario." *Research Journal of Biotechnology* 14 (5): 67–73.

Ren, Deqiang, Xiaojian Fang, Peng Jiang, Guangxu Zhang, Junmei Hu, Xiaoqian Wang, Qing Meng, et al. 2018. "Genetic Architecture of Nitrogen-Deficiency Tolerance in Wheat Seedlings Based on a Nested Association Mapping (NAM) Population." *Frontiers in Plant Science* 9 (June). https://doi.org/10.3389/fpls.2018.00845.

Rieux, Adrien, Samuel Soubeyrand, François Bonnot, Etienne K. Klein, Josue E. Ngando, Andreas Mehl, Virginie Ravigne, Jean Carlier, and Luc de Lapeyre de Bellaire. 2014. "Long-Distance Wind-Dispersal of Spores in a Fungal Plant Pathogen: Estimation of Anisotropic Dispersal Kernels from an Extensive Field Experiment." Edited by Richard A. Wilson. *PLoS ONE* 9 (8): e103225. https://doi.org/10.1371/journal.pone.0103225.

Rosato, Marcela, José A. Galián, and Josep A. Rosselló. 2012. "Amplification, Contraction and Genomic Spread of a Satellite DNA Family (E180) in Medicago (Fabaceae) and Allied Genera." *Annals of Botany* 109 (4): 773–82. https://doi.org/10.1093/aob/mcr309.

Rose, Ray J. 2008. "Medicago Truncatula as a Model for Understanding Plant Interactions with Other Organisms, Plant Development and Stress Biology: Past, Present and Future." *Functional Plant Biology*. https://doi.org/10.1071/FP07297.

Roy, Julien Le, Brigitte Huss, Anne Creach, Simon Hawkins, and Godfrey Neutelings. 2016. "Glycosylation Is a Major Regulator of Phenylpropanoid Availability and Biological Activity in Plants." *Frontiers in Plant Science*. https://doi.org/10.3389/fpls.2016.00735.

Ruggieri, Valentino, Gianluca Francese, Adriana Sacco, Antonietta D'Alessandro, Maria Manuela Rigano, Mario Parisi, Marco Milone, Teodoro Cardi, Giuseppe Mennella, and Amalia Barone. 2014. "An Association Mapping Approach to Identify Favourable Alleles for Tomato Fruit Quality Breeding." *BMC Plant Biology* 14 (1): 337. https://doi.org/10.1186/s12870-014-0337-9.

Rumbolz, J, H -H Kassemeyer, V Steinmetz, H B Deising, K Mendgen, D Mathys, S Wirtz, and R Guggenheim. 2000. "Differentiation of Infection Structures of the Powdery Mildew Fungus Uncinula Necator and Adhesion to the Host Cuticle." *Canadian Journal of Botany* 78 (3): 409–21. https://doi.org/10.1139/b00-016.

Samaj, J. 2003. "From Signal to Cell Polarity: Mitogen-Activated Protein Kinases as

Sensors and Effectors of Cytoskeleton Dynamicity." *Journal of Experimental Botany* 55 (395): 189–98. https://doi.org/10.1093/jxb/erh012.

Sánchez-Vallet, Andrea, Jeroen R Mesters, and Bart P.H.J. Thomma. 2015. "The Battle for Chitin Recognition in Plant-Microbe Interactions." *FEMS Microbiology Reviews* 39 (2): 171–83. https://doi.org/10.1093/femsre/fuu003.

Sarkar, Deepayan. 2008. *Lattice: Multivariate Data Visualization with R*. New York: Springer. ttp://lmdvr.r-forge.r-project.org.

Sasabe, Michiko, and Yasunori Machida. 2006. "MAP65: A Bridge Linking a MAP Kinase to Microtubule Turnover." *Current Opinion in Plant Biology* 9 (6): 563–70. https://doi.org/10.1016/j.pbi.2006.09.010.

Sbeiti, M. ABED AL LATIFF. 2016. "Effect of Climate Change on the Response of Plants and Pathogens, during the Development of Root Diseases Caused by Pathogenic Soil Fungi of the Verticillium Genus, in Two Species of the Medicago Genus." L'école doctorale SDU2E.

Schluttenhofer, Craig, Sitakanta Pattanaik, Barunava Patra, and Ling Yuan. 2014. "Analyses of Catharanthus Roseus and Arabidopsis Thaliana WRKY Transcription Factors Reveal Involvement in Jasmonate Signaling." *BMC Genomics* 15 (1): 502. https://doi.org/10.1186/1471-2164-15-502.

Schnaithmann, Florian, Doris Kopahnke, and Klaus Pillen. 2014. "A First Step toward the Development of a Barley NAM Population and Its Utilization to Detect QTLs Conferring Leaf Rust Seedling Resistance." *Theoretical and Applied Genetics* 127 (7): 1513–25. https://doi.org/10.1007/s00122-014-2315-x.

Schnathorst, W.C. 1981. "Life Cycle and Epidemiology of Verticillium." In *Fungal Wilt Diseases of Plants*, 81–111. Elsevier. https://doi.org/10.1016/B978-0-12-464450-2.50009-7.

Schumann, G. L., and C. J. D'Arcy. 2010. "Essential Plant Pathology." In *Essential Plant Pathology, Second Edition*, i–v. St. Paul, Minnesota U.S.A.: The American Phytopathological Society. https://doi.org/10.1094/9780890546710.fm.

Schwartz, D C, X Li, L I Hernandez, S P Ramnarain, E J Huff, and Y K Wang. 1993. "Ordered Restriction Maps of Saccharomyces Cerevisiae Chromosomes Constructed by Optical Mapping." *Science* 262 (5130): 110 LP – 114. https://doi.org/10.1126/science.8211116.

Scott, Michael F., Olufunmilayo Ladejobi, Samer Amer, Alison R. Bentley, Jay Biernaskie, Scott A. Boden, Matt Clark, et al. 2020. "Multi-Parent Populations in

Crops: A Toolbox Integrating Genomics and Genetic Mapping with Breeding." *Heredity* 125 (6): 396–416. https://doi.org/10.1038/s41437-020-0336-6.

Scott, Paul T., Lisette Pregelj, Ning Chen, Johanna S. Hadler, Michael A. Djordjevic, and Peter M. Gresshoff. 2008. "Pongamia Pinnata: An Untapped Resource for the Biofuels Industry of the Future." *BioEnergy Research* 1 (1): 2–11. https://doi.org/10.1007/s12155-008-9003-0.

Sephton-Clark, Poppy C.S., and Kerstin Voelz. 2018. "Spore Germination of Pathogenic Filamentous Fungi." In *Advances in Applied Microbiology*, 1st ed., 102:117–57. Elsevier Inc. https://doi.org/10.1016/bs.aambs.2017.10.002.

Seymour, Mark, John A. Kirkegaard, Mark B. Peoples, Peter F. White, and Robert J. French. 2012. "Break-Crop Benefits to Wheat in Western Australia – Insights from over Three Decades of Research." *Crop and Pasture Science* 63 (1): 1. https://doi.org/10.1071/CP11320.

Shaner, Gregory. 1977. "The Effect of Nitrogen Fertilization on the Expression of Slow-Mildewing Resistance in Knox Wheat." *Phytopathology* 77 (8): 1051. https://doi.org/10.1094/phyto-67-1051.

Short, Dylan P. G., German Sandoya, Gary E. Vallad, Steven T. Koike, Chang-Lin Xiao, Bo-Ming Wu, Suraj Gurung, Ryan J. Hayes, and Krishna V. Subbarao. 2015. "Dynamics of Verticillium Species Microsclerotia in Field Soils in Response to Fumigation, Cropping Patterns, and Flooding." *Phytopathology®* 105 (5): 638–45. https://doi.org/10.1094/PHYTO-09-14-0259-R.

Siddique, Kadambot H. M., Chris Johansen, Neil C. Turner, Marie-Hélène Jeuffroy, Abul Hashem, Dogan Sakar, Yantai Gan, and Salem S. Alghamdi. 2012. "Innovations in Agronomy for Food Legumes. A Review." *Agronomy for Sustainable Development* 32 (1): 45–64. https://doi.org/10.1007/s13593-011-0021-5.

Singh, B. D., and A. K. Singh. 2015. "Marker-Assisted Plant Breeding: Principles and Practices." In *Marker-Assisted Plant Breeding: Principles and Practices*, 1–514. https://doi.org/10.1007/978-81-322-2316-0.

Slate, Jon. 2005. "Quantitative Trait Locus Mapping in Natural Populations: Progress, Caveats and Future Directions." *Molecular Ecology* 14 (2): 363–79. https://doi.org/10.1111/j.1365-294X.2004.02378.x.

Slatkin, Montgomery. 2008. "Linkage Disequilibrium — Understanding the Evolutionary Past and Mapping the Medical Future." *Nature Reviews Genetics* 9

(6): 477–85. https://doi.org/10.1038/nrg2361.

Son, Yong, Yong-Kwan Cheong, Nam-Ho Kim, Hun-Taeg Chung, Dae Gill Kang, and Hyun-Ock Pae. 2011. “Mitogen-Activated Protein Kinases and Reactive Oxygen Species: How Can ROS Activate MAPK Pathways?” *Journal of Signal Transduction* 2011: 1–6. https://doi.org/10.1155/2011/792639.

Sorkheh, Karim, Lyudmyla V Malysheva-Otto, Michelle G Wirthensohn, Saeed Tarkesh-Esfahani, and Pedro Martínez-Gómez. 2008. “Linkage Disequilibrium, Genetic Association Mapping and Gene Localization in Crop Plants.” www.sbg.org.br.

Stagnari, Fabio, Albino Maggio, Angelica Galieni, and Michele Pisante. 2017. “Multiple Benefits of Legumes for Agriculture Sustainability: An Overview.” *Chemical and Biological Technologies in Agriculture* 4 (1): 2. https://doi.org/10.1186/s40538-016-0085-1.

Stanton-Geddes, John, Timothy Paape, Brendan Epstein, Roman Briskine, Jeremy Yoder, Joann Mudge, Arvind K. Bharti, et al. 2013. “Candidate Genes and Genetic Architecture of Symbiotic and Agronomic Traits Revealed by Whole-Genome, Sequence-Based Association Genetics in Medicago Truncatula.” *PLoS ONE* 8 (5). https://doi.org/10.1371/journal.pone.0065688.

Stich, BenjaminComparison of mixed-model approaches for association mapping, Jens Möhring, Hans Peter Piepho, Martin Heckenberger, Edward S. Buckler, and Albrecht E. Melchinger. 2008. “Comparison of Mixed-Model Approaches for Association Mapping.” *Genetics* 178 (3): 1745–54. https://doi.org/10.1534/genetics.107.079707.

Stram, Daniel. 2014. *Design, Analysis, and Interpretation of Genome-Wide Association Scans (Series: Statistics for Biology and Health)*. http://www.springer.com/us/book/9781461494423.

Sukumaran, Sivakumar, Wenwen Xiang, Scott R. Bean, Jeffrey F. Pedersen, Stephen Kresovich, Mitchell R. Tuinstra, Tesfaye T. Tesso, Martha T. Hamblin, and Jianming Yu. 2012. “Association Mapping for Grain Quality in a Diverse Sorghum Collection.” *Plant Genome* 5 (3): 126–35. https://doi.org/10.3835/plantgenome2012.07.0016.

Svec, David, Ales Tichopad, Vendula Novosadova, Michael W Pfaffl, and Mikael Kubista. 2015. “How Good Is a PCR Efficiency Estimate: Recommendations for Precise and Robust QPCR Efficiency Assessments.” *Biomolecular Detection*

and Quantification 3 (March): 9–16. https://doi.org/10.1016/j.bdq.2015.01.005.

Tai, Helen H., David De Koeyer, Mads Sønderkær, Sanne Hedegaard, Martin Lagüe, Claudia Goyer, Lana Nolan, et al. 2018. “Verticillium Dahliae Disease Resistance and the Regulatory Pathway for Maturity and Tuberization in Potato.” *The Plant Genome* 11 (1): 170040. https://doi.org/10.3835/plantgenome2017.05.0040.

Takahashi, Hideki, Yoshinori Kanayama, Ming Shu Zheng, Tomonobu Kusano, Shu Hase, Masato Ikegami, and Jyoti Shah. 2004. “Antagonistic Interactions between the SA and JA Signaling Pathways in Arabidopsis Modulate Expression of Defense Genes and Gene-for-Gene Resistance to Cucumber Mosaic Virus.” *Plant and Cell Physiology* 45 (6): 803–9. https://doi.org/10.1093/pcp/pch085.

Tang, Haibao, Vivek Krishnakumar, Shelby Bidwell, Benjamin Rosen, Agnes Chan, Shiguo Zhou, Laurent Gentzbittel, et al. 2014. “An Improved Genome Release (Version Mt4.0) for the Model Legume Medicago Truncatula.” *BMC Genomics* 15 (1): 1–14. https://doi.org/10.1186/1471-2164-15-312.

Teixeira, Paulo José PL, Nicholas R. Colaianni, Connor R. Fitzpatrick, and Jeffery L. Dangl. 2019. “Beyond Pathogens: Microbiota Interactions with the Plant Immune System.” *Current Opinion in Microbiology* 49 (September): 7–17. https://doi.org/10.1016/j.mib.2019.08.003.

Thaler, Jennifer S., Parris T. Humphrey, and Noah K. Whiteman. 2012. “Evolution of Jasmonate and Salicylate Signal Crosstalk.” *Trends in Plant Science* 17 (5): 260–70. https://doi.org/10.1016/j.tplants.2012.02.010.

Tharanathan, R. N., and S. Mahadevamma. 2003. “Grain Legumes - A Boon to Human Nutrition.” *Trends in Food Science and Technology*. Elsevier Ltd. https://doi.org/10.1016/j.tifs.2003.07.002.

Thornton, Brenda, and Chhandak Basu. 2011. “Real-Time PCR (QPCR) Primer Design Using Free Online Software.” *Biochemistry and Molecular Biology Education* 39 (2): 145–54. https://doi.org/10.1002/bmb.20461.

Tiwari, Menka, Debasish Pati, Reecha Mohapatra, Binod Bihari Sahu, and Prashant Singh. 2022. “The Impact of Microbes in Plant Immunity and Priming Induced Inheritance: A Sustainable Approach for Crop Protection.” *Plant Stress* 4 (March): 100072. https://doi.org/10.1016/j.stress.2022.100072.

Toueni, Maoulida, Cécile Ben, Aurélie Le Ru, Laurent Gentzbittel, and Martina

Rickauer. 2016. “Quantitative Resistance to Verticillium Wilt in Medicago Truncatula Involves Eradication of the Fungus from Roots and Is Associated with Transcriptional Responses Related to Innate Immunity.” *Frontiers in Plant Science* 7 (September). https://doi.org/10.3389/fpls.2016.01431.

Ugalde, Unai, and Ana Belén Rodriguez-Urra. 2016. “Autoregulatory Signals in Mycelial Fungi.” In *Growth, Differentiation and Sexuality*, edited by Jürgen Wendland, : 10.1007/, 185–202. Cham: Springer International Publishing. https://doi.org/10.1007/978-3-319-25844-7_9.

Undersander, D., Cosgrove, D., Cullen, Ei., Grau, C., and M. Rice, M. E., Renz, M., Sheaffer, C., Shewmaker, G., Sulc. 2011. *Alfalfa Management Guide*. *Alfalfa Management Guide*.

Untergasser, Andreas, Ioana Cutcutache, Triinu Koressaar, Jian Ye, Brant C Faircloth, Maido Remm, and Steven G Rozen. 2012. “Primer3-New Capabilities and Interfaces.” *Nucleic Acids Research* 40 (15): e115–e115. https://doi.org/10.1093/nar/gks596.

Valent, Barbara, and Chang Hyun Khang. 2010. “Recent Advances in Rice Blast Effector Research.” *Current Opinion in Plant Biology* 13 (4): 434–41. https://doi.org/10.1016/j.pbi.2010.04.012.

VanLiere, Jenna M., and Noah A Rosenberg. 2008. “Mathematical Properties of the Measure of Linkage Disequilibrium.” *Theoretical Population Biology* 74 (1): 130–37. https://doi.org/10.1016/j.tpb.2008.05.006.

Viswanathan, R., P. Malathi, A. Ramesh Sundar, S. Aarthi, S. M. Premkumari, and P. Padmanaban. 2005. “Differential Induction of Chitinases and Thaumatin-like Proteins in Sugarcane in Response to Infection by Colletotrichum Falcatum Causing Red Rot Disease.” *Zeitschrift Fur Pflanzenkrankheiten Und Pflanzenschutz* 112 (5): 417–25.

Vleesschauwer, David De, Jing Xu, and Monica Höfte. 2014. “Making Sense of Hormone-Mediated Defense Networking: From Rice to Arabidopsis.” *Frontiers in Plant Science* 5 (November). https://doi.org/10.3389/fpls.2014.00611.

Wang, Dong, Karolina Pajerowska-Mukhtar, Angela Hendrickson Culler, and Xinnian Dong. 2007. “Salicylic Acid Inhibits Pathogen Growth in Plants through Repression of the Auxin Signaling Pathway.” *Current Biology* 17 (20): 1784–90. https://doi.org/10.1016/j.cub.2007.09.025.

Wang, Haihua, Junjie Hao, Xujun Chen, Zhongna Hao, Xia Wang, Yonggen Lou,

Youliang Peng, and Zejian Guo. 2007. “Overexpression of Rice WRKY89 Enhances Ultraviolet B Tolerance and Disease Resistance in Rice Plants.” *Plant Molecular Biology* 65 (6): 799–815. https://doi.org/10.1007/s11103-007-9244-x.

Wang, Minghui, Ning Jiang, Tianye Jia, Lindsey Leach, James Cockram, Robbie Waugh, Luke Ramsay, Bill Thomas, and Zewei Luo. 2012. “Genome-Wide Association Mapping of Agronomic and Morphologic Traits in Highly Structured Populations of Barley Cultivars.” *Theoretical and Applied Genetics* 124 (2): 233–46. https://doi.org/10.1007/s00122-011-1697-2.

Watson, Christine A., Moritz Reckling, Sara Preissel, Johann Bachinger, Göran Bergkvist, Tom Kuhlman, Kristina Lindström, et al. 2017. “Grain Legume Production and Use in European Agricultural Systems.” *Advances in Agronomy* 144 (November): 235–303. https://doi.org/10.1016/bs.agron.2017.03.003.

Watson, L., and M. J. Dallwitz. 1996. “The Families of Flowering Plants: Interactive Identification and Information Retrieval.” *Choice Reviews Online* 33 (10): 33-5710-33–5710. https://doi.org/10.5860/CHOICE.33-5710.

Wees, S. C. M. van, E. A. M. de Swart, J. A. van Pelt, L. C. van Loon, and C. M. J. Pieterse. 2000. “Enhancement of Induced Disease Resistance by Simultaneous Activation of Salicylate- and Jasmonate-Dependent Defense Pathways in Arabidopsisthaliana.” *Proceedings of the National Academy of Sciences* 97 (15): 8711–16. https://doi.org/10.1073/pnas.130425197.

Wenne, Roman. 2018. “Single Nucleotide Polymorphism Markers with Applications in Aquaculture and Assessment of Its Impact on Natural Populations.” *Aquatic Living Resources* 31. https://doi.org/10.1051/alr/2017043.

Westgate, J. M. 1908. “Alfalfa.” *Washington: U. S. Department of Agriculture. p. 5. Retrieved 28 July 2013.*, December.

Westwood, James H., John I. Yoder, Michael P. Timko, and Claude W. DePamphilis. 2010. “The Evolution of Parasitism in Plants.” *Trends in Plant Science* 15 (4): 227–35. https://doi.org/10.1016/j.tplants.2010.01.004.

Wickham, Hadley. 2016. *Ggplot2:: Elegant Graphics for Data Analysis}*. Use R! Cham: Springer International Publishing. https://doi.org/10.1007/978-3-319-24277-4.

Wilhelm; S. 1955. “Longevity of the Verticillium Wilt Fungus in the Laboratory and Field.” *Phytopathology* 45 (3): 180–81.

Wilhelm, Stephen, and Albert O. Paulus. 1980. “How Soil Fumigation Benefits the

California Strawberry Industry." *Plant Disease*. https://www.cabdirect.org/cabdirect/abstract/19800387545.

Wit, P. J. G. M. de. 2007. "How Plants Recognize Pathogens and Defend Themselves." *Cellular and Molecular Life Sciences* 64 (21): 2726–32. https://doi.org/10.1007/s00018-007-7284-7.

Wojtaszek, Przemysław. 1997. "Oxidative Burst: An Early Plant Response to Pathogen Infection." *Biochemical Journal* 322 (3): 681–92. https://doi.org/10.1042/bj3220681.

Wolf, Erick D. De, and Scott A. Isard. 2007. "Disease Cycle Approach to Plant Disease Prediction." *Annual Review of Phytopathology* 45 (1): 203–20. https://doi.org/10.1146/annurev.phyto.44.070505.143329.

Wrzaczek, Michael, Mikael Brosché, and Jaakko Kangasjärvi. 2013. "ROS Signaling Loops — Production, Perception, Regulation." *Current Opinion in Plant Biology* 16 (5): 575–82. https://doi.org/10.1016/j.pbi.2013.07.002.

Xiao, Yingjie, Haijun Liu, Liuji Wu, Marilyn Warburton, and Jianbing Yan. 2017. "Genome-Wide Association Studies in Maize: Praise and Stargaze." *Molecular Plant* 10 (3): 359–74. https://doi.org/10.1016/j.molp.2016.12.008.

Xu, Shan, Michael J. Christensen, Rebecca Creamer, and Yan Zhong Li. 2019. "Identification, Characterization, Pathogenicity, and Distribution of Verticillium Alfalfae in Alfalfa Plants in China." *Plant Disease* 103 (7): 1565–76. https://doi.org/10.1094/PDIS-07-18-1272-RE.

Xu, Y., PFL. Chang, Dong Liu, Meena L Narasimhan, Kashchandra G Raghothama, Paul M Hasegawa, and Ray A Bressan. 1994. "Plant Defense Genes Are Synergistically Induced by Ethylene and Methyl Jasmonate." *The Plant Cell* 6 (August): 1077–85. https://doi.org/10.1105/tpc.6.8.1077.

Yang, Jing, Guihua Duan, Chunqin Li, Lin Liu, Guangyu Han, Yaling Zhang, and Changmi Wang. 2019. "The Crosstalks Between Jasmonic Acid and Other Plant Hormone Signaling Highlight the Involvement of Jasmonic Acid as a Core Component in Plant Response to Biotic and Abiotic Stresses." *Frontiers in Plant Science*. https://doi.org/10.3389/fpls.2019.01349.

Yarwood, C E. 1957. "Powdery Mildews." *Springer* 23 (4): 235–301.

Yin, Cui-Cui, Biao Ma, Derek Phillip Collinge, Barry James Pogson, Si-Jie He, Qing Xiong, Kai-Xuan Duan, et al. 2015. "Ethylene Responses in Rice Roots and Coleoptiles Are Differentially Regulated by a Carotenoid Isomerase-Mediated

Abscisic Acid Pathway." *The Plant Cell* 27 (4): 1061–81. https://doi.org/10.1105/tpc.15.00080.

Young, N. D., Frédéric Debellé, Giles E. D. Oldroyd, Rene Geurts, Steven B. Cannon, Michael K. Udvardi, Vagner A. Benedito, et al. 2011. "The Medicago Genome Provides Insight into the Evolution of Rhizobial Symbioses." *Nature* 480 (7378): 520–24. https://doi.org/10.1038/nature10625.

Young, Nevin Dale, Joann Mudge, and TH Noel Ellis. 2003. "Legume Genomes: More than Peas in a Pod." *Current Opinion in Plant Biology* 6 (2): 199–204. https://doi.org/10.1016/S1369-5266(03)00006-2.

Yu, Jianming, and Edward S. Buckler. 2006. "Genetic Association Mapping and Genome Organization of Maize." *Current Opinion in Biotechnology* 17 (2): 155–60. https://doi.org/10.1016/j.copbio.2006.02.003.

Yu, Jianming, James B Holland, Michael D McMullen, and Edward S Buckler. 2008. "Genetic Design and Statistical Power of Nested Association Mapping in Maize." *Genetics* 178 (1): 539–51. https://doi.org/10.1534/genetics.107.074245.

Yu, Jianming, Gael Pressoir, William H. Briggs, Irie Vroh Bi, Masanori Yamasaki, John F. Doebley, Michael D. McMullen, et al. 2006. "A Unified Mixed-Model Method for Association Mapping That Accounts for Multiple Levels of Relatedness." *Nature Genetics* 38 (2): 203–8. https://doi.org/10.1038/ng1702.

Zander, Peter, T. S. Amjath-Babu, Sara Preissel, Moritz Reckling, Andrea Bues, Nicole Schläfke, Tom Kuhlman, et al. 2016. "Grain Legume Decline and Potential Recovery in European Agriculture: A Review." *Agronomy for Sustainable Development*. Springer-Verlag France. https://doi.org/10.1007/s13593-016-0365-y.

Zare, R. Gams. 2007. "Gibellulopsis, a Suitable Genus for Verticillium Nigrescens, and Musicillium, a New Genus for V. Theobromae." *Nova Hedwigia* 85 (3–4): 463–89. https://doi.org/10.1127/0029-5035/2007/0085-0463.

Zhang, Ning, Lisa A. Castlebury, Andrew N. Miller, Sabine M. Huhndorf, Conrad L. Schoch, Keith A. Seifert, Amy Y. Rossman, et al. 2006. "An Overview of the Systematics of the Sordariomycetes Based on a Four-Gene Phylogeny." *Mycologia* 98 (6): 1076–87. https://doi.org/10.3852/mycologia.98.6.1076.

Zhang, Zhiwu, Elhan Ersoz, Chao Qiang Lai, Rory J. Todhunter, Hemant K. Tiwari, Michael A. Gore, Peter J. Bradbury, et al. 2010. "Mixed Linear Model Approach Adapted for Genome-Wide Association Studies." *Nature Genetics* 42 (4): 355–

60. https://doi.org/10.1038/ng.546.

Zhao, He, Kai-Xuan Duan, Biao Ma, Cui-Cui Yin, Yang Hu, Jian-Jun Tao, Yi-Hua Huang, et al. 2020. “Histidine Kinase MHZ1/OsHK1 Interacts with Ethylene Receptors to Regulate Root Growth in Rice.” *Nature Communications* 11 (1): 518. https://doi.org/10.1038/s41467-020-14313-0.

Zhao, Jian, Koki Fujita, and Kokki Sakai. 2007. “Reactive Oxygen Species, Nitric Oxide, and Their Interactions Play Different Roles in Cupressus Lusitanica Cell Death and Phytoalexin Biosynthesis.” *New Phytologist* 175 (2): 215–29. https://doi.org/10.1111/j.1469-8137.2007.02109.x.

Zhou, Xiaoyi, and Xuehui Huang. 2019. “Genome-Wide Association Studies in Rice: How to Solve the Low Power Problems?” https://doi.org/10.1016/j.molp.2018.11.010.

Zhu, Chengsong, Michael Gore, Edward S. Buckler, and Jianming Yu. 2008. “Status and Prospects of Association Mapping in Plants.” *The Plant Genome* 1 (1): 5–20. https://doi.org/10.3835/plantgenome2008.02.0089.

Zhu, Mengjin, and Shuhong Zhao. 2007. “Candidate Gene Identification Approach: Progress and Challenges.” *International Journal of Biological Sciences* 3 (7): 420–27. https://doi.org/10.7150/ijbs.3.420.

Zimmermann, S., T. Ehrhardt, G. Plesch, and B. Müller-Röber. 1999. “Ion Channels in Plant Signaling.” *Cellular and Molecular Life Sciences* 55 (2): 183–203. https://doi.org/10.1007/s000180050284.

Zurbriggen, Matias D., Néstor Carrillo, and Mohammad-Reza Hajirezaei. 2010. “ROS Signaling in the Hypersensitive Response.” *Plant Signaling & Behavior* 5 (4): 393–96. https://doi.org/10.4161/psb.5.4.10793.

Zvereva, Anna S., and Mikhail M. Pooggin. 2012. “Silencing and Innate Immunity in Plant Defense against Viral and Non-Viral Pathogens.” *Viruses* 4 (11): 2578–97. https://doi.org/10.3390/v4112578.